LEABHARLANN CHOLÁISTE NA TRÍONÓIDE, BAILE ÁTHA CLIATH | TRINITY COLLEGE LIBRARY DUBLIN
Ollscoil Átha Cliath | The University of Dublin

Terms and Conditions of Use of Digitised Theses from Trinity College Library Dublin

Copyright statement

All material supplied by Trinity College Library is protected by copyright (under the Copyright and Related Rights Act, 2000 as amended) and other relevant Intellectual Property Rights. By accessing and using a Digitised Thesis from Trinity College Library you acknowledge that all Intellectual Property Rights in any Works supplied are the sole and exclusive property of the copyright and/or other IPR holder. Specific copyright holders may not be explicitly identified. Use of materials from other sources within a thesis should not be construed as a claim over them.

A non-exclusive, non-transferable licence is hereby granted to those using or reproducing, in whole or in part, the material for valid purposes, providing the copyright owners are acknowledged using the normal conventions. Where specific permission to use material is required, this is identified and such permission must be sought from the copyright holder or agency cited.

Liability statement

By using a Digitised Thesis, I accept that Trinity College Dublin bears no legal responsibility for the accuracy, legality or comprehensiveness of materials contained within the thesis, and that Trinity College Dublin accepts no liability for indirect, consequential, or incidental, damages or losses arising from use of the thesis for whatever reason. Information located in a thesis may be subject to specific use constraints, details of which may not be explicitly described. It is the responsibility of potential and actual users to be aware of such constraints and to abide by them. By making use of material from a digitised thesis, you accept these copyright and disclaimer provisions. Where it is brought to the attention of Trinity College Library that there may be a breach of copyright or other restraint, it is the policy to withdraw or take down access to a thesis while the issue is being resolved.

Access Agreement

By using a Digitised Thesis from Trinity College Library you are bound by the following Terms & Conditions. Please read them carefully.

I have read and I understand the following statement: All material supplied via a Digitised Thesis from Trinity College Library is protected by copyright and other intellectual property rights, and duplication or sale of all or part of any of a thesis is not permitted, except that material may be duplicated by you for your research use or for educational purposes in electronic or print form providing the copyright owners are acknowledged using the normal conventions. You must obtain permission for any other use. Electronic or print copies may not be offered, whether for sale or otherwise to anyone. This copy has been supplied on the understanding that it is copyright material and that no quotation from the thesis may be published without proper acknowledgement.

A numerical, phenotypical and functional characterization of innate T cell populations in CVID

Serena Arduini

TRINITY COLLEGE DUBLIN
10 FEB 2016
ACADEMIC REGISTRY

PhD
Medicine

Ph.D. **2016**

50652326
* 5 0 6 5 2 3 2 6 *

THESIS
11007

Declaration

This thesis has not previously been submitted as an exercise for a degree at the University of Dublin, Trinity College, or any other university, and is entirely the product of my own work.

I agree that the Library may lend or copy this thesis upon request. This permission covers only single copies made for study purposes, subject to normal conditions of acknowledgement.

TRINITY LIBRARY
2 7 JUL 2016
DUBLIN

Thesis 11007

Summary

Common Variable Immunodeficiency (CVID) is a primary antibody deficiency characterized by widespread B cell defects, low serum immunoglobulin levels, recurrent infections and frequent idiopathic complications, including autoimmunity. Both conventional and innate T cells have previously been shown to provide help to B cells maturation and antibody production; innate T cell subsets are furthermore directly and indirectly involved in anti-microbial responses, and can participate in the regulation of inflammatory and autoimmune processes. We therefore followed B cell differentiation and investigated the phenotype and functions of innate T cell subsets in CVID patients with and without complications, aiming to define if these populations could play a role in CVID.

Blood was collected from 27 healthy controls, 21 CVID patients, 3 patients affected by selective IgA deficiency and/or IgG subclass deficiency, 6 patients with secondary hypogammaglobulinemia and 1 patients with idiopathic antibody deficiency attending St. James's Hospital, Dublin. The frequencies and absolute counts of B and T cell populations, including Vδ1, Vδ2 and Vδ3 γδ T cells, invariant natural killer T (iNKT) cells and mucosal-associated invariant T (MAIT) cells were determined by flow cytometry. MAIT cell functionality was assessed by *in vitro* stimulation of whole blood with anti-CD3 and anti-CD28 antibodies or PMA and ionomycin and analysis of phenotypic changes and cytokine expression. Co-cultures of sorted MAIT cells and autologous B cells from healthy donors were set up to determine if MAIT cells could influence B cell maturation and antibody production *in vitro*.

While frequencies of class-switched memory B cells and plasmablasts were significantly decreased in the blood of CVID patients ($p < 0.005$), those of naïve B cells were significantly increased ($p < 0.01$). Vδ1, Vδ2 and Vδ3 γδ T cells were found in normal numbers in the circulation of these individuals, however frequencies and absolute counts of iNKT and MAIT cells were significantly decreased in comparison to healthy donors. Frequencies and numbers of these populations were particularly depleted in patients with complicated CVID ($p < 0.05$). Regardless of complication status, frequencies of MAIT cells expressing activation marker CD69 were significantly higher in unstimulated blood from CVID patients than healthy controls ($p = 0.03$). These cells also produced IL-17A, IL-22 and TNFα significantly more frequently than cells from healthy donors following stimulation with anti-CD3 and anti-CD28 antibodies. In co-cultures with B cells, unstimulated MAIT cells did not affect B cell maturation, but appeared in certain subjects to sustain IgM production.

A defect in B cell class-switching was shown in this cohort of CVID patients to associate with significantly decreased frequencies and absolute counts of both iNKT cells and MAIT cells, implicating these innate T cell subsets in the disease. The particularly low frequencies of iNKT cells and MAIT cells observed in patients with complications are suggestive of an involvement of these cell subsets in the comorbidities accompanying CVID. The strong and likely chronic activation of MAIT cells in patient blood, as well as their enhanced ability to produce IL-17A and IL-22 following antibody-mediated stimulation, are consistent with a role both in infection resolution and in the development of autoimmunity. Although unstimulated MAIT cells were found in this study not to affect B cell differentiation, iNKT cells could play a role in the failed maturation of B cells seen in CVID. These results suggest that MAIT cells and/or iNKT cells may find an immunotherapeutic application in CVID in the future.

To Colin, who is always true.

Acknowledgements

Heartfelt thanks go to my supervisors, Prof Con Feighery and Dr Derek Doherty, for allowing me to take on this project and for being a constant source of advice and support.

Many thanks to the patients who gracefully agreed to be part of this study, without whom this thesis would not be possible. Also thank you to Drs Niall Conlon, Shanti Mahabir and Cariosa Lee-Brennan for welcoming me into the immunology clinic, and to nurses Ann Sloane and Angela Doyle for their invaluable help in arranging my visits and in the collection of samples.

Huge thanks to my fellow PhD students Yasmeen, Éilis and Andreea, who have been there throughout the highs and lows of the past 4 years. It has been a pleasure and a privilege to be able to share this experience with you (just don't ask me to do it again). Also thank you to Tanya, Sarah and Christina, for the great discussions on CVID, the chats and the laughs, and to Vinny, for always being his level-headed, patient self.

Finally, thank you to my family and all those I have left back home, far away but not forgotten.

PhD Output

Original research articles:

Circulating Mucosal-Associated Invariant T cells are depleted and functionally altered in Common Variable Immunodeficiency [Manuscript in preparation]

Meeting presentations:

- HRB PhD Programme in Immunology Annual Research Day, October 14th 2011 [Poster]
- Irish Society for Immunology meeting, September 12-13th 2013 [Poster]
- 16th IMM Annual Meeting, November 8th 2013 [Poster]
- British Society for Immunology Congress, December 2-5th 2013 [Poster]
- UK Primary Immunodeficiency Network Forum, December 6-7th 2013 [Poster]

Courses attended:

- Graduate course in Immunology, Trinity College Dublin, 2011-2012
- Multiparameter Flow Cytometry Course (Flocyte), Galway, November 9th 2012
- FACSCanto II Training (Becton Dickinson), Dublin, October 15-16th 2013

Table of Contents

Declaration i

Summary ii

Acknowledgements v

PhD Output vi

Table of Contents vii

Acronyms and abbreviations 1

CHAPTER 1 - INTRODUCTION 6

1.1 – CVID 7

1.2 – Selective IgA Deficiency and IgG subclass deficiency 10

1.3 – Secondary hypogammaglobulinemia 11

1.4 – Adaptive and innate immunity 11

1.5 – Lymphocyte subsets 13

1.5.1 – B cell subsets 13

1.5.2 – T cell subsets 18

1.5.2.1 – Conventional T cells 18

1.5.2.2 – Innate T cells 20

1.5.2.2.1 – γδ T cells 21

1.5.2.2.2 – iNKT cells 26

1.5.2.2.3 – MAIT cells 30

1.5.2.2.3.1 – MAIT cell development 30

1.5.2.2.3.2 – MR-1 32

1.5.2.2.3.3 – MAIT cell detection and phenotype 33

1.5.2.2.3.4 – MAIT cell functions 34

1.5.2.2.3.5 – MAIT cells in disease 36

1.5.2.2.3.6 – MAIT cell propagation 38

1.5.3 – Other lymphocyte subsets 39

1.5.3.1 – NK cells 39

1.5.3.2 – NT cells 42

1.6 – Immune cell subset abnormalities in CVID 43

1.7 – Aims of the project 45

CHAPTER 2 - MATERIALS AND METHODS 48

2.1 – Materials 49

2.2 – Recipes for solutions and media 56

2.3 – Ethical approval 57

2.4 – Study population 57

2.5 – Classification of patients in clinical phenotypes 60

2.6 – Collection of blood samples 61

2.7 – Cell isolation, count and culture 62

2.7.1 – PBMC isolation by density gradient 62

2.7.2 – Cell counts with Neubauer haemocytometer 62

2.7.3 – Positive selection of $CD3^+$ cells 64

2.7.4 – Negative selection of B cells 64

2.7.5 – Operator-assisted fluorescence-activated cell sorting of MAIT cells 65

2.7.6 - CellTrace Violet Staining 66

2.7.7 – Co-cultures of B cells and MAIT cells 67

2.8 – Flow Cytometry 68

2.8.1 – Principles of flow cytometry 68

2.8.2 – Index of immune cell subsets detected by flow cytometry 70

2.8.3 – Immunophenotyping 71

2.8.4 – Intracellular cytokine staining and activation marker upregulation 72

2.8.5 – Markers of B cell differentiation after co-culture with MAIT cells 73

2.8.6 – Analysis of flow cytometry data 74

2.8.7 – Cytometric Bead Array (CBA) assay 74

2.8.8 – T, B and NK cell enumeration (TruCount test) 78

2.8.9 – Purities of isolated B and T cells 78

2.9 – Statistical analysis 79

CHAPTER 3 - ANALYSIS OF CIRCULATING B CELL SUBSETS IN PATIENTS WITH CVID AND OTHER ANTIBODY DEFICIENCIES 82

3.1 – Introduction 83

3.2 – Hypothesis and aims of the chapter 84

3.3 – Phenotypic analysis of circulating B cell subsets in CVID and secondary hypogammaglobulinemia 85

3.3.1 – Phenotypic analysis of total B, T and NK lymphocytes 85

3.3.2 – Phenotypic analysis of B cell subsets 87

3.4 – Phenotypic analysis of circulating B cell subsets in SIgAD and IgG subclass deficiency 93

3.5 – Phenotypic analysis of circulating B cell subsets in a query diagnosis patient 95

3.6 – Correlations between antibody levels at diagnosis and B cell differentiation status in CVID 97

3.7 – Discussion 99

CHAPTER 4 - ANALYSIS OF CIRCULATING T CELL SUBSETS IN PATIENTS WITH CVID AND OTHER ANTIBODY DEFICIENCIES 105

4.1 – Introduction 106

4.2 – Hypothesis and aims of the chapter 107

4.3 – Phenotypic analysis of circulating T cell subsets in CVID and secondary hypogammaglobulinemia 108

4.3.1 – Phenotypic analysis of conventional T cell subsets 108

4.3.2 – Phenotypic analysis of γδ T cell subsets 110

4.3.3 – Phenotypic analysis of iNKT cells 116

4.3.4 – Phenotypic analysis of MAIT cells 118

4.3.5 – Phenotypic analysis of NT cells 123

4.4 – Phenotypic analysis of circulating T cell subsets in SIgAD and IgG subclass deficiency 126

4.5 – Phenotypic analysis of circulating T cell subsets in a query diagnosis patient 128

4.6 – Determination of associations between frequencies of innate T cell subsets and clinical phenotypes in CVID 129

4.6.1 – Clinical status of the cohort 130

4.6.2 – Associations between frequencies of γδ T cell subsets and clinical phenotypes 132

4.6.3 – Associations between frequencies of iNKT cells and clinical phenotypes 139

4.6.4 – Associations between frequencies of MAIT cells and clinical phenotypes 142

4.7 – Discussion 149

CHAPTER 5 - ANALYSIS OF RELATIONSHIPS BETWEEN FREQUENCIES OR ABSOLUTE COUNTS OF INNATE T CELLS AND OTHER LYMPHOCYTE SUBSETS IN CVID 158

5.1 – Introduction 159

5.2 – Hypothesis and aims of the chapter 161

5.3 – Analysis of statistical correlations between frequencies or counts of Vδ1 γδ T cells and other lymphocyte subsets 162

5.4 – Analysis of statistical correlations between frequencies or counts of Vδ2 γδ T cells and other lymphocyte subsets 165

5.5 – Analysis of statistical correlations between frequencies or counts of Vδ3 γδ T cells and other lymphocyte subsets 167

5.6 – Analysis of statistical correlations between frequencies or counts of iNKT cells and other lymphocyte subsets 168

5.7 – Analysis of statistical correlations between frequencies or counts of MAIT cells and other lymphocyte subsets 170

5.8 – Diagrams of correlations between cell types 174

5.9 – Discussion 176

CHAPTER 6 - FUNCTIONAL PROPERTIES OF MAIT CELLS FROM HEALTHY DONORS AND CVID PATIENTS 181

6.1 – Introduction 182

6.2 – Hypothesis and aims of the chapter 183

6.3 – Upregulation of activation markers by T cells and MAIT cells following *in vitro* stimulation 184

6.3.1 – CD69 expression by T cells and MAIT cells following *in vitro* stimulation 184

6.3.2 – CD40L expression by T cells and MAIT cells following *in vitro* stimulation 189

6.4 – Cytokine production by T cells and MAIT cells following *in vitro* stimulation 193

6.4.1 – Production of TNFα by T cells and MAIT cells following *in vitro* stimulation 193

6.4.2 – Production of IFNγ by T cells and MAIT cells following *in vitro* stimulation 196

6.4.3 – Production of IL-4 by T cells and MAIT cells following *in vitro* stimulation 200

6.4.4 – Production of IL-10 by T cells and MAIT cells following *in vitro* stimulation 203

6.4.5 – Production of IL-17A by T cells and MAIT cells following *in vitro* stimulation 206

6.4.6 – Production of IL-22 by T cells and MAIT cells following *in vitro* stimulation 209

6.5 – Discussion 213

CHAPTER 7 - EFFECTS OF MAIT CELLS ON B CELL MATURATION AND ANTIBODY PRODUCTION 220

7.1 – Introduction 221

7.2 – Hypothesis and aims of the chapter 222

7.3 – Effects of MAIT cells on the differentiation of autologous B cells *in vitro* 223

7.4 – Effects of MAIT cells on antibody production by autologous B cells *in vitro* 226

7.4.1 – Quantification of IgM antibodies in co-cultures of autologous MAIT cells and B cells 226

7.4.2 – Quantification of IgG antibodies in co-cultures of autologous MAIT cells and B cells 229

7.4.3 – Quantification of IgA antibodies in co-cultures of autologous MAIT cells and B cells 232

7.5 – Analysis of correlations between MAIT cell frequencies and circulating antibody levels at diagnosis in CVID patients 235

7.6 – Discussion 238

CHAPTER 8 - DISCUSSION 243

REFERENCES 260

Acronyms and abbreviations

6-FP – 6-formyl pterin

ACTB – β actin

AD-HIES – Autosomal dominant hyper-IgE syndrome

AIHA – Autoimmune haemolytic anaemia

APC – Antigen presenting cell

APC – Allophycocyanin

APRIL – A proliferation-inducing ligand

AT – Atasia telangiectasia

AUC – Area under the curve

BAFF – B-cell-activating factor

BAFF-R – B-cell-activating factor receptor

BCG – Bacillus Calmette-Guérin

Bcl- – B cell lymphoma

BCR – B cell receptor

BFA – Brefeldin A

B_{REG} – Regulatory B (cell)

BSA – Bovine serum albumin

BTK – Bruton tyrosine kinase

C – Constant (region of the BCR)

CAR – Chimeric antigen receptor

CBA – Cytometric bead array (assay)

CCR – C-C motif chemokine receptor

CD – Cluster of differentiation

CD40L – CD40 ligand

cDNA – Complementary deoxyribonucleic acid

CDR3 – Complementarity determining region 3

CLL – Chronic lymphocytic leukaemia

CLR – C-type lectin receptor

CMV – Cytomegalovirus

CpG – C-phosphate-G

CTL – Cytotoxic T lymphocyte

CVID – Common Variable Immunodeficiency

CXCR – C-X-C motif chemokine receptor

Cy5.5 – Cyanine 5.5

Cy7 – Cyanine 7

D – Diverse (region of the BCR)

DAMP – Danger-associated molecular pattern

DBSS – Dried blood spot sample

DC – Dendritic cell

DMSO – Dimethyl sulfoxide

DN – Double negative

DNA – Deoxyribonucleic acid

dsDNA – Double stranded DNA

dsRNA – Double stranded RNA

EAE – Experimental autoimmune encephalomyelitis

EB/AO – Ethidium bromide/acridine orange

EDTA – Ethylenediaminetetraacetic acid

ESID – European Society for Immunodeficiencies

FASL – FAS ligand

FCS – Foetal calf serum

FITC – Fluorescein isothiocyanate

FMO – Fluorescence minus one

FOXP3 – Forkhead box P3

FSC – Forward scatter channel

GATA-3 – GATA binding protein 3

GC – Germinal centre

GM-CSF – Granulocyte macrophage colony-stimulating factor

H – Heavy (chain of the BCR)

HAART – Highly active anti-retroviral therapy

HC – Healthy control

HCV – Hepatitis C virus

HEPES – 4-(2-hydroxyethyl)-1-piperazineethanesulfonic acid

HIGM – X chromosome-linked hyper IgM syndrome

HIV – Human immunodeficiency virus

HLA – Human leukocyte antigen

HMB-PP – (E)-4-hydroxy-3-methy l-2-butenyl pyrophosphate

IBD – Inflammatory bowel disease

IBS – Inflammatory bowel syndrome

ICOS – Inducible T cell costimulator

IEL – Intraepithelial lymphocyte

IFNγ – Interferon γ

IgA – Immunoglobulin A

IgG – Immunoglobulin G

IgM – Immunoglobulin M

IL- – Interleukin

iNK – Immature NK (cell)

iNKT – Invariant natural killer T (cell)

$iNKT_{FH}$ – Follicular helper-like iNKT (cell)

$iNKT_{REG}$ – Regulatory iNKT (cell)

IPP – Isopentenyl pyrophosphate

iPSC – Induced pluripotent stem cell

ITAM – Immunoreceptor tyrosine-based activation motif

iTCR – Invariant TCR

ITIM – Immunoreceptor tyrosine-based inhibition motif

ITP – Idiopathic thrombocytopenic purpura

J – Junction (region of the BCR)

KIR – Killer-cell immunoglobulin-like receptor

KREC – K-deleting recombination excision circle

L – Light (chain of the BCR)

LIP – Lymphoid interstitial pneumonitis

LPMC – *Lamina propria* mononuclear cell

LPS – Lipopolysaccharide

MAC – Membrane attack complex

MAIT – Mucosal-associated invariant T (cell)

MDR – Multiple drug resistance

MEM – Minimum essential medium

MFI – Geometric mean fluorescence intensity

MHC – Major histocompatibility complex

MIC-A – MHC class I polypeptide-related antigen A

MIC-B – MHC class I polypeptide-related antigen B

MMM – Marginal metallophilic macrophage

MOI – Multiplicity of infection

MR-1 – MHC-related molecule 1

mRNA – Messenger RNA

MS – Multiple sclerosis

mTEC – Medullary thymic epithelial cells

MZ – Marginal zone

MZM – Marginal zone macrophage

Myd88 – Myeloid differentiation marker 88

NBS – Nijmegen-breakage syndrome

NEEA – Non-essential amino acids

NF-κB – Nuclear factor κB

NK – Natural killer (cell)

NKG2 – NK group 2

NKR – Natural killer receptor

NKT – Natural killer T (cell)

NLR – NOD-like receptor

NOD1 – Nucleotide-binding oligomerization domain-containing protein 1

NOD2 – Nucleotide-binding oligomerization domain-containing protein 2

NT – Natural T (cell)

PAMP – Pathogen-associated molecular pattern

PBA – PBS with BSA

PBMC – Peripheral blood mononuclear cell

PBS – Phosphate buffered saline

PD-1 – Programmed cell death-1

PD-L2 – Programmed cell death-ligand 2

PE – Phycoerythrin

Pen Strep – Penicillin streptomycin

PerCP – Peridinine chlorophyll protein

PFA – Paraformaldehyde

PHA – Phytohaemagglutinin

PI3K-δ – Phosphoinositide-3-kinase, δ subunit

PID – Primary immunodeficiency

PKC – Protein kinase C

PLC – Peptide loading complex

PLI – Polyclonal lymphocytic infiltration

PLZF – Promyelocytic leukaemia zinc finger

PMA – Phorbol 12-myristate 13-acetate

Poly(I:C) – Polyinosinic-polycytidylic acid

PRR – Pattern recognition receptor

RA – Rheumatoid arthritis

RL-6,7-diMe – 6,7-dimethyl-8-D-ribityllumazine

RL-6-Me-7-OH – 7-hydroxy-6-methyl-8-D-ribityllumazine

RLR – RIG-like receptor

RNA – Ribonucleic acid

ROC – Receiver operating characteristic (curve)

RORγτ – Retinoic acid-related orphan receptor γτ

rRL-6-CH_2OH – Reduced 6-hydroxymethyl-8-d-ribityllumazine

RPM – Revolutions per minute

r_S – Spearman's correlation coefficient

RTOC – Reaggregated thymic organ culture

SAP – SLAM-associated protein

SCID – Severe combined immunodeficiency

SHM – Somatic hypermutation

SIgAD – Selective IgA deficiency

SLE – Systemic lupus erythematosus

SPE-C – Streptococcal pyrogenic exotoxin-C

SSC – Side scatter channel

TACI – Transmembrane activator and CAML interactor

TAP – Transporter associated with antigen processing

T-Bet – T-box expressed in T cells

TCR – T cell receptor

TEC – Thymic epithelial cell

T_{FH} – Follicular helper T (cell)

TGFβ – Tumour growth factor β

T_H – Helper T (cell)

TLR – Toll-like receptor

TNFα – Tumour necrosis factor α

TRAIL – TNF-related apoptosis inducing ligand

TREC – T cell receptor excision circle

T_{REG} – Regulatory T (cell)

TRIF – TIR-domain-containing adapter-inducing interferon-β

TSST-1 – Toxic shock syndrome toxin-1

V – Variable (region of the BCR)

XLA – X-linked agammaglobulinemia

XLP – X-linked lymphoproliferative syndrome

α-GalCer – α-galactosylceramide

β2m – β2-microglobulin

γδ T_{REG} – Regulatory γδ T (cell)

CHAPTER 1

INTRODUCTION

1.1 – CVID

Common variable immunodeficiency (CVID) is, although rare, the most commonly diagnosed primary immunodeficiency. It affects between 1 in 10,000 and 1 in 50,000 individuals,[1] depending on the region considered, and tends to be more frequent in Caucasians, less so amongst Asians and African-Americans.[2] The reasons for the varied prevalence of CVID between ethnicities are unclear so far, but it is postulated that underlying genetic differences play a role, affecting the development of the immune defect, or defects, that cause CVID. Sex, on the other hand, would not appear to be involved in this process, as males and females are diagnosed in similar numbers. CVID can be also diagnosed in all decades of life, and no preferential age at disease onset has been identified. Diagnoses in later life can sometimes reflect a delay by health practitioners in recognizing the heterogeneous symptoms of CVID as the consequence of a single condition. In general, more widespread awareness of primary immunodeficiencies amongst general practitioners is helping to reduce diagnostic delays and to satisfactorily manage the disease from an earlier age, including in children.

The first case of CVID was described in 1953 by Janeway and colleagues.[3] While CVID was initially considered a single disease, it is nowadays thought of as an umbrella definition under which many different conditions, and most likely many causative immune defects, coexist. These disorders share important common features, the most notable being hypogammaglobulinemia, i.e. a reduction of antibody titres in patient serum. Indeed, the diagnostic criteria of the European Society for Immunodeficiencies (ESID), stipulate that an individual is likely to have CVID when all other defined causes of hypogammaglobulinemia have been excluded and the patient presents:

- at greater than 2 years of age, to exclude immunodeficiencies with strong genetic bases;
- with a marked decrease in immunoglobulin G (IgG, at least 2 standard deviations below the mean for age) and a marked decrease in IgM (immunoglobulin M) and/or IgA (immunoglobulin A);
- with absent isohaemagglutinins and/or poor response to vaccines.

Most patients with CVID display reduced IgA levels, but about 50 % are also IgM-deficient. Amongst the conditions that should be excluded during the differential diagnosis are, for example, X-linked agammaglobulinemia (XLA), X-linked lymphoproliferative syndrome (XLP) and secondary antibody deficiency.

A direct consequence of the lack of immunoglobulins, and the second hallmark of CVID, is the development by patients of recurrent infections, mainly of the respiratory and intestinal tracts, but also affecting the skin, eyes and urinary tract. These are most often caused by a limited number of pathogens, including *Haemophilus influenzae*, *Streptococcus pneumoniae*, *Staphylococcus aureus*, *Moraxella catarrhalis*, *Neisseria meningitidis* and *Giardia lamblia*.[4] Respiratory infections, in particular, can range in untreated CVID patients from mild, e.g. rhinitis or sinusitis, to severe, such as pneumonia requiring hospitalization and intravenous administration of antibiotics. If left untreated, they can progress into chronic pulmonary disease and bronchiectasis. Infections tend to diminish in number and intensity once patients are placed on substitutive therapy, consisting of life-long intravenous or subcutaneous IgG infusions. The dose of immunoglobulins administered is initially weight-dependent, and later adjusted for each patient on the basis of his or her response to therapy. Current guidelines suggest to maintain trough immunoglobulin levels of at least 8 g/L.

Beyond hypogammaglobulinemia and recurrent infections, the clinical characteristics of CVID can be very heterogeneous.[2,5] Autoimmune complications are frequent, appearing in 25 to 50 % of patients in a variety of forms, from idiopathic thrombocytopenic purpura (ITP) to primary hypothyroidism, from psoriasis and vitiligo to autoimmune haemolytic anemia (AIHA) or rheumatoid arthritis (RA). Patients can also develop enteropathy, i.e. alterations of the bowel characterized by flattening of the villi and increased frequencies of intraepithelial lymphocytes (IELs) in the intestinal *lamina propria*. Even when enteropathy is not histologically confirmed, many report inflammatory bowel syndrome-like symptoms, including diarrhoea, abdominal cramps, malabsorption and weight loss. Granulomata, lymphadenopathy, hepatomegaly or splenomegaly are frequently observed. Finally, CVID patients are estimated to develop neoplasia (lymphoma, colorectal carcinoma) 8 to 13-fold more often than the general population.[6] All of these conditions are treated symptomatically and on a case by case basis. **Table 1.1** summarizes the most common symptoms and complications of CVID.

CVID is generally considered a sporadic condition, with no cause of disease ever identified for up to 90 % of those affected. However, about 15 % of CVID patients are related in first-degree to individuals with either CVID or selective IgA deficiency (SIgAD), and there have been reports of cases of SIgAD progressing into CVID,[7-9] which suggests CVID and SIgAD may share a genetic association. Particularly interesting is the observation that, in families with more than one member affected by this kind of disorder, a parent with CVID can pass down the defect to the offspring in the shape of IgA deficiency.[9]

Table 1.1 – Most frequent manifestations of CVID

Manifestations of CVID	Type
Recurrent infections	
	Sino-pulmonary infections (rhinitis, sinusitis, otitis, bronchitis, pneumonia)
	Gastro-intestinal infections (giardiasis, *Helicobacter pylori* infection with gastritis)
	Infections at other sites (skin, eyes, urinary tract)
Autoimmunity	Idiopathic thrombocytopenic purpura, autoimmune haemolytic anemia, pernicious anemia, rheumatoid arthritis, primary hypothyroidism, vitiligo, psoriasis
Inflammatory intestinal conditions	Idiopathic CVID enteropathy, inflammatory bowel syndrome (IBS), ulcerative colitis, Crohn's disease
Lymphocytic infiltration of tissues	Granulomata (lungs, liver, lymphoid tissues), lymphadenopathy, hepatomegaly, splenomegaly
Malignancies	Lymphoid malignancies (particularly non-Hodgkin lymphoma), gastric and colorectal carcinoma

Instances of familial CVID, which constitute about 10 % of the total cases, have also been attributed to rare monogenic mutations. The genes involved so far are those for CD19 (cluster of differentiation 19),[10] inducible T cell costimulator (ICOS),[11] and TNF-receptor superfamily members TACI (transmembrane activator and CAML interactor)[12] and BAFF-R (B-cell-activating factor receptor).[13] With the sole exception of ICOS, which is expressed on the surface of T cells, all the proteins encoded by these genes are found in B cell, and all are involved in B cell activation and differentiation. CD19 is phosphorylated and transduces the activation signal following binding of antigen to the B Cell Receptor, while ICOS participates in terminal B cell differentiation into plasma and memory cells. TACI and BAFF-R both recognize BAFF (B-cell-activating factor), a cytokine which induces potent activation, proliferation and differentiation of B cells.

Genetic studies have additionally identified several loci that seem involved in susceptibility to CVID. These include human leukocyte antigen (HLA) class II DR and DQ, which could affect antigen presentation to T helper cells by B cells.[14,15] Loci in the HLA class III region could also play a role,[16,17] particularly as this area is responsible for the production of pro-inflammatory cytokine TNFα (tumour necrosis factor α), a potent mediator involved in autoimmune and inflammatory diseases such as Crohn's disease, rheumatoid arthritis and multiple sclerosis. [18,19] Nonetheless, the molecular bases of CVID remain largely unknown.

1.2 – Selective IgA Deficiency and IgG subclass deficiency

Selective IgA deficiency is a primary immunodeficiency characterised by decreased or undetectable levels of IgA antibodies in the presence of normal IgG and IgM. It is common in Caucasians and Africans, affecting up to about 1 in 200 individuals, while occurrence is much lower amongst Asians.[20]

Despite its high prevalence, SIgAD is less clinically relevant than CVID, as it is often asymptomatic.[21] This is likely due to the compensatory effect of IgG and IgM antibodies, which constitute the bulk of protective immunoglobulins in circulation, as well as to the fact that many individuals retain at least partial secretion of IgA. Symptomatic patients can develop infections, however these are generally fewer and less severe in comparison to those seen in CVID. As well as being found in plasma as a monomer, IgA is secreted by mucosal surfaces in a dimeric form, which plays an important protective role at sites including the intestinal, respiratory and genital tracts. SIgAD patients will therefore most often develop infections of these systems. As in CVID, common affections include sinusitis, bronchitis and pneumonia caused by bacteria including *Haemophilus influenzae* and *Streptococcus pneumoniae*; bronchiectasis can develop as a consequence of untreated recurrent infections.[20] Use of IgG replacement therapy in SIgAD is controversial, as these patients already produce normal levels of IgG antibodies, however anecdotal evidence suggests it can be useful in the worst-affected individuals.

As mentioned in chapter 1.1, SIgAD seems to share a genetic link with CVID. Patients can overtime progress from SIgAD into CVID, and cases of the two diseases seem to cluster in familial units; indeed, SIgAD can present in children of individuals affected by CVID, and first-degree relatives of CVID patients are in general more likely to develop CVID or SIgAD.[7-9] Genetic similarities between the two conditions could help to explain why, like CVID, SIgAD is associated with abnormally high frequencies of autoimmune disorders. Autoimmunity appears in 20-30 % of patients, in a variety of forms, most often as idiopathic thrombocytopenic purpura.[22] An association between SIgAD and lymphoid and gastrointestinal cancers has been suggested, but not definitely identified.[23] Notably, the prevalence of SIgAD is up to 15 times higher amongst sufferers of coeliac disease.[24,25]

IgG subclass deficiency manifests as a selective decrease of plasma antibodies belonging to one or more subclasses of the IgG isotype, i.e. IgG1, IgG2, IgG3 or IgG4. In a subgroup of patients, in which IgG2 and/or IgG4 are usually involved, it appears alongside SIgAD. The causes of these associated defects are unknown, however genetic studies suggest that at least in some patients they could be due to gene deletions.[26]

1.3 – Secondary hypogammaglobulinemia

Secondary hypogammaglobulinemia is characterized by decreased IgG levels. Differently from primary hypogammaglobulinemia, which develops spontaneously, it is acquired following use of certain drugs, traumatic events or certain pathologic conditions. Possible causes of secondary hypogammaglobulinemia are:

- use of corticosteroids or other immunosuppressive drugs, employed in the treatment of autoimmune disorders such as systemic lupus erythematosus and rheumatoid arthritis, as well as following transplantation;
- extensive burns;
- renal and intestinal conditions leading to an increased excretion or loss of immunoglobulins;
- viral infections, e.g. by Epstein-Barr virus, rubella and cytomegalovirus, which can influence B cell maturation in susceptible individuals;
- lymphoid malignancies such as chronic lymphocytic leukaemia (CLL), which affect the function of B cells.

The main symptom of secondary hypogammaglobulinemia are recurrent infections, principally of the respiratory and gastrointestinal tract; bronchiectasis can also develop if infections are left untreated. Similarly to primary antibody deficiencies, therapy for patients with secondary hypogammaglobulinemia consists in the administration of infusions containing IgG antibodies.

1.4 – Adaptive and innate immunity

This chapter means to provide a broad overview of the two arms of the immune system, i.e. innate immunity and adaptive immunity, as well as of their components. The differentiation pathways and phenotypic and functional characteristics of the B, T and NK cell subsets mentioned here are described in more detail in chapter 1.5.

Innate immunity is based on mechanisms that do not require antigen recognition and that do not "adapt", i.e. are available from birth and do not further develop during the life of an individual. Innate responses are less specific than adaptive ones but more rapidly established. They can be mediated by pattern recognition receptors (PRRs), the complement system and innate immune cell populations. PRRs are cellular sensors able to detect different types of molecular patterns, i.e. biological signals characterising unwanted biological events.

Patterns of microbial, viral or fungal origin (pathogen-associated molecular patterns or PAMPs) consist of components the host identifies as non-self, e.g. viral nucleic acids, bacterial products such as lipopolysaccharide (LPS) or flagellin and fungal products such as glucans. Danger-associated molecular patterns (DAMPs), conversely, are endogenous signals of nuclear or cytosolic origin, released by cells in situations of stress; they include heat-shock proteins, cellular nucleic acids and ATP. PRRs can be cytoplasmic or membrane-bound, and are divided on the basis of their structure and function in different classes, including Toll-like receptors (TLRs), NOD-like receptors (NLRs), RIG-like receptors (RLRs) and C-type lectin receptors (CLRs). The complement system is a group of proteins normally found in serum in an inactive state. Following direct contact with pathogens or antibodies, complement components are activated by proteolytic cleavage. Active complement fragments can directly kill pathogens through the formation of membrane attack complexes (MACs), as well as opsonise them for later recognition by immune cells. Opsonised pathogens can be phagocytosed and killed by macrophages, which alongside dendritic cells (DCs) and innate lymphocytes constitute the cellular branch of innate immunity. Innate lymphocytes include several innate T cell subsets, such as invariant natural killer T (iNKT) cells, mucosal-associated invariant T (MAIT cells) and γδ T cell subsets, as well as natural killer (NK) cells.

Adaptive immunity is characterised by an ability to mount responses against specific pathogens, which is developed and refined throughout the life of an individual. It is formed of a cellular component, i.e. B and T lymphocytes, and a humoral component consisting of antibodies. Both B and T lymphocytes express surface receptors, named B or T cell receptors (BCRs or TCRs), able to bind specific antigenic epitopes. Contact of a B or T cell clone with their cognate antigen is followed by rapid activation and expansion of the reactive clone. T lymphocytes can be categorised as cytotoxic T lymphocytes (CTLs) and helper T lymphocytes (T_H), which have effector and regulatory functions respectively; on the basis of their specific roles, helper T lymphocytes can moreover be further classified as T_H1, T_H2, T_H17, T_{REG} (regulatory T cells) and T_{FH} (follicular helper T cells). B lymphocytes are chiefly responsible for the production of antibodies, which constitute humoral immunity. Additionally, they can act as antigen presenting cells (APCs) involved in the activation of T lymphocytes, and have regulatory functions which they express through the production of cytokines.

The cellular components of both adaptive and innate immunity can fulfil their roles through direct cell to cell contact or through the secretion of mediators including cytotoxic

effectors, chemokines and cytokines. **Table 1.2** in chapter 1.5.2.1 summarises the sources and effects of the most common cytokines of lymphocytic origin.

1.5 – Lymphocyte subsets

Lymphocytes are cell populations generated by the bone marrow which, alongside monocytes, macrophages and DCs, constitute cellular immunity. They can have innate as well as adaptive functions and play roles in the production of antibodies, in the elimination of abnormal or infected host cells and in the regulation of immune responses. This chapter describes the lymphocyte populations considered during the present study.

1.5.1 – B cell subsets

Classically, B lymphocytes have been known as cells specialised in the production of antibodies and antigen presentation to T cells. More recently, they have been recognised to play an important role in the regulation of immune functions, through both cytokine production and direct cell contact with other immune cell populations, such as iNKT cells. B cells are identified by their expression of surface marker CD19.

B lymphocytes develop from B lineage lymphoid progenitors in the bone marrow, where they acquire a functional B cell receptor (BCR). This membrane-bound complex is formed by two heavy (H) and two light (L) chains, linked together by disulphide bonds. Each heavy chain of a BCR is composed of a constant (C), a variable (V), a diverse (D) and a junction (J) region, encoded by genes located on chromosome 14. Light chains, on the other hand, feature a C, a V and a J region only, each encoded by genes located on chromosomes 2 or 22. **Figure 1.1** exemplifies the structure of a BCR. The production of both light and heavy chains requires the action of recombinases, enzymes that catalyse a process of so-called somatic or V(D)J recombination.

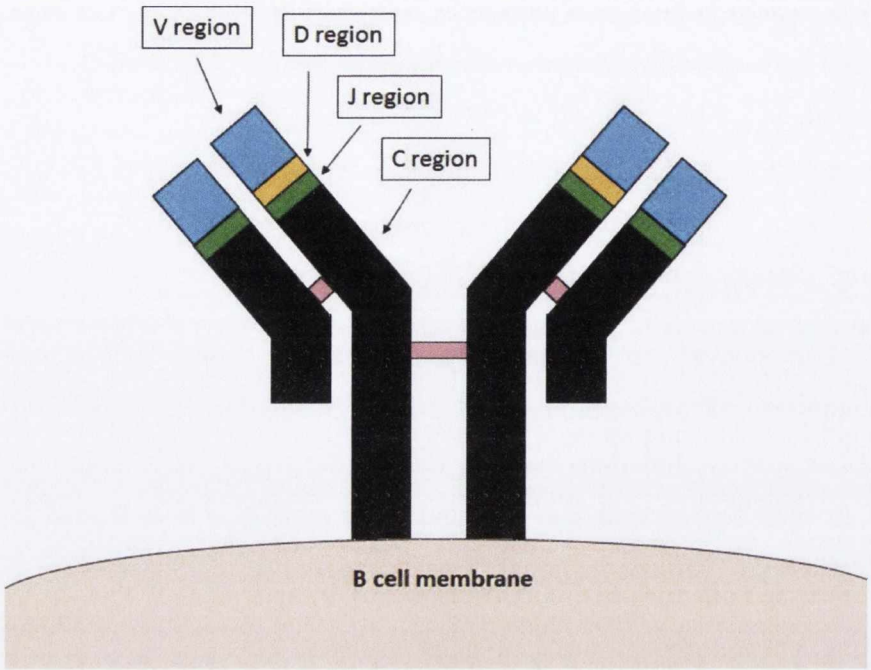


Figure 1.1. Structure of a B cell receptor following V(D)J recombination. The image shows the recombined variable (V, blue), diverse (D, yellow), junction (J, green) and constant (C, black) regions of the BCR. The pink bars represent disulphide bonds linking heavy (long) and light (short) chains together.

Undifferentiated B cells initially contain in their genome gene segments encoding multiple C, V, D and J regions. When heavy chain production is initiated, recombinases progressively select a single J, D and then V gene, assembling in each B cell a unique VDJ region. Through variable VDJ gene segment rearrangement and random insertion or removal of nucleotides at the junctions between them, a huge number of B cell clones with different antigen specificities is generated. Clones expressing functional heavy chain constructs, formed by the selected VDJ region plus a constant Cμ region, are positively selected and undergo clonal expansion. They then see a further round of recombination, this time involving the V and J segments of the light chain genes. Finally, B cells equipped by functional BCRs face negative selection, which eliminates self-reacting clones.

Initially $CD19^+$ and IgM^+, B cells quickly acquire expression of IgD, encoded by constant region Cδ, as they are released in peripheral blood. Although only IgM is secreted and actively participates in humoral responses, both IgM and IgD molecules are expressed on the surface of B cells. Their function at that level seems equivalent, and it is not clear what specific role, if any, IgD may play, although it has been suggested that it could act as a modifier of the signals transduced through surface IgM.[27]

At their most undifferentiated, B cells can be identified in the circulation as transitional B cells, which have been defined in this thesis as having a $CD19^+$ $CD38^+$ $CD24^{high}$

phenotype,[28] and elsewhere in the literature as expressing combinations of these markers and of CD10, IgD and IgM.[29] Importantly, recent studies have defined that the transitional compartment contains the highest frequencies of human regulatory B cells (B_{REGS}), newly discovered IL-10 (interleukin-10) secreting B cells possessing immunomodulatory functions.[30] B_{REGS} have been reliably characterized in mice as $CD19^+$ $CD1d^{high}$ $CD5^+$ cells able to quench T cell-mediated inflammation and contact hypersensitivity reactions, and whose depletion exacerbates inflammation.[31] Unfortunately, no specific markers have so far been identified for them in man, in which their recognition is necessarily based on their functional capabilities, chiefly their ability to generate IL-10.

Depending on their degree of differentiation, transitional B cells can further be distinguished as T1 or T2. T1 cells, i.e. recent bone marrow emigrants, enter the spleen and develop within it into the T2 subset, which eventually generates mature naïve B cells and marginal zone (MZ) B cells.[32,33]

MZ B cells were originally identified in mouse, as an IgM^+ $CD1d^+$ $CD21^{high}$ B cell population expressing low or undetectable levels of IgD.[34] They were given their name due to being a largely stationary subset residing in a well-defined area of the spleen, the marginal zone, where they were observed on the lining of splenic sinusoid in close geographic and functional association with two specific populations of macrophages, marginal metallophilic macrophages (MMMs) and marginal zone macrophages (MZMs).[35] Murine MZ cells carry a non-mutated Ig receptor, and play an important role in responding to pathogenic bacteria and viruses as blood is filtered through the spleen. A search for this population in man has not yielded a perfect match, however a subset of B lymphocytes with characteristics similar to MZ B cells has been observed, which has been termed "MZ-like". Differently from murine MZ B cells, MZ-like B cells are not a fully stationary population, being found both in the MZ of the spleen and in the peripheral circulation; in addition to this, MZ-like B cells express surface IgD^+, being detected by flow cytometry as $CD19^+$ $CD27^+$ IgM^+ IgD^+ events, and possess mutated Ig receptors.[34] Indeed, in the first few years of life of an individual this subset both expands and undergoes a process of somatic mutation that introduces changes in the variable regions of its immunoglobulin genes. MZ-like B cells, however, do not display the restricted clonality seen in class-switched memory B lymphocytes due to successive antigenic challenges.[33] This allows them to mount innate-like responses to antigens from blood-borne pathogens, going through rapid, T cell-independent clonal expansion and then differentiation into plasma cells secreting IgM and IgG antibodies.[36] Individuals with congenital asplenia can form populations of MZ-like B cells, which probably differentiate in alternative sites in secondary lymphoid organs such as the tonsils and the lymph nodes;

MZ-like B cells are however largely lost following removal of the spleen. In both splenectomised and asplenic individuals, circulating MZ-like B cells decrease in number over time, and both groups of patients are more susceptible to infections by encapsulated bacteria including *Streptococcus pneumoniae*, *Haemophilus influenzae* and *Neisseria meningitidis*, underlining the important role of the spleen in anti-bacterial immunity.[33]

Naïve B cells, which are also generated in the spleen, are typically detected in peripheral blood as $CD19^+$ $CD27^-$ IgD^+. Although mature and ready to undergo activation, these B cells are yet to encounter their antigen and do not express memory marker CD27.[37] Further differentiation of naïve cells requires two different stimuli. The first stimulus is contact with soluble cognate antigen, which is specifically recognized and internalized by the BCR, and later presented on their surface through MHC (major histocompatibility complex) class II. The second stimulus consists in physical contact with an armed helper T cell in the T cell area of secondary lymphoid organs, like lymph nodes or the spleen, which is accompanied by recognition of the presented antigen and by the close-range secretion of cytokines by the same helper T cell. This finally induces clonal expansion of B cells to form a primary core of proliferation. The cells so generated can migrate to primary follicles in lymph nodes, where they further differentiate. Alternatively, they can become short-lived plasma cells, responsible for the production of high quantities of IgM typical of primary immune responses, or unswitched memory B cells, characterized in this study as $CD19^+$ $CD27^+$ IgD^+. Notably, a large proportion of unswitched memory B cells also expresses surface IgM. Thus, frequencies of this subset determined by flow cytometry will also include circulating MZ-like B cells.

In primary lymphoid follicles, B cells resume proliferation and form the so called germinal centre (GC). Here, they are selected in successive rounds of proliferation, through processes of somatic hypermutation, which sees mutations interspersed in the V region of immunoglobulin genes, and affinity maturation, which only allows survival of B cells with high affinity for the antigen. Under the stimulus of the cytokine milieu of the GC, B cells also undergo isotype class-switching, undergoing a second recombination event that allows them to transcribe constant region genes Cγ, Cα and Cε. They thus acquire the ability to secrete IgG, IgA and IgE antibodies possessing the same antigen specificity of the original IgM, but higher affinity. In man, in particular, IL-4 has been found to favour the production of IgG and IgE,[38] while IL-5 and TGFβ (tumour growth factor β) induce production of IgA.[39]

Populations of high affinity class-switched memory B cells and plasmablasts are therefore formed. Class-switched memory B cells were defined in this study as $CD19^+$

$CD27^+$ IgD^-, while plasmablasts were identified as $CD19^+$ $CD24^-$ $CD38^{high}$. Both class-switched memory B cells and plasmablasts can produce non-dividing long-lived plasma cells, residing in dedicated niches in the spleen and bone marrow and responsible for maintaining stable levels of protective immunoglobulins in circulation; plasmablasts can additionally give rise to short-lived plasma cells, providing robust shorter term defences.[40] Finally, there exists a little-studied population of $CD19^+$ $CD27^-$ IgD^- (double negative) B cells, which could represent exhausted memory B cells that have lost expression of the CD27 marker.[41]

Figure 1.2 summarises the differentiation process of B cells, from the bone marrow through to the generation of plasma cells. **Table 1.2**, in chapter 1.5.2.1, summarises the main cytokines produced by lymphocytes, including B cells, as well as their functions.

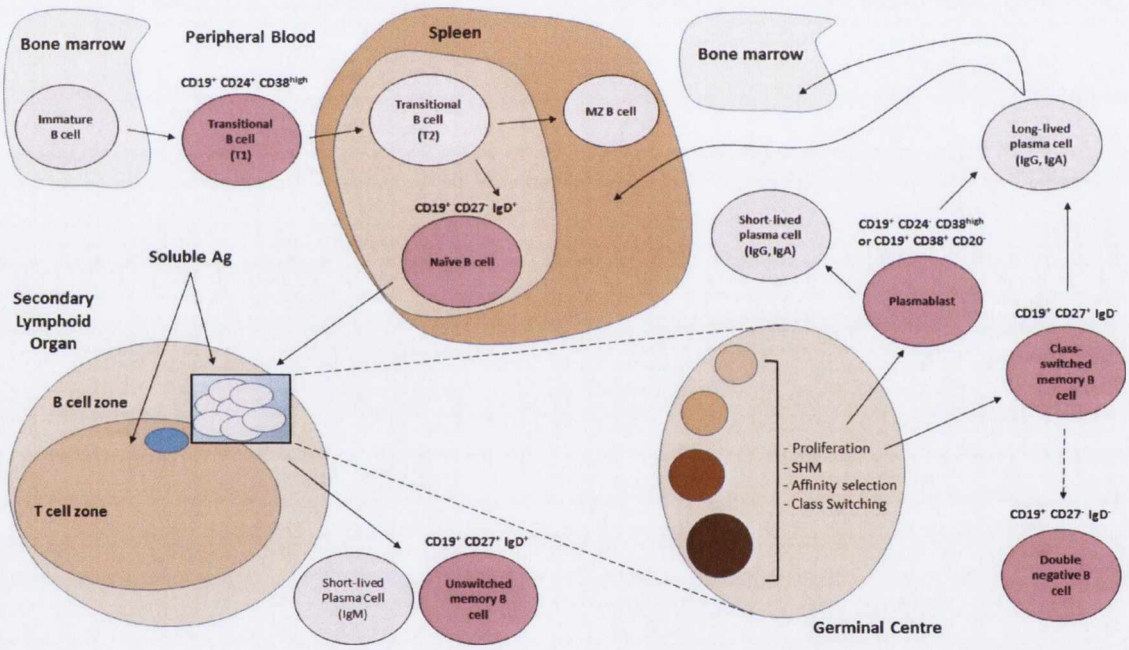


Figure 1.2. B cell differentiation, from bone marrow precursors through to long-lived plasma cells. Immature B cells, generated from B lineage precursors in the bone marrow, are released into peripheral blood and migrate as early transitional B cells (T1) to the spleen, where they mature into naïve B cells. A portion of late transitional B cells (T2) also gives rise to marginal zone (MZ) B cells, a resident spleen population. Naïve B cells gather in the B cell zone of secondary lymphoid organs (shaded blue rectangle), where they come in contact with cognate soluble antigen and with armed T cells with the same antigen specificity (in turquoise). Following activation, they differentiate into IgM-producing short-lived plasma cells or unswitched memory B cells, or else proliferate in GCs, undergoing somatic hypermutation (SHM), affinity selection and class-switching. These processes generate plasmablasts, as well as terminally differentiated populations of class-switched memory B cells and plasma cells. Long-lived plasma cells return to the bone marrow and to the spleen, where they are responsible for the production of up to 80 % of circulating antibodies. $CD27^-$ IgD^- B cells, possibly a population of exhausted memory B cells, may also originate from class-switched memory B cells following their loss of CD27 expression. The B cell populations phenotyped during this study are highlighted in the image in dark pink, with the markers used for their detection indicated above each subset.

1.5.2 – T cell subsets

T cells have been subdivided here into conventional T cells and innate T cells, with the latter group comprising iNKT cells, MAIT cells and Vδ1, Vδ2 and Vδ3 γδ T cells. Although these populations exhibit widely different characteristics, they are recognizable as a whole by their surface expression of the CD3 marker.

1.5.2.1 – Conventional T cells

T lymphocyte development begins in the bone marrow with the production of T-lineage lymphoid progenitors. Once released from the bone marrow these progenitors migrate to the thymus, where they proliferate and initiate a two-stage selection process.

Initially identified as triple negative ($CD3^-$ $CD4^-$ $CD8^-$), thymocytes undergo somatic recombination between genes encoding the T cell receptor (TCR) complex, in a process alike that already described for B cells (chapter 1.5.1.1). Similarly to distinct heavy and light chains recognizable in the BCR, conventional TCRs are formed by an α and a β chain; generation of β chains requires VDJ recombination, while α chains are produced by VJ recombination. Alongside their TCR, thymocytes also acquire expression of CD3, CD4 and CD8, and as such are referred to as double positive ($CD3^+$ $CD4^+$ $CD8^+$). Although CD4 or CD8 expression will later be lost by T cells during differentiation, the CD3 complex appears on the surface of all T cells from this stage onwards, acting as a co-receptor to the TCR. It is formed by heterodimers of an ε and either γ or δ chain, plus a ζ chain homodimer indispensable for the transduction of signals from the TCR to the cell cytoplasm. **Figure 1.3** schematises the structure of a TCR/CD3 co-receptor complex.

Upon acquisition of their receptor and co-receptors, double positive thymocytes migrate to the thymic cortex, where they face a first round of selection. Clones are selected on the basis of their ability to recognize self-antigen presented by the MHC class I or II of thymic epithelial cells (TECs); only clones which bind and have appropriate affinity for the antigen receive a survival signal. The type of MHC complex presenting the antigen also affects thymocyte differentiation: cells which recognize antigens presented by MHC class II will tend to downregulate CD8 and maintain CD4 expression; vice versa, those recognizing antigens presented by MHC class I will tend to downregulate CD4 and maintain CD8 expression. The CD4 and CD8 molecules, which act as co-receptors to CD3 on the surface of T cells, will influence cell function, allowing to broadly classify T cells as either $CD8^+$ cytotoxic T lymphocytes or $CD4^+$ helper T lymphocytes.

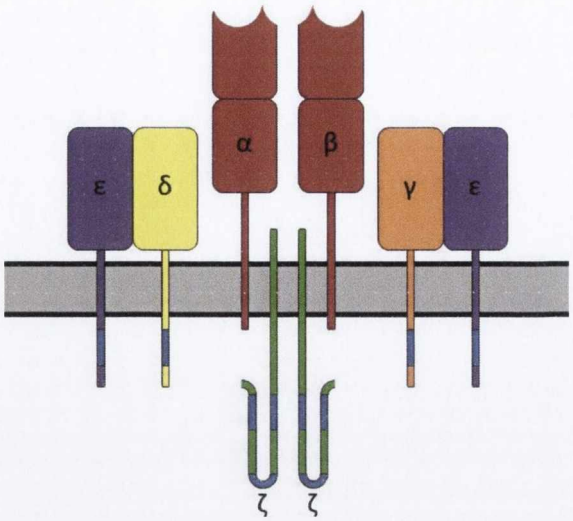


Figure 1.3. Structure of a TCR/CD3 complex. The image shows the α and β chains of the TCR (red), flanked by the CD3 co-receptor. CD3 is composed of heterodimers of ε (purple) and either δ (yellow) or γ (orange) chains, plus homodimeric ζ chains (green/blue) necessary for intracellular signal transduction. Image courtesy of Wikipedia.

Following successful positive selection, thymocytes emerge into the thymic medulla as (mainly) single positive cells, either $CD3^+$ $CD4^+$ $CD8^-$ or $CD3^+$ $CD4^-$ $CD8^+$, ready for a second selection step. In the medulla, cells are presented with self-antigen by either medullary thymic epithelial cells (mTEC), expressing MHC class I, or thymic DCs, expressing MHC class II. Thymocytes that bind the antigen are for the most part negatively selected and induced to initiate apoptosis, with the exception of a small population of $CD4^+$ cells which will later become regulatory T cells.

Cells that survive both positive and negative selection are released from the thymus as naïve mature T cells and migrate towards the periphery. These recent thymic emigrants, as they are also known, may eventually come in contact with their cognate antigen, presented by MHC class I or II molecules. Their activation requires binding of the presented antigen by the CDR3 (complementarity determining region 3) area of their TCR and parallel costimulation through co-receptor CD28. Once activated, T cells are armed and can provide the second stimulus necessary for B cell maturation, as well as exert specific functions, which as previously stated depend on their expression of either CD4 or CD8.

$CD8^+$ cytotoxic lymphocytes act as effector cells, actively screening for and recognizing anomalous cells and killing them through a localized cytotoxic response. They are particularly important in the elimination of tumour cells or cells infected by viruses, which are identified due to the presentation of abnormal or viral antigens through MHC class I molecules. CTLs produce large quantities of perforin and granzyme B, which are stored in

granules in the cytoplasm. When an abnormal cell is detected, CTLs dock to it, open pores in its membrane through a confined release of perforin and finally infuse it with granzyme B, which triggers the caspase cascade and initiates apoptosis.

$CD4^+$ helper T cells, initially described as T_H0, differentiate into one of several subsets and begin to produce diverse panels of cytokines, through which they sustain and modulate the immune response:

- T_H1 cells produce IL-2, IFNγ (interferon γ) and TNFα, and are involved in inflammation and responses to intracellular pathogens;
- T_H2 cells produce IL-4, IL-5 and IL-13, important for B cell differentiation and antibody production, as well as responses to parasites;
- T_H17 cells produce IL-17 and IL-22, which play a key role both in responses to bacterial pathogens and in autoimmunity;
- T_{REG} cells produce IL-10 and/or TGFβ, central in immune suppression;
- T_{FH} cells produce IL-21, favouring affinity maturation and isotype switching of B cells in follicles.

Table 1.2 summarises the principal sources and effects of common cytokines of lymphocytic origin. Although differential cytokine production has long been used to distinguish T_H subsets, they are better defined by their expression of master regulators of transcription. In this regard, T_H1 cells express transcription factor T-Bet (T-box expressed in T cells), T_H2 cells express GATA-3 (GATA binding protein 3), T_H17 cells express RORγτ (retinoic acid-related orphan receptor γτ), T_{REG} cells express FOXP3 (forkhead box P3) and T_{FH} cells express Bcl-6 (B cell lymphoma 6). Interestingly, a stable hybrid phenotype expressing both T-bet and GATA-3, and with the ability to produce both T_H1 and T_H2 cytokines, can also be produced following parasitic infection.[42]

For the purposes of this study, conventional T cells have been defined as $CD3^+$ $CD56^-$, and subdivided in $CD4^+$ $CD8^-$, $CD4^-$ $CD8^+$ and $CD4^-$ $CD8^-$ (double negative) subsets.

1.5.2.2 – Innate T cells

A particular class of T cells, defined "innate T cells", lies at the hinge of adaptive and innate immunity. These lymphocytes express TCRs, which mediate antigen-recognition, however they respond to conserved molecular structures and are able to mount rapid immune responses, similar to innate cells. Five subsets, known as Vδ1, Vδ2 and Vδ3 γδ T cells, iNKT cells and MAIT cells, possess TCRs that are either totally invariant, i.e. composed of fixed combinations of αβ or γδ chains, or that display a low degree of variation. Other innate T

cells, expressing variable TCRs, can be grouped according to their restriction to MHC-like molecules such as CD1a, CD1b and CD1c.

γδ T cells, iNKT cells and MAIT cells constitute a first line of defence in immunity and are involved in the recognition and removal of microbial antigens and tumour cells. They moreover possess regulatory and immunomodulating functions, producing cytokines which can shape the host's broader immune response (**Table 1.2**). Furthermore, both Vδ2 γδ T cells and iNKT cells have recently been recognized to sustain B cell differentiation and maturation, promoting the production of antibodies.

1.5.2.2.1 – γδ T cells

Similar to conventional T cells, γδ T cells develop in the thymus and express CD3, CD4 and CD8, however their TCR is composed of a γ and a δ chain, which are selected during V(D)J recombination in place of an α and a β chain.[43] While conventional T cells display huge TCR diversity, selective pressures applied on the γδ population during thymic somatic recombination translate into the biased production of cell subsets displaying typical associations of Vγ and Vδ chains. Research in mouse suggest that following selection in the thymus, these subsets migrate to definite tissues and organs at specific times during foetal development and persist there, forming oligoclonal populations (**Figure 1.4**).[44]

Importantly, the Vδ2 γδ T cell subset, which is the most prominent in man, does not have a mouse equivalent. This raises doubts on the suitability of mice models for γδ T cell studies. Three major populations of γδ T cells have been identified in human tissues. They are named on the basis of their δ chain type as Vδ1, Vδ2 and Vδ3. The Vδ2 subset, which constitutes up to 5 % of circulating T lymphocytes and up to 80 % of circulating γδ T cells, is by far the best studied and appears reliably as a Vγ9-Vδ2 population. The other two γδ T cell subsets are found at low frequencies in blood, but make up a large proportion of the intraepithelial lymphocytes found in the skin, intestine and respiratory and reproductive tract.[45] **Table 1.3** summarizes the known human γδ T cell subsets and the tissues they predominantly home to; all information is from Bonneville et al.[46]

γδ T cell activation is controlled by the TCR and other co-receptors. As shown in **Figure 1.5**, these include both PRRs, such as toll-like receptors and dectin-1, and natural killer receptors (NKRs), such as NKG2D (Natural Killer group 2, member D).

Table 1.2 – Common lymphocyte-derived cytokines

Cytokine	Source	Activities
IL-2	All T cells NK cells B cells	Induction of clonal T cell proliferation and NK cell activation. Promotion of the proliferation of activated B cells in the presence of IL-4.
IL-4	T_H2 cells iNKT cells γδ T cell subsets B cells	Induction of T_H2 cell development and proliferation. Suppression of T_H1 cell development. Promotion of B cell proliferation, MHC class II expression and isotype-switching to IgG1, gG4 and IgE. Enhancement of mast cell function.
IL-5	T_H2 cells iNKT cells Vδ1 γδ T cells Vδ2 γδ T cells	Promotion of B cell proliferation and isotype-switching to IgA. Promotion of eosinophil proliferation and activation.
IL-10	T_{REG} cells B_{REG} cells iNKT cells Vδ1 γδ T cells Vδ2 γδ T cells	Inhibition of pro-inflammatory cytokine synthesis. Promotion of IgG1 and IgG3 isotype-switching in B cells. Suppression of functions of macrophages and DCs, including IL-12 production. Inhibition of antigen presentation. Suppression of cell-mediated immunity.
IL-13	T_H2 cells iNKT cells NK cells	Inhibition of pro-inflammatory cytokine synthesis. Promotion of B cell isotype-switching to IgE. Induction of collagen production by fibroblasts and mucus production by epithelia.
IL-17	T_H17 cells iNKT cells Vδ1 γδ T cells Vδ3 γδ T cells MAIT cells	Recruitment of monocytes and neutrophils to sites of inflammation, through stimulation of chemokine production. Induction of synthesis of microbial peptides and pro-inflammatory cytokines, including TNFα. Promotion of anti-bacterial responses. Induction of autoimmunity. Potentiation of IL-22-induced effects.
IL-21	T_H1 cells T_{FH} cells iNKT cells	Induction of proliferation of bone marrow NK cells, as well as activated T and B cells. Regulation of CTL and NK cell activity in tumour clearance. Promotion of affinity maturation and isotype-switching of B cells in primary follicles. Promotion of follicular activities of γδ T cells.
IL-22	T_H17 cells MAIT cells NK cells	Promotion of tissue repair. Promotion of anti-bacterial responses at mucosal surfaces. Induction of autoimmunity. Potentiation of IL-17-induced effects.
IFNγ	T_H1 cells INKT cells γδ T cell subsets MAIT cells NK cells B cells	Promotion of T_H1 cell differentiation. Promotion of MHC class I and II presentation. Activation of granulocytes, CTLs and NK cells. Promotion of cell-mediated immunity. Induction of macrophage activation and microbicidal function. Promotion of IgG3 isotype-switching by B cells.
TNFα	T_H1 cells iNKT cells γδ T cell subsets MAIT cells NK cells B cells	Promotion of acute phase protein production by hepatocytes. Promotion of vascular endothelial permeability and enhancement of vascular adhesion molecule expression. Promotion of neutrophil activation. Induction of fever.

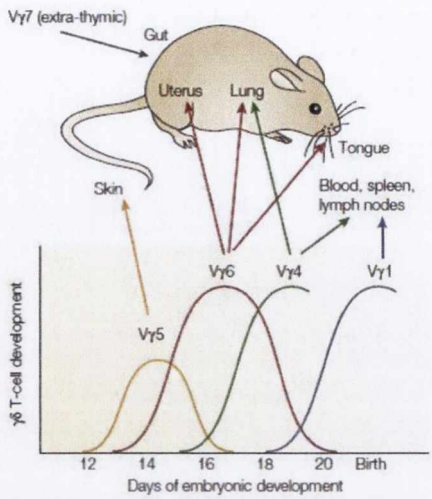


Figure 1.4. Embryonic development and migration of murine γδ T cell subsets. Different subsets of γδ T cells migrate to specific peripheral tissues at different stages during embryonic development. Image from Carding and Egan.[44]

Table 1.3. Distribution of γδ T cell subsets in human tissues

Subset	Location
Vγ9Vδ2	Peripheral blood
Vδ1	Thymus
	Spleen
	Dermis
	Liver
	Intestinal epithelia
Vδ3	Liver
	Intestinal epithelia

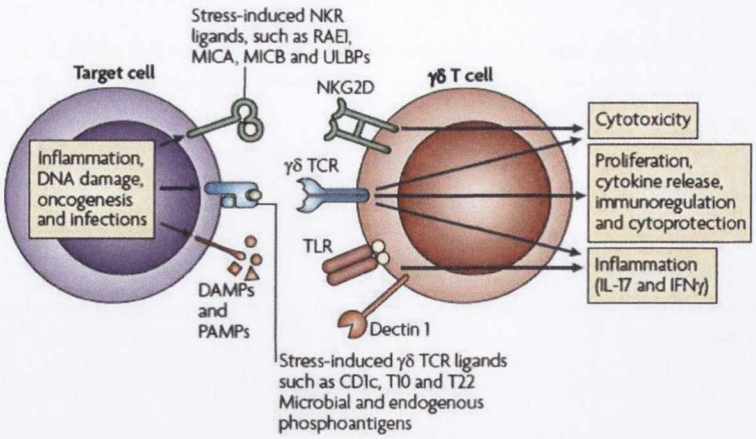


Figure 1.5. Activation signals recognized by γδ T cells. γδ T cells can recognize stimuli produced by damaged, transformed or infected cells through three different types of receptors, i.e. the γδ TCR, natural killer receptors (NKRs) such as NKG2D and pattern recognition receptors like toll-like receptors (TLR) and dectin-1, binding PAMPs and DAMPs (pathogen- or danger-associated molecular patterns). The response of the γδ T cell will be different depending on the kind(s) of receptor involved in its stimulation. Image from Bonneville *et al.*[46]

γδ T cells are not MHC-restricted and recognize protein and non-protein antigens produced by stressed, virally infected or transformed host cells and by pathogens. The Vδ2 subset responds to phosphoantigens,[47] in the form of (E)-4-hydroxy-3-methyl-2-butenyl pyrophosphate (HMB-PP) and isopentenyl pyrophosphate (IPP). Recent research indicates that detection of these molecules by Vδ2 cells requires their presentation by butyrophilin BTN3A1.[48] Direct involvement of the TCR is also assumed, as transfection with cDNA (complementary deoxyribonucleic acid) constructs coding for the Vγ9 and Vδ2 TCR chains enables antigen recognition by TCR$^-$ Jurkat cells in a dose-dependent manner.[49] HMB-PP is of prokaryotic origin and is produced as an intermediate of the non-mevalonate pathway of IPP biosynthesis found in many pathogenic bacteria; IPP is also generated by eukaryotic cells, and in particularly high quantities upon transformation. Interestingly, Vδ2 cells are about 10^4 times less sensitive to mammalian phosphoantigens than to microbial ones, permitting swift activation in the presence of microbial infection and response towards the host tissues only at high concentrations of self-antigens.[47] This γδ T cell subset is also depleted in the blood of patients co-infected with HIV (human immunodeficiency virus) and *M. tuberculosis*[50] and responds in culture to macrophages infected with influenza antigens.[51] These findings, alongside the demonstrated cytotoxic and cytokine-secreting abilities of Vδ2 cells,[51-53] implicate this population in immunoregulation[54] and surveillance against bacteria, tumours and virally infected cells.[55-57] Vδ2 γδ T cells can moreover affect the functions of other innate immune populations. In the presence of HMB-

PP, they can for example interact with monocytes, inducing the secretion of pro-inflammatory mediators including cytokines TNFα and IFNγ and the differentiation of monocytes into IL-12-generating DCs *in vitro*.[58,59] The same mechanism is observed in wild type mice following intranasal administration of antituberculotic BCG (Bacillus Calmette-Guérin) vaccine, ultimately resulting in the priming of DCs to IL-12 production and, consequently, in the induction of a T_{H1}-type immune response.[60] As DCs are key for antigen presentation to $CD8^+$ T cells in mycobacterial infections, insufficient conditioning of DCs in TCR-$\delta^{-/-}$ mice, which lack γδ T cells, translates in suboptimal production of IFNγ by cytotoxic lymphocytes in the lungs of these animals upon BCG vaccination and impaired protection from subsequent challenges with *M. tuberculosis*.[60] Secretion of GM-CSF (granulocyte macrophage colony-stimulating factor), IFNγ and TNFα by human Vδ2 cells can also induce differentiation of neutrophils into APC-like cells, thus mediating the presentation of previously phagocytosed and processed bacterial antigens to both $CD4^+$ and $CD8^+$ αβ T cells.[61] Neutrophils can reciprocally activate and induce the proliferation of Vδ2 cells in the presence of monocytes and of a cytokine milieu including TNFα, facilitating their access to HMB-PP by means of pathogen digestion.[62]

Finally, a subset of Vδ2 γδ T cells expressing follicle-homing chemokine receptor CXCR5 (C-X-C motif receptor 5) has been found to provide help to autologous B cells, secreting IL-2, IL-4 and IL-10 and aiding IgM, IgG and IgA production in the presence of IPP.[63] These Vδ2 γδ T cells express surface markers ICOS and CD40L (CD40 ligand), involved in the mediation of B cell/T cell interactions, as well as T_{FH}-lineage transcriptional regulator Bcl-6.[64] Polarisation of Vδ2 cells towards a follicular helper phenotype can be induced in culture in the presence of phosphoantigens and IL-21, a mediator produced *in vivo* by conventional T_{FH} cells and known to influence the behaviour of GC B cells in a paracrine way.[64] It has therefore been hypothesized that the development of a follicular Vδ2 γδ T cell phenotype may be favoured in lymphoid tissues by the availability of T_{FH}-produced IL-21. Interestingly, Vδ2 γδ T cells are disseminated in secondary lymphoid organs[65] and have previously been identified in clusters within GCs.[66] Previous studies in SCID mice, which are devoid of T and B cells, have moreover shown formation of GCs following adoptive reconstitution of B cell and γδ T cell pools.[67]

Subsets of Vδ1 γδ T cells recognize antigens presented by CD1c and CD1d.[68,69] Upon activation through CD1d, they secrete T_H1-type cytokines and can exert cytotoxic functions, lysing target cells through perforin- and FAS-mediated mechanisms; they moreover produce granulysin, a protein with potent anti-microbial properties. As in the case of Vδ2 γδ T cells, their responses are dependent on the presence of a functional TCR, as proved through

transfection experiments. Vδ1 γδ T cells are also known to bind MHC class I polypeptide-related antigen A and B (MIC-A and MIC-B), which are broadly produced by stressed intestinal cells.[70] Although the functions of this γδ T cell subset are not well known, they have been implicated in anti-bacterial, anti-tumour and anti-viral responses.[71-73] It has also been shown that TCR stimulation in the presence of TGFβ and IL-2 can induce a regulatory phenotype in this cell subset, including the expression of T_{REG} marker FoxP3. These regulatory γδ T cells (γδ T_{REG}) can reduce the proliferation of $CD4^+$ T cells and are decreased in the circulation of systemic lupus erythematosus (SLE) patients.[74]

Vδ3 cells are the least studied amongst the three γδ T cell subsets, and little information is available on them. They are nonetheless known to include CD1d-restricted cells that produce T_H1, T_H2 and T_H17 cytokines upon stimulation and that can exert cytotoxic action against CD1d-positive target cells.[75] Reports also exist about their expansion and possible involvement in different pathologic conditions, such as cytomegalovirus infection,[76] chronic lymphocytic leukaemia[77] and possibly HIV infection.[78]

1.5.2.2.2 – iNKT cells

Natural killer T (NKT) cells are a subset of innate immune cells initially defined by their expression of surface markers typical of both T and NK cells, including CD3, CD16, CD56 and CD161, and by the constitutive production of cytotoxic molecules such as perforin and granzymes. Within this broader population, further research has allowed to identify a subset of so-called invariant NKT (iNKT) cells, characterized by an invariant Vα24-Jα18 Vβ11 TCR and positive or negative for CD161 expression.[79]

Like conventional T cells, iNKT cells develop in the thymus, where they acquire their invariant TCR following somatic V(D)J recombination. Distinctly from other T cells, though, double positive ($CD3^+$ $CD4^+$ $CD8^+$) thymocytes, rather than thymic epithelial cells, are responsible for the presentation of lipid self-antigens to the TCR of early iNKT cells in the thymic cortex.[80] Although the exact nature of the self-antigens involved in this process is not known, their presentation must take place through MHC class I-like, limitedly polymorphic molecule CD1d. Further differentiation of iNKT cells is strictly dependent on the expression of transcription factor promyelocytic leukaemia zinc finger (PLZF), which is responsible for their effector properties and their innate-like phenotype.[81,82] PLZF also influences the localization of these cells once they are released in the circulation, directing them to the liver and the spleen; in its absence, this subset preferentially homes to the lymph

nodes. A second transcription factor, T-bet, controls the maturation of iNKT cells in the periphery, after they exit the thymus at an early stage of differentiation.[83]

Mature iNKT cells respond to lipid or glycolipid antigens and are CD1d-restricted.[84] Similar to the self-antigens involved in their differentiation, the natural antigens they recognize in the periphery are not well known, however there are reports they can be activated by lipids contained in the walls of gram negative bacteria from the *Sphingomonas* and *Ehrlichia* species, protozoa such as *Leishmania donovani* and mycobacteria. This could hint at the original function of iNKT cells, as these microorganisms do not produce LPS and would therefore be less recognizable than other microbial pathogens through Toll-like receptor 4 (TLR4).[85]

In the absence of a recognised, potent natural ligand for iNKT cells, studies on this population have relied on α-galactosylceramide (α-GalCer), a synthetic analogue of α-galactosylceramide agelasphin-9b, a lipid naturally produced in a marine sponge. Early studies with α-GalCer carried much promise, as iNKT cells stimulated with this compound displayed potent anti-tumour and anti-metastatic effects in mouse.[86,87] Unfortunately, subsequent studies in man have failed to replicate this anti-neoplastic action. Current research is focusing on structurally modified variants of α-GalCer, in hopes they will yield a breakthrough in this sense.

α-GalCer itself has nonetheless been invaluable for the study of iNKT cell responses to *in vitro* stimulation, as treatment with the compound promotes their cytotoxic and effector functions. Indeed, their expression of cytotoxic mediators, although constitutive, increases by several folds following treatment with α-GalCer, together with that of FAS ligand (FASL), TNFα and TNF-related apoptosis inducing ligand (TRAIL).[88] The recognition of target cells can be direct, as in the case of CD1d-expressing tumour cells, or mediated by APCs. [88,89]

iNKT cells can in some occasions exert direct cytotoxicity. They for example secrete IFNγ and releases cytolytic mediator granulysin in the presence of $CD1d^{+}$ monocytes, macrophages or monocyte-derived DCs pulsed with α-GalCer and infected by *Mycobacterium tuberculosis*, displaying anti-mycobacterial activities.[90] This innate T cell subset can also directly or indirectly affect the functions of several other immune cell types, including monocytes, DCs, NK cells, T cells and B cells. *In vitro*, iNKT cells can for example induce the maturation of monocytes into DCs with suppressive properties. The maturation process requires expression of CD1d by monocytes and secretion of GM-CSF and IL-13 by iNKT cells, but does not necessitate α-GalCer. The tolerogenic DCs obtained express high surface levels of inhibitory ligand PD-L2 (programmed cell death-ligand 2),

produce IL-10 and inhibit T cell proliferation and activation *in vivo*.[91,92] Administration of α-GalCer to mouse models has allowed to study the effects of CD1d-dependent iNKT cell activation on NK cells and resting DCs. Activation of hepatic and splenic NK cells, manifesting as upregulation of CD69 surface expression, IFNγ secretion, enhanced proliferation and cytotoxicity, has been demonstrated following early generation of IFNγ by stimulated iNKT cells.[93,94] Splenic DCs, on the other hand, respond to the administration of α-GalCer and ovalbumin by processing and presenting both molecules, secreting IFNγ and TNFα and upregulating the expression of costimulatory surface molecules CD80, CD86 and CD40. iNKT cell-conditioned DCs display higher efficiency in the presentation of antigen to naive $CD4^+$ and $CD8^+$ T cells, thus enhancing T cell-mediated immunity.[95,96] iNKT cells play an additional role in the polarisation of T cell responses, due to their ability to secrete a wide range of cytokines.[97] $CD4^+$, $CD8^+$ and double negative (DN, $CD4^-$ $CD8^-$) iNKT cells have all been found to produce T_H1-type (IFNγ and TNFα) and T_H2-type (IL-4, IL-5, IL-13) cytokines, often simultaneously; the $CD4^+$ subset can also produce IL-10, while the DN subset can generate IL-17.[98] T_H1 cytokines promote pro-inflammatory and cytotoxic cellular responses, while T_H2 cytokines and IL-10 mediate humoral responses and immunosuppression.

Finally, iNKT cells possess direct and indirect B cell helper functions. They can respond to cognate antigen presented by B cells through CD1d, normally in the spleen, or to noncognate self-antigen presented by DCs (**Figure 1.6**).[99] In the first case, iNKT cells themselves take on a follicular helper-like role and phenotype (termed $iNKT_{FH}$)[100] aiding B cell proliferation and maturation and the production of IgM and IgG antibodies.[101] This kind of mechanism could be particularly important for B cells involved in the production of anti-lipid antigen antibodies, which are for example found in the serum of individuals affected by malaria, autoimmune diabetes and systemic lupus erythematosus. When presentation is performed by DCs, on the other hand, the help given to B cells is more indirect, depending on cytokine production by both iNKT and DCs, as well as antigen presentation by the latter, which results in the activation of conventional $CD4^+$ T_{FH} cells; it is these T_{FH} cells that are then ultimately responsible for stimulating B cell responses.[102] Due to their mechanisms of action, cognate help is also described as "innate", while noncognate help is often termed "adaptive". Although both pathways see the formation of plasmablasts and GCs and production of class-switched antibodies, cognate help stimulates only limited affinity maturation of B cells and does not result in the production of memory B cells; noncognate help, on the contrary, results in full affinity maturation and in the generation of both long-lived plasma cells and memory B cells.[99] Importantly, induction of

noncognate help also takes place when α-GalCer is presented by DCs to iNKT cells, opening the way for a possible use of this compound alongside polysaccharidic antigens in vaccines.[103] iNKT cells participating in noncognate help do not need to display a follicular helper phenotype.

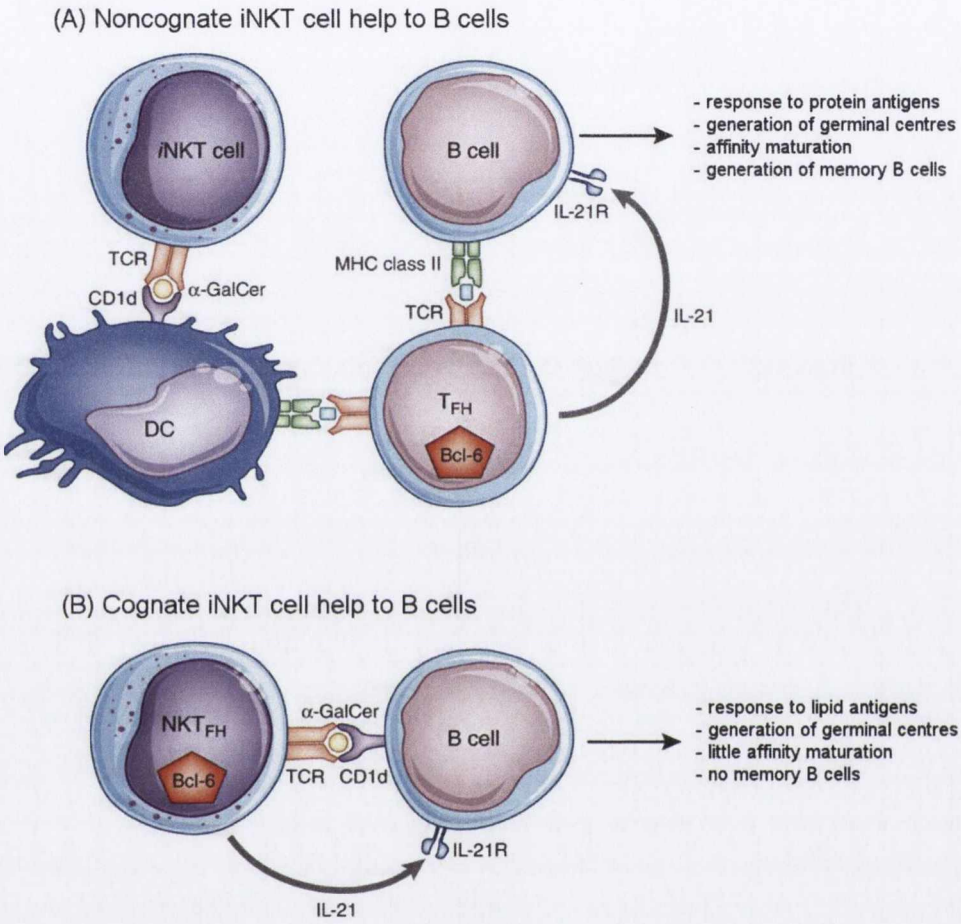


Figure 1.6. iNKT cells can provide cognate and noncognate help to B cells. iNKT cells provide noncognate help (A) by responding to and reciprocally stimulating $CD1d^+$ dendritic cells (DC) presenting lipid antigens, which in turn activate $CD4^+$ follicular helper T cells (T_{FH}). Antibody responses are ultimately induced by T_{FH} cells, through recognition of cognate antigen presented by B cells and paracrine secretion of IL-21. Cognate help (B) requires the direct presentation of lipid antigen by B cells to follicular helper iNKT cells (NKT_{FH}) through CD1d. NKT_{FH} cells respond to the stimulation by paracrinely secreting IL-21 and stimulating antibody production. Both kinds of B cell help result in the generation of GCs, but only noncognate stimuli induce affinity maturation and the differentiation of B cells into memory B cells. Noncognate help supports production of antibodies against protein antigens, while cognate help is thought to be involved in the production of antibodies against lipid antigens. Image modified from Lehuen and Fazilleau.[104]

1.5.2.2.3 – MAIT cells

Mucosal-associated invariant T (MAIT) cells were first identified some 15 years ago. They are innate T lymphocytes characterized in man by the expression of a Vα7.2-Jα33 TCR chain paired with a limited range of Vβ chains, mainly Vβ13 and Vβ2.[105] Similar to other innate T cells, they have a "poised effector" phenotype in the periphery. They home chiefly to the liver, where they represent up to 50 % of the resident T lymphocyte population, and to the *lamina propria* of the intestine, where they constitute 5 to 10 % of total T cells. They also feature in the lung and in peripheral blood at frequencies similar to those seen in the gut, but are essentially absent from lymph nodes.[106] As a whole, this population is abundant in man but relatively rare in other animal species, such as mouse and cattle.

MAIT cells are activated by intermediates produced in the *de novo* riboflavin/vitamin B2 pathway found in many but not all species of bacteria and yeasts, including *Escherichia coli*, *Staphylococcus aureus* and *Candida albicans*.[107] Antigen presentation to MAIT cells is mediated by MHC-like molecule MR-1 (MHC-related molecule 1), to which the population is restricted. The ubiquitous expression of MR-1 in tissues, as well as the strongly conserved sequence of both MR-1 and the population's TCR, are suggestive of the important role played by MAIT cells.

1.5.2.2.3.1 – MAIT cell development

MAIT cells are assumed to enter the thymus as $CD3^-$ $CD4^-$ $CD8^-$ precursors and acquire CD3 expression and a functional TCR in the cortex of the organ, following a somatic recombination process biased towards pairings of the Vα7.2 chain with Vβ2, Vβ13 and Vβ22 chains. They then migrate to the thymic medulla.

Mouse reaggregated thymic organ cultures (RTOCs) and bone marrow chimeras have both been employed to study the thymic stages of MAIT cell differentiation. RTOCs are tridimensional culture systems in which thymic stromal cells, obtained from disaggregated foetal thymus lobes, are supplemented with thymocytes at the desired differentiation stage. Bone marrow chimeras are generated by transplanting donor bone marrow in recipient mice following irradiation. Work in these systems has revealed that the thymic selection of MAIT cells requires the presence of a population of double positive thymocytes expressing MR-1, while it is independent of triple negative and single positive thymocytes, thymic B cells, DCs, macrophages or epithelial cells.[108] In this respect, MAIT cell development follows mechanisms similar to those already described for iNKT cells. Although MR-1 is normally undetectable on the surface of primary cells, the loading of double positive thymocytes with

bacterial ligand translates in a slight but reproducible upregulation of the protein on their surface. This most likely results from a recall of preformed MR-1 from storage sites within cells to their surface, where the molecule is thought to form a stable complex with a currently unknown endogenous ligand.[108] MAIT cells develop normally in mice doubly deficient for the transporter associated with antigen processing (TAP) and for MHC-groove-blocking invariant chain Ii, which are instead indispensable for the thymic selection of conventional T cells.[109]

MAIT cells exit the thymus as naïve cells,[110] acquiring CD161 expression within it or immediately upon migration. They then reach secondary lymphoid organs, including the spleen and mesenteric lymph nodes; it is only later, at a more advanced maturation stage, that they home to other peripheral sites such as the liver and the lungs, and lastly the small intestine. Throughout this process, gradually, they acquire expression of transcription factor PLZF and of IL-18Rα, while their CD8α co-receptor tends to transform from CD8αβ to CD8αα.[111] Notably, human foetal MAIT cells resident in non-lymphoid peripheral sites already possess the ability to respond to bacterial antigen and produce IFNγ, IL-17A and IL-22.[111] Data from germ-free mice indicate that MAIT cells do not expand in the absence of a commensal microbiome, but can be rescued by feeding a monospecific microbial diet.[109,112] Accordingly, analysis of human cord blood evidenced a small population of $CD161^{+}$ IL-$18R\alpha^{+}$ naive MAIT cells, which rapidly swells after birth following colonization of human tissues by microorganisms, until stable adult-like frequencies are reached around 2 years of age.[106]

Experiments in chimeric mice lacking T and B cells or T cells only have shown that B cells are also required for the expansion of murine MAIT cells.[109] Interestingly, the presence of even a small number of B lymphocytes, in the form of an IgA-producing population located in the intestine of an otherwise B cell-deficient mouse model, proved sufficient in this setting to support MAIT cell expansion. Data from four XLA patients, who due to a mutation in the Bruton tyrosine kinase (BTK) gene are either devoid or display very low frequencies of B cells, seem to support the observations in mice. Transcripts for the invariant TCR of MAIT cells have been reported in these individuals at very low to normal frequencies; it has been proposed that, similar to the mouse model previously mentioned, this could be due to the presence of a residual B cell population, undetectable in peripheral blood but located at gut level.[109] Taken together, these data suggest that the quality of the interactions between MAIT cell and B cells is more important than the quantity of B cells available for the interaction itself. The role of B cells in this setting could also be varied: they could for example be involved in direct interactions with MAIT cells, perhaps

presenting microbial antigens to them in their role as APCs, or foster indirect interactions depending on other cell types such as DCs or epithelial cells. In the second scenario, DCs could internalize microbial antigens and activate B cells, which would then supply a stimulatory or co-stimulatory signal driving the expansion and maturation of MAIT cells.[110]

Like iNKT cells, MAIT cells express transcription factor PLZF, which has lately been linked in both cell types to a particular propensity to apoptosis through activation of the caspase cascade.[113] However, while iNKT cells require PLZF since the first stages of thymic development, MAIT cells only express it once in the periphery.[111] Similarly, MAIT cell development does not depend on the SAP (SLAM-associated protein)/Fyn/NF-κB (nuclear factor κB) pathway iNKT cells rely on, as MAIT cell numbers remain normal in SAP-deficient patients, who instead present with undetectable levels of iNKT cells.[110] Notwithstanding the similarities between the two cell types, these observations highlight the important differences in the mechanisms underlying the development and differentiation of iNKT cells and MAIT cells.

1.5.2.2.3.2 – MR-1

MR-1 is an MHC-1b-like molecule, encoded on human chromosome 1 by the same genetic locus as CD1d. It is ubiquitously expressed in human cells and evolutionarily conserved in mammals including sheep, rat, mouse, opossum, cattle and man, to the point that its human and murine forms share 90 % sequence identity.[114] Its structure and fold are similar to that of the conventional MHC class I complex, featuring three extracellular domains and a small antigen-binding cleft, surrounded by two α-helical regions and resting on a platform of β-sheets (**Figure 1.7**).[107] Its function is strictly dependent on the availability of a β2-microglobulin (β2m) chain, to which it is non-covalently attached.[109] MR-1 can be detected intracellularly in $\beta2m^-$ cells, but not on their surface, confirming that the β2m chain plays a stabilizing role.[115]

The expansion of MAIT cells in transgenic mouse models is dependent on MR-1 but independent of TAP, which together with tapasin, calreticulin and ERp57 forms the peptide loading complex (PLC) required for the functioning of classical MHC class I.[109] Nonetheless, MR-1 appears to rely on a folding process similar to MHC class I and has been immunoprecipitated with antibodies specific for all members of the PLC.[115]

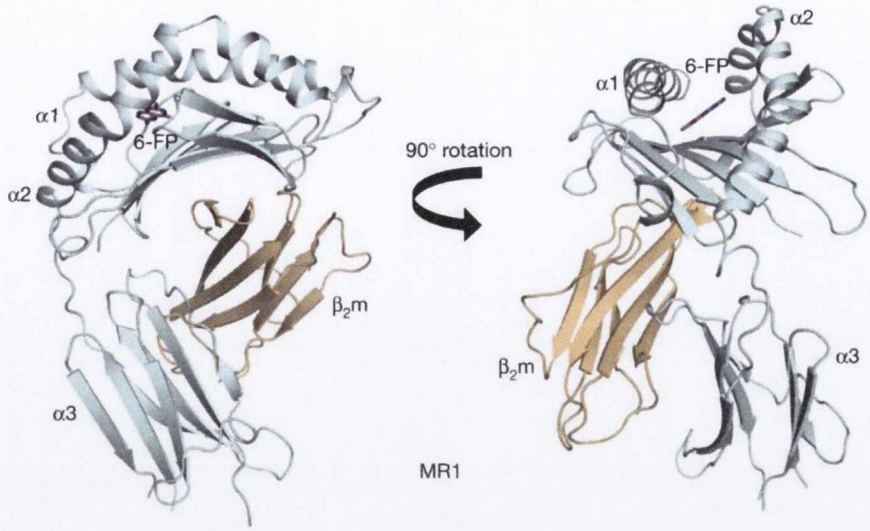


Figure 1.7. Structure of MR-1. The image shows the α-helix domains α1 and α2, β-sheet domain α3 and ligand 6-formyl pterin (6-FP) nested in the antigen cleft. In its functional form, MR-1 associates with an accessory β2-microglobulin (β2m) chain. Image from Kjer-Nielsen *et al.*[107]

At resting state, MR-1 is found mainly within the cytoplasm of cells, in the endoplasmic reticulum, in an unassembled state. It is only when required that it appears to release chaperone molecules, undergo loading with antigen and shuttle to the cell surface.[115] This translocation process most likely depends on endocytosis, as activation of MAIT cells in the presence of microbial agents is blocked when endocytosis or intracellular trafficking are inhibited in APCs.[112]

1.5.2.2.3.3 – MAIT cell detection and phenotype

There exists a consensus that detection of MAIT cells requires a combination of an anti-invariant TCR antibody and CD161, and that they appear as a distinct Vα7.2^{+} CD161^{high} population. Vα7.2^{+} populations expressing lower levels of CD161, i.e. either CD161^{int} or CD161^{-}, have been less studied, but seem to comprise cells with phenotypic and functional features different from those of MAIT cells. The vast majority of CD161^{low} cells are also not defined by the Vα7.2 invariant TCR chain, instead displaying a variety of TCRs.[116,117]

Peripheral blood MAIT cells have additionally been phenotyped as CD45RA^{-} CD45RO^{+}, indicating a memory phenotype, and also as CD27^{+}, CD62L^{low}, CD122^{int}, CD127^{high} and CD95^{high}, which identifies them as memory effector cells. Phenotypic analysis of their chemokine receptor expression found them to be CCR7 (C-C motif receptor 7) negative CCR5^{high} CCR6^{high} CXCR6^{high} CCR9^{int}, confirming they are able to home to the liver and the intestine, but not to the lymph nodes.[106,110] It has moreover been suggested

that MAIT cells share a transcriptional signature which includes chemokine receptors CCR2, CCR6, CXCR6 and CCR9, transcription factors PLZF and RORγτ and cytokine receptors IL-12R, IL-23R and IL-18Rα.[116] Interestingly, this transcriptional signature appears to overlap that of a wider population of $CD161^{high}$ $CD8^+$ cells, which like MAIT cells express RORγτ and secrete IL-17 and IL-22; $CD8^+$ MAIT cells constitute 80 to 90 % of this broader immune subset.[117]

$CD8^+$ and $CD4^-$ $CD8^-$ cells account for the majority of MAIT cells. $CD8^+$ MAIT cells overwhelmingly express CD8αα homodimers instead of the more usual CD8αβ associations found in MHC-restricted immune cells.[118,119] $CD4^+$ MAIT cells can be detected by flow cytometry alongside the $CD8^+$ and double negative subsets in human and murine adult and cord blood,[109,116] however this subset fails to display upregulation of activation marker CD69 when incubated with APCs loaded with bacteria that produce MAIT cell antigens.[112] As a consequence of this, $CD4^+$ MAIT cells are considered non-functional and generally not reported on. This may change in light of recent research employing modified MR-1 tetramers loaded with riboflavin-derived antigen rRL-6-CH_2OH (reduced 6-hydroxymethyl-8-d-ribityllumazine), which allow the detection of MAIT cells on the basis of their functional abilities rather than their phenotype.[118] Interestingly, these compounds identify $CD4^+$ MAIT cells both in man and in mouse. The TCRs of tetramer-isolated MAIT cells may also feature a wider variety of β chains than previously expected.

1.5.2.2.3.4 – MAIT cell functions

The functions of MAIT cells are currently the subject of intense study, with evidence quickly accumulating that they are involved in responses against bacteria, yeasts and mycobacteria.

Following *in vitro* stimulation, MAIT cells upregulate their production of cytotoxic mediators granulysin and perforin, which are stored in basophilic granules in their cytoplasm.[120] They additionally secrete granzyme A and B and a variety of cytokines: TNFα is abundantly produced upon treatment with anti-CD3 and anti-CD28 antibodies, while the more robust stimulus of PMA (phorbol 12-myristate 13-acetate) and ionomycin is necessary to obtain strong secretion of IL-2, IFN-γ and IL-17.[106] T_H2 cytokines (IL-4, IL-5, IL-13), IL-10 and TGF-β, do not seem to be routinely secreted by MAIT cells, although secretion of IL-4 has been reported in elderly individuals.[121]

MAIT cells have been documented to degranulate and exert direct cytotoxicity against $MR\text{-}1^+$ epithelial cells following infection by cytoplasmic bacteria producing appropriate

antigens.[120] MAIT cells are also known to respond to stimulation by APCs carrying bacterial antigen by upregulating activation marker CD69 and producing T_H1 and T_H17 cytokines IL-2, TNF-α, IFN-γ, IL-17 and IL-22.[106,112,116] These processes can be mediated by a number of different APCs, including DCs, macrophages, epithelial and fibroblastic cells.[112] They are without exception dependent on MR-1, as they are blocked by an anti-MR-1 antibody, and are influenced by the MOI (multiplicity of infection), i.e. the infectant/APC ratio. MAIT cells also recognise antigen presented by neutrophils, generating GM-CSF, IFNγ and TNFα which in turn promote the acquisition of an APC-like phenotype by neutrophils themselves and the activation of αβ T cell-mediated responses.[61] The cytokines available in the surrounding environment most likely affect the response of MAIT cells, whose production of IFNγ is modulated by the availability of IL-12 and IL-18.[122]

Only microbial species possessing a pathway for the *de novo* generation of riboflavin can activate MAIT cells. Several metabolic intermediates produced in this pathway can act as their antigens, the most powerful identified so far being rRL-6-CH_2OH (**Figure 1.8**).[107]

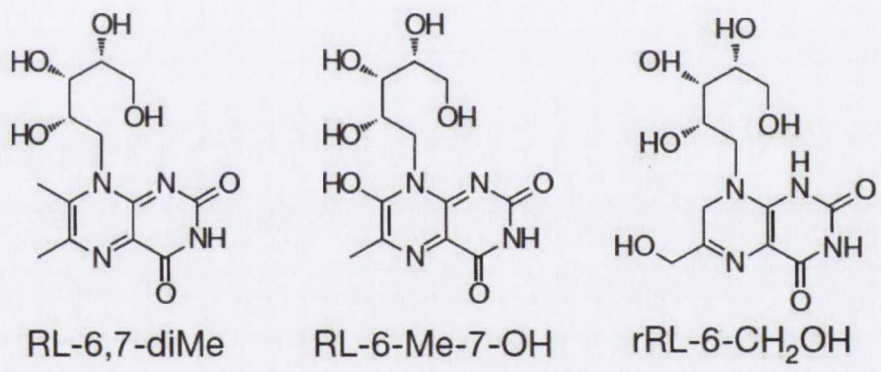


Figure 1.8. MAIT cell antigens. MAIT cells can be activated by several metabolites produced during the *de novo* generation of riboflavin. Activating metabolites characterised to date are 6,7-dimethyl-8-D-ribityllumazine (RL-6,7-diMe, left), 7-hydroxy-6-methyl-8-D-ribityllumazine (RL-6-Me-7-OH, centre) and 6-hydroxymethyl-8-D-ribityllumazine (rRL-6-CH_2OH, right). Image from Kjer-Nielsen et al.[107]

MAIT cell activation has specifically been observed after incubation of APCs with *Escherichia coli*, *Staphylococcus aureus*, *Staphylococcus epidermis*, *Pseudomonas aeruginosa*, *Klebsiella pneumoniae*, *Lactobacillus casei*, *Salmonella typhimurium*, *Candida albicans*, *Saccharomyces cerevisiae*, *Mycobacterium tuberculosis* and *Mycobacterium bovis*.[107,123,124] Microorganisms that do not feature a riboflavin production pathway, such as species of *Streptococcus*, *Enterococcus faecalis* and *Listeria monocytogenes*, fail to provide the necessary stimulus, as do microbial species that only recover riboflavin from the surrounding environment through transporter systems. Activation does not take place in the

absence of the antigen when APCs are stimulated by PAMPs, including LPS, CpG (C-phosphate-G) nucleic acid, dsRNA (double strand ribonucleic acid) synthetic analogue Poly(I:C) (polyinosinic-polycytidylic acid) and bacterial lipoprotein analogue Pam_3CSK_4 peptidoglycan. On the other hand, APCs deficient in adaptor proteins Myd88 (myeloid differentiation marker 88) and TRIF (TIR-domain-containing adapter-inducing interferon-β) and in cellular bacterial sensors NOD1 and NOD2 (nucleotide-binding oligomerization domain-containing proteins 1 and 2) can still suitably activate MAIT cells.[112]

The poised effector status of MAIT cells, their recognition of microbial antigens and their homing to tissues in frequent contact with microorganisms, such as the intestine and the lungs, strongly suggest that they primarily act as a first line of defence against a defined group of non-viral pathogens. This role is likely fulfilled in complementary ways, on one hand through exertion of direct cytotoxic effects, and on the other by modulation of the cytokine milieu that affects the behaviour of other immune cells at the site of infection. With regard to this, it has been hypothesized that their high expression of multiple drug resistance (MDR) protein ABCB1, which allows them to survive successive chemotherapy cycles, plays a role in their ability to survive and operate in a microorganism-rich environment, protecting them against toxic substances produced by the microbiome.[106]

Finally, mounting evidence links MAIT cells to the suppression and/or induction of autoimmunity; more information about this topic is supplied in chapter 1.5.2.2.3.5.

1.5.2.2.3.5 – MAIT cells in disease

Information about the behaviour of MAIT cells in disease is rather scant. These cells are regularly found at lower frequencies in the peripheral blood of individuals fighting infections, for example patients with pulmonary bacterial pathologies,[112] active tuberculosis[123] and sepsis.[125] Mouse studies have focused on bacterial loads in infected animals rather than peripheral blood MAIT cell frequencies, showing for example that MR-1$^-$ animals, which do not develop MAIT cells, display higher microbial burdens following experimental infection with *Mycobacterium bovis*.[124] The most accredited explanation for these findings is that, upon infection, MAIT cells migrate from peripheral blood and infiltrate infection sites, where they exert their anti-microbial functions; indeed, they have been observed in lung lesions in two patients diagnosed with *Mycobacterium tuberculosis*,[112] as well as in mouse lung tissue during pulmonary infection by *Francisella tularensis*.[126] It has nonetheless been noted that *in vitro* and *in vivo* mouse studies do not always give consistent results.[124] In fact, *in vivo* infections with several microorganisms capable of activating

MAIT cells in culture are not better controlled in $MR1^+$ mice in comparison to $MR\text{-}1^-$ animals.[112,127] This could be due to the fact that native MAIT cell populations are very small in mice, and possibly functionally redundant to T and B cells in many cases. Use of transgenic mouse models overexpressing the Vα19 chain, homologous to the human Vα7.2 chain, is complicated by the fact that the composition of the whole T cell compartment is altered in these mice, with over 50 % of T cells expressing the invariant TCR chain.[106]

A rapidly growing number of reports in mouse models suggest that MAIT cells could play a role in the regulation of autoimmunity and inflammation. Chiba and colleagues have reported that $MR\text{-}1^-$ mice are less susceptible to the onset of induced arthritis and display a less severe arthritic phenotype; the same mice reconstituted with MAIT cells, conversely, develop severe arthritis.[128] Quite in opposition to this, an overrepresentation of MAIT cells in non-obese diabetic mice delays the onset of the diabetes.[129] MAIT cells also seem to inhibit the induction and progression of experimental autoimmune encephalomyelitis (EAE), a mouse model of multiple sclerosis (MS), which manifests in exacerbated form in $MR\text{-}1^-$ mice.[130]

In man, research in relapsing/remitting MS patients has uncovered an inverse correlation between disease activity and MAIT cell frequencies in peripheral blood.[131] The lower frequencies of MAIT cells in the circulation of MS patients with high disease activity have been linked to their possible migration to inflammatory lesions, which would mirror their behaviour at infection sites. This idea is supported by recently published work on inflammatory bowel diseases (IBDs), which describes an enrichment in MAIT cells in inflamed intestinal tissue from patients affected by Crohn's disease and ulcerative colitis and a parallel depletion of this population in peripheral blood.[132] Some non-peer-reviewed evidence is also available that MAIT cells are present in psoriatic lesions.[133] Interestingly, although this subset is found at similar frequencies in healthy skin, $CD8^+$ MAIT cells producing IL-17A were exclusively detected in psoriasis. This resonates with the observation that MAIT cells from IBD patients secrete significantly more IL-17A and/or IL-22 upon *in vitro* stimulation,[132] implicating either or both of these cytokines in the mediation of autoimmunity by these cells. MAIT cells have also been observed to suppress IFNγ production by T cells in culture, highlighting their possible role in the modulation of T_H1 responses *in vivo*.[131]

Although MAIT cells were initially identified as having anti-viral properties, this idea has since been dismissed. Nonetheless, their frequencies are reportedly decreased in the blood of patients infected by HIV, alone or in combination with *Mycobacterium tuberculosis*, from the early stages of infection.[134-136] As they are not actively infected by

the virus, their depletion could be due to their recall to peripheral tissues, or alternatively to activation-induced cell death. The latter would be consistent with the fact that residual circulating MAIT cells express an activated and exhausted phenotype. Notably, their numbers do not recover following long term highly active anti-retroviral therapy (HAART). Because of this, it has been suggested that the loss of MAIT cells could be implicated in the diminished ability of HIV^+ patients to respond to opportunistic infections by microorganisms including *Mycobacterium tuberculosis* and mucocutaneous *Candida albicans*.

As previously stated, MAIT cells constitute up to 50 % of total liver T lymphocytes. Interestingly, an enrichment in $CD161^{high}$ $CD8\alpha\alpha^+$ T cells, the majority of which are MAIT cells, has previously been identified in the liver of patients with chronic hepatitis C in comparison with their peripheral blood.[116] A recent poster presentation at the International Liver Congress 2014 provided evidence that, although MAIT cells are not infected by hepatitis C virus (HCV), they are activated in the presence of IL-18 secreted by resident Kupffer cells following inflammasome activation.[137] This cytokine then stimulates them to generate IFNγ, which has both anti-viral and anti-fibrogenic properties. MAIT cells could therefore indirectly participate in the processes that determine virus persistence and liver fibrosis. In this regard, it is worth remembering that IL-17A and IL-22, which are also produced by this cell type following stimulation, have pro-fibrogenic and hepatoprotective functions, respectively.

1.5.2.2.3.6 – MAIT cell propagation

In contrast to conventional T cells, MAIT cells are not easily expanded in culture. Attempts have been made to cultivate them in the presence of phytohaemagglutinin (PHA), IL-2, IL-7 and IL-15, without obtaining satisfying results.[106,116] Similarly, *in vitro* expansion in the presence of IL-2, IL-4 and IL-7 has previously been reported as unsuccessful.[138] It has been found that these cells seldom express Ki67, a proliferation marker, do not enter the cellular cycle and are normally found in G_0 phase.[106,116] Leeansyah and colleagues have however reported that adult MAIT cells are capable of limited proliferation in response to incubation with whole cell *Escherichia coli*, anti-CD28 antibody and IL-2; through this method they were also able to induce satisfactory propagation of foetal MAIT cells, which express naturally higher levels of Ki67.[111] They have moreover suggested that addition of IL-18 and IL-12 could improve MAIT cell growth *in vitro*, as these cytokines can activate this subset independently of TCR ligation.[122] It should however be noted that, to date, functional proliferating populations of adult MAIT cells have only

been obtained *in vitro* using an induced pluripotent stem cell (iPSC)-based approach which requires the reprogramming of MAIT cells into iPSC and their subsequent redifferentiation.[139]

1.5.3 – Other lymphocyte subsets

1.5.3.1 – NK cells

Natural Killer cells are a subset of immune cells initially generated in the bone marrow from the same lymphocytic progenitors that also produce B and T cells. Their differentiation process is not as well dissected as that of other lymphocyte populations, but immature NK (iNK) cells can be identified both in the bone marrow and in the liver of mice. These precursors lack the complete array of phenotypic markers that normally characterize NK cells, but express NK1.1 and can lyse target cells through a TRAIL-mediated process.[140] $CD161^+$ $CD56^-$ cells with equivalent functions can be generated *in vitro* from human progenitors,[141] suggesting this is a common differentiation stage for this cell type. It is not clear how and where NK cells conclude their maturation, although several sites have been proposed, including the bone marrow, the liver, the spleen and lymph nodes. Once their differentiation is complete, however, NK cells depend for their homeostasis on the availability of two cytokines, IL-15 and TGFβ. IL-15 boosts NK cell numbers, promoting their proliferation through the expression of anti-apoptotic factor Bcl-2,[142] while TGFβ has the opposite effect, slowing their development.[143]

Mature NK cells are large lymphocytes found in a variety of tissues and organs in the human body, such as blood, the spleen, the liver, the lymph nodes, the omentum, the lungs and, during gestation, the uterus. They display a $CD3^-$ $CD56^+$ phenotype and are generally $CD8^+$ or $CD4^-$ $CD8^-$, but lack a TCR. They can also be further subdivided on the basis of their expression of CD16 and the intensity of their CD56 expression, in a $CD56^{bright}$ $CD16^-$ and a $CD56^{dim}$ $CD16^+$ subset. Both populations are involved in the elimination of virus-infected and transformed cells, however $CD56^{dim}$ cells display the strongest cytotoxic characteristics, whereas $CD56^{bright}$ cells have more of an immunoregulatory role.[144]

Both NK cell subsets share a common activation mechanism. Differently from cytotoxic $CD8^+$ lymphocytes, which recognize viral or anomalous self-antigens presented through MHC class I, NK cells can detect abnormal cells through their lack of surface expression of classical and non-classical MHC class I molecules. As MHC class I is downregulated upon

infection or transformation, NK cells fill a niche which would otherwise be left unguarded by the adaptive arm of the immune system. MHC expression sampling is carried out through a variety of surface receptors: some of these are activating, meaning that they induce cytotoxicity against the target cell when engaged; others are inhibiting, as they suppress the "natural" cytotoxic response of NK cells. Engagement of stimulatory receptors or lack of engagement of inhibitory receptors can both trigger cytotoxicity. The highly polymorphic family of killer-cell immunoglobulin-like receptors (KIRs) includes both activating and inhibiting members (**Figure 1.9**). Stimulatory KIRs like KIR2DS1 have short intracellular tails containing an immunoreceptor tyrosine-based activation motif (ITAM), and transduce signals by recruiting adaptor molecules which in turn bind and activate tyrosine kinase enzymes. Inhibitory KIRs such as KIR2DL1, on the other hand, have long intracellular tails containing immunoreceptor tyrosine-based inhibition motifs (ITIMs), through which they directly bind and activate tyrosine phosphatase enzymes. Nomenclature is similar for both groups, with the name of each receptor indicating its number of extracellular domains (e.g. 2D), the length of the intracellular tail (S for short or L for long) and the specific gene it is encoded by (e.g. 1).

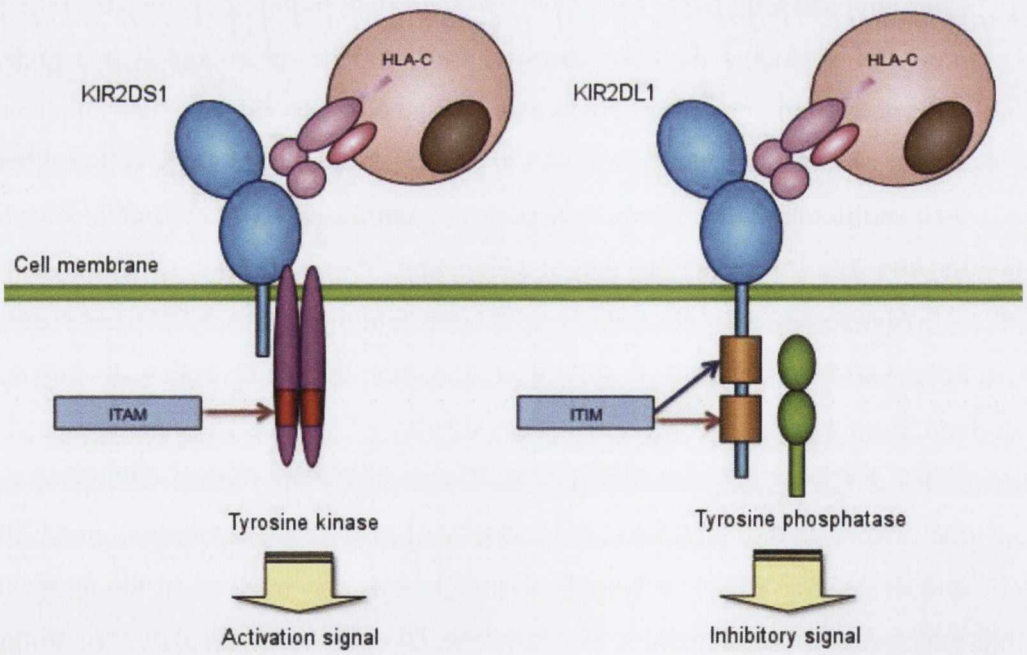


Figure 1.9. Stimulatory and inhibitory KIRs. NK cell responses are controlled by stimulatory and inhibitory KIRs, which sample the expression of MHC class-I molecules like HLA-C on the surface of cells. Stimulatory KIRs, such as KIR2DS1, transduce activation signals through the cell membrane by means of an ITAM domain which recalls tyrosine kinases. Inhibitory KIRs like KIR2DL1, conversely, transduce inhibitory signals through an ITIM domain which recalls tyrosine phosphatases. Image modified from Maeda et al.[145]

In addition to KIRs, NK cells also possess other kinds of receptors, such as the members of the NK group 2 (NKG2) family. Four of the five receptors composing the family, i.e. NKG2A, NKG2B, NKG2C and NKG2E, dimerise with surface antigen CD94 and express inhibitory (NKG2A, NKG2B) or stimulatory (NKG2C, NKG2E) functions following binding of non-classical MHC class I molecule HLA-E. NKG2D, on the other hand, exists on the surface of NK cells as a homodimer and recognises non-classical MHC class I-like molecules MICA and MICB, which are highly expressed by cells in situations of stress.

$CD56^{dim}$ NK cells, as already mentioned, have superior cytolytic abilities and embody the "typical" NK phenotype. They constitutively produce cytotoxic substances such as granzymes and perforin, which are stored in cytoplasmic granules. Once activated, they dock against the target cell and release the content of these granules through its membrane and into the cytoplasm, triggering apoptosis. $CD56^{dim}$ NK cells can produce pro-inflammatory cytokines, namely IFNγ and TNFα, although in limited quantities.

$CD56^{bright}$ NK cells have a less extensive receptor repertoire than $CD56^{dim}$ cells, lacking inhibitory KIRs CD158a, CD158b and NKB1.[146] They also have a two-fold reduced ability to form conjugates with potential target cells, and their granules contain about ten times less cytotoxic mediators than those of $CD56^{dim}$ cells.[146] They are, however, much stronger producers of IFNγ and TNFα (**Table 1.2**, chapter 1.5.2.1), constitutively express the high affinity form of IL-2 receptor and are enriched in lymph nodes. Indeed, production of IL-2 by lymph node T cells further stimulates IFNγ secretion by $CD56^{bright}$ NK cells.[147] As such, this subset has a definite role in the modulation of the cytokine milieu in the surrounding environment and participates in the bridging of innate and adaptive immune responses. Interestingly, IL-2 can also promote the acquisition of CD16 expression by $CD56^{bright}$ NK cells; it has been suggested that this could be part of a naturally occurring mechanism of conversion to the $CD56^{dim}$ subset *in vivo*.[148]

Although NK cells are classically thought of as purely innate immune cells, recent studies have demonstrated that they display a degree of immunological memory, which had previously been strictly associated with adaptive immunity. In fact, long-lived "memory" cells emerge from the large, clonally expanded populations of NK cells that are formed in response to the first contact with a viral pathogen. These cells with memory characteristics can react more rapidly to a second infection, including when used for adoptive transfer in infection-naïve animals, conferring superior protection.[149,150]

1.5.3.2 – NT cells

The heterogeneous subset of cells identified in this thesis as "natural T" (NT) consists of T lymphocytes that, similarly to iNKT cells, present surface markers typical of both T and NK cells, particularly CD3 and CD56. Differently from iNKT cells, though, they can operate in either a MHC-restricted or in a CD1d-restricted way. Their TCR can be composed of αβ or γδ chains, and they expand *in vitro* following expression of CD56 by $CD3^+$ cells, rather than upregulation of CD3 by $CD56^+$ ones.[151,152] Notably, CD56 can be induced on the surface of T lymphocytes by anti-CD3 and TCR stimulation, and its induction is directly proportional to the increase of MHC-unrestricted cytotoxicity and cytokine production.[153] A combination of IL-2 and IL-12 has been found to be induce strong development of this cell type *in vitro*.[151]

NT cells have potent cytolytic functions, and can kill both myeloid leukaemia and B cell lymphoma tumour cells.[152,154] As expression of CD56, but not CD8, correlates in this subset with cytotoxicity,[152] they probably act in a way similar to natural killer cells, being activated by stimulatory surface receptors in the presence of appropriate cytokines. Cytotoxicity can also be initiated by the presentation of antigens through MHC molecules, in a cytotoxic T lymphocyte-like fashion. Upon stimulation, NT cells secrete a range of T_H1 and T_H2 cytokines, such as IL-2, IFNγ, TNFα, IL-4 and IL-13, in some cases simultaneously.[155,156] **Table 1.4** summarizes the main characteristics of NT cells; all information was sourced from Kelly-Rogers *et al.*[153] Alongside other populations of unconventional T cells, such as γδ T cells and iNKT cells, this subset seems to have functions common to both innate and adaptive immunity, and as such is probably important in bridging the two arms of the immune system.

Table 1.4 - Main characteristics of NT cells

Feature	Details
TCR	αβ or γδ
Restriction	MHC- or CD1d-restricted
Surface receptors	CD3 Various combinations of NK cell markers (CD56, CD16, CD94/NKG2, CD161, NKG2D, KIRs)
CD4/CD8 status	$CD4^+$, $CD8^+$ or $CD4^-$ $CD8^-$
Localization	Less than 5 % of T cells in peripheral blood Up to 50 % of T cells in the liver and intestine
Functions	Granzyme and perforin-mediated cytotoxicity (NK-like or TCR-mediated) Cytokine production (T_H1- and T_H2-type cytokines)

1.6 – Immune cell subset abnormalities in CVID

Although CVID is a complex and diverse disease, numerous phenotyping studies have over time described common numerical abnormalities in the immune cell populations of patients. These affect first and foremost the B cell compartment, reflecting the heavy involvement of B cells in the disease and their inability to correctly differentiate into antibody-secreting plasma cells. Although percentages of circulating total B cells are usually normal or at most slightly decreased, patients display increased frequencies of naive B cells and a parallel steep depletion of class-switched memory B cells; the transitional B cell subset can also be expanded.[157] Three different classification systems, usually referred to as "Paris",[158] "Freiburg"[159] and "EUROclass",[160] have sought to subdivide patients into groups on the basis of their B cell phenotype and clinical presentation.

In addition to B cells, conventional T cells also exhibit aberrations. It is for example known that T cell proliferation in response to mitogens is frequently poor in CVID.[5] The CD4/CD8 status of circulating T cells is often altered, with subgroups of patients displaying a decrease in $CD4^+$ and/or an increase in $CD8^+$ T cell frequencies.[161,162] $CD4^+$ and $CD8^+$ naïve T cells are particularly depleted,[163] while activated $CD8^+$ T cells expressing HLA-DR are more frequently found in the blood of CVID patients.[164] A recent study has uncovered diminished proliferation and exhaustion of $CD4^+$ T cells responsible for anti-bacterial responses in reaction to bacterial translocation and high endotoxemia in CVID.[165] The observed expansion of $CD8^+$ T cells, on the other hand, seems to be at least in part a consequence of cytomegalovirus (CMV) infection, which is well known to drive the accumulation of late effector cells specific for CMV proteins; a correlation has also been documented between CMV infection and the inflammatory complications of CVID.[166] Increased frequencies of $CD8^+$ T cells have furthermore been linked to splenomegaly[162] as well as to autoimmune complications of the disease.[167] Regulatory T cells are likely to also play a part in the high occurrence of autoimmunity in CVID, as patients exhibit decreased frequencies of this subset.[168]

Not much is known about innate immune cell subsets in the disease, however a numerical decrease of iNKT cells has been observed.[169] As iNKT and B cell homeostasis have previously been linked and a correlation has been defined between low frequencies of iNKT cells and class-switched memory B cells in CVID patients, it has been suggested that this innate T cell subset could be involved in the failed differentiation of B cells in CVID. In addition to this, there have been reports of a numerical decrease in NK cells[170] and of functional anomalies affecting DCs.[171,172]

Table 1.5 summarizes what is known so far with regard to anomalies in the different immune cell subsets in CVID.

Besides cellular anomalies, CVID patients also display widespread TLR9 signalling abnormalities, and therefore an impaired response to bacterial PAMPs such as CpG dsDNA (double strand deoxyribonucleic acid).[175,176] Interestingly, the ability to respond to CpG signalling through TLR9 has been linked to isotype class switching, in a pathway involving IL-10.[177]

Table 1.5 – Immune cell subsets abnormalities in CVID patients

Parent population	Subset	Anomalies
B cells		The total frequencies of B cells can be normal or slightly reduced. A minority of patients have very low B cell frequencies.
	Naïve B cells	Increased frequencies.
	Transitional B cells	Increased frequencies in a subgroup of patients.
	Memory B cells	Reduced frequencies of class-switched memory B cells. Some CVID patients are able to respond to vaccination,[173,174] but this may be a transient response.
T cells		A sizeable portion of patients exhibit decreased proliferative response to mitogens.
	Helper T cells	$CD4^+$ cells are often decreased.
	Cytotoxic T cells	$CD8^+$ T cell frequencies are increased in a subgroup of patients; this strongly associates with splenomegaly.
	T_{REG}	Decreased in CVID patients.
	iNKT cells	Decreased in CVID patients.
NK cells		Decreased in CVID patients.
Dendritic cells		Functional anomalies in the ability of DCs to stimulate and activate other immune cells.

1.7 – Aims of the project

CVID is a relatively common but poorly understood immunodeficiency. A substantial amount of information is available describing the role of B cells in the disease and associations between their frequencies and phenotypes and the clinical presentation of patients. This is due to the fact that CVID is first and foremost characterized by a non-functional B cell compartment and by the inability, on the patients' part, to sustain a satisfactory humoral response against pathogens. Evidence of the possible involvement of other immune cell populations in the disease has also been gathered, including conventional T cells, regulatory T cells, NK cells and DCs, however innate T cell subsets have been largely overlooked. Additionally, while some effort has been made to classify CVID patients on the basis of their conventional T cell phenotype, no data of this kind is currently available for innate T cell populations. This is all the more surprising as a number of studies in recent years have provided proof that innate T cells, similarly to conventional T cells, are involved in sustaining B cell activation, proliferation and antibody production. Innate T cells can moreover counter bacterial and fungal infections, support the activation of adaptive responses via the differentiation and stimulation of antigen presenting cells, and polarise the wider immune response by generating early bursts of cytokines.

The overarching hypothesis of the work presented in this thesis is that a defect in innate T cell immunity could be involved in the aetiology of CVID or its complications. We investigated this proposition by numerically, phenotypically and functionally characterizing B cells and innate T cells from healthy individual and CVID patients. The data obtained are presented here in five chapters, corresponding to five specific research questions.

Chapter 3. Is B cell maturation impaired in CVID, and if so, what differentiation stage does this impairment affect? We investigated this matter by determining the frequencies and absolute numbers of circulating transitional, naïve and unswitched memory B cells, class-switched memory B cells, $CD27^-$ IgD^- B cells and plasmablasts in patient and control groups.

Chapter 4. May T cells, particularly innate T cell subsets, play a role in CVID and in its associated complications? We explored this possibility by determining the frequencies and absolute numbers of circulating T cells, iNKT cells, MAIT cells, Vδ1, Vδ2 and Vδ3 γδ T cells, as well as the CD4/CD8 status of these cell subsets, in healthy individuals and in CVID patients with and without complications.

Chapter 5. Is CVID characterised by unusual interactions between B and innate T cell subsets, and if so, may these hint at novel mechanisms of disease? We sought to identify these interactions by defining the existence of statistical correlations between frequencies or absolute counts of previously phenotyped B cell and innate T cell subsets in the blood of healthy individuals and CVID patients.

Chapter 6. Are MAIT cells, found during this study to be depleted in the circulation of patients with CVID, functionally altered in the disease? We investigated this question by examining the activation status and cytokine profile of MAIT cells before and after *ex vivo* stimulation with anti-CD3 and anti-CD28 antibodies or PMA and ionomycin.

Chapter 7. Can MAIT cells promote the maturation of B cells, and/or induce antibody production? We explored this *in vitro*, by determining the differentiation status and quantifying the antibody production of isolated B cells cultured in the presence or in the absence of total autologous MAIT cells for up to 7 days.

CHAPTER 2

MATERIALS AND METHODS

2.1 – Materials

The experiments presented in this thesis required the use of several types of materials. Antibodies specific for surface clusters of differentiation (CDs) were employed in flow cytometry experiments for the identification of different lymphocyte populations (**Table 2.1**). These antibodies were commercially conjugated to fluorochromes fluorescein isothiocyanate (FITC), phycoerythrin (PE), peridinine chlorophyll protein (PerCP), pacific blue or allophycocyanin (APC). Antibodies conjugated with tandem fluorochromes PE.Cy7, PerCP.Cy5.5 and APC.Cy7, derived from the association of PE, PerCP and APC with cyanine 5.5 (Cy5.5) or cyanine 7 (Cy7), were also used. In addition to fluorochrome-conjugated antibodies, some non-antibody-based flow cytometry stains were employed for the detection of specific cell subsets, cell death and proliferation (**Table 2.2**).

Cell cultures required the use of sterile materials (**Table 2.3**). Non-conjugated antibodies directed against stimulatory surface receptors allowed to induce T cell stimulation *in vitro* (**Table 2.4**).

Solutions and buffers needed during experiments were either prepared in-house from chemical powders (**Table 2.5**) or commercially available in ready-made form (**Table 2.6**).

General laboratory reagents for cell isolation, count, stimulation and flow cytometry (**Table 2.7**), plasticware (**Table 2.8**) and equipment (**Table 2.9**) were also used in the execution of the experiments.

Table 2.1. Fluorochrome-conjugated antibodies for flow cytometry

Manufacturer	Antibody	Clone
BD Biosciences *Oxford, UK*	anti-CD1d-PE	CD1d42
	anti-IgD-PE	IA6-2
	anti-Invariant NKT cell-PE	6B11
	Multitest 6-color TBNK Reagent (anti-CD3-FITC/ CD16+CD56-PE/ CD45-PerCP/CD19-APC)	/
Beckman Coulter *High Wycombe, UK*	anti-Vδ3-APC	Polyclonal, conjugated in house
Biolegend *San Diego, CA, USA*	anti-CD3-PacificBlue	HIT3a
	anti-CD3-PE.Cy7	HIT3a
	anti-CD4-FITC	SK3
	anti-CD4-PE.Cy7	SK3
	anti-CD5-PerCP.Cy5.5	UCHT2
	anti-CD8a-APC.Cy7	HIT8a
	anti-CD8a-PE	HIT8a
	anti-CD8a-Pacific Blue	HIT8a
	anti-CD19-PacificBlue	HIB19
	anti-CD38-PE.Cy7	HIT2
	anti-CD56-PE.Cy7	HCD56
	anti-CD69-PE	FN50
	anti-CD154-PE	24-31
	anti-CD161-FITC	HP-3G10
	anti-CD161-PerCP.Cy5.5	HP-3G10
	anti-IgD-PE	IA6-2
	anti-IFNγ-PE	4S.B3
	anti-IL-4-PE	8D4-8
	anti-IL-10-PE	JES3-19F1
	anti-IL-17a-PE	BL168
	anti-IL-22-PE	BG/IL22
	anti-TNFα-PE	MAb11
	anti-Vα7.2-APC	3C10
	anti-Vδ2-PE	B6
eBioscience *Hatfield, UK*	anti-CD38-PE.Cy7	HIT2
ImmunoTools *Friesoythe, Germany*	anti-CD24-FITC	SN3
	anti-CD27-FITC	LT27
Thermo Fisher Scientific *Logan, UT, USA*	anti-Vδ1-FITC	TS8.2

Table 2.2. Non-antibody-based stains for flow cytometry

Manufacturer	Reagent	Fluorochrome
Molecular Probes *Leiden, The Netherlands*	CellTrace Violet	/
	LIVE/DEAD Fixable Aqua dead cell stain	/
NIH Tetramer Facility *Atlanta, USA*	CD1d Tetramer (unloaded or loaded with PBS-57)	APC

Table 2.3. Cell culture reagents

Manufacturer	Reagent
Biosera *Boussens, France*	Foetal Calf Serum (FCS)
Gibco *Renfrew, UK*	2-mercaptoethanol, 50 mM
	HEPES buffer solution (1M)
	L-glutamine 200 mM (100x)
	MEM amino acids (50x)
	MEM NEAA (100x), non-essential amino acids
	Pen Strep solution (10,000 U/mL penicillin, 10 mg/mL streptomycin)
	PBS pH 7.4 (1x)
	RPMI 1640 (1x) + GlutaMAX
	Sodium pyruvate 100 mM (100x)
Hyclone *Cramlington, UK*	Foetal Calf Serum (FCS)

Table 2.4. Antibodies for cell stimulation

Manufacturer	Antibody	Clone
Biolegend *San Diego, CA, USA*	Ultra-LEAF Purified anti-CD3	OKT3
	Ultra-LEAF Purified anti-CD28	CD28.2

Table 2.5. Solids

Manufacturer	Reagent
Fisher Scientific *Loughborough, UK*	di-Sodium hydrogen orthophosphate anhydrous (Na_2HPO_4)
	Potassium phosphate monobasic (KH_2PO_4)
	Sodium chloride (NaCl)
Sigma-Aldrich *Poole, UK*	Potassium chloride (KCl)
	Saponin from Quillaja bark
	Sodium azide (NaN_3)

Table 2.6. Ready-made buffers

Manufacturer	Reagent
BD Biosciences *Oxford, UK*	FACS Lysing Solution
Chemcruz *Heidelberg, Germany*	Paraformaldehyde solution 4 % in PBS

Table 2.7. General laboratory reagents

Manufacturer	Reagent
Axis-Shield *Dundee, UK*	Lymphoprep
BD Biosciences *Oxford, UK*	CBA Human IgA Flex Set
	CBA Human IgG Flex Set
	CBA Human IgM Flex Set
	CBA Human Immunoglobulin Master Buffer Kit
	CS&T research beads
	FACS Clean solution
	FACSFlow Sheath Fluid
	FACS Shutdown solution
Biolegend *San Diego, CA, USA*	Monensin solution (1000x)
DuPont *Wilmington, DE, USA*	Virkon
eBioscience *Hatfield, UK*	OneComp eBeads
Fisher Scientific *Hampton, NH, USA*	Bovine serum albumin (BSA) Protease free powder, heat shock treated
Innova Biosciences *Cambridge, UK*	Lightning-link APC-XL conjugation kit
Miltenyi Biotec *Bergish Gladbach, Germany*	MACS CD3 microbeads
Sigma-Aldrich *Poole, UK*	Acridine orange solution
	Brefeldin A
	Dimethyl sulfoxide (DMSO) solution, $\geq$ 99.5%
	Ethidium bromide solution
	Ionomycin calcium salts from Streptomyces
	Phorbol 12-myristate 13-acetate
Stemcell Technologies *Grenoble, France*	EasySep Human B cell enrichment kit

Table 2.8. Plasticware

Manufacturer	Device
BD Biosciences *Oxford, UK*	Falcon 5 mL polypropylene round bottom tubes
	Falcon 5 mL polypropylene round bottom tubes, sterile
	Falcon 5 mL polystyrene round bottom tubes
	TruCount tubes
Corning *Corning, NY, USA*	96 well cell culture cluster, round bottom with lid, tissue culture treated
	Stripettes, 5 mL
	Stripettes, 10 mL
	Stripettes, 25 mL
Miltenyi Biotec *Bergish Gladbach, Germany*	30 μm pre-separation filters
	MACS LS separation columns
Sarstedt *Nümbrecht, Germany*	0.2 - 10 μL pipette tips
	15 mL tubes
	50 mL tubes
Semperit *Vienna, Austria*	Semperguard latex gloves, powder-free
Thermo Fisher Scientific *Logan, UT, USA*	SureOne non-filter pipet tips, 1 – 200 μL
	SureOne non filter pipet tips, 100 – 1250 μL
	30 mL tubes

Table 2.9. Equipment

Manufacturer	Device
AGB Scientific *Dublin, Ireland*	AGB 1000 hot plate and stirrer
Beckman Coulter *Oxford, UK*	Cyan ADP flow cytometer
	MoFlo XDP high speed sorter
Becton Dickinson *High Wycombe, UK*	FACSCanto II flow cytometer
Eppendorf *Hamburg, Germany*	5810 centrifuge
Gemmy *Taipei, Taiwan*	Water bath
HANNA Instruments *Woonsocket, RI, USA*	pH20 pH meter
IKA *Staufen im Breisgau, Germany*	Genius 3 vortex
Miltenyi Biotec *Bergish Gladbach, Germany*	MACS Midi magnet
	MACSMix roller
Nikon *Tokyo, Japan*	Eclipse E200 microscope with 10x, 20x and 40x lenses
Ohaus *Pine Brook, NJ, USA*	Adventurer Pro precision balance
RS Biotech *Irvine, UK*	Galaxy S CO_2 incubator
Scientific Industries *Bohemia, NY, USA*	Vortex Genie 2
Stemcell Technologies *Grenoble, France*	EasySep magnet
Telstar Laboratory Equipment *Woerden, The Netherlands*	CleanAir Biosafety cabinet
Thermo Fisher Scientific *Logan, UT, USA*	0.2 – 2 µL Finnpipette F2
	2 – 20 µL Finnpipette F2
	20 – 200 µL Finnpipette F2
	100 – 1000 µL Finnpipette F2
	Fisherbrand motorized pipette filler

2.2 – Recipes for solutions and media

The recipes described in this chapter pertain to the way solutions and media were prepared.

10x PBS (phosphate buffered saline) – The following salts were weighted on a precision balance:

- 80 g NaCl;
- 2 g KCl;
- 14.4 g Na_2HPO_4;
- 2.4 g KH_2PO_4.

After adding distilled water, the suspension was mixed on a magnetic stirrer until complete solubilisation was achieved. The pH was then adjusted to between 7 and 7.4 and the volume of the solution brought up to 1 L.

PBA (PBS with BSA)

- for phenotyping studies: 1x PBS was supplemented with 1.5 % BSA (bovine serum albumin) and 0.02 % sodium azide;
- for intracellular cytokine staining and activation marker upregulation studies: 1x PBS was supplemented with 0.5 % BSA and 0.02 % sodium azide.

0.2 % saponin solution – 0.1 g of saponin powder were dissolved in 50 mL PBA. The solution was freshly made before every use.

Complete Culture Medium – 500 mL RPMI 1640 + GlutaMAX were supplemented with:

- 60 mL FCS (foetal calf serum);
- 12 mL HEPES (4-(2-hydroxyethyl)-1-piperazineethanesulfonic acid) buffer solution (1 M);
- 12 mL 50x MEM (minimum essential medium) amino acids;
- 6 mL 100x MEM NEAA (non-essential amino acids);
- 6 mL sodium pyruvate (100 mM);
- 5 mL 1x L-glutamine;
- 5 mL Pen Strep (penicillin streptomycin) solution;
- 600 µL 2-mercaptoethanol (50 mM).

All solutions were sterile. The same medium was used for B cells, MAIT cells and MAIT cell-depleted T cells.

EB/AO (ethidium bromide/acridine orange) – 0.8 mL of 4 mg/ml ethidium bromide solution were mixed with 2 ml of 1 mg/ml acridine orange solution.

Miltenyi buffer for $CD3^+$ cell enrichment – 50 mL of sterile PBS were supplemented with:

- 833 µL 30 % BSA, sterile-filtered;
- 400 µL 250 mM EDTA (ethylenediaminetetraacetic acid), sterile-filtered.

The buffer was freshly prepared on the morning of each enrichment procedure and kept on ice when not in use.

EasySep B cell separation buffer – 500 mL of sterile PBS were supplemented with:

- 10 mL (2 %) sterile heat-inactivated FCS;
- 2 mL 250 mM EDTA, sterile-filtered.

The buffer was refrigerated between uses but kept at room temperature when in use.

2.3 – Ethical approval

Full consideration was given to the ethical implications of this study. Ethical approval was requested and obtained from the Joint Research Ethics committee of St. James's Hospital and Federated Dublin Voluntary Hospitals for a study on blood samples from immunodeficient patients attending the immunology clinic in St. James's Hospital, Dublin. The title of the approved study was "Investigations into the molecular defects associated with primary immunodeficiency disorders".

2.4 – Study population

Peripheral blood samples for immunophenotyping were obtained from 31 patients, of which:

- 21 were diagnosed with CVID (13 males, 8 females; median age 38 years; age range 22 to 82 years old);
- 1 was diagnosed with selective IgA deficiency (female, age 26);
- 2 were diagnosed with selective IgA deficiency and IgG2 subclass deficiency (1 male, 1 female; ages 35 and 73 years old, respectively). These two individuals belonged to the same family unit;

- 6 were diagnosed with secondary antibody deficiency (2 males, 4 females; median age 60.5; age range 46 to 69). In 5 of these patients, hypogammaglobulinemia was most likely caused by chronic treatment with steroids, while in the 6th patient, it was secondary to a thymoma, which had been surgically removed;
- 1 (male, age 23) did not satisfy the requirements for diagnosis of any of the previously mentioned conditions. The antibody deficit of this patient presented in the first months of life in the form of low IgA, IgM and IgG2 levels leading to the development of chest infections, including pneumonia requiring hospitalization at age 4 months. Due to the severity of the infections he was placed on IgG replacement therapy at around age 1. IgA and IgM levels were borderline normal at the time samples were collected for this study, nonetheless therapy could not be interrupted as he had previously developed severe bacterial infections (mastoiditis, pneumonia and meningitis) when the intervals between infusions were made longer than 6 weeks. XLA, as well as CD40L, CD40 and properdin deficiency, had been tested for and excluded during differential diagnosis. A strong family history of meningitis had been identified in males on his mother's side, suggesting he could be affected by an X-linked immunodeficiency. Recent genetic testing has excluded that his condition could depend on a mutation in the gene encoding PI3K-δ (Phosphoinositide-3-kinase, δ subunit).

For the purposes of this immunophenotyping study, patients were divided in 4 groups:

- CVID (n = 21);
- secondary antibody deficiency (n = 6);
- selective IgA deficiency and/or IgG2 subclass deficiency (n = 3);
- query diagnosis (n = 1).

The control cohort included 27 individuals (14 males, 13 females; median age 34 years; age range 22 to 66 years old). None had a history of immune-mediated illnesses.

Figure 2.1 shows the median ages of the patients and controls recruited. Although the median ages of healthy controls and CVID patients were comparable, the median age of patients with secondary hypogammaglobulinemia was significantly higher than that of healthy controls.

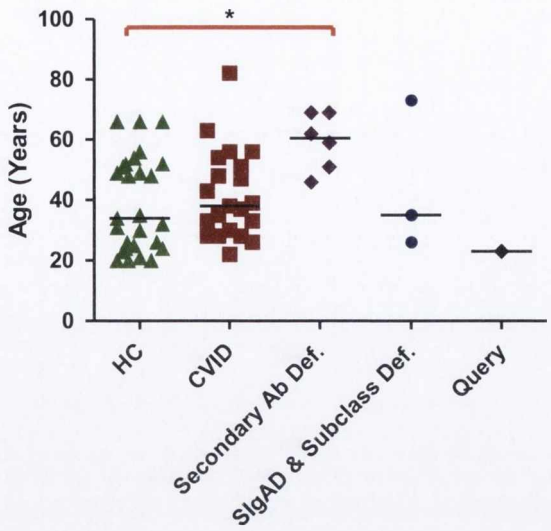


Figure 2.1. Median ages of the patient and control groups for immunophenotyping. The graph shows the median ages of groups of healthy controls (HC), CVID patients (CVID), secondary antibody deficiency patients (Secondary Ab Def.), selective IgA deficiency and/or IgG2 subclass deficiency patients (SIgAD & Subclass Def.). It also shows the age of a single query diagnosis patient (Query). Statistical analysis was performed on the first three groups (HC, CVID and Secondary Ab Def.), using a Kruskal-Wallis test plus Dunn's post-hoc test; no statistics was performed on the remaining groups due to insufficient subject numbers. * $p < 0.05$.

For functional work on T cells and MAIT cells, peripheral blood samples were collected from:

- 7 definitively diagnosed CVID patients, free from complications (6 males, 1 female; median age 39; age range 27 to 57);
- 5 definitively diagnosed CVID patients, affected by complications (3 males, 2 females; median age 34; age range 30 to 55);
- 6 healthy controls, with no history of immune-mediated illnesses (3 males, 3 females; median age 30.5; age range 25 to 53).

The 12 CVID patients recruited for this portion of the study were part of the cohort originally recruited for immunophenotyping. As shown in **Figure 2.2,** the median ages of the three groups were comparable.

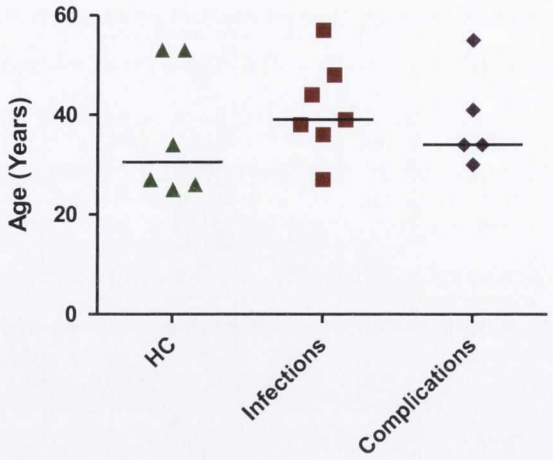


Figure 2.2. Median ages of the patient and control groups for functional work. The graph shows the median ages of groups of healthy controls (HC), CVID patients with infections only (Infections) and CVID patients with infections and complications (Complications). Statistical analysis was performed using a Kruskal-Wallis test plus Dunn's post-hoc test.

2.5 – Classification of patients in clinical phenotypes

The medical records of patients were accessed with the aim of collecting clinical information that could later be correlated with experimental data. In order to obtain results consistent with those currently available in the literature, it was decided to adopt a clinical classification system first defined by Chapel *et al.* in a study involving more than 300 CVID patients.[178] On the basis of their clinical status, the patients recruited to the present study were therefore assigned to one or more of the following five phenotypes:

- *No complications* – patients with infections only;
- *Autoimmunity* – patients with infections plus autoimmune complications, including both cytopaenias and organ-specific autoimmune conditions, such as rheumatoid arthritis, systemic lupus erythematosus, seronegative arthritis (meeting the American Rheumatism Association criteria), Graves' disease, primary thyroid failure, insulin-dependent diabetes mellitus, pernicious anemia, atrophic gastritis (biopsy-proven with antral sparing), chronic autoimmune haemolytic anemia, chronic immune thrombocytopenia, persistent unexplained neutropenia, psoriasis, vitiligo. Transient arthropathies were not considered a manifestation of autoimmunity;
- *Polyclonal Lymphocytic Infiltration (PLI)* – patients with infections plus complications such as lymphoid interstitial pneumonitis (LIP), unexplained granuloma (biopsy-proven), unexplained hepatomegaly (detected by clinical

examination or ultrasound), extensive and persistent lymphadenopathy (detected by palpation, ultrasound or CT scan). Crohn's disease was not considered a manifestation of PLI;

- *Enteropathy* – patients with infections plus biopsy-proven lymphocytic infiltration of the *lamina propria* and villous atrophy. As the manifestations and symptoms of CVID enteropathy are similar to those of coeliac disease, only patients insensitive to gluten withdrawal were classified in this phenotype.
- *Malignancy* – patients with infections plus lymphoid malignancies, such as non-Hodgkin's lymphoma.

Importantly, these phenotypes were defined by Chapel and colleagues to account only for complications intrinsically linked to CVID. According to this principle, conditions such as bronchiectasis and splenomegaly, often observed in CVID and initially considered as part of the classification, were later excluded. Bronchiectasis was considered to be consequence of recurrent pulmonary infections rather than of the underlying immune defect causing CVID. Splenomegaly, on the other hand, was found to associate with a number of other complications, suggesting its development could be due to a variety of causes, rather than secondary to CVID pathogenesis specifically.

Although the patients recruited to this study were classified according to the criteria detailed above, the results reported in this thesis refer more generally to individuals affected by "infections only" or "complications". This is due to the fact that subject numbers were not sufficient to allow for every complication type to be considered singularly. As such, throughout this report, the "infections only" group includes patients belonging to the "no complication" phenotype, while the "complications" group comprises patients exhibiting autoimmunity, PLI, enteropathy and/or malignancy.

2.6 – Collection of blood samples

For patients receiving intravenous immunoglobulin infusions at the Immunology clinic in St. James's Hospital every three weeks, blood samples were collected just before infusions. For patients on home therapy, either on intravenous infusions every three weeks or on weekly subcutaneous infusions, blood samples were collected during biannual patient reviews. All patients read and signed informed consent forms before being recruited to the study. Both patients and healthy controls were infection-free at the time of sample collection.

Blood was collected in EDTA Vacutainer tubes for immunophenotyping and enumeration of cells, or in sodium heparin Vacutainer tubes for functional studies on cytokine production and activation marker upregulation by T cells and MAIT cells. Autologous MAIT cells and B cells for co-culture experiments were isolated from blood packs donated by the Irish Blood Transfusion Service.

Samples were always processed within 4 hours of collection. When sterility had to be maintained, samples were handled within a class II biosafety cabinet with appropriate sterile techniques. Appropriate personal protection devices were always worn, including gloves and a lab coat. Any blood residue was disposed of by inactivation in diluted Virkon for at least 1 hour, followed by autoclaving of the remaining material.

2.7 – Cell isolation, count and culture

2.7.1 – PBMC isolation by density gradient

This technique allows to obtain purified preparations of peripheral blood mononuclear cells (PBMCs), i.e. lymphocytes and monocytes.

A non-irradiated buffy coat donated by the Irish Blood Transfusion Service (30-50 mL) was diluted 1:2 to 1:4 with sterile PBS. The diluted blood was layered on Lymphoprep reagent in a 2:1 ratio and centrifuged at 400 g for 25 minutes with brakes applied. Following centrifugation, the components of the buffy coat separated on the basis of their density, as shown in **Figure 2.3**. The PBMCs were collected with a sterile pastette and divided in two 50 mL tubes. The cells were then washed twice, both times bringing the total volume of the suspension up to 50 mL with sterile PBS, centrifuging at 400 g for 10 minutes and discarding the supernatant by inversion. Finally, the cells were resuspended in 30 mL of sterile PBS and counted with a Neubauer haemocytometer.

2.7.2 – Cell counts with Neubauer haemocytometer

EB/AO, a mixture containing 16 µg/mL ethidium bromide and 10 µg/mL acridine orange in PBS, was used to count cells, diluting 10 µL of cell suspension in 190 µL of staining solution. Under UV light, ethidium bromide highlights dead cells in orange, while acridine orange stains live cells green. The count was performed using a Neubauer haemocytometer, whose counting grid is shown in **Figure 2.4**.

At least 100 cells and 2 large quadrants (1 mm x 1 mm) in opposite corners were counted, to ensure accuracy. The number obtained from the count was divided by the number of quadrants, then multiplied by the dilution factor applied (20) and again by the conversion factor of the chamber (10^4), obtaining the number of cells per mL.

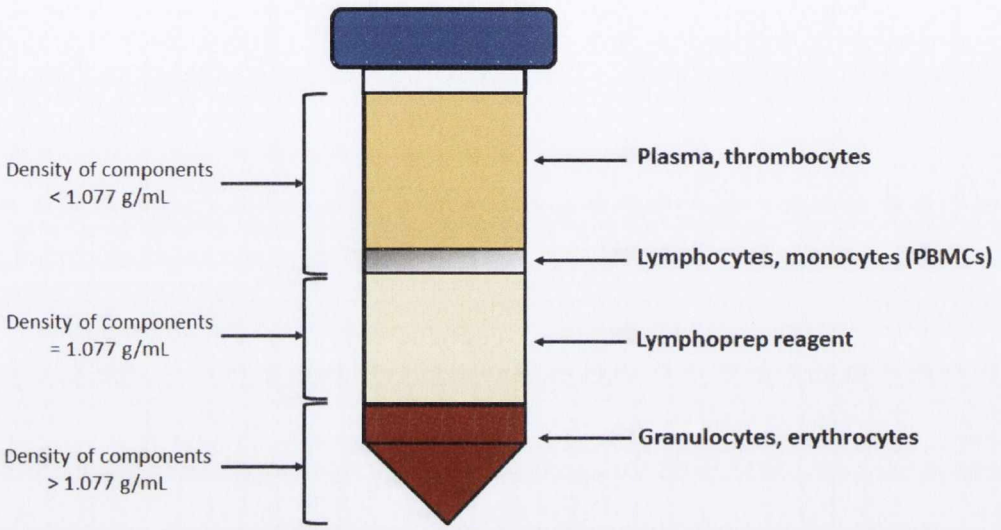


Figure 2.3. Separation of blood components in Lymphoprep reagent. Following layering of blood on Lymphoprep and centrifugation, blood components separate according to their density. Peripheral blood mononuclear cells (PBMCs) gather in a white-coloured ring, separated from granulocytes and erythrocytes by the Lymphoprep reagent.

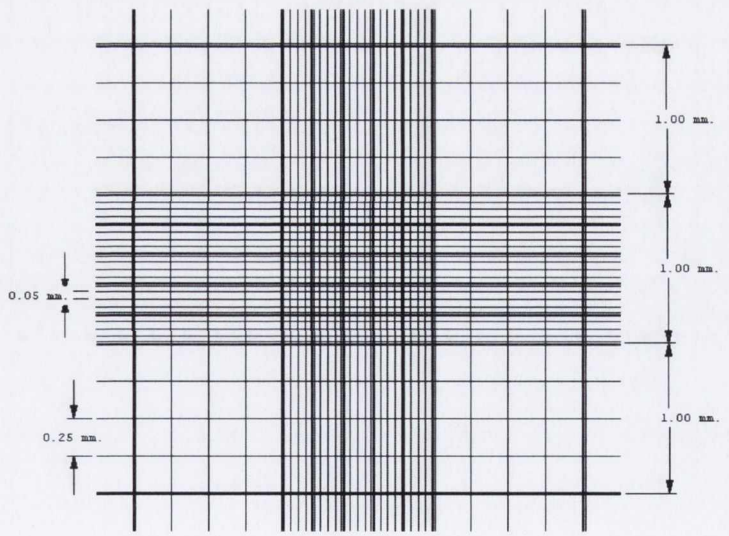


Figure 2.4. Organization of the counting grid in a Neubauer chamber. Image courtesy of Hausser Scientific (www.hausserscientific.com).

2.7.3 – Positive selection of $CD3^+$ cells

As MAIT cells are relatively rare, constituting approximately 1 to 10 % of total T cells, enriched preparations of $CD3^+$ cells were obtained from PBMCs in order to simplify sorting. To this end, a positive selection Miltenyi MACS kit specific for $CD3^+$ cells was used. All solutions utilised in this protocol were pre-cooled and kept on ice when possible, to prevent non-specific cell labelling. Volumes given are for 1 x 10^7 cells and were scaled up or down as necessary, except where otherwise noted.

PBMCs were centrifuged at 300 g for 10 minutes. The supernatant was removed with a pipette, and the cell pellet resuspended in 20 µL of Miltenyi buffer. After adding 5 µL of CD3 Microbeads, the cell suspension was mixed thoroughly and incubated at 4 °C for 15 minutes. Excesses of Microbeads were washed away by topping the mixture up to 10 mL with Miltenyi buffer and centrifuging at 300 g for 10 minutes; the volume of this wash was not scaled up. While the cells were being centrifuged, a Miltenyi LS separation column was prepared in a MACS Midi magnet, with a 30 µm pre-separation filter on top, and rinsed with 3 mL of Miltenyi buffer. A fresh collection tube was then placed underneath the column. After removing the supernatant with a pipette, the cells were resuspended in 500 µL of buffer and fed into the column, which was then washed 3 times, each time with 3 mL buffer. The effluent resulting from this process, comprising unlabelled $CD3^-$ cells, was kept aside for later use in the negative selection of B cells.

Upon completion of the washes, the column was removed from the magnet and placed in a new collection tube. 5 mL of Miltenyi buffer were pipetted in the column and immediately flushed out with the plunger supplied, thus isolating the labelled $CD3^+$ cell fraction. $CD3^+$ and $CD3^-$ cells were counted with a Neubauer haemocytometer, then centrifuged at 1500 RPM (revolutions per minute) for 7 minutes. Finally, the $CD3^+$ fraction was resuspended in PBS plus 2 % FSC at 10 x 10^6 cells/mL, in preparation for sorting; the $CD3^-$ fraction, on the other hand, was resuspended in complete RPMI medium for later use in B cell isolation.

2.7.4 – Negative selection of B cells

B cell isolation made use of a negative selection EasySep kit and EasySep magnet, and $CD3^-$ cells as a starting material; all steps in this protocol were performed at room temperature. $CD3^-$ cells were suspended in complete medium at 50 x 10^6 cells/mL. 1 mL of the suspension was placed in a 15 mL tube and centrifuged at 1500 RPM for 7 minutes; the

pelleted cells were then resuspended in 1 mL EasySep buffer. After adding 50 µL of Human B cell Enrichment cocktail, the tube was thoroughly mixed and incubated at room temperature for 10 minutes. 75 µL of EasySep D Magnetic Particles, vortexed for 30 seconds to ensure the absence of aggregates, were added. The tube was again fully mixed and incubated at room temperature for 5 minutes. At the end of the incubation, the total volume of the mixture was brought up to 5 mL with EasySep buffer; the suspension was mixed gently by pipetting up and down, to avoid the detachment of beads from the labelled cells. The tube was then placed uncapped in the EasySep magnet and set aside for 5 minutes. Finally, the magnet and tube were inverted over a fresh 15 mL vessel, collecting the unlabelled B cells. The isolated cells were counted with a Neubauer haemocytometer.

2.7.5 – Operator-assisted fluorescence-activated cell sorting of MAIT cells

In order to set up co-cultures of MAIT cells and B cells, MAIT cells had to be isolated by operator-assisted fluorescence-activated sorting. This chapter describes the protocol applied for the preparation of the cells to be isolated; see chapter 2.8 for more information about basic flow cytometry principles and staining protocols used for immunophenotyping and functional studies.

Positively selected $CD3^+$ cell preparations were resuspended at densities of up to 5 x 10^7 cells/mL in PBS containing 2 % FCS and stained with appropriate amounts of anti-CD161 and anti-Vα7.2 antibodies. OneComp eBeads were stained at the same time to obtain single stains, adding 1 test of a PerCp.Cy5.5- or APC-conjugated antibody of choice to one drop of beads. Both cells and beads were incubated at 4 °C for 30 minutes. Following staining, cells and beads were washed with 2 mL of non-complete RPMI medium and centrifuged at 1500 RPM for 7 minutes. The cells were resuspended in up to 1.5 mL of complete medium plus 2 % FCS, then passed through a Miltenyi Biotec 30 µm pre-separation filter to eliminate clumps. The single stains were resuspended in 200 µL of PBS. An unstained control was prepared dispersing 0.5 x 10^6 $CD3^-$ cells in 1 mL RPMI plus 2 % FCS; $CD3^-$ cells were used, rather than $CD3^+$ cells, as these were the most abundantly available. Recipient tubes containing 0.5 mL of complete medium were also brought to the sorter, as collection vessels for sorted MAIT cells and MAIT cell-depleted T cells.

The cells where run on a MoFlo XDP high speed sorter by Dr Eamon Breen, manager of the flow cytometry facility of the Institute for Molecule Medicine, St. James's Hospital, Dublin.

2.7.6 - CellTrace Violet Staining

CellTrace is a non fluorescent esteric reagent. Once added to cells, it permeates them and is converted in their cytoplasm into a fluorescent amine-reactive compound that irreversibly binds cellular amines and is retained through successive cellular divisions. During the cellular division process, the fluorescent compound is equally divided between daughter cells, resulting in the "dilution" of the dye in successive generations (**Figure 2.5**).

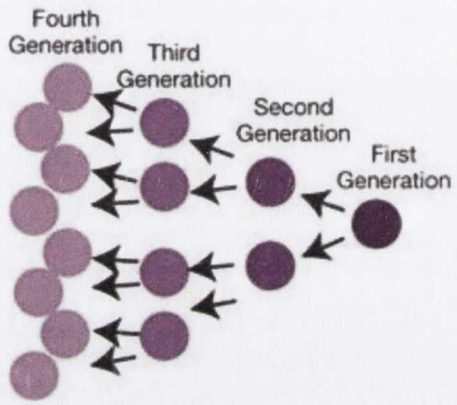


Figure 2.5. Progressive attenuation of CellTrace fluorescence in successive rounds of cell division. Image courtesy of Life Technologies (www.lifetchnologies.com).

Upon acquisition of a CellTrace-stained sample on a flow cytometer, proliferation will therefore be detected in a histogram as the presence of peaks at fluorescence intensities lower than the parent population (**Figure 2.6**).

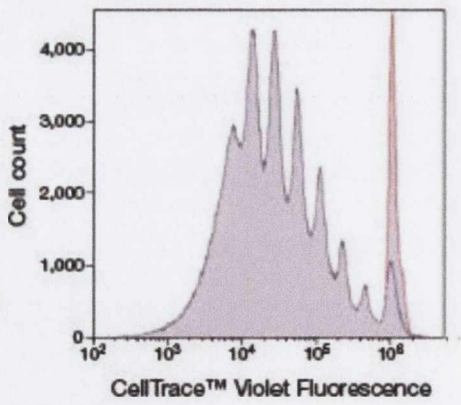


Figure 2.6. Visualisation of proliferation in flow cytometry histogram following staining with CellTrace. The image shows the proliferation of $CD4^+$ T cells following 7 day stimulation of PBMCs with anti-CD3 antibody and IL-2. The peak rimmed in red marks the fluorescence of the unstimulated parent population, with the highest content of the fluorescent reagent. The other peaks at progressively lower fluorescence intensities are successive cell generations. Image courtesy of Life Technologies (www.lifetchnologies.com).

Some of the experiments presented in this thesis required the co-culturing of B cells and MAIT cells for up to 7 days. After 3 and 7 days of co-culture, B cells were stained for differentiation markers CD27 and IgD, defining the frequencies of increasingly differentiated populations, i.e. naïve B cells ($CD27^-$ IgD^+), unswitched memory B cells ($CD27^+$ IgD^+) and class-switched memory B cells ($CD27^+$ IgD^-). It was considered that as the frequencies of these populations were defined by the same markers, and therefore relative to each other, each could be influenced by the death or proliferation of the others. CellTrace staining was therefore included to account for B cell proliferation in culture.

Before staining, a vial of CellTrace Violet was thawed from -20 °C and reconstituted with 20 µL of DMSO, generating a 5 mM stock. Negatively isolated B cells were resuspended in PBS at 5 x 10^5 cells/mL. A working solution of CellTrace, obtained diluting the original 5 mM stock 1:5 in PBS, was added at 1 µL/mL of cell suspension. After incubating the cells at 37 °C for 20 minutes, 5 volumes of complete RPMI medium warmed to 37 °C were added to the mixture. The cells were then incubated at 37 °C for a further 5 minutes, allowing the free protein in the medium to bind the unused dye and quench the staining reaction. Finally, the preparation was centrifuged at 1500 RPM for 7 minutes and resuspended in complete culture medium at a density of 10^6 cells/mL, ready for plating.

2.7.7 – Co-cultures of B cells and MAIT cells

Negatively selected, CellTrace-stained B cells were co-cultured with sorted MAIT cells or MAIT cell-depleted T cells in order to investigate their effects on the differentiation status of B cells. Before plating, all cells were resuspended in complete RPMI medium at a density of 10^6 cells/mL. A small aliquot of B cells was kept aside in order to determine the differentiation status of each donor's B cells at time zero. The remaining cells were seeded in 96-well round bottom plates, as follows:

- B cells only (negative control);
- B cells plus MAIT cells (1:1 ratio);
- B cells plus MAIT cell-depleted T cells (1:1 ratio).

All wells were seeded at a final density of 2 x 10^5 cells and in a final volume of 200 µL of medium per well. The plates were then sealed with parafilm and incubated at 37 °C in an atmosphere enriched with 5 % CO_2 for 3 or 7 days. At these times, the supernatants from the co-cultures were removed and frozen at -20 °C for later quantification of antibody isotype levels by cytometric bead array assay, while the co-cultured B cells were immediately stained for differentiation markers CD27 and IgD and analysed by flow cytometry.

2.8 – Flow Cytometry

2.8.1 – Principles of flow cytometry

In flow cytometry, single cells of interest stained with fluorochrome-conjugated antibodies can be studied to find out more about their physical and functional characteristics, as well as separated from other cells on the basis of their properties. Flow cytometry systems are formed of different parts, i.e. fluidics, optics and electronics. The fluidics system is composed of a tubing apparatus carrying a solution called "sheath fluid" through the machine. The sheath fluid constitutes a vehicle for single cell suspensions, which are channelled in the centre of its stream through a nozzle and towards an "interrogation point". The interrogation point is the key site of the optics system, which is composed of a set of lasers, filters, mirrors and photomultiplier tubes. The lasers used in flow cytometry machines are typically identified by the colour of visible light they are excited by, e.g. as violet (405 nm), blue (488 nm) and red (640 nm). Light from the lasers hits cells at the interrogation point, exciting the fluorochrome-conjugated antibodies they are stained with and causing them to emit fluorescence (**Figure 2.7**).

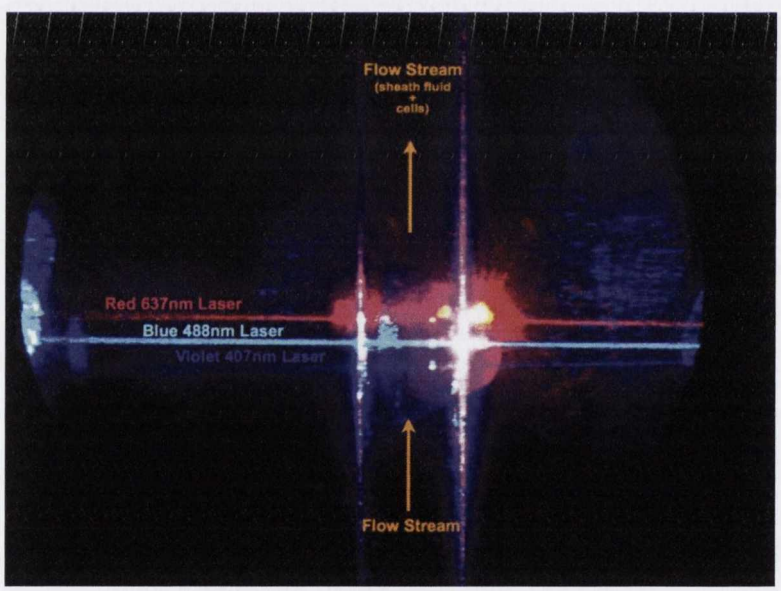


Figure 2.7. Laser light crosses the sheath fluid stream at the interrogation point of a flow cytometer. Image courtesy of the Flow Cytometry Core Facility of the New York University College of Dentistry (www.nyu.edu).

This emitted light is collected by detectors placed either in front of the laser source (forward scatter channel/FSC) or at a 90° angle (side scatter channel/SSC and fluorescence detectors). Amongst these detectors, the forward and side scatter channels collect

information regarding the physical properties of cells, specifically their size (FSC) and their complexity or granularity (SSC). The other detectors are serviced by a system of mirrors and bandpass filters that allow them to collect fluorescence at specific wavelengths. Photomultiplier tubes can amplify the signal detected before it is sent on for digitization and interpretation. **Figure 2.8** gives a schematic representation of the workings of detectors in a flow cytometer.

While both fluidics and optics are found in the main body of a flow cytometer, its electronics are mostly external and include a computer and dedicated software. Once collected, the fluorescent signal is converted into digital form and presented graphically on a computer screen. This allows the operator to display and analyse it as necessary.

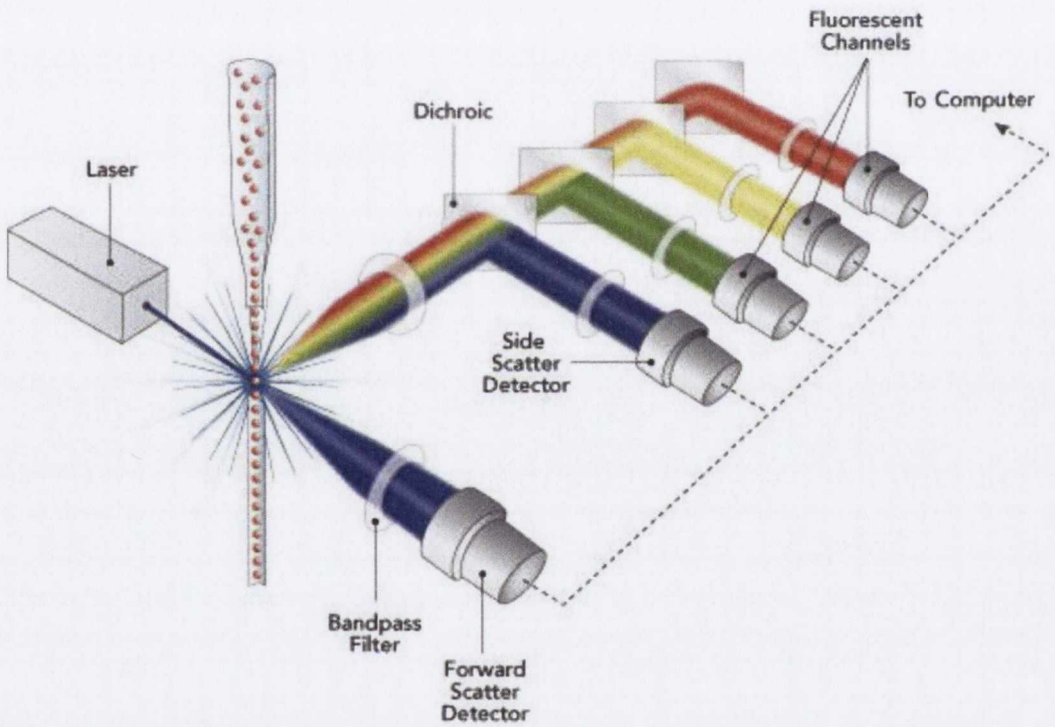


Figure 2.8. Schematic representation of light detectors in a flow cytometer. Cells hit by laser light at the interrogation point emit fluorescence. Specific fluorescence wavelengths are selected by a system of bandpass filters and dichroic mirrors, and collected by detectors (forward scatter detector, side scatter detector and fluorescent channel detectors). Following detection, the signal is digitised and sent to a computer for further analysis. Image courtesy of Semrock (www.semrock.com).

The flow cytometry systems employed during this study were of two types. Standard flow cytometers, in which cells are interrogated and then discarded into a waste collection vessel, were used to gather evidence about the properties of immune cell subsets. Operator-assisted fluorescence-activated cell sorting, on the other hand, was employed to recover fluorochrome-stained cells following their selection by the cytometer. In sorting systems,

cells of interest are identified at the interrogation point on the basis of their fluorescence emission, then allowed to separate into a steady stream of single droplets, which are given a positive or negative charge. Their charge causes them to be attracted to oppositely-charged "deflection plates" and collected in separate vessels as required (**Figure 2.9**).

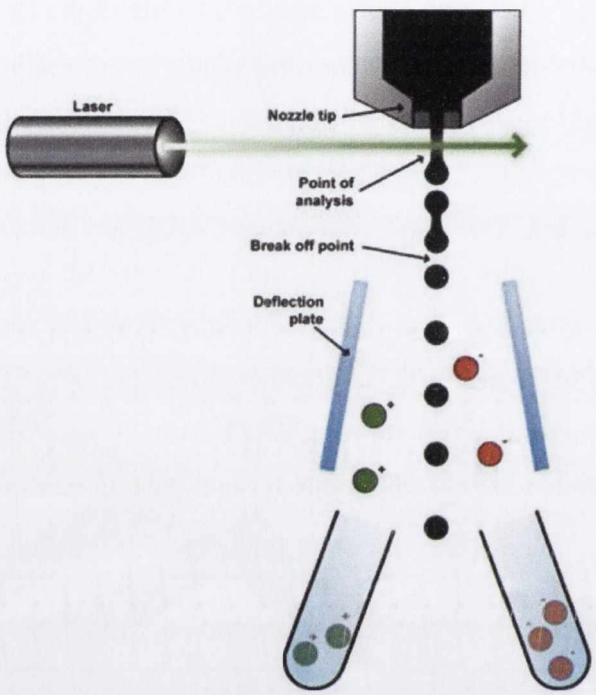


Figure 2.9. Schematic representation of fluorescence-activated cell sorting. In a sorting system, cell of interest are identified at the point of analysis following interrogation by a laser. They are then allowed to separate in single droplets of fluid and given a positive or negative charge. The droplets are selected as they pass between oppositely-charged deflection plates, or eliminated if devoid of charge. Image courtesy of Abcam (www.abcam.com).

2.8.2 – Index of immune cell subsets detected by flow cytometry

The cell subsets detected in this study included B, T, NK cells and their subpopulations, as summarized in **Table 2.10**.

iNKT cell frequencies were also determined in two different ways, using either an anti-invariant-TCR (iTCR) antibody or a CD1d tetramer. The antibody recognizes the junction between the Vα24 and Jα18 chains found in the TCR of iNKT cells; the tetramer is a synthetic compound constituted of four molecule of CD1d loaded with PBS-57, an α-GalCer analogue. The two methods detect iNKT cells at comparable frequencies,[179] however the anti-iTCR antibody is incapable of distinguishing between cells expressing the Vβ11 chain, i.e. iNKT cells, and other β chains (V.P. O'Reilly, unpublished data). The tetramer,

conversely, specifically marks iNKT cells on the basis of their ability to bind α-GalCer presented through CD1d.

Table 2.10. Summary of phenotyped B, T and NK cell populations

Cell subset	Phenotype
B cell subsets	
B cells (as per TruCount test)	$CD45^+$ $CD19^+$
Transitional B cells	$CD19^+$ $CD24^{high}$ $CD38^{high}$
Naive B cells	$CD19^+$ $CD27^-$ IgD^+
Unswitched memory B cells	$CD19^+$ $CD27^+$ IgD^+
Class-switched memory B cells	$CD19^+$ $CD27^+$ IgD^-
Double negative B cells	$CD19^+$ $CD27^-$ IgD^-
Total IgD^+ B cells	$CD19^+$ IgD^+
Plasmablasts	$CD19^+$ $CD24^-$ $CD38^{high}$
T cell subsets	
T cells (as per TruCount test)	$CD45^+$ $CD3^+$
iNKT cells (with anti-iTCR antibody)	$CD3^+$ Vα24-Jα18
iNKT cells (with CD1d Tetramer)	$CD3^+$ Tetramer-binding$^+$
Vδ1 γδ T cells	$CD3^+$ $V\delta1^+$
Vδ2 γδ T cells	$CD3^+$ $V\delta2^+$
Vδ3 γδ T cells	$CD3^+$ $V\delta3^+$
MAIT cells	$CD3^+$ $V\alpha7.2^+$ $CD161^{high}$
Other lymphocyte subsets	
NK cells (as per TruCount test)	$CD45^+$ $CD3^-$ CD16/$CD56^+$
NT cells	$CD3^+$ $CD56^+$

2.8.3 – Immunophenotyping

Prior to the phenotyping of B, T and NK cell populations, LIVE/DEAD Fixable Aqua dead cell stain was reconstituted with 50 μL DMSO per vial. 100 μL of EDTA whole blood were added to flow cytometry tubes containing appropriate antibody panels and 1 μL of the reconstituted dead cell stain, vortexed and incubated for 15 minutes at room temperature in the dark. Red blood cells were lysed by adding 1 mL of FACS Lysing Solution to each tube, vortexing and incubating for a further 15 minutes at room temperature in the dark. The tubes were then centrifuged at 1500 RPM for 7 minutes. After discarding the supernatants, cells were washed with 2 mL of PBA per tube, vortexed and centrifuged again at 1500 RPM for 7 minutes. Finally, the supernatants were discarded and the cells were resuspended in 0.5 % PFA (paraformaldehyde). Samples were acquired with a Cyan ADP flow cytometer within 12 hours of their fixation.

2.8.4 – Intracellular cytokine staining and activation marker upregulation

As staining of whole blood had previously been performed to determine the phenotype of immune populations, a whole blood approach was also adopted to assess cytokine production and activation marker upregulation by T cells and MAIT cells. This methodology did not require the use of PBMC preparations, with multiple advantages over the protocols traditionally used in the laboratory. Indeed, it was not only quicker to perform, but also improved the final yield of cells, avoiding loss of material during the preparation of samples. In addition to this, as unmanipulated whole blood was used, the responses reported in this thesis for unstimulated samples can be considered a direct reflection of the baseline status of cells. The method, originally by BD Biosciences, was applied as previously described by Meddows-Taylor and colleagues,[180] with some modifications. All blood samples were processed within 4 hours of collection. The markers investigated were:

- cytokines TNFα, IFNγ, IL-4, IL-10, IL-17a and IL-22;
- CD69 and CD40L, early activation markers expressed by T cells within 2 to 4 hours of their stimulation. The functions and ligand of CD69 are not currently well known, however its upregulation has long been used as an indicator of T cell proliferation and cytokine production *in vitro*.[181] CD40L's function is to mediate interactions between T cells and APCs by binding CD40, which is constitutively expressed on the surface of B cells, macrophages and DCs; its upregulation marks T cell activation and suggests an intact ability to interact with these cell types.[182]

15 mL conical bottom polypropylene tubes were used in this protocol for incubations as they had previously been shown by BD Biosciences to be the type of vessel most suitable for the assay. For all determinations, whole blood was left unstimulated or incubated with either:

- 1 µg/mL anti-CD3 and 10 µg/mL anti-CD28 antibodies;
- 10 ng/mL PMA and 1 µg/mL ionomycin. An equal volume of non-complete RPMI medium was added to all blood samples stimulated with PMA and ionomycin.

For cytokine determination, 10 µg/mL brefeldin A (BFA) were added to both unstimulated and stimulated tubes. Similarly, 1x monensin was added to both unstimulated and stimulated tubes, alongside 3 µL of anti-CD40L-PE antibody, when studying CD40L upregulation. Neither BFA nor monensin were required for the determination of CD69 upregulation. After adding all the required reagents, the tubes were gently vortexed and incubated at 37 °C in 5 % CO_2 for either 8 hours (cytokines) or 4 hours (activation markers), with the caps slightly loosened. It should be noted that downregulation of the TCR, and therefore of Vα7.2, was

noticed in whole blood samples stimulated with anti-CD3 antibody, particularly for incubations longer than 8 hours and for concentrations of anti-CD3 antibody equal to 5 μg/mL and over (data not shown). This influenced the choice of the incubation times and concentration of anti-CD3 antibody used in these experiments, as detection of MAIT cells relies on the presence of detectable Vα7.2.

At the end of the incubation, EDTA solution was added to each tube at a final concentration of 2 mM. The tubes were then vortexed vigorously and incubated at room temperature for 15 minutes. The material was vortexed again on high setting for 10 seconds, then transferred into previously-labelled flow cytometry tubes, using 200 μL of blood for cytokine determination and 100 μL for CD40L and CD69 analysis. Anti-CD161-PerCp.Cy5.5 and anti-Vα7.2-APC surface antibodies were added to the flow cytometry tubes alongside an appropriate amount of dead cell stain. The samples were then incubated at room temperature for 15 minutes in the dark. Following surface staining, 1 or 2 mL of 1x BD FACS Lysing solution were added to each tube, depending on the amount of blood to lyse. The tubes were mixed gently and incubated for 10 minutes at room temperature, then washed with 2 mL PBA each and centrifuged at 1500 RPM for 7 minutes.

After lysis, cells were permeabilised with 50 μL of 0.2 % saponin solution per tube, vortexing and incubating at 4 °C for 10 minutes in the dark. Antibodies for intracellular staining were added, following dilution in 0.2 % saponin solution up to a total volume of 50 μL. In addition to cytokines, CD3, CD4 and CD8 were always stained for intracellularly, as these markers showed a tendency to downregulate following cell stimulation with PMA and ionomycin (data not shown). Anti-CD69-PE antibody was also used for intracellular staining throughout these experiments, in order to measure both surface and intracellular stores of this molecule. Upon addition of the antibodies, the tubes were vortexed and incubated at 4 °C for 30 minutes in the dark. They were then washed with 2 mL PBA and centrifuged at 1500 RPM for 7 minutes. After discarding the supernatant, they were fixed with 1 % PFA for 30 minutes at 4 °C in the dark, washed with 2 mL of PBA and resuspended in 200 μL of the same buffer. All samples were run on a Cyan ADP flow cytometer within 12 hours of their fixation.

2.8.5 – Markers of B cell differentiation after co-culture with MAIT cells

Following co-culture with MAIT cells or MAIT cell-depleted T cells, B cells were assessed for their expression of CD27 and IgD, which together define three distinct

populations: naïve B cells, unswitched memory B cells and class-switched memory B cells. After removing and storing the supernatants, the co-cultured cells were transferred to flow cytometry tubes, washed with 2 mL of PBS and centrifuged at 1500 RPM for 7 minutes. LIVE/DEAD Fixable Aqua dead cell stain, reconstituted with 50 μL of DMSO to form a stock solution, was diluted 1:1000 in PBS. A staining mix, including 40 μL of diluted dead cell stain plus appropriate antibodies for the surface markers of interest, was added to the flow cytometry tubes after discarding the supernatants. After incubating at room temperature for 15 minutes in the dark, the tubes were washed with 2 mL of PBS, centrifuging again at 1500 RPM for 7 minutes. The cells were acquired on a FACSCanto II flow cytometer immediately after staining, forgoing fixation.

2.8.6 – Analysis of flow cytometry data

This chapter refers to the analysis of flow cytometry data obtained from immunophenotyping, intracellular cytokine staining and activation marker upregulation studies, as well as from co-culture experiments. **Figure 2.10** shows the gating strategy adopted. For the gating strategy used during analysis of CBA (cytometric bead array) assays, see chapter 2.8.7.

FMO (fluorescence minus one) controls, in which all antibodies in a cell subset-specific panel are included, except for one, were used to aid the gating of immune populations. For immunophenotyping, blood from at least one healthy control was run alongside that of patients on any given day, as a quality control. Although blood samples were always processed within 4 hours of collection, a dead cell stain was always included, in order to exclude dead cells from analysis.

2.8.7 – Cytometric Bead Array (CBA) assay

A flow cytometry-based CBA assay was employed to determine the levels of IgA, IgM and IgG antibodies secreted by B cells during 3 or 7 day co-cultures with MAIT cells or MAIT cell-depleted T cells. The CBA assay is a sandwich method, in that beads of known size and fluorescence bind the analyte, which is then bound by a fluorescent detection reagent. Events possessing the fluorescence of both the beads and the detection reagent can be detected by flow cytometry. Due to intrinsic assay limitations, IgM and IgA detection was multiplexed, while IgG antibodies had to be quantified separately.

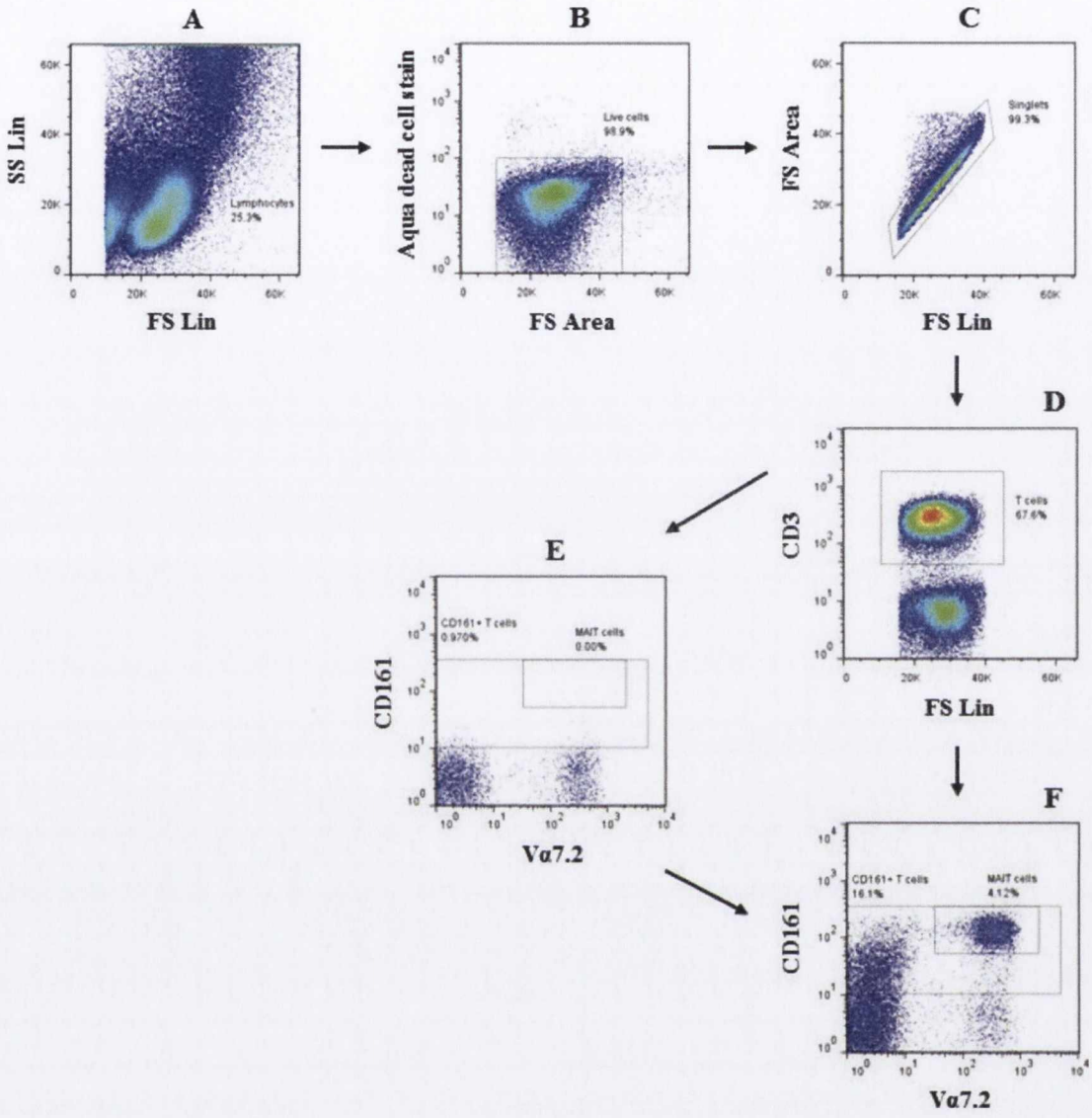


Figure 2.10. Gating strategy for analysis of flow cytometry data. Lymphocytes were initially selected on the basis of their physical characteristics in an FS Lin (Forward Scatter, Linear) vs SS Lin (Side Scatter, Linear) dot plot (A). Live cells, showing as negative following staining with LIVE/DEAD Fixable Aqua dead cell stain, were then identified (B). Doublet analysis allowed to exclude doublets and only analyse singlets (C). The parent population of interest, i.e. T, B or NK cells, was gated (D). With the help of FMO controls (E) subpopulations of interests were defined within the parent populations (F).

Pellets of lyophilised standard were reconstituted in 1 mL each of the supplied Assay Diluent and allowed to equilibrate at room temperature for 15 minutes. The stocks obtained were used directly (for IgM and IgA determinations) or further diluted 1:31 with assay diluent (for IgG determinations) to obtain top standards. Both top standards were then serially diluted 1:2 8 times, up to a final dilution of 1:256. **Table 2.11** summarises the

concentrations of the top and diluted standards used. A further tube containing only assay diluent was used as a zero-concentration standard.

Table 2.11. Concentrations of the standards used in CBA assays.

	Concentration in ng/mL in each serial dilution tube								
Assay	**Top standard**	**1:2**	**1:4**	**1:8**	**1:16**	**1:32**	**1:64**	**1:128**	**1:256**
IgM/IgA	2730	1365	682.5	341.3	170.6	85.3	42.7	21.3	10.7
IgG	430	215	107.5	53.8	26.9	13.4	6.7	3.4	1.7

50x Capture Beads were diluted to 1x in the Capture Bead Diluent provided; similarly, 50x PE Detection Reagent was diluted to 1x in Detection Reagent Diluent. In a 96-well round bottom plate, 25µL of diluted capture beads were added to 25 µL of either standard or medium samples from the co-cultures, mixed gently and incubated at room temperature in the dark for 1 hour. At the end of the incubation, the wells were washed with 200 µL of Wash Buffer and the plates centrifuged at 200 g for 5 minutes. After removing the supernatant, 25 µL of diluted detection reagent were added to the wells, and the plates incubated at room temperature in the dark for 2 hours. The plates were again washed with 200 µL wash buffer and centrifuged at 200 g for 5 minutes. Following removal of the supernatant and resuspension in 100 µL of wash buffer, the samples were immediately acquired on a FACSCanto II flow cytometer. **Figure 2.11** presents the gating strategy used during acquisition. Data from the assay were collected as fluorescence intensities in the PE channel.

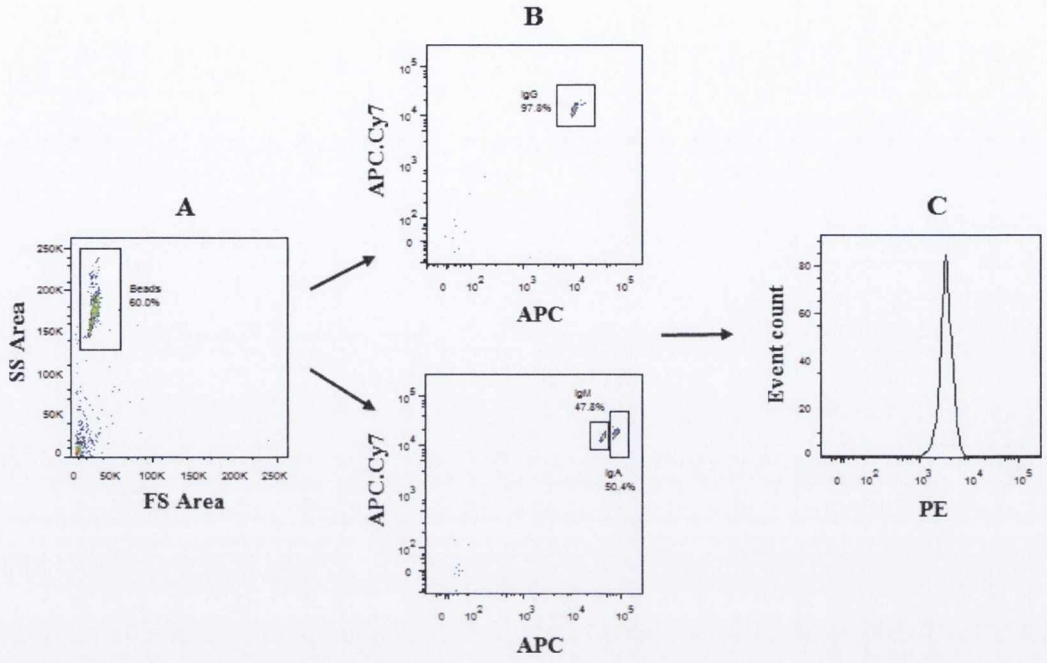


Figure 2.11. Gating strategy for CBA assay acquisition. Beads were initially selected on the basis of their physical characteristics in a forward scatter (FS) versus side scatter (SS) dot plot (A). Populations of IgG-positive (top) or IgM-positive and IgA-positive (bottom) events were then identified (B). Data for each population were collected as fluorescence intensities in the PE channel (C).

When analysing the data, the immunoglobulin concentration of the unknown samples was determined by interpolating their geometric mean fluorescence intensity (MFI) values with those obtained for standard controls of known concentration. **Figure 2.12** shows peaks obtained from standards for the determination of IgM and IgA antibodies.

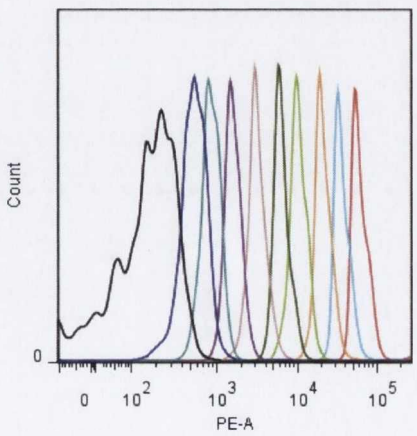


Figure 2.12. MFI peaks for IgM/IgA antibodies standards. The image shows an overlay of the fluorescence intensity peaks obtained from standards used for the determination of IgM antibodies. The peaks correspond to concentrations of 2730 ng/mL (red), 1365 ng/mL (sky blue), 682.5 ng/mL (orange), 341.3 ng/mL (neon green), 170.6 ng/mL (dark green), 85.3 ng/mL (caramel), 42.7 ng/mL (purple), 21.3 ng/mL (teal), 10.7 ng/mL (dark blue) and 0 ng/mL (black), respectively.

2.8.8 – T, B and NK cell enumeration (TruCount test)

Flow cytometry data are expressed as relative frequencies, however absolute counts of immune cell subsets were also determined in the present investigation. Conversion of frequencies into absolute counts was achieved through the use of TruCount tubes and Multitest 6-color TBNK Reagent, both by BD Biosciences. 5 μL of TBNK reagent, an antibody cocktail against T, B and NK cells, were added to TruCount tubes, which contain known quantities of pelleted beads. 50 μL of EDTA whole blood were then reverse-pipetted into each tube and incubated for 15 minutes at room temperature in the dark. Finally, red blood cells were lysed adding 450 μL of FACS Lysing Solution and incubating at room temperature in the dark for a further 15 minutes; the samples were not washed, as the buffer is designed to allow a "lyse-no-wash" preparation procedure. Processed samples were run on a FACSCanto II flow cytometer in the Central Pathology Laboratory of St. James's Hospital within 48 hours.

TruCount test reports included absolute counts and frequencies of total B cells, total T cells, total NK cells and total lymphocytes in the sample; absolute counts were expressed as number of cells/μL of blood. Absolute counts of B and T cell subsets were calculated dividing the absolute count obtained from TruCount tests for the parent population by 100 and then multiplying by the frequencies identified for each cell subset by flow cytometry.

2.8.9 – Purities of isolated B and T cells

The purity of sorted MAIT cells and MAIT cell-depleted T cells, as well as of B cells isolated by negative selection using magnetic beads, was assessed by flow cytometry. 10 μL of B cell and MAIT cell-depleted T cell suspensions were added to 90 μL PBS and stained for 15 minutes at room temperature with 2 μL anti-CD3-Pacific Blue and 1 μL anti-CD19-Pacific Blue antibodies, respectively. No antibodies were added to MAIT cells as they had previously been stained in order to undergo sorting. Following incubation, MAIT cell-depleted T cells and B cells were washed with 2 mL PBS and centrifuged at 1500 RPM for 7 minutes. All samples were then resuspended in 200 μL PBS and immediately run on a FACSCanto II flow cytometer, forgoing fixation. The populations of interest were visualized as follows:

- MAIT cells, as $CD161^{high}$ and $V\alpha7.2^{+}$ events;
- MAIT cell-depleted T cells, as $CD3^{+}$ events;
- B cells, as $CD19^{+}$ events.

Purities were in the range of:

- 91.1 - 96.8 % for MAIT cells;
- 99.4 - 99.9 % for MAIT cell-depleted T cells;
- 96.3 - 99.6 % for B cells.

Figure 2.13 shows flow cytometry dot plots representative of purities obtained for the three cell subsets.

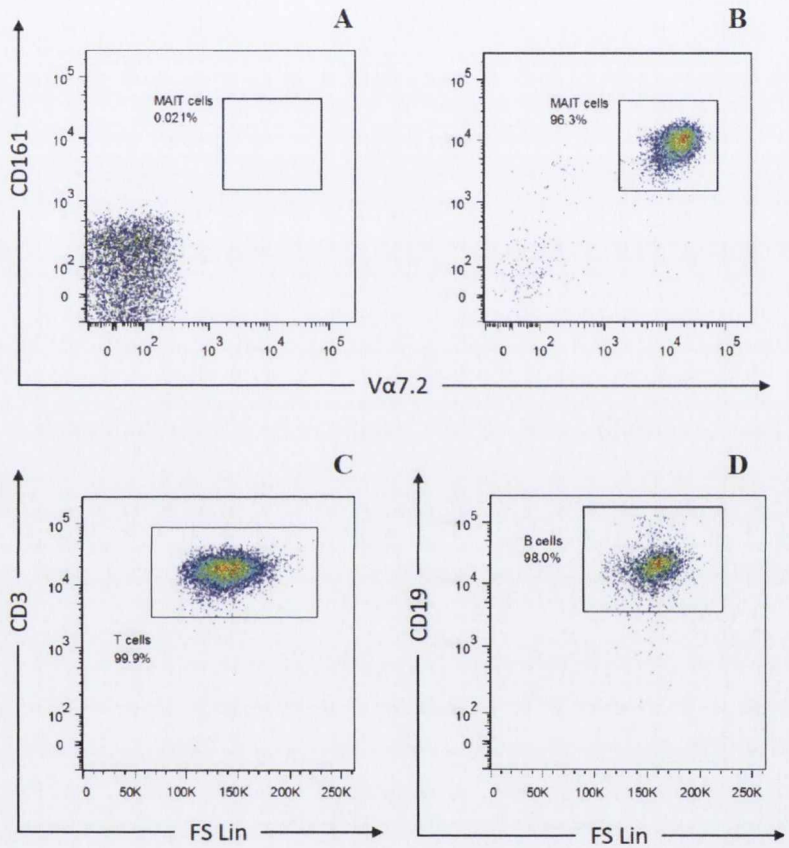


Figure 2.13. Flow cytometry dot plots representative of the purities of isolated B cells, MAIT cells and MAIT cell-depleted T cells. Top-row flow cytometry dot plots show the percentages of events included in a MAIT cell gate in an unstained sample (A) and in a sample sorted with anti-Vα7.2 and anti-CD161 antibodies (B). Bottom-row flow cytometry dot plots show the purities obtained for MAIT cell-depleted T cells (C) and B cells (D).

2.9 – Statistical analysis

Statistical analysis was performed in GraphPad Prism version 5, conservatively assuming all data were non-parametric. Thus, differences between two groups or conditions were defined performing a two-tailed Mann-Whitney test; differences between three or more

groups were probed using the Kruskal-Wallis test plus Dunn's post-hoc test. Results were considered significant for P values lower than 0.05.

Prism 5 did not supply exact P values for Kruskal-Wallis tests, but indicated a p value range:

- * stood for $p < 0.05$;
- ** stood for $p < 0.01$;
- *** stood for $p < 0.001$.

In order to define the discriminatory power of total IgD^+ B cell frequencies as a possible diagnostic test, the individuals recruited to the study were divided in two groups, on the basis of their being affected by a primary immunodeficiency:

- healthy controls and secondary antibody deficiency patients were considered not affected by a primary immunodeficiency (controls);
- CVID, SIgAD and IgG subclass deficiency patients were considered affected by a primary immunodeficiency (patients).

The sensitivity (or true positive rate) of the test was calculated according to the equation (A/A+C), where A stands for true positive and C for false negative results defined using a threshold of 90.3%. The specificity (or true negative rate) of the test was similarly calculated according to the equation (D/B+D), where D stands for true negative and B for false positive results defined using the same 90.3% threshold. A ROC (receiver operating characteristic) curve was also calculated in GraphPad Prism to define the accuracy of the test, i.e. its ability to discriminate between individuals affected and not affected by primary immunodeficiencies. The area under the curve (AUC) obtained was used to express the discriminatory power of the test, which was considered:

- poor, for AUC values of 0.6 to 0.7;
- fair, for AUC values of 0.7 to 0.8;
- good, for AUC values of 0.8 to 0.9;
- excellent, for AUC values of 0.9 to 1.

In chapter 5, correlations between frequencies or absolute counts of innate T cells and other cell types were defined using Spearman's correlation coefficient; a regression line is also shown in correlation graphs. Spearman's correlation coefficient values were interpreted as follows:

- 0 - 0.49, no correlation to weak correlation;
- 0.50 - 0.69, moderate correlation;
- 0.70 - 0.89, strong correlation;
- 0.90 - 1.00, very strong correlation.

CHAPTER 3

ANALYSIS OF CIRCULATING B CELL SUBSETS IN PATIENTS WITH CVID AND OTHER ANTIBODY DEFICIENCIES

3.1 – Introduction

Numerous studies have defined that, notwithstanding its heterogeneity, CVID is characterised by altered frequencies of certain B cell subsets in the blood of patients. In fact, CVID patients often display:[157,5]

- normal or slightly decreased total B cell frequencies;
- increased naïve and sometimes transitional B cell frequencies;
- decreased class-switched memory B cell and plasmablast frequencies.

The "Paris", "Freiburg" and "EUROclass" classification systems have sought to associate B cell phenotyping results with the clinical characteristics of CVID patients. The Paris study[158] made use of two surface markers, CD27 and IgD, to define three different B cell populations, i.e. naïve B cells, unswitched memory B cells and class-switched memory B cells. On the basis of their frequencies, patients were divided in groups MB0 (almost absent memory B cells), MB1 (defective class-switched but normal unswitched memory B cells) or MB2 (normal memory B cells). Most of the 59 CVID patients who participated in the study were classified as MB0 (27 patients, 47 %) and MB1 (19 patients, 33 %), with the least assigned to the MB2 group (11 patients, 19 %). Splenomegaly, lymphoid proliferation and granulomatous disease were all detected at a higher prevalence in group MB0. Splenomegaly also appeared in group MB1, but autoimmunity was found in all three groups.

The study which generated the Freiburg classification[159] employed similar phenotypic markers to subdivide 30 patients in two groups: group I (77 % of the cohort) displayed significantly reduced numbers of class-switched memory B cells, defined as $CD27^+$ IgD^- IgM^-; in group II, on the other hand, the frequencies of this population were comparable to those of healthy controls. Group I patients were further split into group Ia and group Ib on the basis of their frequencies of $CD21^-$ B cells (> 20 % or < 20 % of total B cells, respectively), with CVID patients affected by splenomegaly and autoimmune cytopaenias found to cluster in group Ia. The biological role of $CD21^-$ B cells is unclear at this time; it has been variably suggested that they could constitute a population of polyclonal, IgD^+ innate-like B cells[183] or a subset of anergic, autoreactive naïve B cells.[184] Interestingly, low expression of CD21 has also been found to identify a population of early transitional B cells, characterised by the production of autoreactive antibodies.[185]

The EUROclass trial[160] was a European multicentre study involving 303 patients, carried out with the intent of merging the Paris and Freiburg classifications in a single scheme. The resulting categorisation seeks to identify patients on the basis of their B cell defect, separating them in three groups:

- individuals with absent or almost absent B cells (< 1 %), i.e. with early B cell differentiation defects;
- individuals with severely reduced class-switched memory B cells (< 2 %), i.e. affected by defective GC development;
- individuals with expanded transitional B cells (> 9 %) or $CD21^{low}$ B cells (> 10 %). The defect causing the expansion of these B cell subsets is to date not understood, but these patients often present with complications, particularly lymphadenopathy, which associates with high frequencies of transitional B cells, and splenomegaly, which associates with high frequencies of $CD21^-$ B cells.

Taken together, the Paris, Freiburg and EUROclass studies have had an important impact, ending previous attempts to classify patients on the basis of *in vitro* immunoglobulin production by their B cells and allowing to shed some light on the pathogenic mechanisms of the disease. The three classifications also have prognostic implications, allowing to identify subgroups of patients at higher risk of developing complications.

3.2 – Hypothesis and aims of the chapter

Since the publication of the Paris, Freiburg and EUROclass studies, phenotypic analysis of B cell subsets has emerged as one of the most useful tools for the investigation of CVID, both in a research and in a clinical setting. Phenotyping was therefore employed to define the B cell status of the patients recruited to this study, providing a frame of reference for their comparison with other CVID cohorts. Our hypothesis was that the patients would exhibit a block in B cell maturation at the isotype class-switching stage. More specifically, our aims for this chapter were:

1. to define if B cell maturation was impaired in the cohort of CVID patients recruited, and if so, what differentiation stage this impairment affected. In order to explore this, we determined the frequencies and absolute counts of total B cells, transitional and naïve B cells, unswitched and class-switched memory B cells, $CD27^-$ IgD^- B cells and plasmablasts. Results from CVID patients are presented alongside those from a smaller group of individuals affected by secondary antibody deficiency, acting as internal controls. Some data from patients with selective IgA deficiency/IgG subclass

deficiency, and from a single immunodeficient patient with a query diagnosis, are also included;

2. to determine if a direct link existed between the numbers of naïve and memory B cells available in the circulation of patients and their serum antibody levels. We reasoned that, if a class-switching defect was the main event causing low antibody production, levels of IgM antibodies in the blood of CVID patients would correlate with the frequencies of unswitched memory B cells, while those of IgG and IgA antibodies would not correlate with the frequencies of class-switched memory B cells. In order to investigate this possibility we built on the B cell data gathered by immunophenotyping, probing the existence of statistical correlations between frequencies of naïve, unswitched memory and class-switched memory B cells and the levels of IgM, IgG and IgA antibodies measured in the blood of CVID patients at diagnosis.

3.3 – Phenotypic analysis of circulating B cell subsets in CVID and secondary hypogammaglobulinemia

3.3.1 – Phenotypic analysis of total B, T and NK lymphocytes

Total B, T and NK cell frequencies and absolute numbers were determined simultaneously, using the BD Biosciences TBNK enumeration system described in chapter 2.8.8.

In accordance with the literature,[157] total B cell frequencies were found to be comparable in CVID patients and healthy controls; they were however significantly reduced in in the peripheral blood of secondary antibody deficiency patients ($p < 0.05$). NK and T cell frequencies were unaffected in either patient group (**Figure 3.1**).

With regard to absolute B, T and NK cell counts, CVID and secondary antibody deficiency patients exhibited a generalized lymphopenia, displaying lower numbers of all lymphocyte types in comparison to healthy controls, however only B cell counts were significantly affected in both patient groups ($p < 0.05$ for CVID patients, $p < 0.01$ for secondary antibody deficiency patients, **Figure 3.2**).

Thus, frequencies of T, B and NK cells were comparable in the blood of CVID and healthy age-matched controls, however absolute counts of the three lymphocyte populations

were generally decreased in the circulation of CVID patients in comparison to controls, and significantly so for B cells.

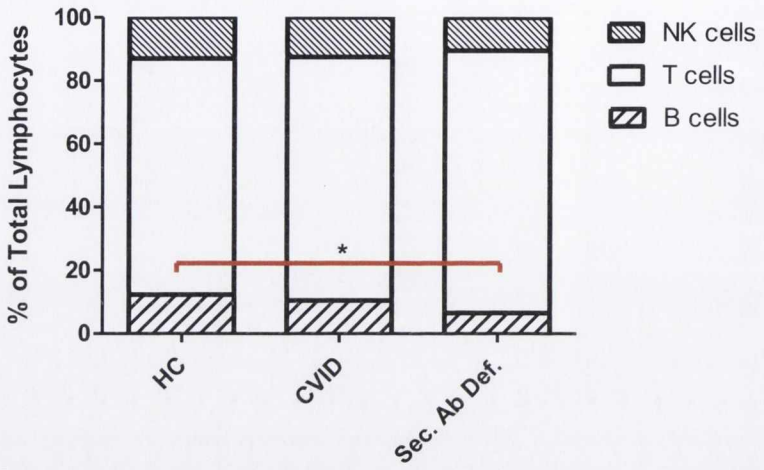


Figure 3.1. Frequencies of T, B and NK cells in the peripheral blood of healthy controls, patients with CVID and patients with secondary antibody deficiency. Whole blood from healthy controls (HC, n = 26), CVID patients (CVID, n = 21) and secondary antibody deficiency patients (Sec. Ab Def., n = 6) was analysed by flow cytometry following staining with Multitest 6-color TBNK Reagent, a cocktail of antibodies recognising B cells ($CD45^+$ $CD19^+$ events), T cells ($CD45^+$ $CD3^+$ events) and NK cells ($CD45^+$ $CD3^-$ $CD16/CD56^+$ events). Statistically significant differences in the frequencies of B, T and NK cells amongst different patient groups were identified performing a Kruskal-Wallis test plus Dunn's post hoc test. * $p < 0.05$, comparing frequencies of total B cells.

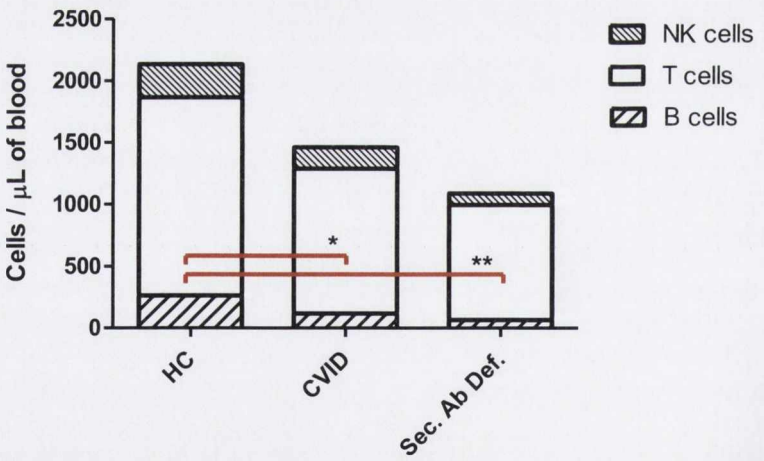


Figure 3.2. Absolute counts of T, B and NK cells in the peripheral blood of healthy controls, patients with CVID and patients with secondary antibody deficiency. Whole blood from healthy controls (HC, n = 26), CVID patients (CVID, n = 21) and secondary antibody deficiency patients (Sec. Ab Def., n = 6) was analysed by flow cytometry following staining with Multitest 6-color TBNK Reagent, a cocktail of antibodies recognising B cells ($CD45^+$ $CD19^+$ events), T cells ($CD45^+$ $CD3^+$ events) and NK cells ($CD45^+$ $CD3^-$ $CD16/CD56^+$ events). Statistically significant differences in the absolute counts of B, T and NK cells amongst different patient groups were identified performing a Kruskal-Wallis test plus Dunn's post hoc test.. * $p < 0.05$; ** $p < 0.01$, comparing absolute counts of total B cells.

3.3.2 – Phenotypic analysis of B cell subsets

Several B cell populations were found to be significantly increased or decreased in the blood of CVID patients. These include subsets defined by markers CD27 and IgD, i.e. naïve, unswitched memory, class-switched memory and double negative ($CD27^-$ IgD^-) B cells, as seen in the representative flow cytometry plots in **Figure 3.3**. It should be noted that four healthy controls had to be excluded from the analysis of these B cell populations, due to anomalies in the distribution of flow cytometry data noticed during acquisition of their samples.

Frequencies of naive B cells, shown in **Figure 3.4**, were significantly increased in the blood of CVID patients in comparison to both healthy controls ($p < 0.01$) and secondary antibody deficiency patients ($p < 0.005$). Absolute counts of naive B cells were the lowest in secondary antibody deficiency patients, in comparison to both healthy controls ($p < 0.01$) and CVID patients ($p < 0.05$). The frequencies and absolute numbers of unswitched memory B cells, on the contrary, were similar in all three groups of individuals (**Figure 3.5**).

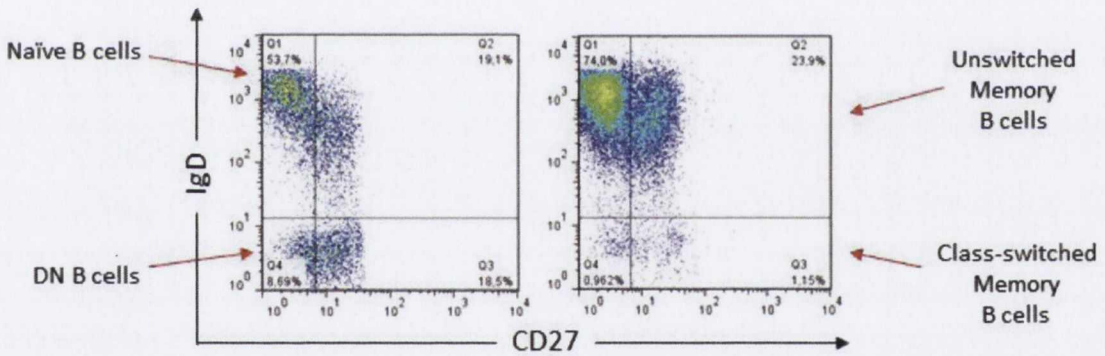


Figure 3.3. Determination of four B cell subsets by CD27/IgD staining. The representative flow cytometry dot plots shown display the four population defined by CD27/IgD staining in whole blood from a healthy control (left) and a CVID patient (right), following gating on $CD19^+$ cells. DN = double negative.

Frequencies and absolute counts of class-switched memory B cells (**Figure 3.6**) were significantly decreased in the peripheral blood of CVID patients in comparison to both healthy controls ($p < 0.005$) and secondary antibody deficiency patients ($p < 0.005$ for frequencies, $p < 0.05$ for absolute counts). Double negative B cells (**Figure 3.7**) behaved in a way similar to class-switched memory B cells, being found at significantly decreased frequencies in CVID patients in comparison to healthy subjects ($p < 0.005$) and secondary antibody deficiency patients ($p < 0.01$); their absolute counts were also decreased in CVID patients in comparison to healthy controls ($p < 0.005$).

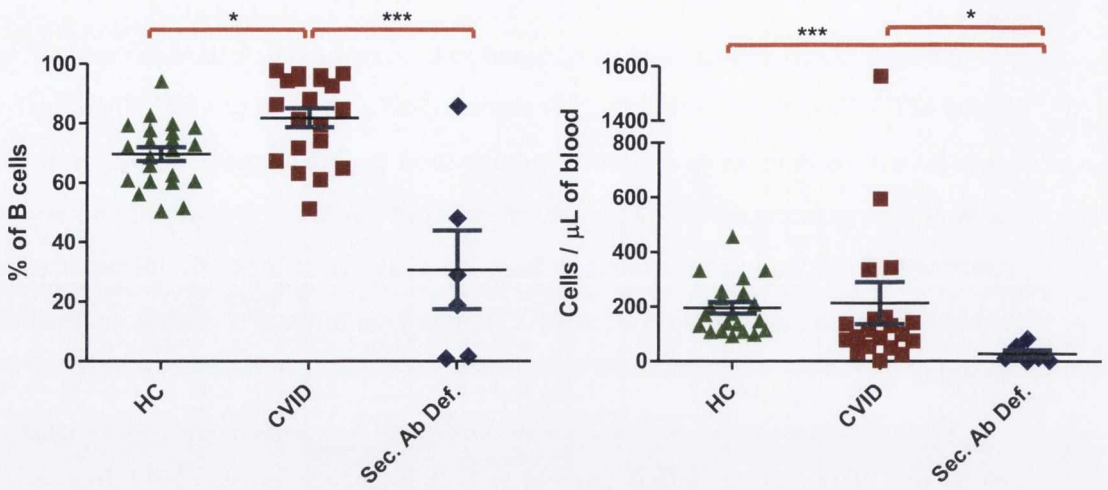


Figure 3.4. Frequencies and absolute counts of naive B cells. The figures show the frequencies (left) and absolute numbers (right) of naive B cells, defined as $CD19^+$ $CD27^-$ IgD^+ events, as determined by flow cytometry in whole blood from healthy controls (HC, n = 22), CVID patients (CVID, n = 20) and secondary antibody deficiency patients (Sec. Ab Def., n = 6). Statistical analysis was performed employing a Kruskal-Wallis test plus Dunn's post hoc test.* $p < 0.05$; *** $p < 0.005$.

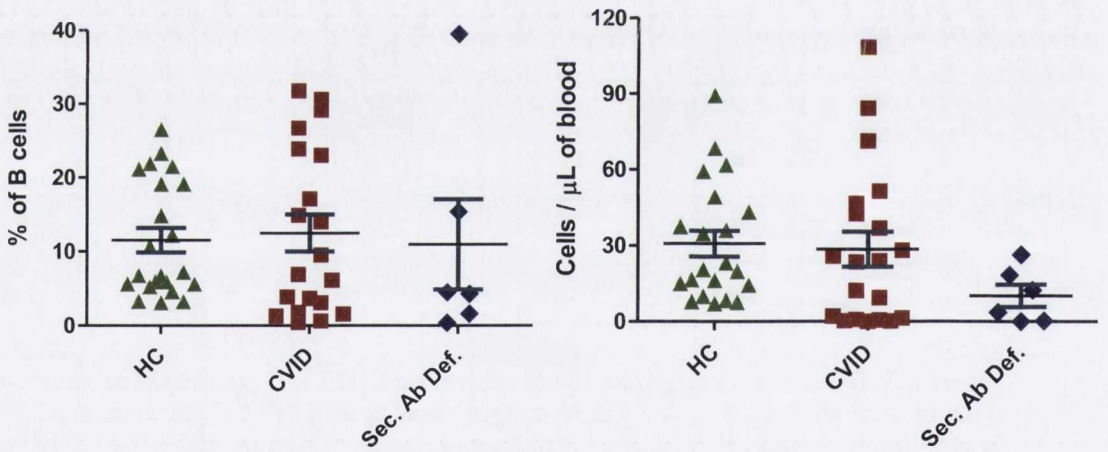


Figure 3.5. Frequencies and absolute counts of unswitched memory B cells. The figures show the frequencies (left) and absolute numbers (right) of unswitched memory B cells, defined as $CD19^+$ $CD27^+$ IgD^+ events, as determined by flow cytometry in whole blood from healthy controls (HC, n = 22), CVID patients (CVID, n = 20) and secondary antibody deficiency patients (Sec. Ab Def., n = 6). Statistical analysis was performed employing a Kruskal-Wallis test plus Dunn's post hoc test.

As three out of four populations described by the association of CD27 and IgD markers were detected at anomalous frequencies in the peripheral blood of CVID patients, an attempt was made to re-analyse the data in a simplified fashion, using only a single marker at a time. Dividing B cells into $CD27^-$ and $CD27^+$ subgroups proved poorly descriptive, as all significances previously identified were lost; **Figure 3.8** shows as an example the results

obtained from the analysis of the $CD27^+$ B cell subset. Analysis of IgD^- and IgD^+ B cells, on the other hand, appeared to be more informative, as IgD^+ B cells were found at significantly higher frequencies in CVID patients than in healthy controls or secondary antibody deficiency patients (**Figure 3.9**).

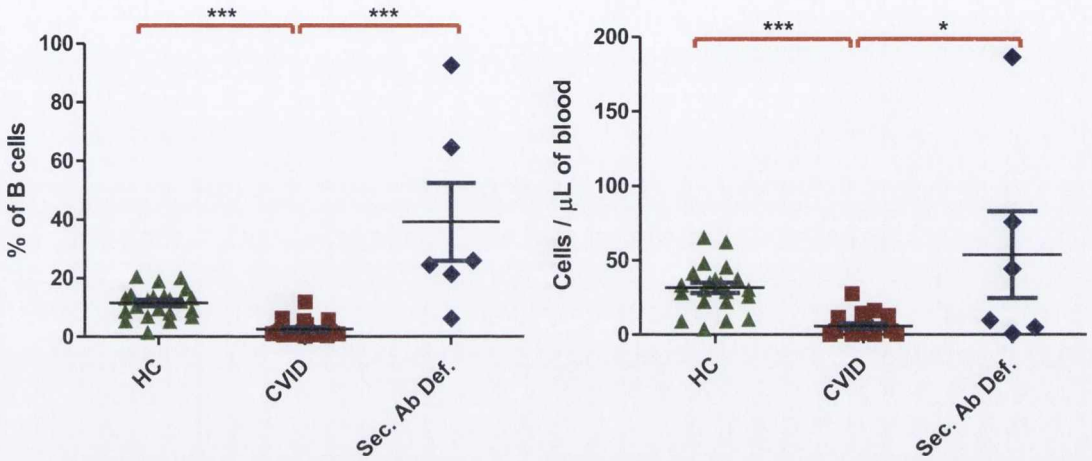


Figure 3.6. Frequencies and absolute counts of class-switched memory B cells. The figures show the frequencies (left) and absolute numbers (right) of class-switched memory B cells, defined as $CD19^+$ $CD27^+$ IgD^- events, as determined by flow cytometry in whole blood from healthy controls (HC, n = 22), CVID patients (CVID, n = 20) and secondary antibody deficiency patients (Sec. Ab Def., n = 6). Statistical analysis was performed employing a Kruskal-Wallis test plus Dunn's post hoc test. * $p < 0.05$; *** $p < 0.005$.

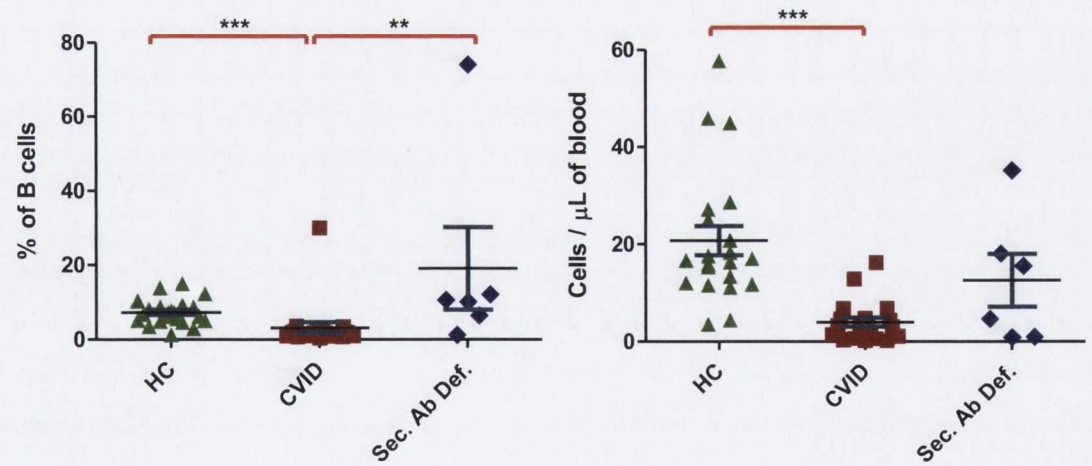


Figure 3.7. Frequencies and absolute counts of double negative B cells. The figures show the frequencies (left) and absolute numbers (right) of double negative B cells, defined as $CD19^+$ $CD27^-$ IgD^- events, as determined by flow cytometry in whole blood from healthy controls (HC, n = 22), CVID patients (CVID, n = 20) and secondary antibody deficiency patients (Sec. Ab Def., n = 6). Statistical analysis was performed employing a Kruskal-Wallis test plus Dunn's post hoc test. ** $p < 0.01$; *** $p < 0.005$.

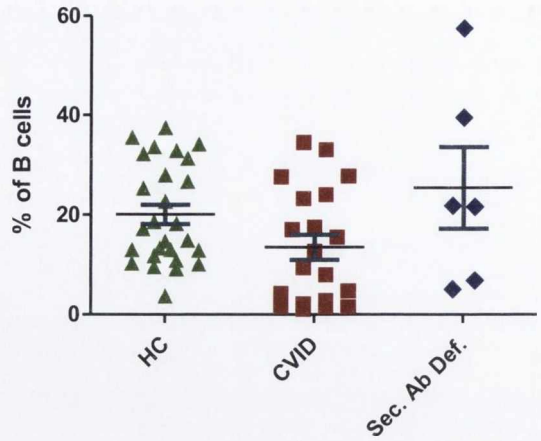


Figure 3.8. Frequencies of CD27$^+$ B cells. The figure shows the frequencies of CD19$^+$ CD27$^+$ B cells, as determined by flow cytometry in whole blood from healthy controls (HC, n = 26), CVID patients (CVID, n = 20) and secondary antibody deficiency patients (Sec. Ab Def., n = 6). Statistical analysis was performed employing a Kruskal-Wallis test plus Dunn's post hoc test.

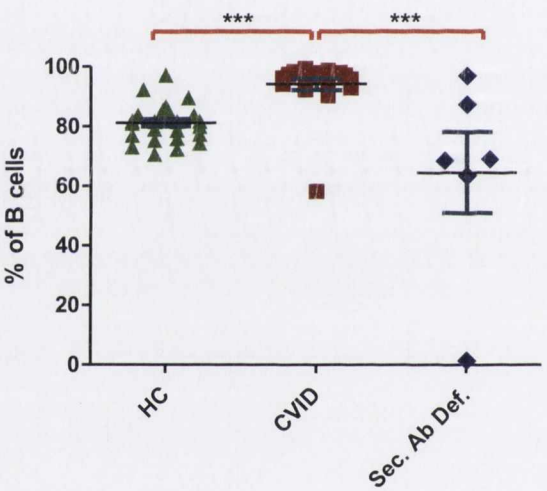


Figure 3.9. Frequencies of IgD$^+$ B cells. The figure shows the frequencies of CD19$^+$ IgD$^+$ B cells, as determined by flow cytometry in whole blood from healthy controls (HC, n = 26), CVID patients (CVID, n = 20) and secondary antibody deficiency patients (Sec. Ab Def., n = 6). Statistical analysis was performed employing a Kruskal-Wallis test plus Dunn's post hoc test. *** $p < 0.005$.

Frequencies of plasmablasts, identified in this study as CD19$^+$ CD38^{high} CD24$^-$ cells, were significantly reduced in CVID in comparison to healthy individuals ($p < 0.005$); counts of this population were additionally found to be significantly lower in both CVID ($p < 0.005$) and secondary antibody deficiency patients ($p < 0.05$) than in controls (**Figure 3.10**).

Analysis of phenotyping data for transitional B cells did not yield significant results. Nonetheless, as shown in **Figure 3.11**, the peripheral blood frequencies of this cell subset appeared increased for a number of CVID patients and for one of the secondary antibody

deficiency patients; their absolute counts were also raised in three patients belonging to the CVID cohort.

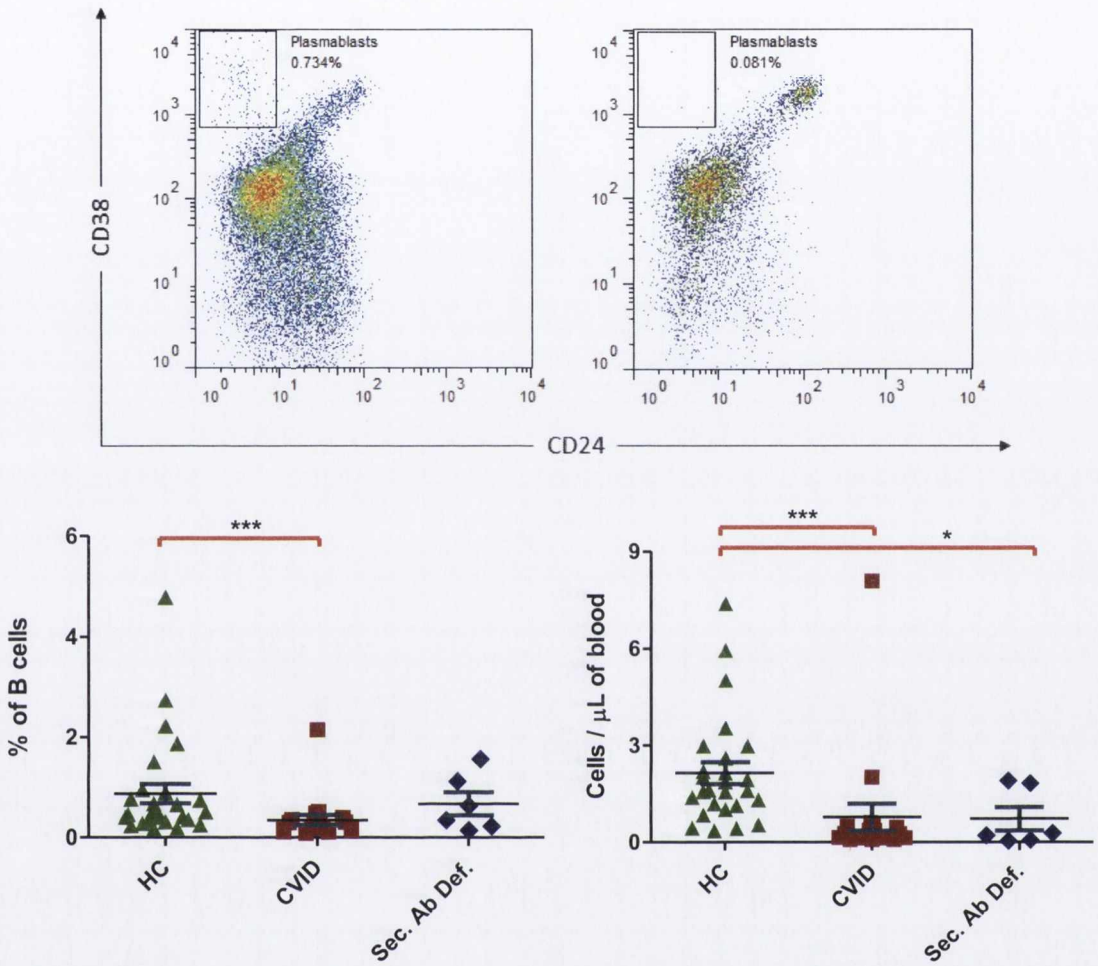


Figure 3.10. Representative dot plots, frequencies and absolute counts of plasmablasts. The representative flow cytometry dot plots in the figure (top) show plasmablasts, detected as $CD24^{-}$ $CD38^{high}$ events following gating on $CD19^{+}$ B cells, in whole blood from a healthy control (left) and a CVID patient (right). The scatter plots (bottom) show the frequencies (left) and absolute numbers (right) of plasmablasts, as determined by flow cytometry in whole blood from healthy controls (HC, n = 27), CVID patients (CVID, n = 19) and secondary antibody deficiency patients (Sec. Ab Def., n = 6). Statistical analysis was performed employing a Kruskal-Wallis test plus Dunn's post hoc test. * $p < 0.05$; *** $p < 0.005$.

Thus, anomalies appeared in the frequencies and absolute counts of a number of B cell subsets. More specifically, these patients displayed significantly increased percentages of naïve B cells, as well as significantly decreased frequencies of memory B cells, plasmablasts and $CD27^{-}$ IgD^{-} B cells, in comparison to healthy controls. Percentages of transitional B cells and unswitched memory B cells were generally similar to those found in the circulation of healthy donors, although some patients appeared to display increased frequencies of the

former cell type. In terms of absolute counts, numbers of naïve, transitional and unswitched memory B cells in the circulation of CVID patients were comparable to those found in healthy donors, while their counts of circulating class-switched memory B cells, plasmablasts and $CD27^-$ IgD^- B cells were significantly reduced.

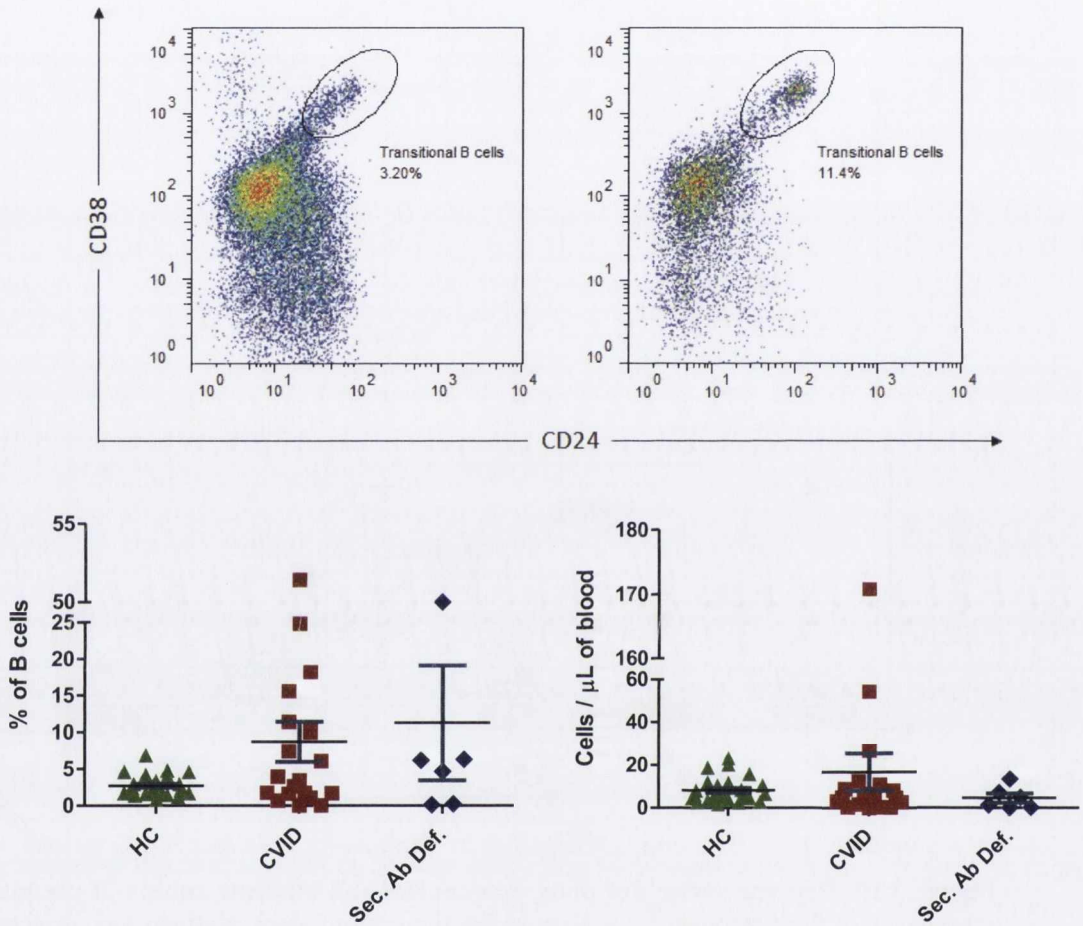


Figure 3.11. Representative dot plots, frequencies and absolute counts of transitional B cells. The representative flow cytometry dot plots in the figure (top) show transitional B cells, detected as $CD24^+$ $CD38^{high}$ events following gating on $CD19^+$ B cells, in whole blood from a healthy control (left) and a CVID patient (right). The scatter plots (bottom) show the frequencies (left) and absolute numbers (right) of transitional B cells, as determined by flow cytometry in whole blood from healthy controls (HC, n = 27), CVID patients (CVID, n = 20) and secondary antibody deficiency patients (Sec. Ab Def., n = 6). Statistical analysis was performed employing a Kruskal-Wallis test plus Dunn's post hoc test.

3.4 – Phenotypic analysis of circulating B cell subsets in SIgAD and IgG subclass deficiency

This patient group was formed by only three individuals. One of them was affected by selective IgA deficiency (SIgAD), while the remaining two presented with both SIgAD and IgG subclass deficiency. The latter two individuals were also part of the same family unit. This chapter presents a selection of results from these patients, and a brief summary of the data not shown. It should be noted that four healthy controls had to be excluded from the analysis of naïve, unswitched memory, class-switched memory and $CD27^-$ IgD^- B cells, due to anomalies in the distribution of flow cytometry data noticed during acquisition of their samples.

The three patients displayed frequencies and absolute counts similar to those seen in healthy controls for total B cells, transitional B cells, naïve B cells (**Figure 3.12**), unswitched memory B cells, class-switched memory B cells (**Figure 3.13**) and plasmablasts.

Frequencies and absolute counts of $CD27^-$ IgD^- B cells, however, were significantly decreased in their peripheral blood ($p = 0.01$ and $p = 0.03$, respectively; **Figure 3.14**), while frequencies of total IgD^+ B cells were significantly increased ($p = 0.01$; **Figure 3.15**).

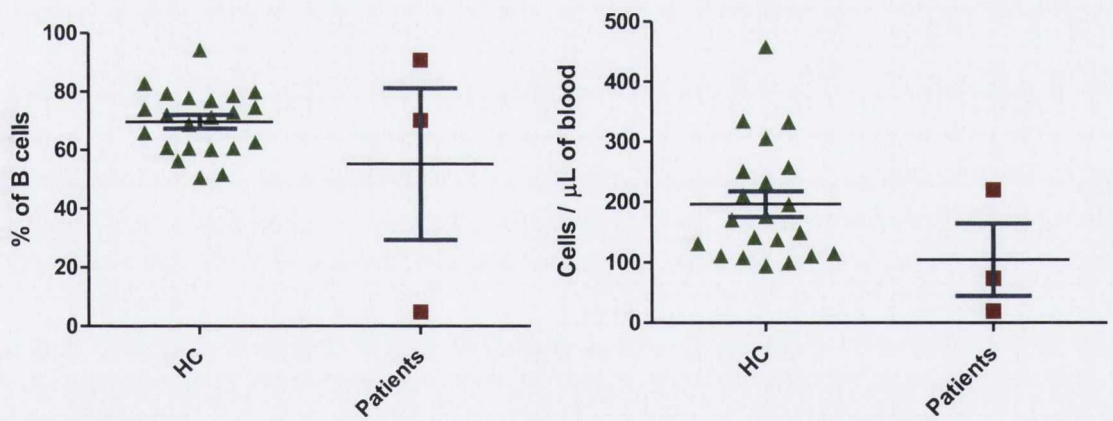


Figure 3.12. Frequencies and absolute counts of naïve B cells. The figures show the frequencies (left) and absolute numbers (right) of naïve B cells, defined as $CD19^+$ $CD27^-$ IgD^+ events, as determined by flow cytometry in whole blood from healthy controls (HC, n = 22) and patients with SIgAD/IgG subclass deficiency (Patients, n = 3). Statistical analysis was performed employing a two-tailed Mann-Whitney test.

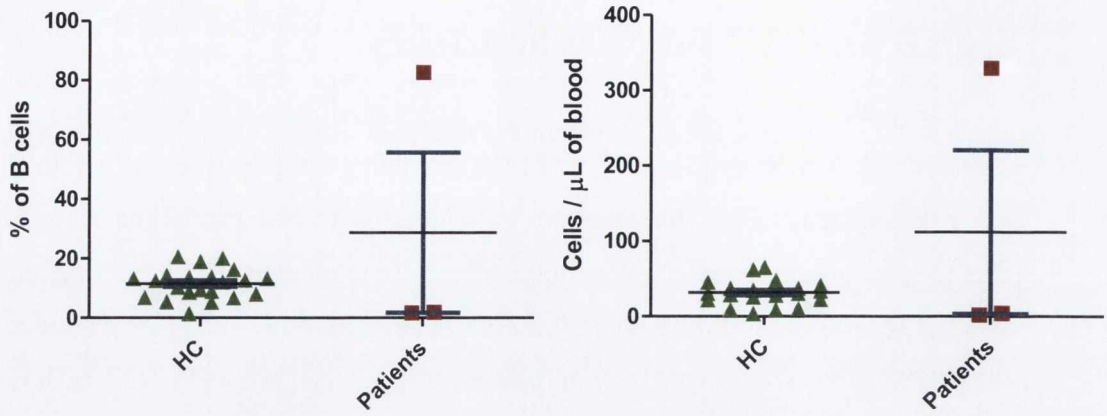


Figure 3.13. Frequencies and absolute counts of class-switched memory B cells. The figures show the frequencies (left) and absolute numbers (right) of class-switched memory B cells, defined as $CD19^+$ $CD27^+$ IgD^- events, as determined by flow cytometry in whole blood from healthy controls (HC, n = 22) and patients with SIgAD/IgG subclass deficiency (Patients, n = 3). Statistical analysis was performed employing a two-tailed Mann-Whitney test.

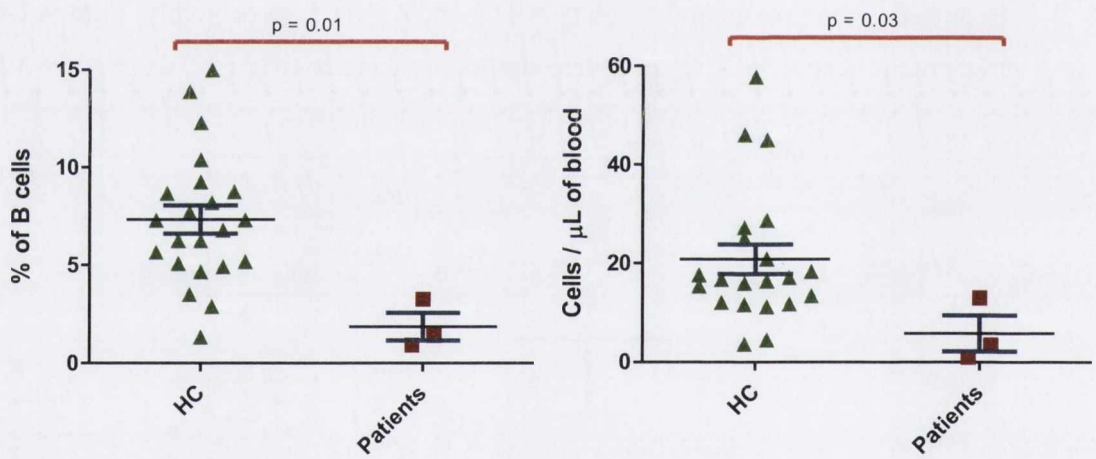


Figure 3.14. Frequencies and absolute counts of $CD27^-$ IgD^- B cells. The figures show the frequencies (left) and absolute numbers (right) of $CD19^+$ $CD27^-$ IgD^- B cells, as determined by flow cytometry in whole blood from healthy controls (HC, n = 22) and patients with SIgAD/IgG subclass deficiency (Patients, n = 3). Statistical analysis was performed employing a two-tailed Mann-Whitney test.

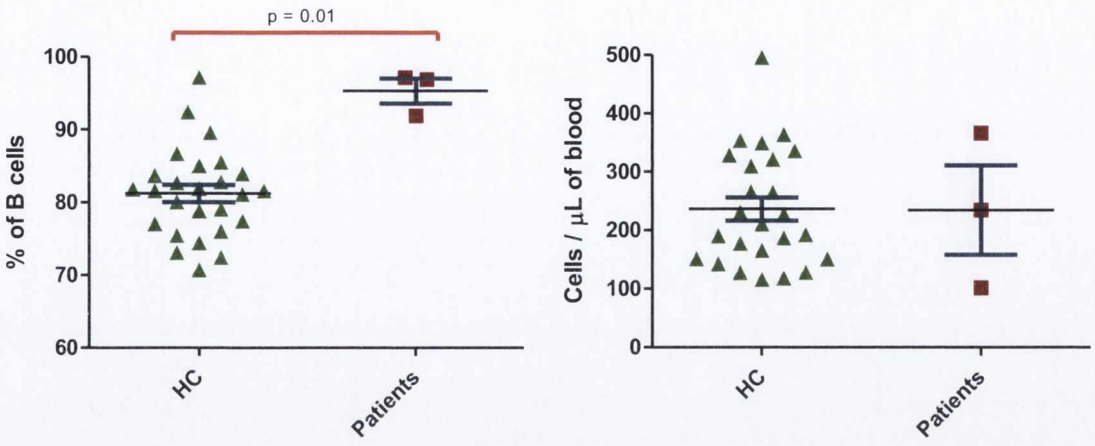


Figure 3.15. Frequencies and absolute counts of IgD$^+$ B cells. The figures show the frequencies (left) and absolute numbers (right) of total CD19$^+$ IgD$^+$ B cells, as determined by flow cytometry in whole blood from healthy controls (HC, n = 26) and patients with SIgAD/IgG subclass deficiency (Patients, n = 3). Statistical analysis was performed employing a two-tailed Mann-Whitney test.

3.5 – Phenotypic analysis of circulating B cell subsets in a query diagnosis patient

Although initially classified as having CVID, one of the patients enrolled in this study was later excluded from that cohort due to the very early onset of his immunodeficiency, which caused life-threatening infections in the form of meningitis from the age of 1 month. A history of similar infections in males on the maternal side of the patient's family suggests that his condition may have genetic bases and be X-linked, although no causative mutation has so far been identified (see chapter 2.4 for details). A single round of immunophenotyping performed on blood from this patient highlighted several features that set him apart both from healthy controls and from other immunodeficient patients taking part in this study. This chapter contains preliminary observations derived from this case study. As absolute counts vary widely between individuals, only frequencies are reported in this case. It should be noted that four healthy controls had to be excluded from the analysis of naïve, unswitched memory, class-switched memory and CD27$^-$ IgD$^-$ B cell populations, due to anomalies in the distribution of flow cytometry data noticed during acquisition of their samples.

Frequencies of total B cells were high in the circulation of this patient, constituting 25.45 % of total lymphocytes (normal range 5 to 19 %); at 676.3 cells/µL, his absolute counts of B cells also appeared elevated in comparison to healthy donors (normal range 99 to 618

cells/μL), although there was no evidence of uncontrolled B cell proliferation. For most cell populations, the patient displayed frequencies and absolute counts in line with those seen in healthy controls. In contrast to the scenario typical of CVID, his naïve B cell frequencies tended to be low, while those of class-switched memory B cells rested in the upper range of healthy control values (**Figure 3.16**). $CD27^-$ IgD^- B cells and total IgD^+ B cells were also found in his blood at normal frequencies (**Figure 3.17**), whereas they were previously reported in this thesis as significantly decreased and increased, respectively, in both CVID patients and patients with SIgAD/IgG subclass deficiency.

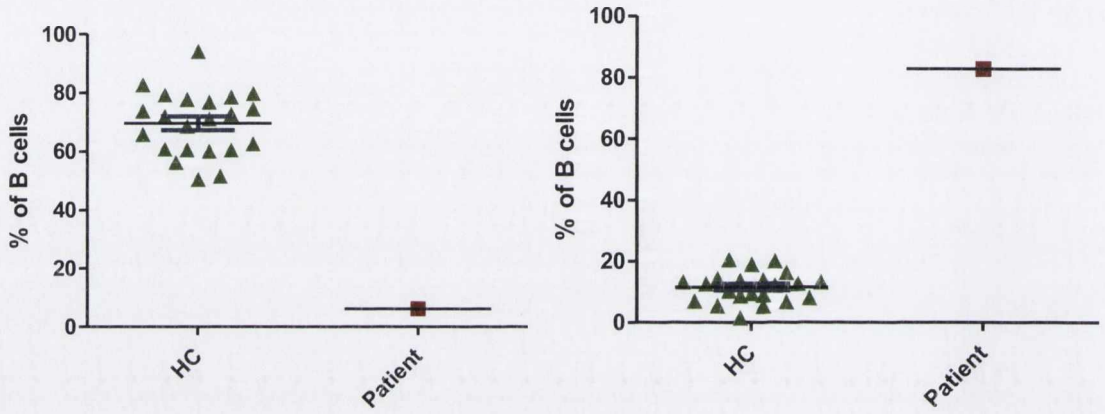


Figure 3.16. Frequencies of naïve and class-switched memory B cells in the blood of a query diagnosis patient. The scatter plots show the frequencies of naive B cells (defined as $CD19^+$ $CD27^-$ IgD^+ events, left) and class-switched memory B cells (defined as $CD19^+$ $CD27^+$ IgD^- events, right), as determined by flow cytometry in whole blood from healthy controls (HC, n = 22) and a query diagnosis patient (Patient). No statistical analysis was performed on these data.

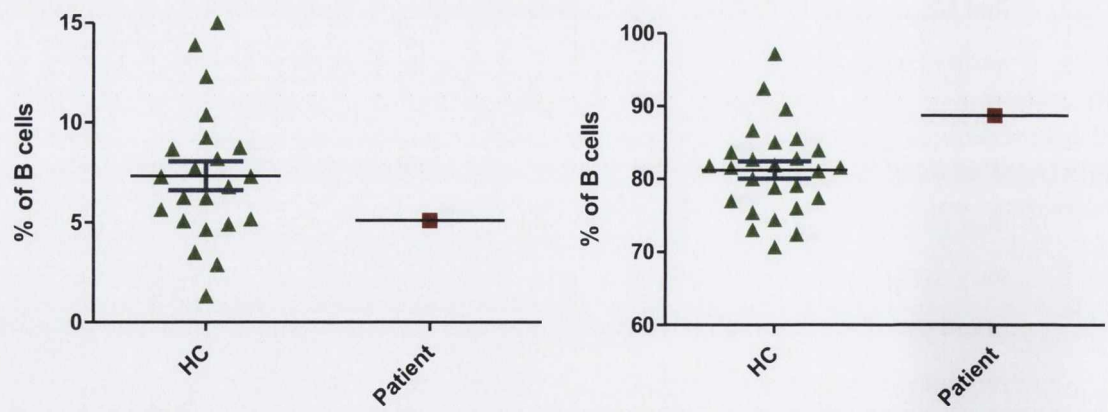


Figure 3.17. Frequencies of $CD27^-$ IgD^- B cells and IgD^+ B cells in the blood of a query diagnosis patient. The scatter plots show the frequencies of double negative B cells (defined as $CD19^+$ $CD27^-$ IgD^- events, left) and those of total IgD^+ B cells (defined as $CD19^+$ IgD^+ events, right), as determined by flow cytometry in whole blood from healthy controls (HC, n = 22 for DN B cells and n = 26 for IgD^+ B cells) and a query diagnosis patient (Patient). No statistical analysis was performed on these data.

3.6 – Correlations between antibody levels at diagnosis and B cell differentiation status in CVID

As shown in chapter 3.2.2, naïve, unswitched memory and class-switched memory B cells were found at abnormal frequencies and numbers in the circulation of CVID patients. In order to investigate if these anomalies could be linked to abnormal antibody production, we correlated the frequencies and absolute counts of each of these B cell populations with the levels of circulating IgM, IgG and IgA antibodies recorded at the time of diagnosis. No significant results were obtained correlating the frequencies or absolute counts of class-switched memory B cells with the levels of the three antibody isotypes (**Figure 3.18**). Similarly, no significant correlations were identified for naïve and unswitched memory B cells (data not shown). It should however be noted that these correlations are based on historical antibody level data, collected as noted at diagnosis, and in many cases years previously. For more accurate results, these correlations should be performed again, using antibody level data obtained on the same date as the samples used for the determination of class-switched memory B cell frequencies and absolute counts.

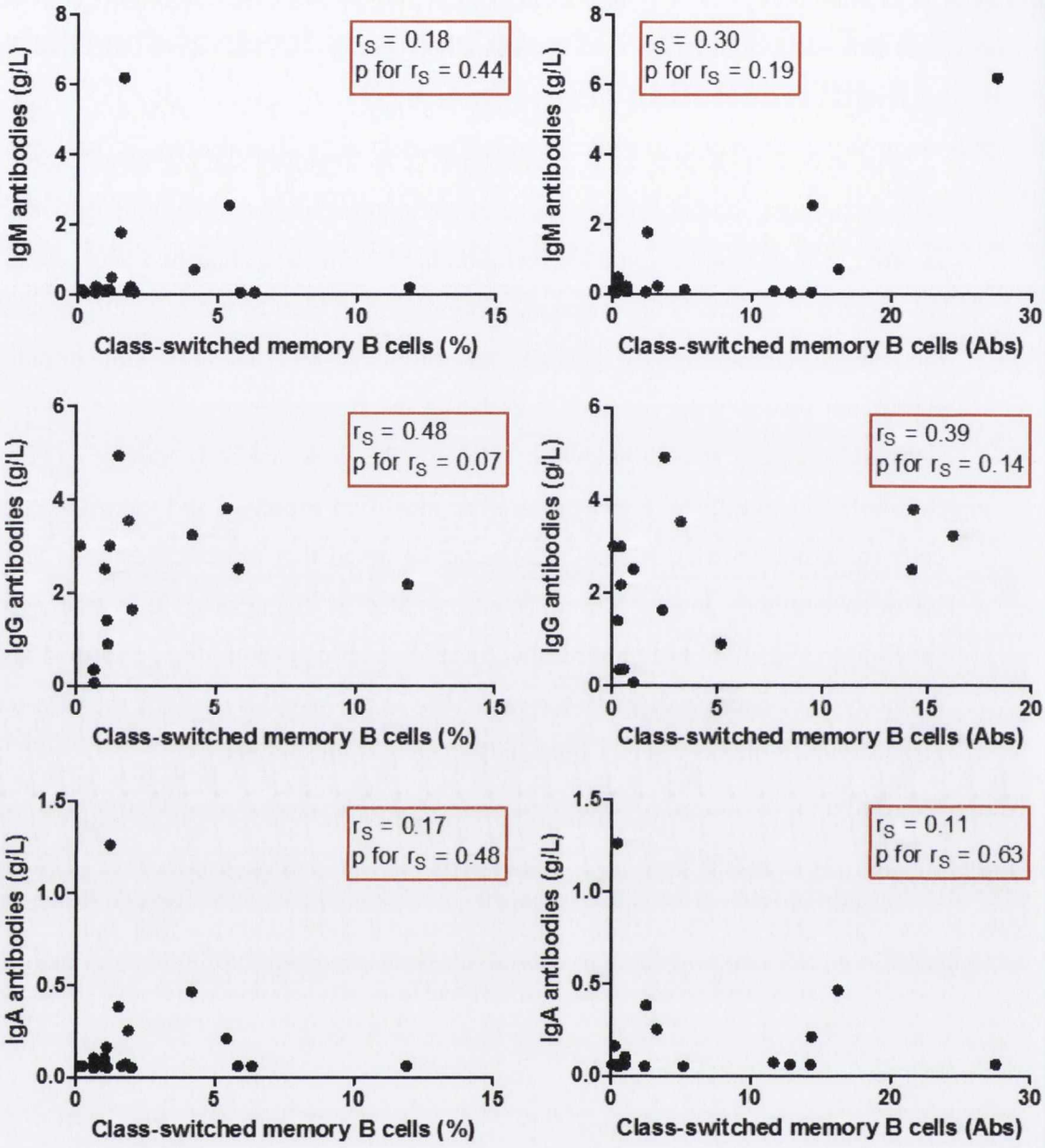


Figure 3.18. Correlations between frequencies or absolute counts of class-switched memory B cells and antibody levels. Frequencies (left column) or absolute counts (right column) of class-switched memory B cells, identified by flow cytometry in whole blood samples collected from CVID patients as $CD19^+$ $CD27^+$ IgD^- events, were correlated with the levels of IgM (top), IgG (middle) or IgA (bottom) antibodies measured in the circulation of the same patients at diagnosis. The strength of correlations was expressed through a Spearman's correlation coefficient (r_S).

3.7 – Discussion

The data collected in this chapter provide information on the phenotypes of B cell populations in patients with antibody deficiencies, particularly CVID. Although frequencies of total B cells in the blood of the CVID patients recruited were comparable to those of healthy age-matched controls, these individuals exhibited significantly decreased absolute counts of this population. Anomalies also appeared in the frequencies and absolute counts of a number of B cell subsets. More specifically, these patients displayed significantly increased percentages of naïve B cells, as well as significantly decreased frequencies of fully differentiated subsets, including both memory B cells and plasmablasts. Percentages of transitional B cells and unswitched memory B cells were generally similar to those found in the circulation of healthy donors, although some patients appeared to display increased frequencies of the former cell type. Frequencies of $CD27^-$ IgD^- B cells were significantly decreased. In absolute count terms, this meant that these individuals had in their circulation numbers of naïve, transitional and unswitched memory B cells comparable to those of healthy donors, but significantly reduced counts of class-switched memory B cells, plasmablasts and $CD27^-$ IgD^- B cells. Counts and frequencies of naïve, unswitched memory and class-switched memory B cells were later correlated with the levels of IgM, IgG and IgA antibodies measured in the circulation of CVID patients at diagnosis, however no significant relationships were identified.

The immunophenotyping data gathered confirm the results obtained in other patient cohorts and offer clues with regard to the biological mechanisms at the basis of CVID, supporting the idea that it is characterised by a block in B cell antibody class-switching. As reviewed in chapter 1.5.1.1, activated naïve B cells undergo processes of somatic hypermutation, affinity maturation and isotype class-switching in GCs, specialised lymph node structures which are ultimately responsible for the generation of differentiated B cell subsets including class-switched memory B cells, plasmablasts and long-lived plasma cells. Individuals affected by homozygous deletions of the ICOS gene, known to cause a CVID-like syndrome, display profound defects in GC formation.[186] The same mutation affects the generation of follicular helper T cells, which are virtually absent in the circulation of $ICOS^{-/-}$ patients.[187] Recent literature suggests that altered GC functions may also occur in non ICOS-induced CVID, although to a somewhat lesser extent. More specifically, immunohistochemistry performed on lymph node biopsies obtained from 10 patients with CVID complicated by benign lymphoproliferation detected some normal GCs alongside as high numbers of hyperplastic and poorly-defined ones.[188] It has therefore been suggested

that a GC output deficiency, rather than a defect in GC formation, could be involved in the B cell abnormalities observed in CVID, at least in patients with lymphadenopathy. Interestingly, a GC output deficiency would account for all the immunophenotyping data obtained in this study, blocking the differentiation of mature B cell types such as class-switched memory B cells and plasmablasts while allowing for normal or increased frequencies and counts of transitional, naïve, and unswitched memory B cells (**Figure 3.19**). It should be noted that frequencies of $CD27^-$ IgD^- B cells, not enumerated in previous CVID cohorts, were found in this study to be significantly decreased in the circulation of patients. Should the GC hypothesis be definitively proven, this finding would support the notion of this subset being a highly differentiated, exhausted population of class-switched memory B cells characterised by downregulated CD27 expression.[41]

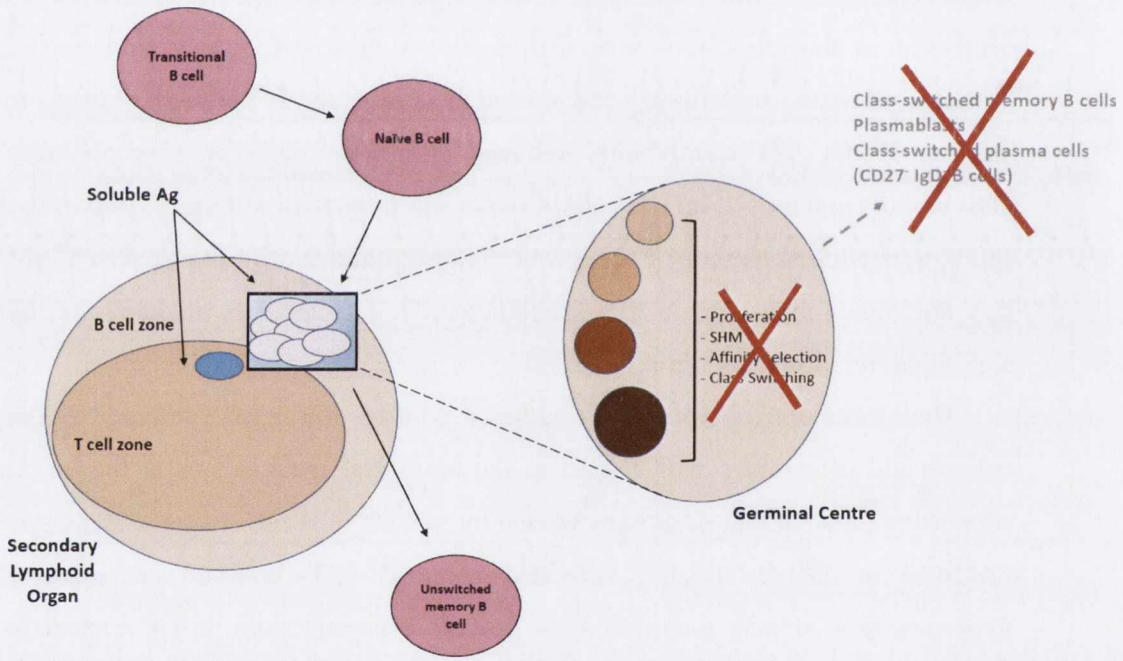


Figure 3.19 – Consequences of a germinal centre output deficiency. The immunophenotyping data collected during this study support the hypothesis that the B cell abnormalities typically found in CVID may be the consequence of a GC output defect. Such a defect would not affect the maturation of transitional, naïve and unswitched memory B cells. It would however lead to decreased frequencies of differentiated B cell subsets including class-switched memory B cells and plasmablasts, whose generation depends on GC processes. $CD27^-$ IgD^- B cells are shown in brackets amongst differentiated B cell subsets on the right because their differentiation pathway has yet to be completely defined. The turquoise oval represents an armed T cell with the same antigen specificity as the naïve T cell approaching the secondary lymphoid organ. SHM = somatic hypermutation.

Although a class-switching defect appears to be what ultimately causes CVID in this and other patient cohorts, it is important to stress that CVID itself is not a monolithic disease, but rather a collection of disorders resulting from a range of possible B cell abnormalities.

Indeed, single patients in a cohort may not present with defects in class-switching, instead exhibiting early blocks in the generation of B cells, or late abnormalities specifically affecting the differentiation of plasmablasts. This heterogeneity could explain why no significant correlation was identified between the frequencies and absolute counts of naïve, unswitched memory or class-switched memory B cells and the antibody levels recorded in the circulation of CVID patients at diagnosis. The lack of a correlation also suggests that other factors, in addition to B cell numbers alone, are involved in determining unsuccessful antibody production in CVID. Importantly, the accuracy of the correlations performed is decreased due to the use of historical data. More accurate results could be produced by using antibody level data measured on the same date as the blood samples used for the determination of frequencies and absolute counts of class-switched memory B cells. This would however not be possible for IgG antibodies, as all patients recruited to this study were on IgG replacement therapy.

CVID could be thought of as belonging to a spectrum of antibody deficiencies of varying severity, which would include selective IgA deficiency, IgG subclass deficiency and secondary antibody deficiency as well as diseases like XLA, causing agammaglobulinemia. The data presented in this chapter, however, strongly suggest that the B cell compartment of primary antibody deficiency patients is inherently different from that of individuals that have developed a secondary antibody deficiency. In fact, subjects affected by secondary antibody deficiency appeared in this study to display frequencies of naïve B cells, class-switched memory B cells, $CD27^-$ IgD^- B cells and plasmablasts very similar to those of healthy donors. In these patients, functional defects of terminally differentiated B cells, i.e. plasmablasts and plasma cells, are therefore a more likely cause of hypogammaglobulinemia than a block in B cell differentiation. Alternatively, they may suffer from a generalised reduction in the numbers of B cells available for differentiation and antibody production, manifesting as total B cell lymphopenia.

At this time, the differential diagnosis of antibody deficiencies is complex and time consuming, and must rely on the use of several tools, including the determination of serum immunoglobulin levels, medical history and family history of an individual. Phenotyping of B cell populations, particularly using CD27 and IgD markers, can be of help in a diagnostic context, although the results obtained need to be carefully evaluated alongside all other assessments. We propose that the determination of total IgD^+ B cell frequencies could be an additional tool useful in the definition of the primary or secondary nature of a patient's hypogammaglobulinemia. 22 out of 23 patients with primary antibody deficiencies recruited to this study (95.6 %, including both CVID and SIgAD/IgG subclass deficiency patients),

displayed frequencies of IgD^+ B cells of 90.3 % and above. Conversely, when considering both healthy donors and secondary antibody deficiency patients, who displayed similar B cell profiles, only 3 out of 32 individuals (9.4 %) exhibited frequencies above that threshold (**Figure 3.20**). Interestingly, the only patient with a query diagnosis included in the study, although very close to the 90.3 % threshold, could not be recognised as having a primary immunodeficiency. This could mean that this approach may only be useful in distinguishing CVID-like primary conditions, in which percentages of IgD^+ B cells are driven up by the accumulation of naïve B cells and unswitched memory B cells, and class-switched memory B cells and $CD27^-$ IgD^- B cells are depleted. Within this group of patients and healthy donors, measurements of IgD^+ B cell frequencies could distinguish patients with primary antibody deficiencies with a sensitivity (true positive rate) of 95.65 % and a specificity (true negative rate) of 90.62 %. When visualised in a ROC curve, this would correspond to an AUC of 0.92, synonymous of excellent accuracy ($p < 0.0001$, **Figure 3.21**).

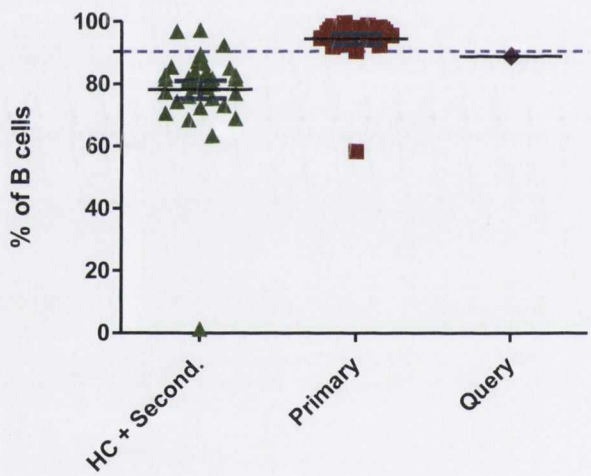


Figure 3.20 – Possible use of IgD^+ B cell frequencies as a diagnostic tool. The individuals recruited to the study were divided according to their frequencies of $CD19^+$ IgD^+ B cells, as previously determined by flow cytometry, considering a threshold of 90.3 % (blue dotted line). Healthy controls (HC, n = 26) and secondary antibody deficiency patients (Second., n = 6) typically exhibited frequencies of this B cell subset below the threshold, while primary antibody deficiency patients (Primary, including CVID patients, n = 20, as well as SIgAD/IgG subclass deficiency patients, n = 3) generally displayed frequencies above that value. The threshold chosen for the test did not identify a query patient (Query) as having a primary antibody deficiency.

It is unclear at this time why patients affected by CVID-like primary immunodeficiencies would present with increased frequencies of IgD^+ B cells in their circulation. There is however evidence to suggest that loss of IgD during B cell differentiation is dependent on the passage of B cells through GCs and on the activation of

T cell-dependent immunity. Indeed, patients deficient in CD40 or CD40L, and thus incapable of generating GCs, have been found to possess a noticeable population of so called "natural effector" B cells, characterised by a $CD27^+$ IgD^+ IgM^+ phenotype and by a limited replication history in comparison to $CD27^+$ IgD^- B cells.[189-192] Counts of class-switched memory B cells ($CD27^+$ IgD-, or CD27+ IgG^+/IgA^+), on the other hand, were very significantly decreased in the circulation of these patients in comparison to healthy individuals. It is therefore possible that the GC defect hypothesised to be involved in CVID could be the cause of both the decreased frequencies of class-switched memory B cells and the increased frequencies of IgD^+ B cells identified in the peripheral blood of patients.

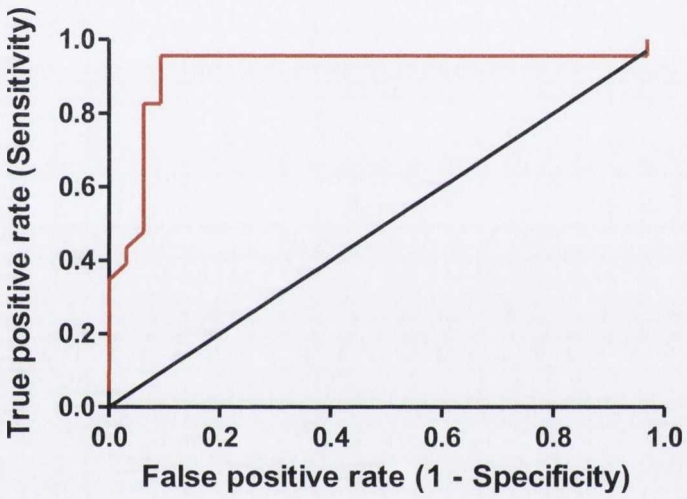


Figure 3.21 – ROC curve of IgD^+ B cell frequencies as a diagnostic tool. The ROC curve in the image (in red) expresses the discriminatory power of $CD19^+$ IgD^+ B cell frequencies in determining if an individual is affected by a CVID-like primary immunodeficiency (AUC = 0.92, $p < 0.0001$). The curve was obtained by plotting $CD19^+$ IgD^+ B cell frequencies from healthy controls and secondary antibody deficiency patients against those of CVID, SIgAD and IgG subclass deficiency patients. The black line defines an AUC of 0.5, at which the test would be considered to have null discriminatory power.

Taken together, the data collected in this chapter support our hypothesis that CVID patients exhibit a block in B cell maturation at the isotype class-switching stage. Mounting evidence supports the hypothesis that a GC output defect may be at the root of the poor antibody production observed in these individuals. Our analysis also suggests that frequencies of total IgD^+ B cells may be useful in assessing the primary or secondary nature of disease in new patients with hypogammaglobulinemia.

CHAPTER 4

ANALYSIS OF CIRCULATING T CELL SUBSETS IN PATIENTS WITH CVID AND OTHER ANTIBODY DEFICIENCIES

4.1 – Introduction

Clinically speaking, CVID is characterised by the development of recurrent infections and by heterogeneous, idiopathic complications including autoimmunity, granulomas, enteropathy and malignancies. The B cell abnormalities described in chapter 3 and in previous literature undoubtedly play a role in both these processes. IgG infusions decrease the number and frequency of infections in CVID patients, proving that insufficient levels of circulating immunoglobulins are in large part responsible for their occurrence. As reviewed in chapter 1.6 and 3.1, numerical abnormalities in several B cell populations have additionally been found to associate with the complications of CVID. High frequencies of transitional B cells have for example been linked to lymphadenopathy, while patients with high frequencies of $CD21^-$ B cells are known to be at increased risk of developing splenomegaly.[160]

In contrast to the wealth of data describing B cell abnormalities, relatively little information is available in the literature about the status of T cell- and innate cell-mediated immunity in CVID. Decreased frequencies of regulatory T cells[168] and NK cells[170] have been identified in distinct cohorts. CVID patients also display generally decreased frequencies of circulating $CD4^+$ T cells and/or increased frequencies of $CD8^+$ T cells in comparison to healthy donors.[161,162] Abnormalities affecting the $CD4^+$ and $CD8^+$ T cell subsets appear to involve a depletion of naïve cells and an accumulation of activated, memory cell types.[163,164] Although the causes of these alterations are not definitely known, they may depend on a combination of factors of pathogenic origin. Bacterial translocation and endotoxemia have for example been found to affect the proliferative abilities and functions of $CD4^+$ T cells,[165] while CMV infection has been deemed at least partly responsible for the expansion of $CD8^+$ T cells seen in CVID patients.[166] Similar to B cells, links have been identified between altered frequencies of circulating T cell populations and complications of CVID. Specifically, abnormal frequencies of $CD8^+$ T cells in the peripheral blood of patients significantly associate with both splenomegaly[162] and autoimmune complications.[167,178]

Of the currently known innate T cell populations, only iNKT cells have been the object of some investigation in CVID. Although it has been known for some time that this population is depleted in the blood of patients,[169] a correlation between iNKT cell frequencies and lymphoproliferative complications, specifically splenomegaly, has only been uncovered by Gao and colleagues last year.[193] An attempt by the same group to expand iNKT cells from CVID patients *in vitro* was largely unsuccessful, prompting them to suggest

that this cell subset may be functionally altered in the disease. This could have far-reaching implications, as iNKT cells can affect the functions of a number of cell types involved in the fight against infections, including monocytes, DCs and T cells (see chapter 1.5.2.2.2). iNKT cells are furthermore known to play a role in the mediation of B cell responses, both by directly responding to lipid antigen presented by B cells and by supporting T_{FH} cells in the activation of B cell differentiation and antibody production.[99] Numerical and functional abnormalities in this cell subset could therefore impact immunoglobulin levels in the blood of patients.

4.2 – Hypothesis and aims of the chapter

In this chapter, we investigated the frequencies, absolute counts and phenotypic characteristics of T lymphocytes, in patients affected by primary and secondary antibody deficiencies as well as in healthy donors. The hypothesis under investigation was that these populations, and particularly innate T cell subsets, could play a role in CVID and in its associated complications. Our specific aims for this chapter were therefore:

1. to determine the frequencies and absolute counts of conventional T cells, NT cells and innate T cell subsets, i.e. iNKT cells, MAIT cells and Vδ1, Vδ2 and Vδ3 γδ T cells, in the circulation of patients affected by primary and secondary antibody deficiencies and healthy individuals. The CD4/CD8 status of these populations was also investigated, determining in each case the frequencies and absolute counts of $CD4^+$ ($CD4^+$ $CD8^-$), $CD8^+$ ($CD4^-$ $CD8^+$) and double negative ($CD4^-$ $CD8^-$) subsets. In order to maintain consistency with the structure adopted in chapter 3, the results obtained from CVID patients are presented alongside those from secondary antibody deficiency patients. A selection of results from patients with SIgAD and IgG subclass deficiency, as well as from a single patient with a query diagnosis, is also included;

2. to probe the existence of associations between the clinical status of CVID patients, following their allocation to appropriate clinical phenotypes, and the frequencies of innate T cell populations, as well as of their $CD4^+$, $CD8^+$ and double negative subpopulations.

4.3 – Phenotypic analysis of circulating T cell subsets in CVID and secondary hypogammaglobulinemia

This section presents the immunophenotyping results obtained for both conventional T cells and innate T cell subsets Vδ1, Vδ2 and Vδ3 γδ T cells, iNKT cells, MAIT cells and NT cells. For every population, data on frequencies and absolute counts are supplied. Data on the frequencies and absolute counts of $CD4^+$, $CD8^+$ and double negative (DN, $CD4^-$ $CD8^-$) cells within each subsets are also included for CVID patients. **Figure 4.1** shows the strategy employed for the gating of CD4/CD8 populations within the total T cell population; the same approach was employed for innate T cell subsets, after identification of the population of interest. See chapter 3.2.1 for data on the frequencies and absolute counts of total T and NK cells, as determined by the BD Biosciences TBNK enumeration system described in chapter 2.8.8.

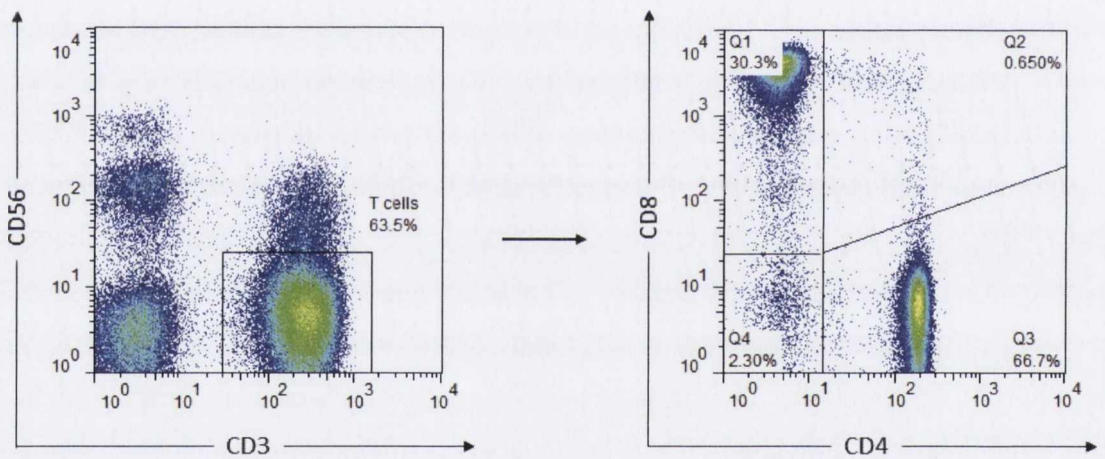


Figure 4.1. Gating strategy for CD4/CD8 T cell subsets. Total T cells were first identified in flow cytometry plots as $CD3^+$ $CD56^-$ events (left), and subsequently divided on the basis of their expression of CD4 and/or CD8 (right).

4.3.1 – Phenotypic analysis of conventional T cell subsets

As shown in chapter 3.2.1, the overall frequencies and absolute counts of T cells were not significantly altered in either CVID patients or patients with secondary antibody deficiency. The frequencies of $CD4^+$ and $CD8^+$ T cells were however abnormal in the peripheral blood of CVID patients. More specifically, percentages of $CD4^+$ T cells were found to be significantly decreased ($p = 0.04$), while those of $CD8^+$ T cells were significantly increased ($p = 0.02$) in comparison to healthy controls (**Figure 4.2**). In terms of absolute

counts, $CD4^+$ and DN T cells were found in significantly lower numbers in CVID patients ($p = 0.002$ and 0.008, respectively; **Figure 4.3**).

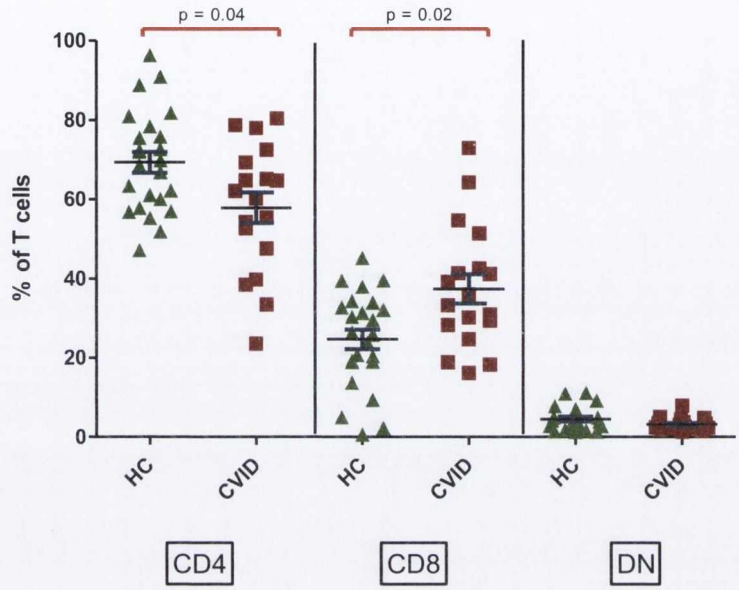


Figure 4.2. Frequencies of $CD4^+$, $CD8^+$ and double negative T cells. T cells, detected by flow cytometry as $CD3^+$ $CD56^-$ events in whole blood from healthy controls (HC, n = 24) and CVID patients (CVID, n = 18), were subdivided on the basis of their positivity or negativity for CD4 and CD8 in $CD4^+$ ($CD4^+$ $CD8^-$), $CD8^+$ ($CD4^-$ $CD8^+$) and double negative (DN, $CD4^-$ $CD8^-$) subsets. Statistical analysis was performed employing a two-tailed Mann-Whitney test.

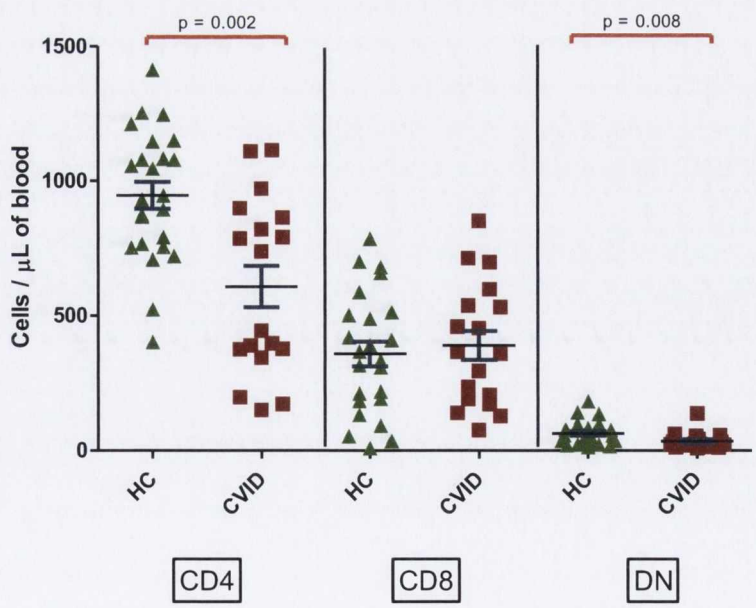


Figure 4.3. Absolute counts of $CD4^+$, $CD8^+$ and double negative T cells. T cells, detected by flow cytometry as $CD3^+$ $CD56^-$ events in whole blood from healthy controls (HC, n = 24) and CVID patients (CVID, n = 18), were subdivided on the basis of their positivity or negativity for CD4 and CD8 in $CD4^+$ ($CD4^+$ $CD8^-$), $CD8^+$ ($CD4^-$ $CD8^+$) and double negative (DN, $CD4^-$ $CD8^-$) subsets. Statistical analysis was performed employing a two-tailed Mann-Whitney test.

4.3.2 – Phenotypic analysis of γδ T cell subsets

This study provided an opportunity to gauge the frequencies, counts and CD4/CD8 status of γδ T cell subsets. As shown in **Figures 4.4 to 4.6**, no significant alteration was detected in the frequencies or absolute counts of Vδ1, Vδ2 or Vδ3 γδ T cell subsets in the peripheral blood of CVID patients in comparison to healthy controls. Frequencies of all three subsets and absolute counts of Vδ1 and Vδ3 cells were also comparable between healthy controls and patients with secondary antibody deficiency, however absolute counts of Vδ2 γδ T cells were significantly decreased in this patient group ($p < 0.05$).

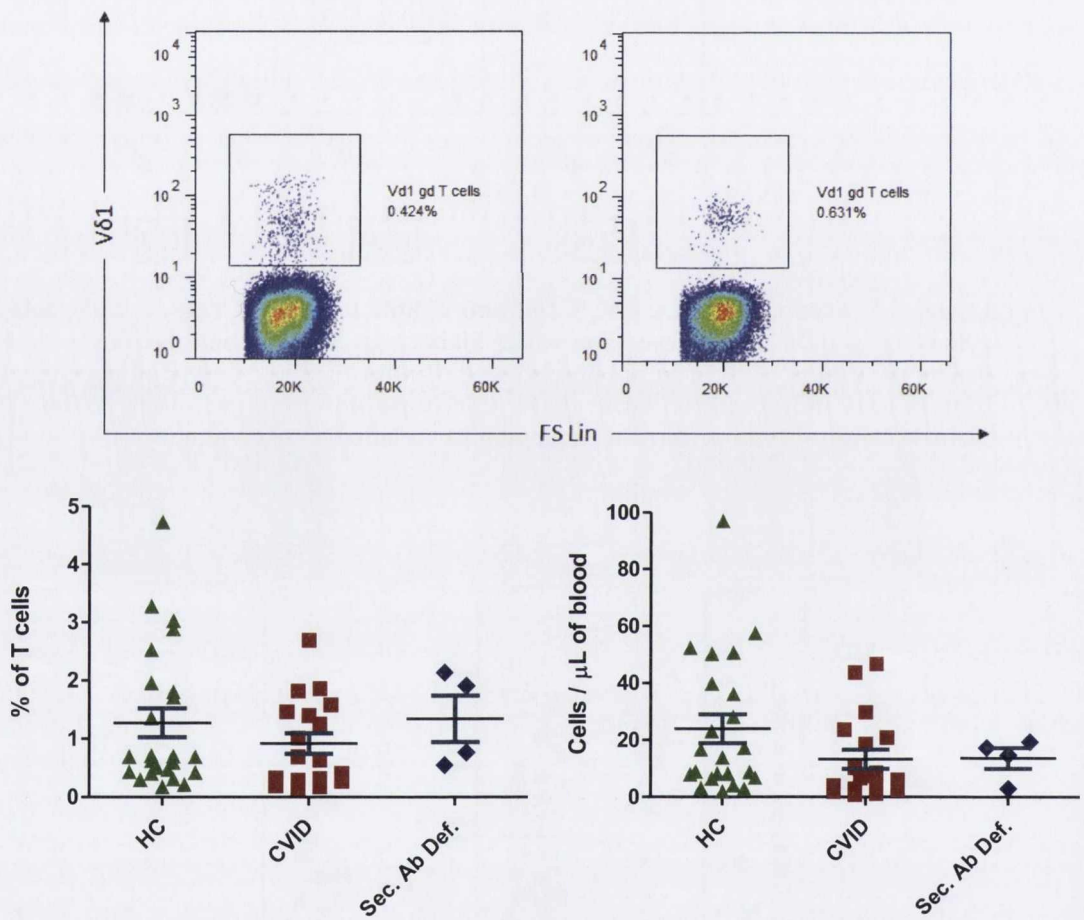


Figure 4.4. Representative dot plots, frequencies and absolute counts of Vδ1 γδ T cells. The representative flow cytometry dot plots in the figure (top) show Vδ1 γδ T cells, detected as Vδ1 TCR^+ events following gating on $CD3^+$ T cells, in whole blood from a healthy control (left) and of a CVID patient (right). The scatter plots (bottom) show the frequencies (left) and absolute numbers (right) of Vδ1 γδ T cells, as determined by flow cytometry in whole blood from healthy controls (HC, n = 24), CVID patients (CVID, n = 18) and secondary antibody deficiency patients (Sec. Ab Def., n = 4). Statistical analysis was performed employing a Kruskal-Wallis test plus Dunn's post hoc test.

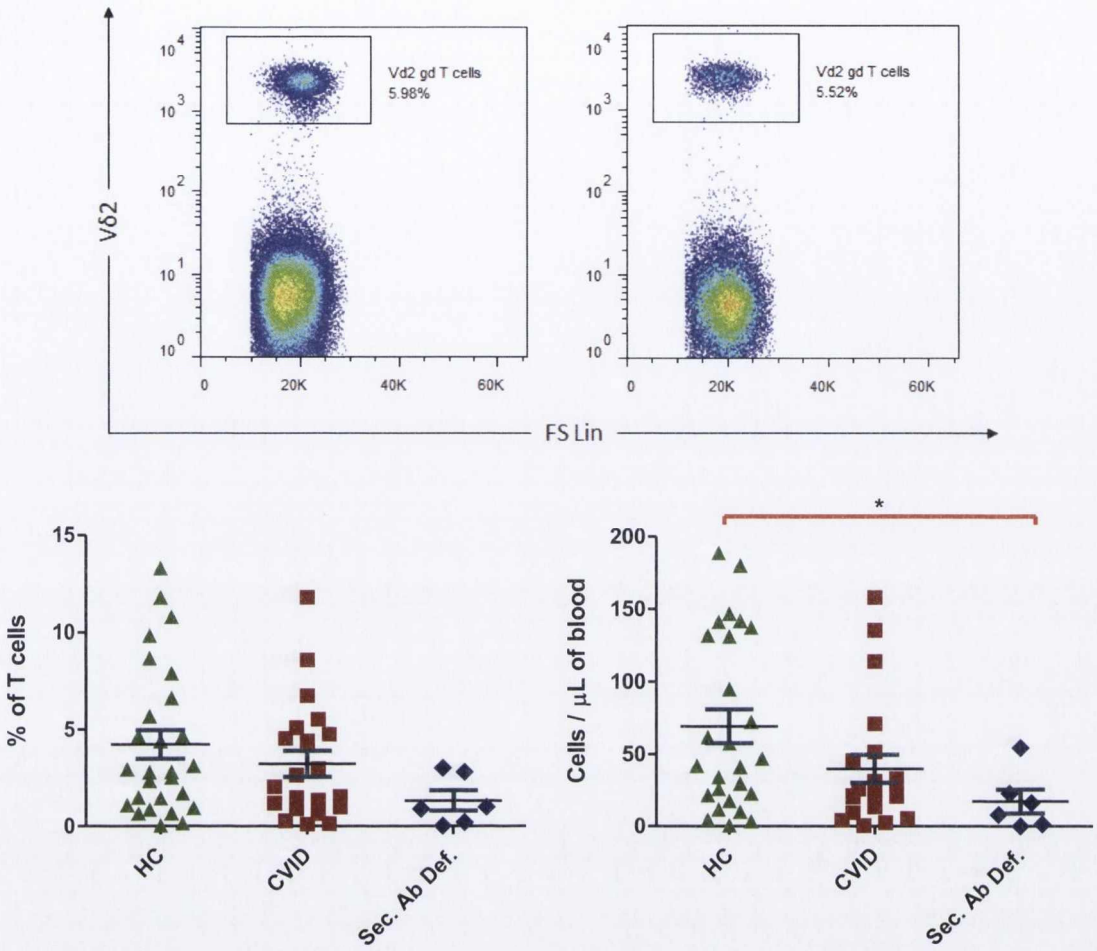


Figure 4.5. Representative dot plots, frequencies and absolute counts of Vδ2 γδ T cells. The representative flow cytometry dot plots in the figure (top) show Vδ2 γδ T cells, detected as Vδ2 TCR^+ events following gating on $CD3^+$ T cells, in whole blood from a healthy control (left) and of a CVID patient (right). The scatter plots (bottom) show the frequencies (left) and absolute numbers (right) of Vδ2 γδ T cells, as determined by flow cytometry in whole blood from healthy controls (HC, n = 27), CVID patients (CVID, n = 21) and secondary antibody deficiency patients (Sec. Ab Def., n = 6). Statistical analysis was performed employing a Kruskal-Wallis test plus Dunn's post hoc test. * $p < 0.05$.

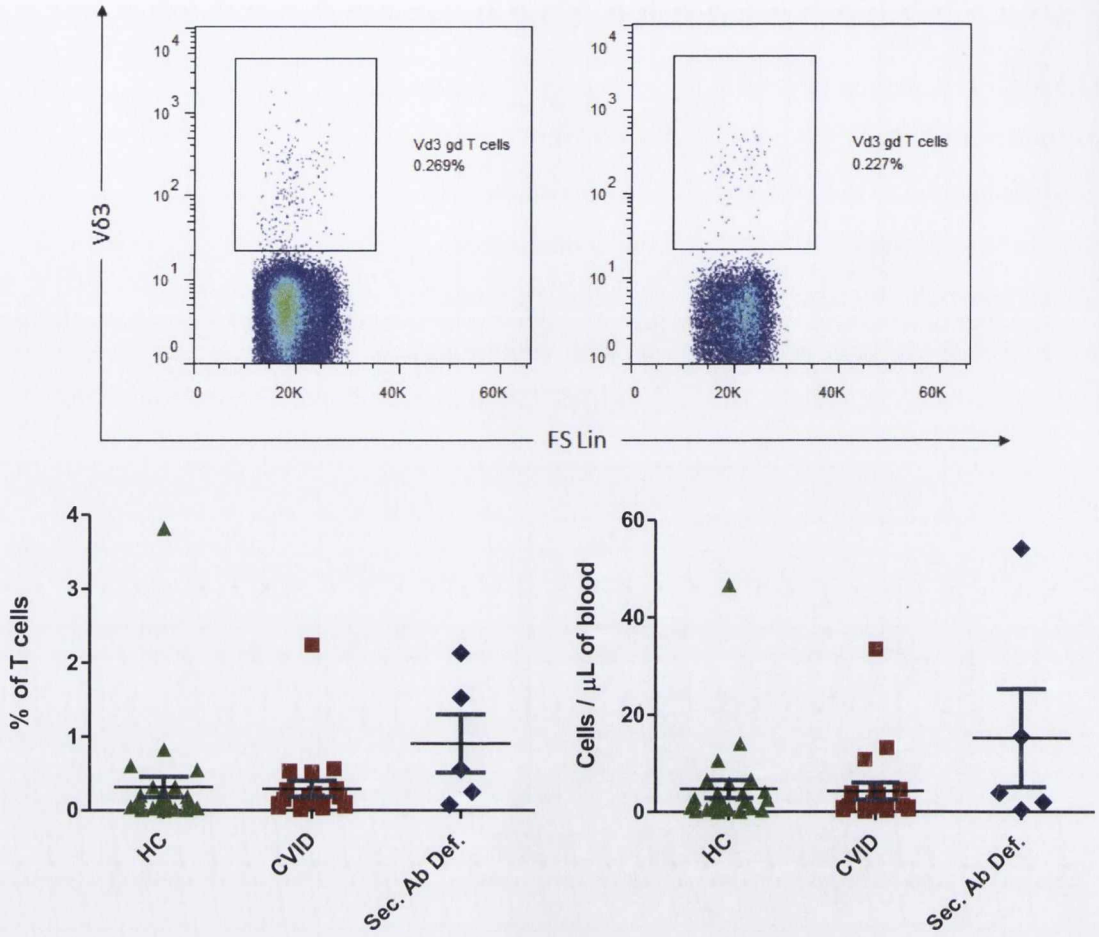


Figure 4.6. Representative dot plots, frequencies and absolute counts of Vδ3 γδ T cells. The representative flow cytometry dot plots in the figure (top) show Vδ3 γδ T cells, detected as Vδ3 TCR^+ events following gating on $CD3^+$ T cells, in whole blood from a healthy control (left) and of a CVID patient (right). The scatter plots (bottom) show the frequencies (left) and absolute numbers (right) of Vδ3 γδ T cells, as determined by flow cytometry in whole blood from healthy controls (HC, n = 27), CVID patients (CVID, n = 20) and secondary antibody deficiency patients (Sec. Ab Def., n = 5). Statistical analysis was performed employing a Kruskal-Wallis test plus Dunn's post hoc test.

No significant differences were identified with regard to the frequencies of $CD4^+$, $CD8^+$ and double negative cells for any of the three γδ T cell subset in CVID patients (**Figures 4.7 to 4.9**). Absolute counts of $CD4^+$ and double negative Vδ1 cells, as well as $CD4^+$ Vδ2 cells, were however decreased in CVID patients in comparison to healthy controls ($p = 0.005$, 0.03 and 0.0009, respectively; **Figures 4.10 and 4.11**). Absolute counts of Vδ3 γδ T cells were not affected (**Figure 4.12**).

Thus, frequencies and absolute of all three γδ T cell populations, as well as the frequencies of their $CD4^+$, $CD8^+$ and double negative subsets, were found to be comparable in CVID patients and healthy controls. Significantly decreased counts, of $CD4^+$ and double

negative Vδ1 γδ T cells, as well as of $CD4^+$ Vδ2 γδ T cells, were however observed in the circulation of CVID patients in comparison to healthy controls.

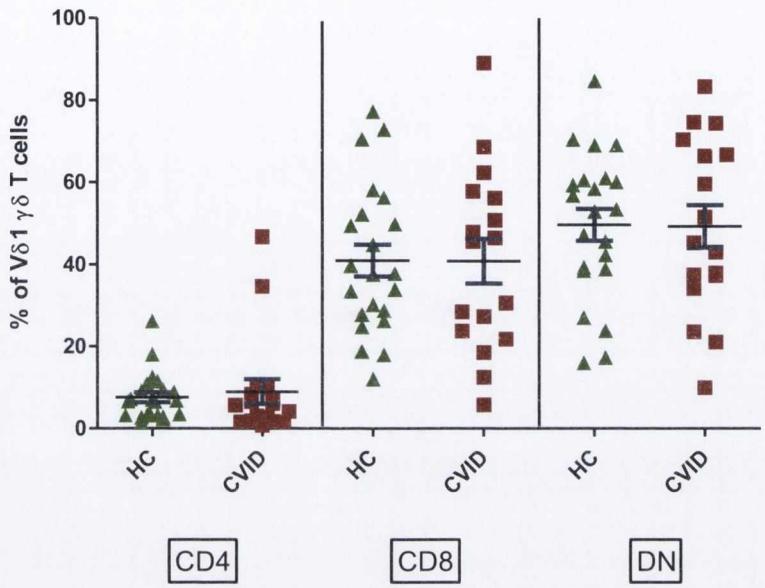


Figure 4.7. Frequencies of $CD4^+$, $CD8^+$ and double negative Vδ1 γδ T cells. Vδ1 γδ T cells, detected by flow cytometry as $CD3^+$ Vδ1 TCR^+ events in whole blood from healthy controls (HC, n = 22) and CVID patients (CVID, n = 17) were subdivided on the basis of their positivity or negativity for CD4 and CD8 in $CD4^+$ ($CD4^+$ $CD8^-$), $CD8^+$ ($CD4^-$ $CD8^+$) and double negative (DN, $CD4^-$ $CD8^-$) subsets. Statistical analysis was performed employing a two-tailed Mann-Whitney test.

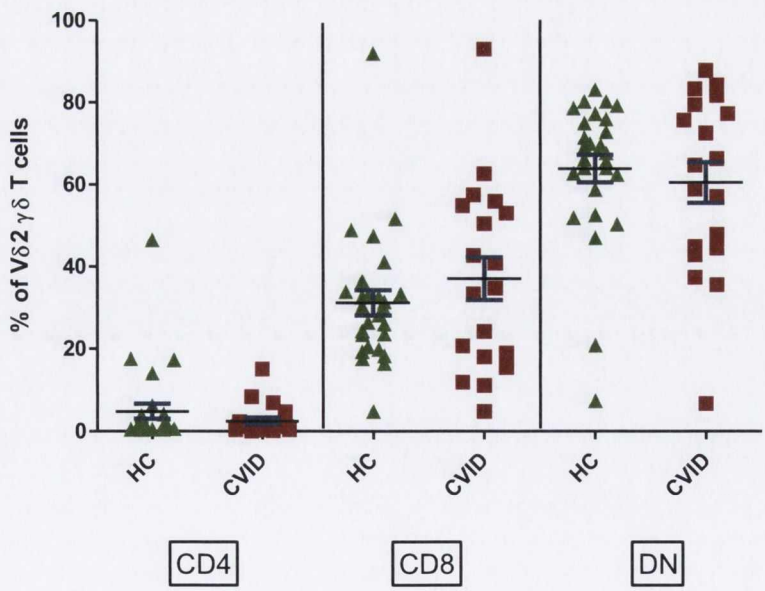


Figure 4.8. Frequencies of $CD4^+$, $CD8^+$ and double negative Vδ2 γδ T cells. Vδ2 γδ T cells, detected by flow cytometry as $CD3^+$ Vδ2 TCR^+ events in whole blood from healthy controls (HC, n = 27) and CVID patients (CVID, n = 19) were subdivided on the basis of their positivity or negativity for CD4 and CD8 in $CD4^+$ ($CD4^+$ $CD8^-$), $CD8^+$ ($CD4^-$ $CD8^+$) and double negative (DN, $CD4^-$ $CD8^-$) subsets. Statistical analysis was performed employing a two-tailed Mann-Whitney test.

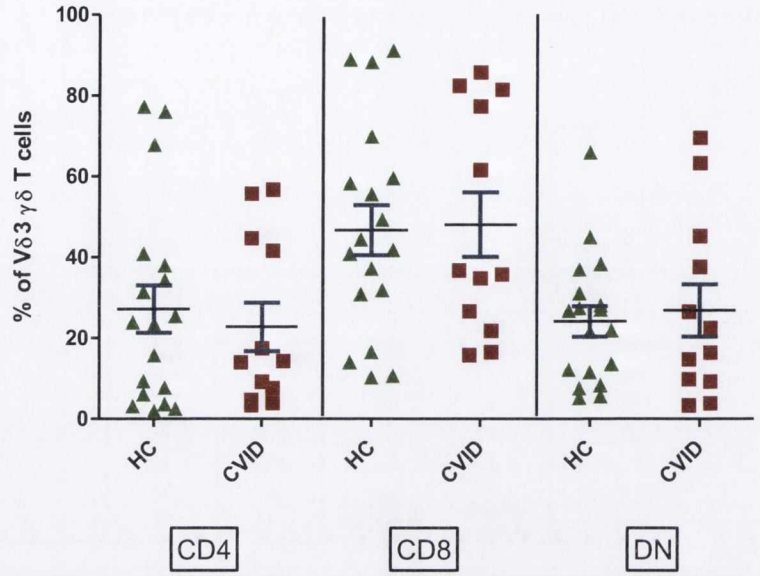


Figure 4.9. Frequencies of CD4$^+$, CD8$^+$ and double negative Vδ3 γδ T cells. Vδ3 γδ T cells, detected by flow cytometry as CD3$^+$ Vδ3 TCR$^+$ events in whole blood from healthy controls (HC, n = 18) and CVID patients (CVID, n = 12) were subdivided on the basis of their positivity or negativity for CD4 and CD8 in CD4$^+$ (CD4$^+$ CD8$^-$), CD8$^+$ (CD4$^-$ CD8$^+$) and double negative (DN, CD4$^-$ CD8$^-$) subsets. Statistical analysis was performed employing a two-tailed Mann-Whitney test.

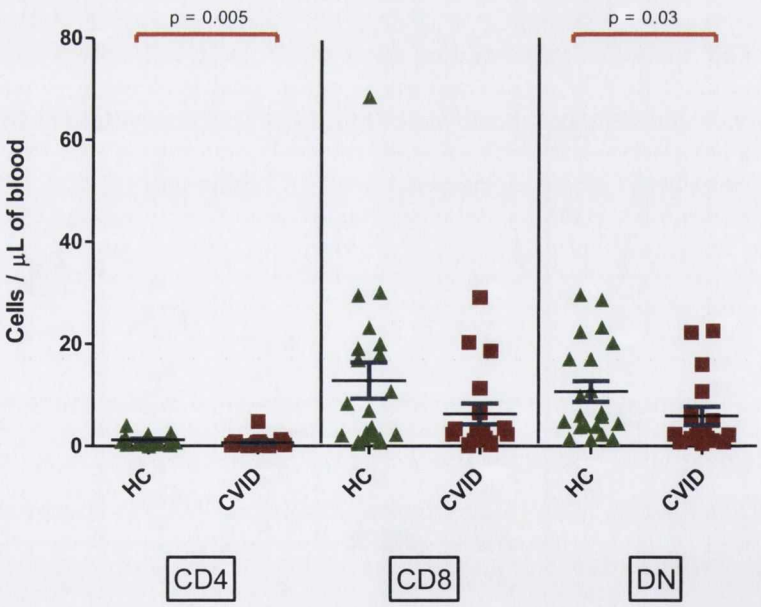


Figure 4.10. Absolute counts of CD4$^+$, CD8$^+$ and double negative Vδ1 γδ T cells. Vδ1 γδ T cells, detected by flow cytometry as CD3$^+$ Vδ1 TCR$^+$ events in whole blood from healthy controls (HC, n = 21) and CVID patients (CVID, n = 17) were subdivided on the basis of their positivity or negativity for CD4 and CD8 in CD4$^+$ (CD4$^+$ CD8$^-$), CD8$^+$ (CD4$^-$ CD8$^+$) and double negative (DN, CD4$^-$ CD8$^-$) subsets. Statistical analysis was performed employing a two-tailed Mann-Whitney test.

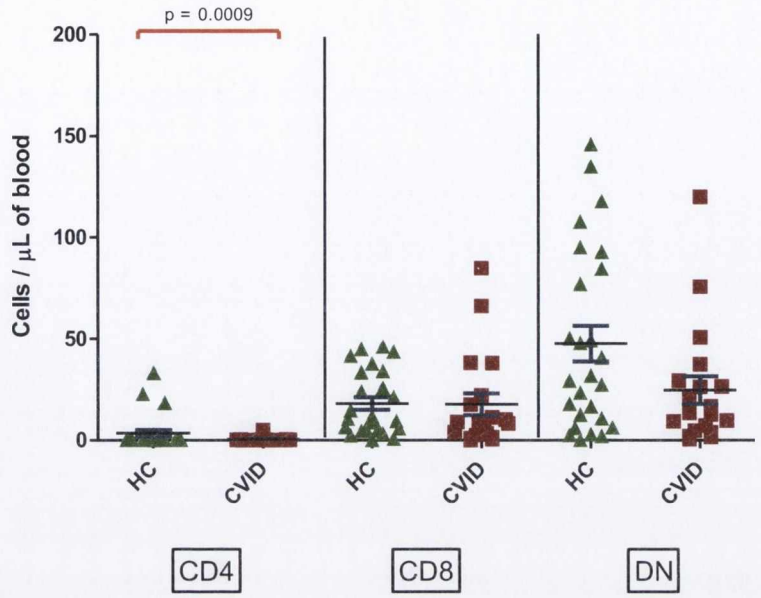


Figure 4.11. Absolute counts of CD4$^+$, CD8$^+$ and double negative Vδ2 γδ T cells. Vδ2 γδ T cells, detected by flow cytometry as CD3$^+$ Vδ2 TCR$^+$ events in whole blood from healthy controls (HC, n = 26) and CVID patients (CVID, n = 19) were subdivided on the basis of their positivity or negativity for CD4 and CD8 in CD4$^+$ (CD4$^+$ CD8$^-$), CD8$^+$ (CD4$^-$ CD8$^+$) and double negative (DN, CD4$^-$ CD8$^-$) subsets. Statistical analysis was performed employing a two-tailed Mann-Whitney test.

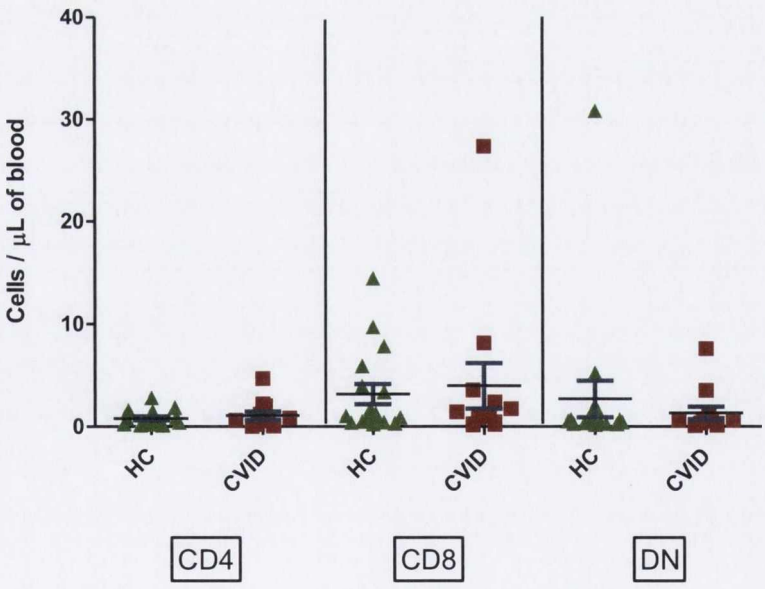


Figure 4.12. Absolute counts of CD4$^+$, CD8$^+$ and double negative Vδ3 γδ T cells. Vδ3 γδ T cells, detected by flow cytometry as CD3$^+$ Vδ3 TCR$^+$ events in whole blood of healthy controls (HC, n = 17) and CVID patients (CVID, n = 12) were subdivided on the basis of their positivity or negativity for CD4 and CD8 in CD4$^+$ (CD4$^+$ CD8$^-$), CD8$^+$ (CD4$^-$ CD8$^+$) and double negative (DN, CD4$^-$ CD8$^-$) subsets. Statistical analysis was performed employing a two-tailed Mann-Whitney test.

4.3.3 – Phenotypic analysis of iNKT cells

iNKT cells were detected in two ways, employing either an antibody targeting the Vα24-Jα18 invariant chain of their TCR or a CD1d tetramer loaded with α-GalCer analogue PBS-57. **Figure 4.13** shows representative flow cytometry dot plots of iNKT cells as identified by the two methods, whose merits have been discussed in chapter 2.82.

Antibody-mediated detection of iNKT cells was used throughout this study with good results. It allowed us to determine that frequencies and absolute counts of this population were severely decreased in comparison to healthy controls in both CVID ($p < 0.005$) and secondary antibody deficiency patients ($p < 0.01$ for frequencies and $p < 0.005$ for absolute counts; **Figure 4.14**).

Although initially satisfactory, use of the CD1d tetramer became increasingly challenging as the compound began to detect high levels of background. These issues affected both samples containing PBS-57-loaded tetramer and controls prepared with an unloaded version of the compound (**Figure 4.15**). Although the roots of this problem have never been identified, the tetrameric molecule may have degraded over time, allowing it to non-specifically bind other targets. As a consequence of this, the majority of the data obtained by using the CD1d tetramer had to be discarded, including all available data on secondary antibody deficiency patients and most of those derived from healthy controls. What results could be salvaged showed a trend similar to that already seen using antibody detection, pointing to a decrease in iNKT cell frequencies in CVID patients and identifying a significant decrease ($p < 0.05$) in the absolute counts of this population in comparison to healthy controls (**Figure 4.16**).

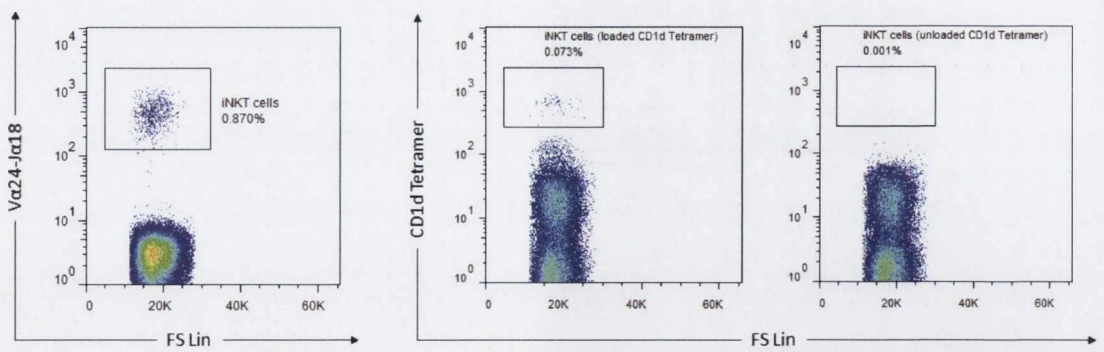


Figure 4.13. Representative flow cytometry dot plots of iNKT cells. Following gating on $CD3^+$ cells, iNKT cells were detected in whole blood from the same individual as either $V\alpha24\text{-}J\alpha18^+$ events (left) or as cells binding a PBS-57-loaded CD1d tetramer (centre). Unloaded CD1d tetramer was also used to test for non-specific tetramer binding (right).

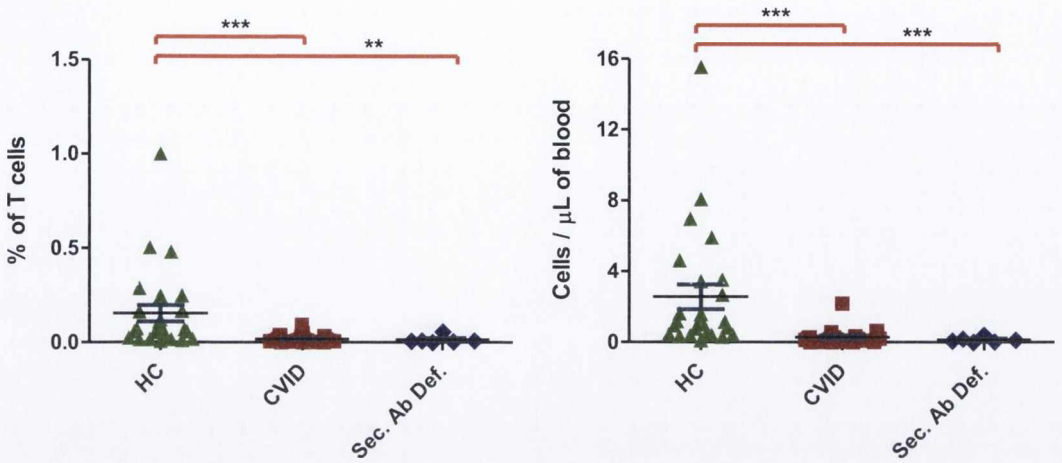


Figure 4.14. Frequencies and absolute counts of Vα24-Jα18$^+$ iNKT cells. The scatter plots show the frequencies (left) and absolute numbers (right) of iNKT cells, detected by flow cytometry as CD3$^+$ Vα24-Jα18$^+$ events in whole blood from healthy controls (HC, n = 26), CVID patients (CVID, n = 21) and secondary antibody deficiency patients (Sec. Ab Def., n = 6). Statistical analysis was performed employing a Kruskal-Wallis test plus Dunn's post hoc test. ** $p < 0.01$; *** $p < 0.001$.

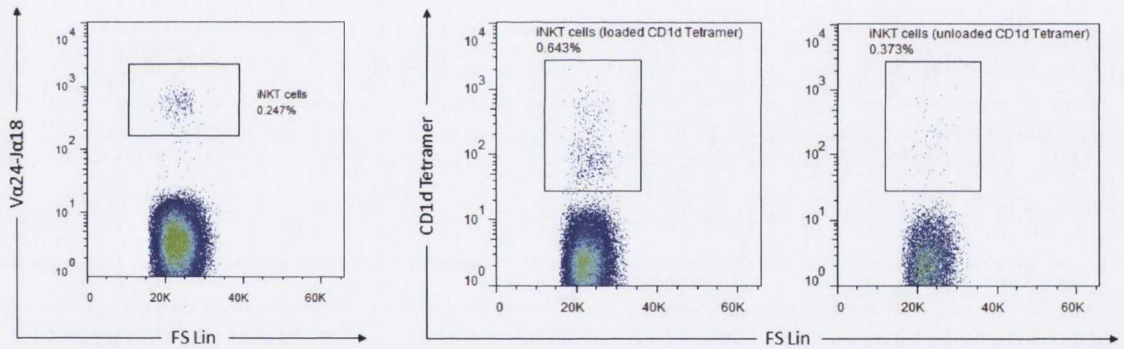


Figure 4.15. High background levels in samples containing CD1d tetramer. Following acquisition by flow cytometry and gating on CD3$^+$ cells, iNKT cells were detected in whole blood from the same individual as either Vα24-Jα18$^+$ events (left) or as cells binding a PBS-57-loaded CD1d tetramer (centre). Unloaded CD1d tetramer was also used to test for non-specific tetramer binding (right).

iNKT cells are rare in peripheral blood, constituting around 0.01 % of T cells in healthy controls and, as seen, being almost absent in patients. Anti-CD4 and anti-CD8 antibodies were included in all staining panels for iNKT cells, however the extremely low number of events collected during the acquisition of samples made it impossible to determine the CD4/CD8 status of this population.

Thus, frequencies and absolute counts of iNKT cells were found to be very significantly decreased in the circulation of CVID patients in comparison to healthy controls.

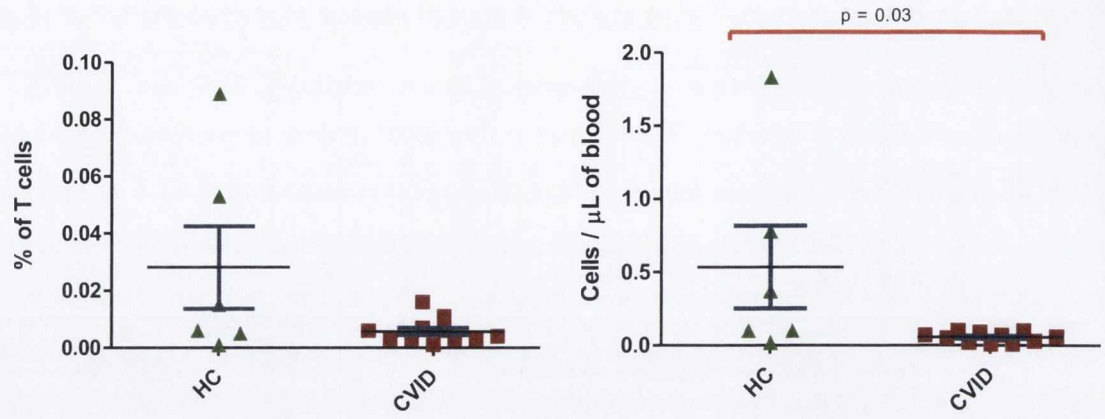


Figure 4.16. Frequencies and absolute counts of CD1d-tetramer$^+$ iNKT cells. The scatter plots show the frequencies (left) and absolute numbers (right) of iNKT cells, detected by flow cytometry as CD3$^+$ CD1d-tetramer-binding events, in whole blood from healthy controls (HC, n = 6) and CVID patients (CVID, n = 11). Statistical analysis was performed employing a two-tailed Mann-Whitney test.

4.3.4 – Phenotypic analysis of MAIT cells

MAIT cells were reliably detected as a well-defined population of Vα7.2$^+$ cells expressing high levels of CD161. As shown in **Figure 4.17**, frequencies ($p < 0.05$) as well as absolute counts ($p < 0.01$) of this subset were found to be decreased in the circulation of both CVID and secondary antibody deficiency patients in comparison to healthy controls.

The frequencies of CD4$^+$ and CD8$^+$ MAIT cells in the peripheral blood of CVID patients were also altered, being increased ($p = 0.009$) and decreased ($p = 0.047$), respectively, when compared to healthy donors (**Figure 4.18**). CVID patients also displayed lower absolute counts of CD8$^+$ and double negative MAIT cells ($p = 0.002$ and $p = 0.03$, respectively; **Figure 4.19**).

As said, MAIT cells are defined as CD3$^+$ cells expressing markers CD161 and Vα7.2. Previous research in mouse models and in XLA patients has also shown that this cell population depends on B cells for its expansion after birth.[109] For these reasons, the reduced frequencies and counts of MAIT cells observed in patients with immune deficiencies could depend on a generalized decrease of CD161 expression by T cells, or be the consequence of decreased B cell frequencies. A comparison of CD161$^+$ T cell frequencies and counts showed no significant differences in the expression of this marker by healthy controls and patients (**Figure 4.20**). Similarly, no significant correlation was identified between the frequencies or absolute counts of MAIT cells and total B cells in CVID patients (**Figure 4.21**).

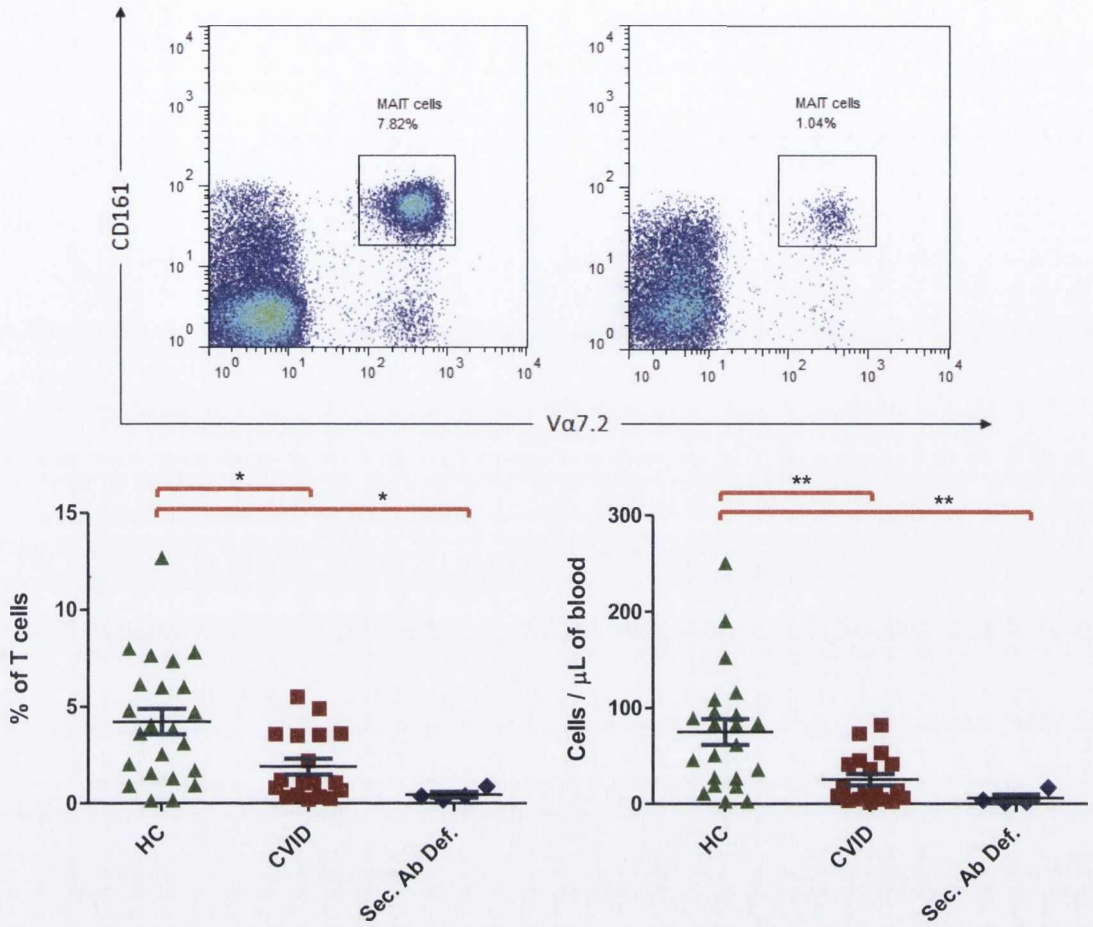


Figure 4.17. Representative dot plots, frequencies and absolute counts of MAIT cells. The representative flow cytometry dot plots in the figure (top) show MAIT cells, detected as Vα7.2$^+$ CD161^{high} events following gating on CD3$^+$ T cells, in whole blood from a healthy control (left) and of a CVID patient (right). The scatter plots (bottom) show the frequencies (left) and absolute numbers (right) of MAIT cells, as determined by flow cytometry in whole blood from healthy controls (HC, n = 23), CVID patients (CVID, n = 18) and secondary antibody deficiency patients (Sec. Ab Def., n = 4). Statistical analysis was performed employing a Kruskal-Wallis test plus Dunn's post hoc test. * $p < 0.05$; ** $p < 0.01$.

In order to compare frequencies of different B cell subsets in patients with high or low numbers of MAIT cells, CVID patients were divided in two groups displaying frequencies of MAIT cells either lower or equal to/higher than 2.2 % of total T cells, respectively. The threshold of 2.2 % was selected on the basis of the immunophenotyping results obtained for the population. Frequencies of MAIT cells were found to be significantly different in the two groups of patients ($p = 0.001$, **Figure 4.22**), however no significant result was identified following comparison of the frequencies of total and transitional B cells, naïve B cells, unswitched and class-switched memory B cells and CD27$^-$ IgD$^-$ B cells in the two groups. Scatter plots for naïve, unswitched memory, class-switched memory and CD27$^-$ IgD$^-$ B cells

are shown in **Figure 4.23**. The correlation analysis and division of patients according to low or high MAIT cell frequencies was not performed for secondary antibody deficiency patients as data were available for only four of them.

Thus, frequencies and absolute counts of MAIT cells were found to be significantly decreased in the circulation of CVID patients in comparison to healthy controls; these changes were not associated with diminished frequencies of CD161-expressing T cells or decreased frequencies or counts of B cells in patients. Differences in MAIT cell frequencies in the blood of patients did not associate with altered frequencies of total and transitional B cells, naïve B cells, unswitched and class-switched memory B cells and $CD27^-$ IgD^- B cells. Frequencies and absolute counts of $CD4^+$, $CD8^+$ and double negative MAIT cells were also anomalous in blood samples from CVID patients in comparison to healthy controls.

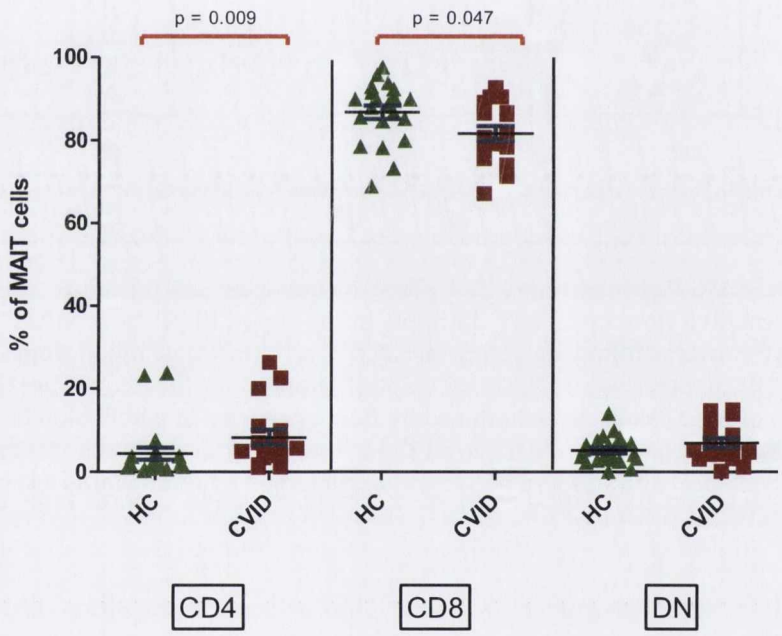


Figure 4.18. Frequencies of $CD4^+$, $CD8^+$ and double negative MAIT cells. MAIT cells, detected by flow cytometry as $CD3^+$ $V\alpha7.2^+$ $CD161^{high}$ events in whole blood from healthy controls (HC, n = 21) and CVID patients (CVID, n = 17) were subdivided on the basis of their positivity or negativity for CD4 and CD8 in $CD4^+$ ($CD4^+$ $CD8^-$), $CD8^+$ ($CD4^-$ $CD8^+$) and double negative (DN, $CD4^-$ $CD8^-$) subsets. Statistical analysis was performed employing a two-tailed Mann-Whitney test.

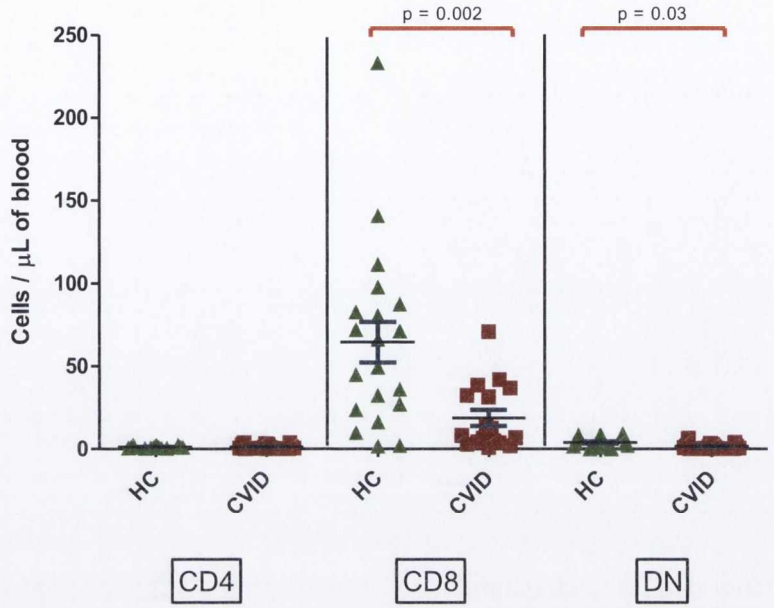


Figure 4.19. Absolute counts of CD4$^+$, CD8$^+$ and double negative MAIT cells. MAIT cells, detected by flow cytometry as CD3$^+$ Vα7.2$^+$ CD161^{high} events in whole blood from healthy controls (HC, n = 20) and CVID patients (CVID, n = 17) were subdivided on the basis of their positivity or negativity for CD4 and CD8 in CD4$^+$ (CD4$^+$ CD8$^-$), CD8$^+$ (CD4$^-$ CD8$^+$) and double negative (DN, CD4$^-$ CD8$^-$) subsets. Statistical analysis was performed employing a Kruskal-Wallis test plus Dunn's post hoc test.

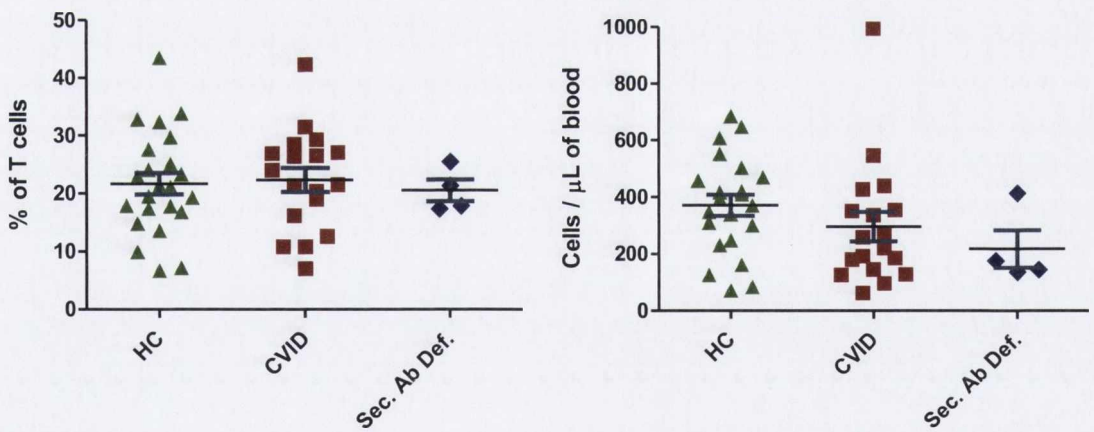


Figure 4.20. Frequencies and absolute counts of CD161$^+$ T cells. The scatter plots show the frequencies (left) and absolute numbers (right) of CD161$^+$ T cells, detected by flow cytometry as CD3$^+$ CD161$^+$ events, in whole blood from healthy controls (HC, n = 23), CVID patients (CVID, n = 18) and secondary antibody deficiency patients (Sec. Ab Def., n = 4). Statistical analysis was performed employing a Kruskal-Wallis test plus Dunn's post hoc test.

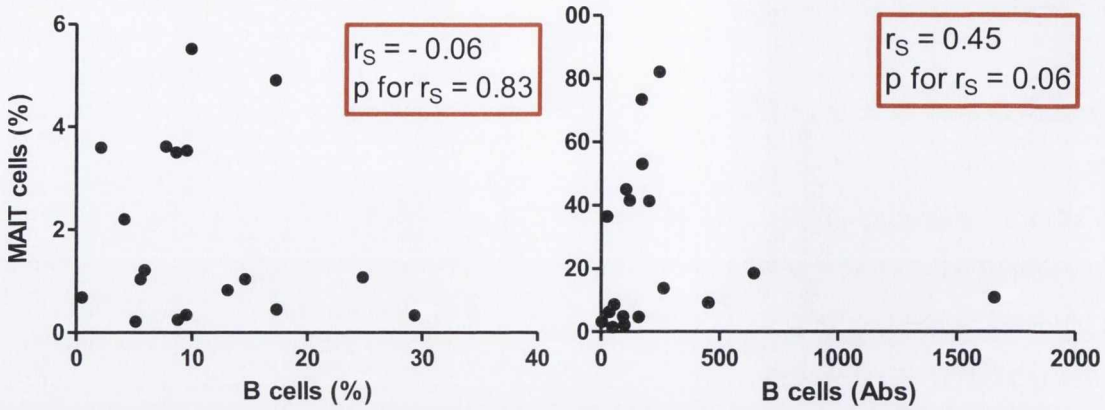


Figure 4.21. Correlations between frequencies and absolute counts of MAIT cells and total B cells in CVID patients. Frequencies and absolute counts of MAIT cells, detected as $CD3^+$ $V\alpha7.2^+$ $CD161^{high}$ events, were determined by flow cytometry in whole blood samples from CVID patients. Frequencies and absolute counts of B cells were determined by flow cytometry in whole blood samples from CVID patients, staining the samples with Multitest 6-color TBNK Reagent in TruCount tubes. The degree of correlation between frequencies (%, left) and absolute numbers (Abs, right) of MAIT cells and B cells was expressed using Spearman's correlation coefficient (r_S). p = p value.

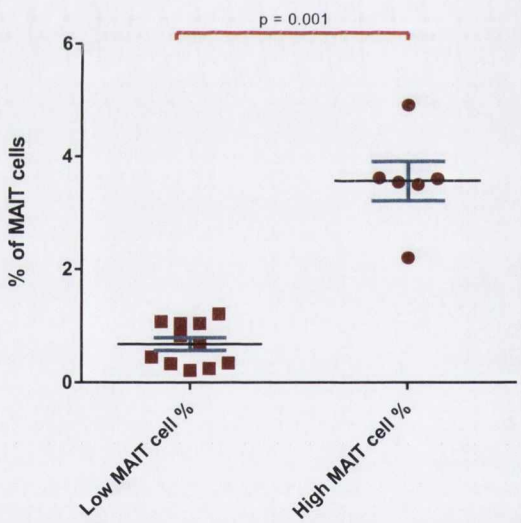


Figure 4.22. Division of CVID patients according to their frequencies of MAIT cells. MAIT cells were detected by flow cytometry as $CD3^+$ $V\alpha7.2^+$ $CD161^{high}$ events in whole blood samples from CVID patients. The patients were then divided on the basis of their frequencies of MAIT cells, in a group with frequencies lower than 2.2 % (Low MAIT cell %, n = 11) and a group with frequencies equal to or higher than 2.2 % (High MAIT cell %, n = 6). Statistical analysis was performed employing a two-tailed Mann-Whitney test.

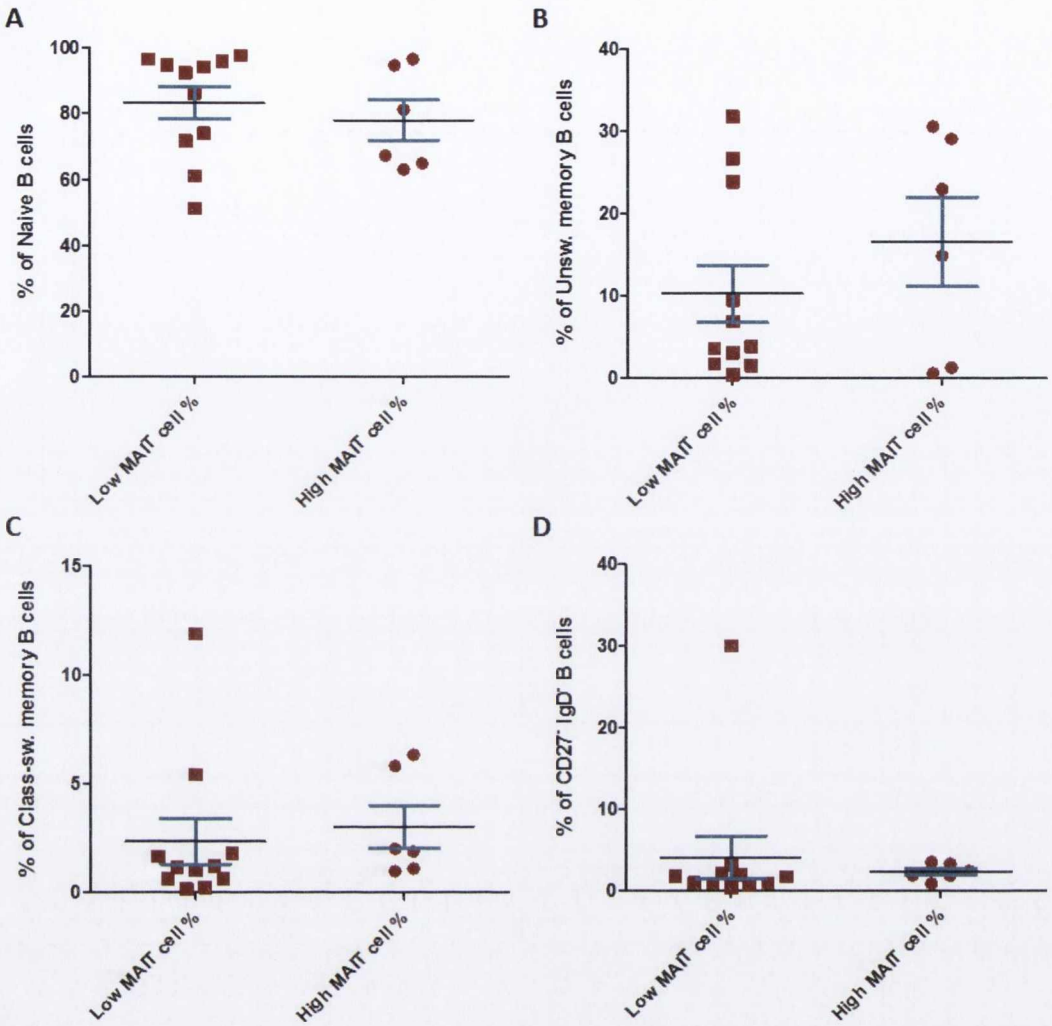


Figure 4.23. Numbers of B cell populations in CVID patients divided according to their frequencies of circulating MAIT cells. Frequencies of B cells were determined by flow cytometry in whole blood samples from CVID patients, detecting naïve B cells ($CD19^+$ $CD27^-$ IgD^+ events), unswitched memory B cells ($CD19^+$ $CD27^+$ IgD^+ events), class-switched memory B cells ($CD19^+$ $CD27^+$ IgD^- events) and $CD27^-$ IgD^- B cells. The frequencies of B cells in CVID patients with low (< 2.2 %, n = 11) and high (≥ 2.2 %, n = 6) frequencies of MAIT cells, similarly detected in whole blood samples as $CD3^+$ $V\alpha7.2^+$ $CD161^{high}$ events, were then compared. Statistical analysis was performed employing a two-tailed Mann-Whitney test.

4.3.5 – Phenotypic analysis of NT cells

NT cells were identified in this study as $CD3^+$ $CD56^+$ events. No significant differences were detected when comparing the frequencies or absolute counts of this population in the circulation of CVID patients, secondary antibody deficiency patients and healthy controls (**Figure 4.24**). Similarly, frequencies and absolute counts of $CD4^+$, $CD8^+$ and double

negative NT cells were found to be similar in the circulation of healthy donors and CVID patients (**Figure 4.25 and 4.26**).

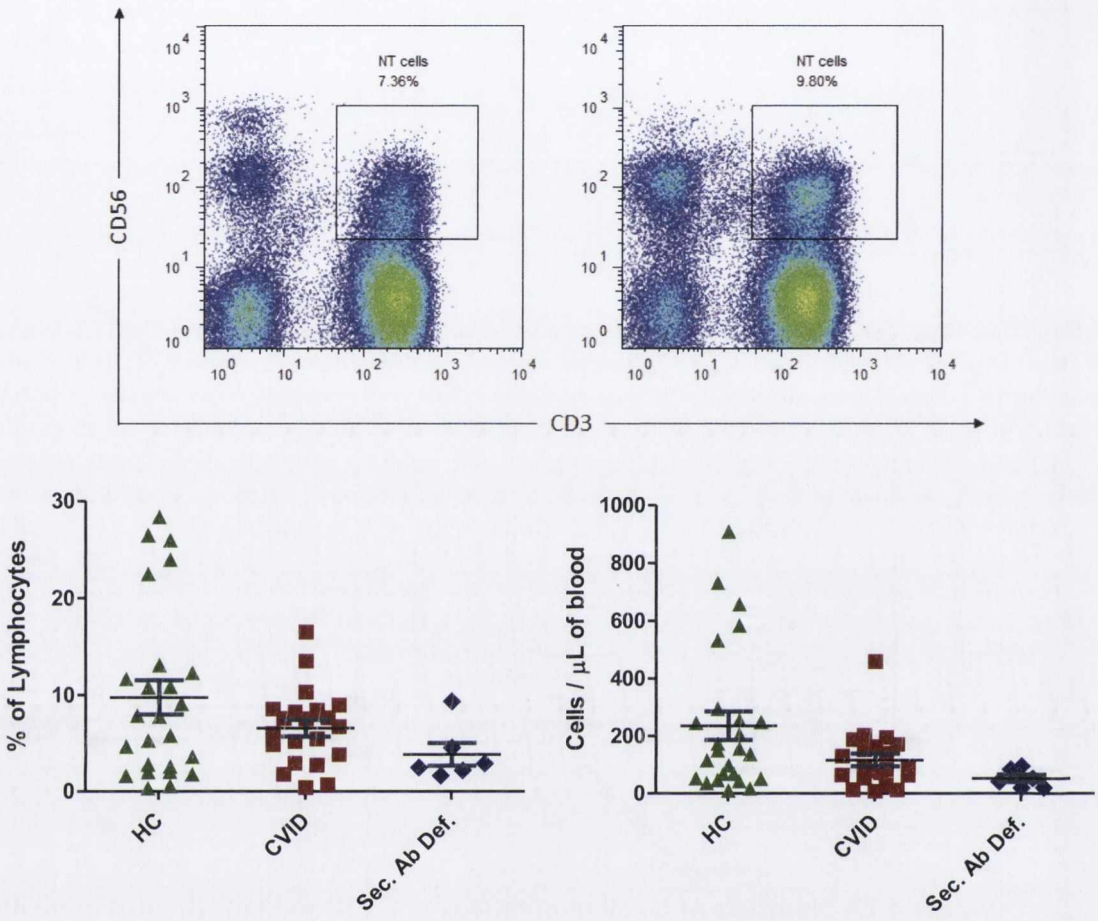


Figure 4.24. Representative dot plots, frequencies and absolute counts of NT cells. The representative flow cytometry dot plots in the figure (top) show NT cells, detected as $CD3^+$ $CD56^+$ events, in whole blood from a healthy control (left) and of a CVID patient (right). The scatter plots (bottom) show the frequencies (left) and absolute numbers (right) of NT cells, as determined by flow cytometry in whole blood from healthy controls (HC, n = 25), CVID patients (CVID, n = 21) and secondary antibody deficiency patients (Sec. Ab Def., n = 6). Statistical analysis was performed employing a Kruskal-Wallis test plus Dunn's post hoc test.

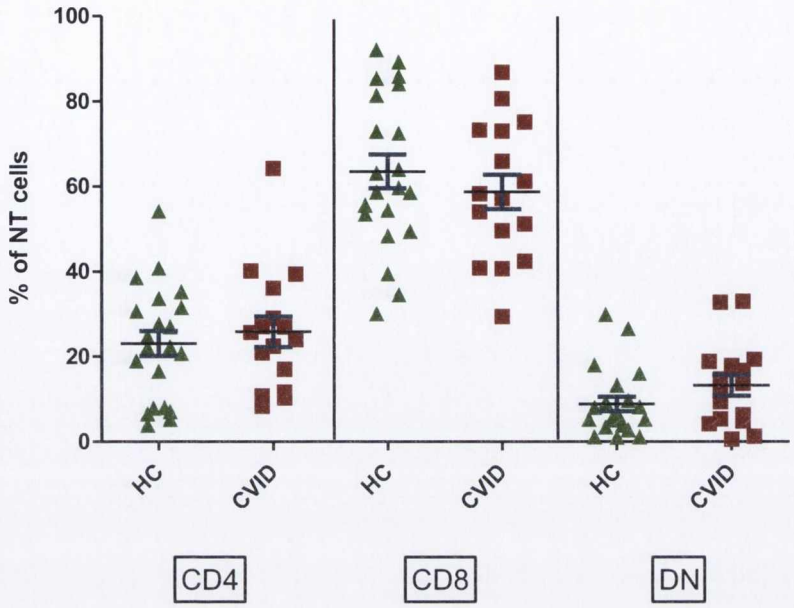


Figure 4.25. Frequencies of $CD4^+$, $CD8^+$ and double negative NT cells. NT cells, detected by flow cytometry as $CD3^+$ $CD56^+$ events in whole blood from healthy controls (HC, n = 21) and CVID patients (CVID, n = 16) were subdivided on the basis of their positivity or negativity for CD4 and CD8 in $CD4^+$ ($CD4^+$ $CD8^-$), $CD8^+$ ($CD4^-$ $CD8^+$) and double negative (DN, $CD4^-$ $CD8^-$) subsets. Statistical analysis was performed employing a two-tailed Mann-Whitney test.

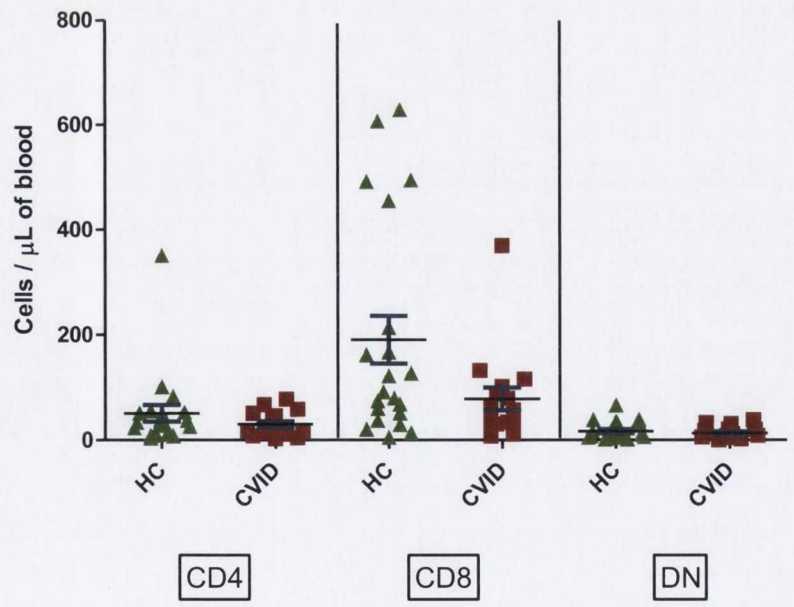


Figure 4.26. Absolute counts of $CD4^+$, $CD8^+$ and double negative NT cells. NT cells, detected by flow cytometry as $CD3^+$ $CD56^+$ events in whole blood from healthy controls (HC, n = 21) and CVID patients (CVID, n = 16), were subdivided on the basis of their positivity or negativity for CD4 and CD8 in $CD4^+$ ($CD4^+$ $CD8^-$), $CD8^+$ ($CD4^-$ $CD8^+$) and double negative (DN, $CD4^-$ $CD8^-$) subsets. Statistical analysis was performed employing a two-tailed Mann-Whitney test.

4.4 – Phenotypic analysis of circulating T cell subsets in SIgAD and IgG subclass deficiency

Only three patients with SIgAD and/or IgG subclass deficiency were recruited to this study. Of these, one presented with SIgAD exclusively; the remaining two were closely related and affected by both conditions. This chapter presents a selection of results from these donors, and a brief summary of the data not shown.

The three patients displayed normal frequencies and absolute counts of total T cells, NK cells, NT cells, Vδ2 and Vδ3 γδ T cells (data not shown). Similar to CVID patients, iNKT cells were decreased in these individuals in comparison to healthy donors (**Figure 4.27**), both in frequencies ($p = 0.03$) and in absolute counts ($p < 0.05$). Vδ1 γδ T cells were also significantly depleted ($p = 0.04$ for frequencies and $p = 0.03$ for absolute counts; **Figure 4.28**). MAIT cell frequencies and counts, which were altered in the larger CVID cohort, were comparable to those of healthy controls, although their frequencies tended to be low (**Figure 4.29**).

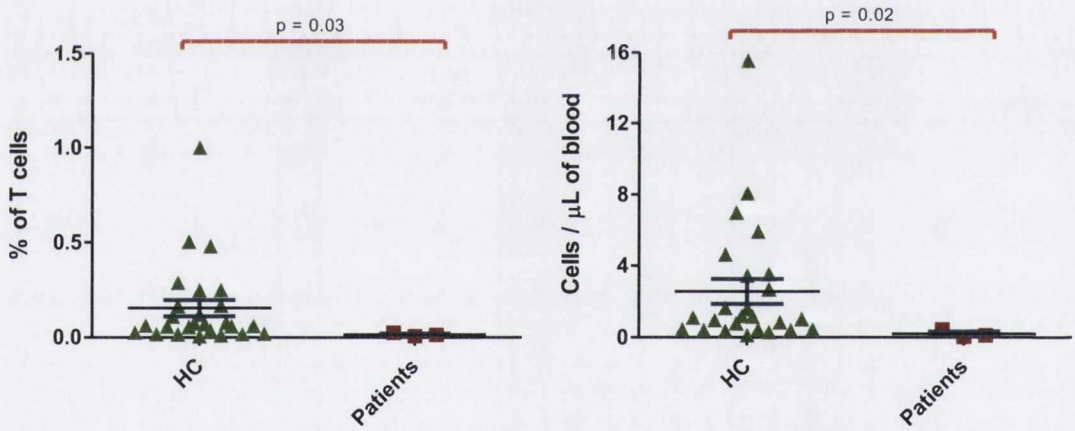


Figure 4.27. Frequencies and absolute counts of Vα24-Jα18$^+$ iNKT cells. The scatter plots show the frequencies (left) and absolute numbers (right) of iNKT cells, detected by flow cytometry as CD3$^+$ Vα24-Jα18$^+$ events in whole blood from healthy controls (HC, n = 26) and SIgAD/IgG subclass patients (Patients, n = 3). Statistical analysis was performed employing a two-tailed Mann-Whitney test.

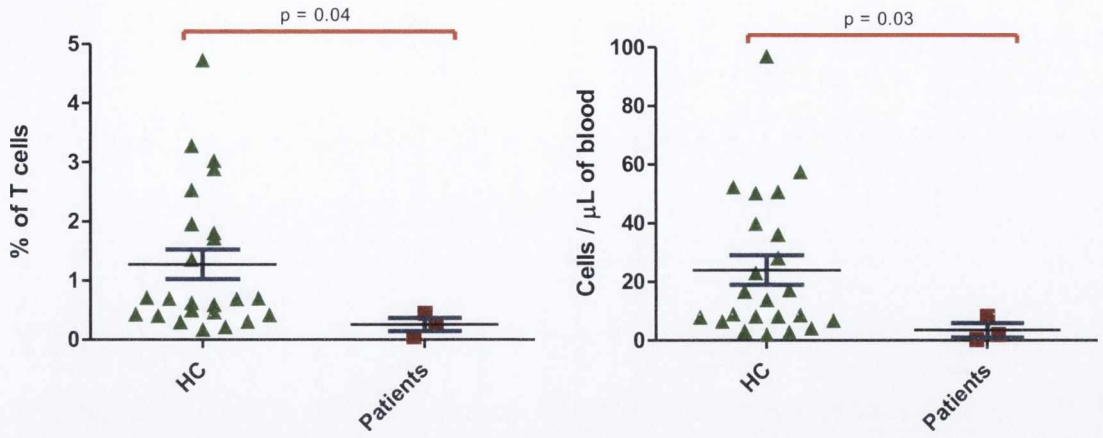


Figure 4.28. Frequencies and absolute counts of Vδ1 γδ T cells. The scatter plots show the frequencies (left) and absolute numbers (right) of Vδ1 γδ T cells, detected by flow cytometry as $CD3^+$ Vδ1 TCR^+ events in whole blood from healthy controls (HC, n = 24) and SIgAD/IgG subclass patients (Patients, n = 3). Statistical analysis was performed employing a two-tailed Mann-Whitney test.

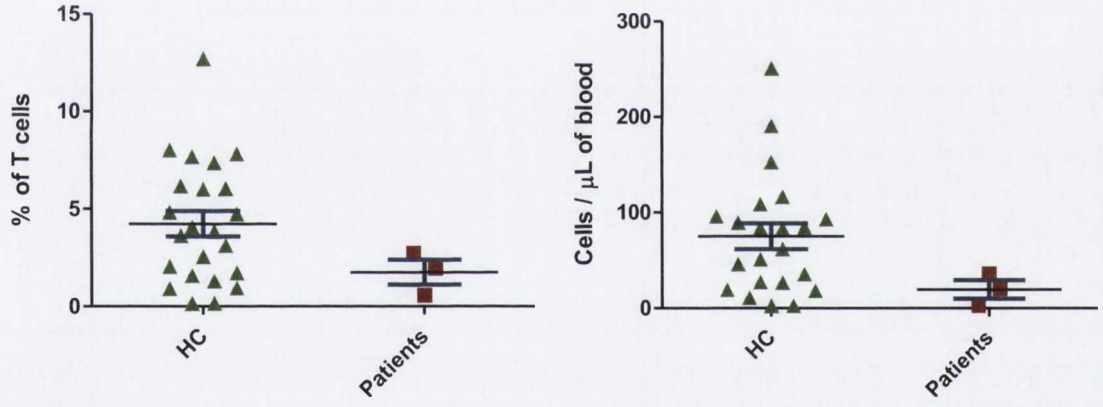


Figure 4.29. Frequencies and absolute counts of MAIT cells. The scatter plots show the frequencies (left) and absolute numbers (right) of MAIT cells, detected by flow cytometry as $CD3^+$ $V\alpha7.2^+$ $CD161^{high}$ events in whole blood from healthy controls (HC, n = 23) and SIgAD/IgG subclass patients (Patients, n = 3). Statistical analysis was performed employing a two-tailed Mann-Whitney test.

4.5 – Phenotypic analysis of circulating T cell subsets in a query diagnosis patient

The data reported here refer to a single male individual whose antibody deficiency was found to differ from CVID, SIgAD, IgG subclass deficiency and secondary deficiency. This patient's immunodeficiency had an early onset, becoming established and causing life-threatening infections, in the form of meningitis, from the age of 1 month. A history of similar infections in males belonging to the maternal side of the patient's family suggests that the condition may have genetic bases and be X-linked, however no causative mutation has so far been identified (see chapter 2.4 for further details). This chapter contains preliminary observations derived from a single round of immunophenotyping performed on blood from this patient. As absolute counts vary widely between individuals, only frequencies are reported in this case.

While frequencies of B cell subsets had previously been found to be largely normal (chapter 3.4), those of some T cell populations were peculiar. iNKT cells were detected at extremely high frequencies, above 1.5 % of total T cells (**Figure 4.30**). Although not as strikingly high, MAIT cell and Vδ2 γδ T cell frequencies also fell in the upper range of healthy control values (**Figure 4.31**). Counts of these populations were also notably high (data not shown). On the other hand, percentages of total T cells, Vδ1 and Vδ3 γδ T cells, NK cells and NT cells were unremarkable (data not shown).

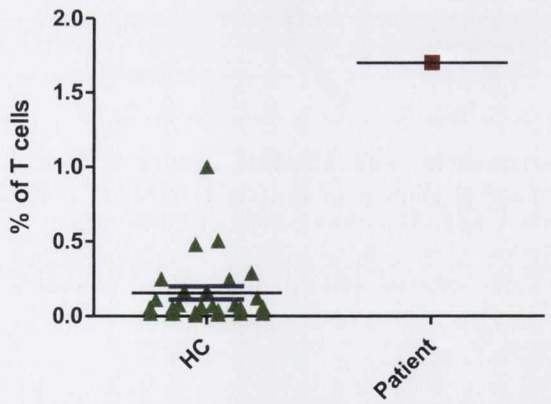


Figure 4.30. Frequencies of Vα24-Jα18$^+$ iNKT cells in the blood of a query diagnosis patient. The scatter plot shows the frequencies of iNKT cells, detected by flow cytometry as CD3$^+$ Vα24-Jα18$^+$ events in whole blood from healthy controls (HC, n = 26) and from a query diagnosis patient (Patient, n = 1). No statistical analysis was performed on these data.

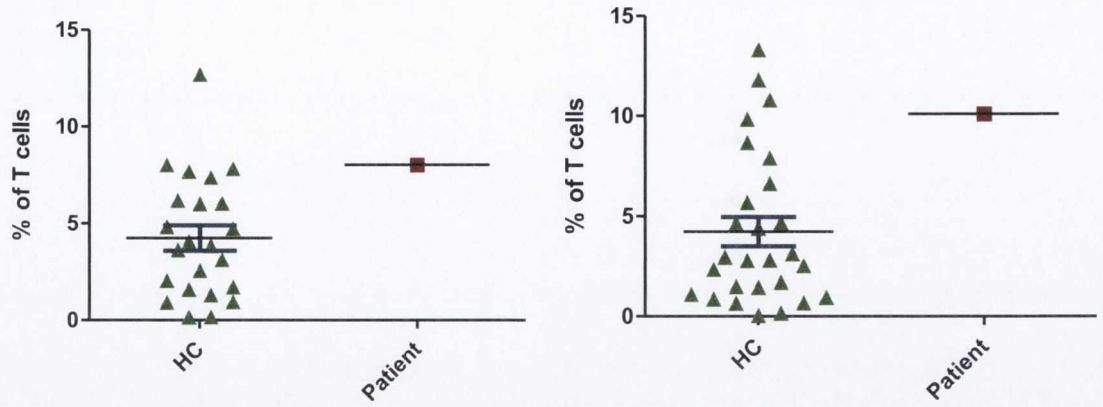


Figure 4.31. Frequencies of MAIT cells and Vδ2 γδ T cells in the blood of a query diagnosis patient. The scatter plots show the frequencies of MAIT cells (defined as $CD3^+$ $V\alpha7.2^+$ $CD161^{high}$ events, left) and Vδ2 γδ T cells (defined as $CD3^+$ Vδ2 TCR^+ events, right), detected by flow cytometry in whole blood from healthy controls (HC, n = 23 and n = 27, respectively) and from a query diagnosis patient (Patient, n = 1). No statistical analysis was performed on these data.

4.6 – Determination of associations between frequencies of innate T cell subsets and clinical phenotypes in CVID

This subchapter describes the associations existing between the clinical status of CVID patients, following their allocation to appropriate clinical phenotypes, and the frequencies of innate T cell populations, as well as their $CD4^+$, $CD8^+$ and double negative subpopulations. It should be noted that data obtained from healthy individuals were not included in the statistical analysis performed for this section of the thesis. A choice was made to exclude them, on the basis of the fact that statistically significant differences in the frequencies and absolute counts of innate T cells and their CD4/CD8 subsets in healthy controls and CVID patients had already been described at length in chapter 4.3. This chapter, on the contrary, explores whether statistically significant differences may exist in the composition of the innate T cell compartment of CVID patients with complications or with infections only. In doing so, it attempts to shed light on possible links between anomalies in innate T cell immunity and the severity of the disease.

4.6.1 – Clinical status of the cohort

As described in chapter 2.5, five distinct clinical phenotypes have previously been defined for CVID in a study by Chapel and colleagues.[178] These are:

- No complications (infections only);
- Autoimmunity;
- Polyclonal lymphocytic infiltration (PLI);
- Enteropathy;
- Lymphoid Malignancies.

CVID patients enrolled in the current study were assigned to one or more of these phenotypes on the basis of their clinical status. Broadly speaking, individuals who only developed infections were allocated to the "no complications" group, while patients who presented with infections as well as complications were categorized into one or more of the remaining phenotypes. In some cases, significant associations were detected in CVID between the frequencies of innate T cell subsets and clinical phenotypes. When this occurred, data from patients with other antibody deficiencies were added to the analysis, to define if the association was likely to be restricted to CVID or a feature of antibody deficiencies as a whole. Donors with SIgAD, IgG subclass deficiency, secondary antibody deficiency and query diagnosis were therefore categorised using the same criteria applied to CVID patients.

As shown in **Table 4.1**, 12 CVID patients (60 %) were categorized as "infections only", while 8 (40 %) had some sort of complication. Of these, 7 (87.5 %) presented with autoimmune manifestations, while one was affected by polyclonal lymphocytic infiltration exclusively. Two of the patients with autoimmune conditions were also categorized as belonging to the enteropathy and PLI phenotypes, respectively. Amongst the 3 patients with SIgAD and IgG subclass deficiency, 1 presented with autoimmunity. Finally, 1 out of 6 patients with secondary hypogammaglobulinemia displayed both autoimmunity and PLI.

Due to the small size of the cohort recruited, and the limited number of patients with complications, it was not possible to perform statistical analysis considering single complication phenotypes. Because of this, results from patients with complications are always presented together, comparing them with results from patients with infections only. Graphs representing discrete complication phenotypes are sometimes supplied in the text for completeness, but no statistical analysis was performed on these.

Table 4.1. Clinical status and complication phenotypes of recruited patients

Cohort	No. of patients	Sex	Age	Complications	Clinical phenotype
CVID	12	6M/6F	22 - 63	No	Infections only
	1	M	28	Autoimmune hepatitis	Autoimmunity
	1	M	33	AHA, ITP, possible autoimmune neutropenia, psoriasis	Autoimmunity
	1	F	33	Primary hypothyroidism, vitiligo, alopecia	Autoimmunity
	1	F	56	Pernicious anemia, primary hypothyroidism, atrophic gastritis, psoriasis	Autoimmunity
	1	M	39	Psoriasis	Autoimmunity
	1	M	54	Psoriasis, enteropathy*	Autoimmunity, Enteropathy
	1	F	28	Psoriasis, lymphadenopathy	Autoimmunity, PLI
	1	M	51	Non-caseating granuloma	PLI
SIgAD, IgG subclass deficiency	2	1M/1F	35/26	No	Infections only
	1	F	73	Psoriasis, primary hypothyroidism	Autoimmunity
Query diagnosis	1	M	23	No	Infections only
Secondary antibody deficiency	5	2M/3F	46 - 69	No	Infections only
	1	F	59	SLE, Sjogren's syndrome, antiphospholipid syndrome, ITP, hepatomegaly	Autoimmunity, PLI

* Flattening of duodenal villi and infiltration of intraepithelial lymphocytes was confirmed on biopsy for the patient classified as belonging to the enteropathy phenotype. Several other patients reporting recurrent intestinal symptoms were not included in this phenotype for lack of histological evidence of inflammation upon biopsy, or when the condition was ascribed to infectious causes.

4.6.2 – Associations between frequencies of γδ T cell subsets and clinical phenotypes

Vδ1, Vδ2 and Vδ3 γδ T cell frequencies and absolute counts had previously been found to be comparable in CVID patients and healthy controls (chapter 4.2.2). Similarly, no significant differences were identified in the frequencies and cell counts of these cell types in CVID patients with and without complications (**Figures 4.32 to 4.34**). Frequencies and absolute counts of Vδ1 and Vδ2 γδ T cells, however, appeared somewhat decreased in CVID patients with complications.

When frequencies (**Figure 4.35**) and absolute counts (**Figure 4.36**) of $CD4^+$, $CD8^+$ and double negative Vδ1 γδ T cells were considered, no significant differences were identified between CVID patients with infections only and CVID patients with complications, although counts of $CD8^+$ and double negative cells displayed a non-significant decrease.

A significant increase ($p = 0.03$) in the frequencies of $CD4^+$ Vδ2 γδ T cells was noted in CVID patients with complications as opposed to patients with infections only, however no significant change was identified for $CD8^+$ or double negative cells belonging to this subset (**Figure 4.37**); this is probably due to the fact that the percentage increase in $CD4^+$ γδ T cell frequencies seen in patients with complications is too small to sufficiently alter the medians of the $CD8^+$ or double negative cells for this patient population, on the basis of which the Mann-Whitney test employed for statistical analysis calculates statistical significance. In terms of absolute counts (**Figure 4.38**), this translated in comparable counts of $CD4^+$ Vδ2 γδ T cells in the blood of the two patient groups, while counts of $CD8^+$ cells were significantly decreased in the circulation of patients with complications ($p = 0.03$). Counts of double negative Vδ2 γδ T cells were also decreased in samples collected from patients with complications in comparison to patients with infections only, although not significantly so.

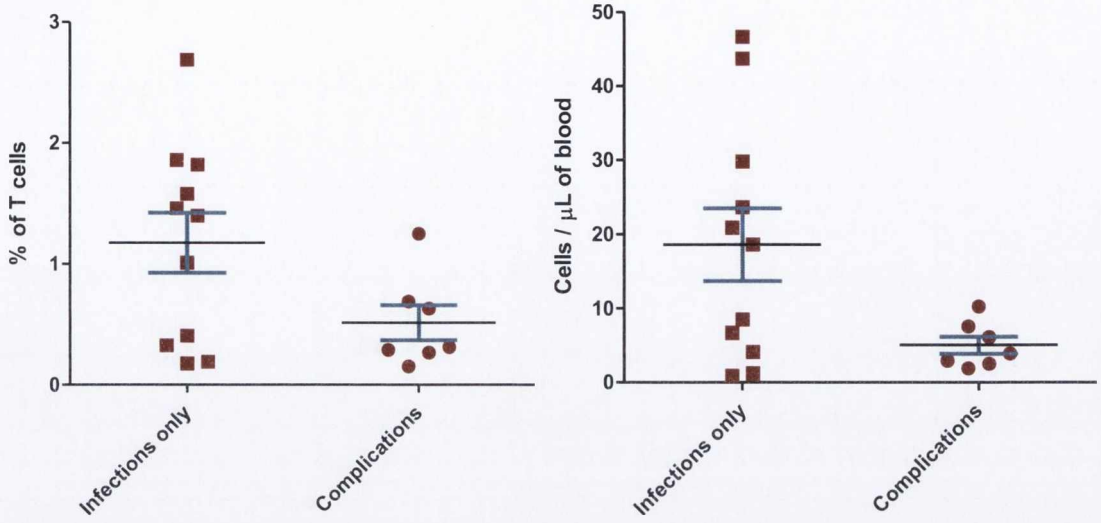


Figure 4.32. Frequencies and absolute counts of Vδ1 γδ T cells in CVID patients with or without complications. The scatter plots show the frequencies (left) and absolute counts (right) of Vδ1 γδ T cells, detected by flow cytometry as $CD3^+$ Vδ1 TCR^+ events, in whole blood from CVID patients with infections only (n = 11) or with infections and complications (Complications, n = 7). Statistical analysis was performed employing a two-tailed Mann-Whitney test.

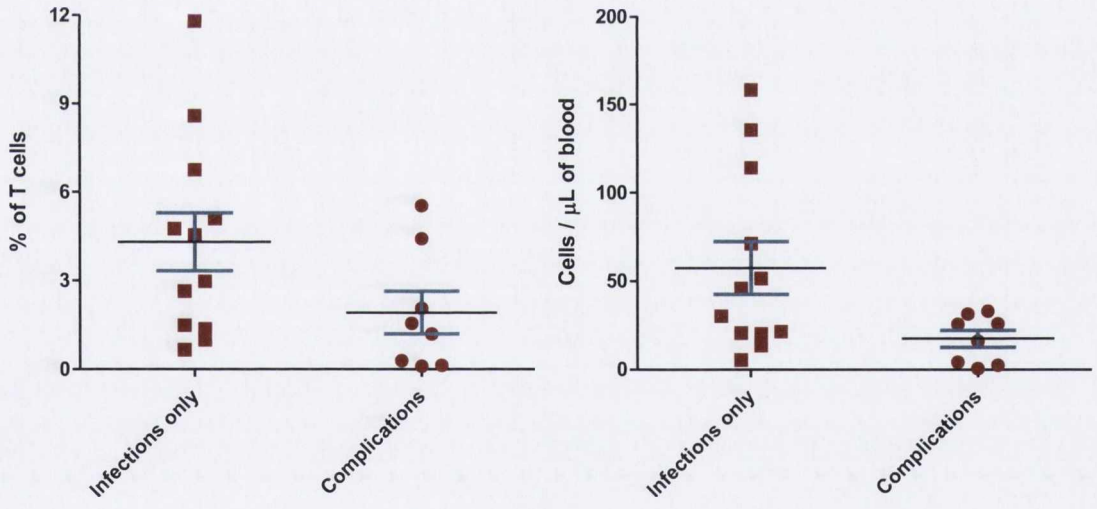


Figure 4.33. Frequencies and absolute counts of Vδ2 γδ T cells in CVID patients with or without complications. The scatter plots show the frequencies (left) and absolute counts (right) of Vδ2 γδ T cells, detected by flow cytometry as $CD3^+$ Vδ2 TCR^+ events, in whole blood from CVID patients with infections only (n = 12) or with infections and complications (Complications, n = 8). Statistical analysis was performed employing a two-tailed Mann-Whitney test.

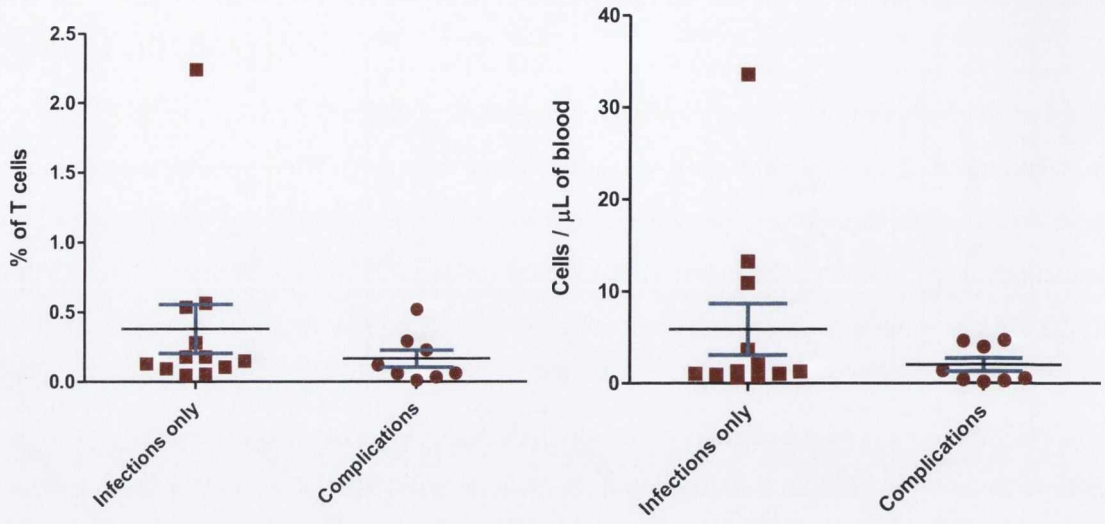


Figure 4.34. Frequencies and absolute counts of Vδ3 γδ T cells in CVID patients with or without complications. The scatter plots show the frequencies (left) and absolute counts (right) of Vδ3 γδ T cells, detected by flow cytometry as $CD3^+$ Vδ3 TCR^+ events, in whole blood from CVID patients with infections only (n = 12) or with infections and complications (Complications, n = 8). Statistical analysis was performed employing a two-tailed Mann-Whitney test.

No significant differences were noted in the frequencies of $CD4^+$, $CD8^+$ and double negative Vδ3 γδ T cells detected in the blood of CVID patients with infections only or CVID patients with complications (**Figure 4.39**). Differences between absolute counts of these populations could not be investigated, due to the insufficient number of data points obtained for CVID patients with complications.

Thus, Vδ1, Vδ2 and Vδ3 γδ T cells, as well as their $CD4^+$, $CD8^+$ and double negative subsets, were generally detected at similar frequencies in the peripheral blood of CVID patients with infections only or with infections and complications. The exceptions to these were the frequencies of $CD4^+$ Vδ2 γδ T cells and the counts of $CD8^+$ Vδ2 γδ T cells, which were significantly increased and decreased, respectively, in patients with complications in comparison to patients with infections only.

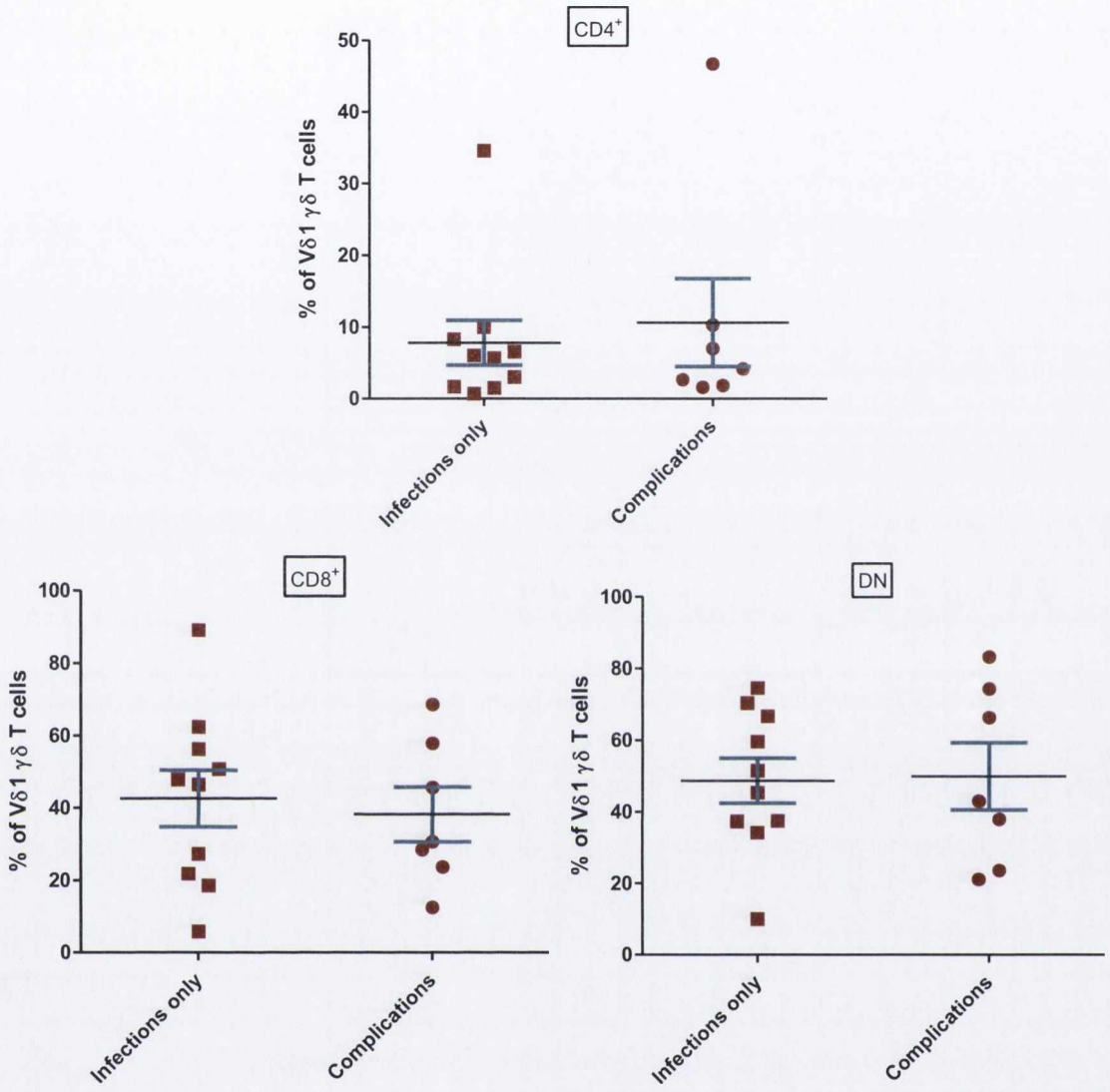


Figure 4.35. Frequencies of $CD4^+$, $CD8^+$ and double negative Vδ1 γδ T cells in CVID patients with or without complications. The scatter plots show the frequencies of $CD4^+$ (top), $CD8^+$ (bottom left) and double negative (DN, bottom right) Vδ1 γδ T cells, detected by flow cytometry as $CD3^+$ Vδ1 TCR^+ events, in whole blood from CVID patients with infections only (n = 10) or with infections and complications (Complications, n = 7). Statistical analysis was performed employing a two-tailed Mann-Whitney test.

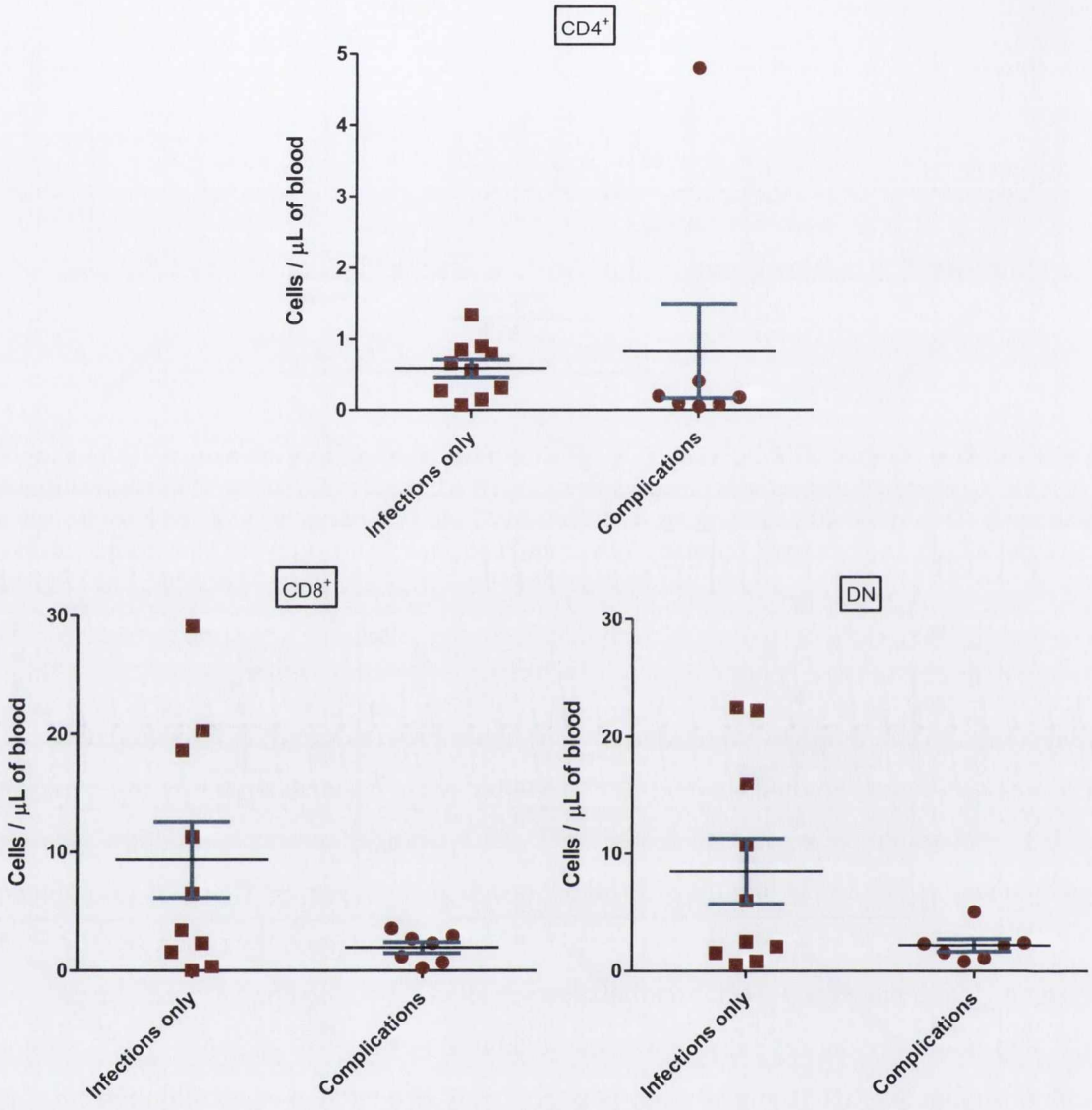


Figure 4.36. Absolute counts of $CD4^+$, $CD8^+$ and double negative Vδ1 γδ T cells in CVID patients with or without complications. The scatter plots show the absolute counts of $CD4^+$ (top), $CD8^+$ (bottom left) and double negative (DN, bottom right) Vδ1 γδ T cells, detected by flow cytometry as $CD3^+$ Vδ1 TCR^+ events, in whole blood from CVID patients with infections only (n = 10) or with infections and complications (Complications, n = 7).). Statistical analysis was performed employing a two-tailed Mann-Whitney test.

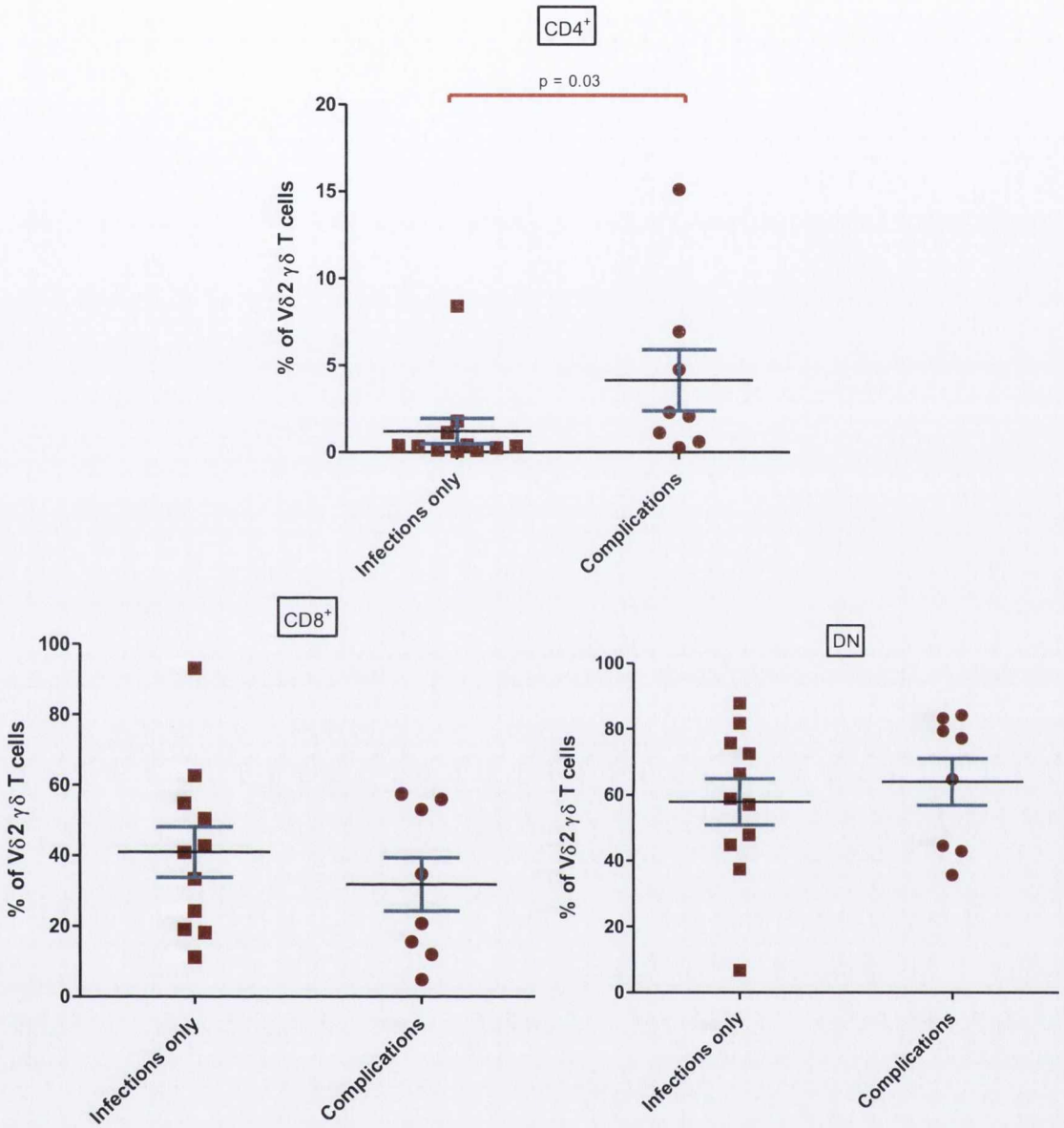


Figure 4.37. Frequencies of $CD4^+$, $CD8^+$ and double negative Vδ2 γδ T cells in CVID patients with or without complications. The scatter plots show the frequencies of $CD4^+$ (top), $CD8^+$ (bottom left) and double negative (DN, bottom right) Vδ2 γδ T cells, detected by flow cytometry as $CD3^+$ Vδ2 TCR^+ events, in whole blood from CVID patients with infections only (n = 11) or with infections and complications (Complications, n = 8).). Statistical analysis was performed employing a two-tailed Mann-Whitney test.

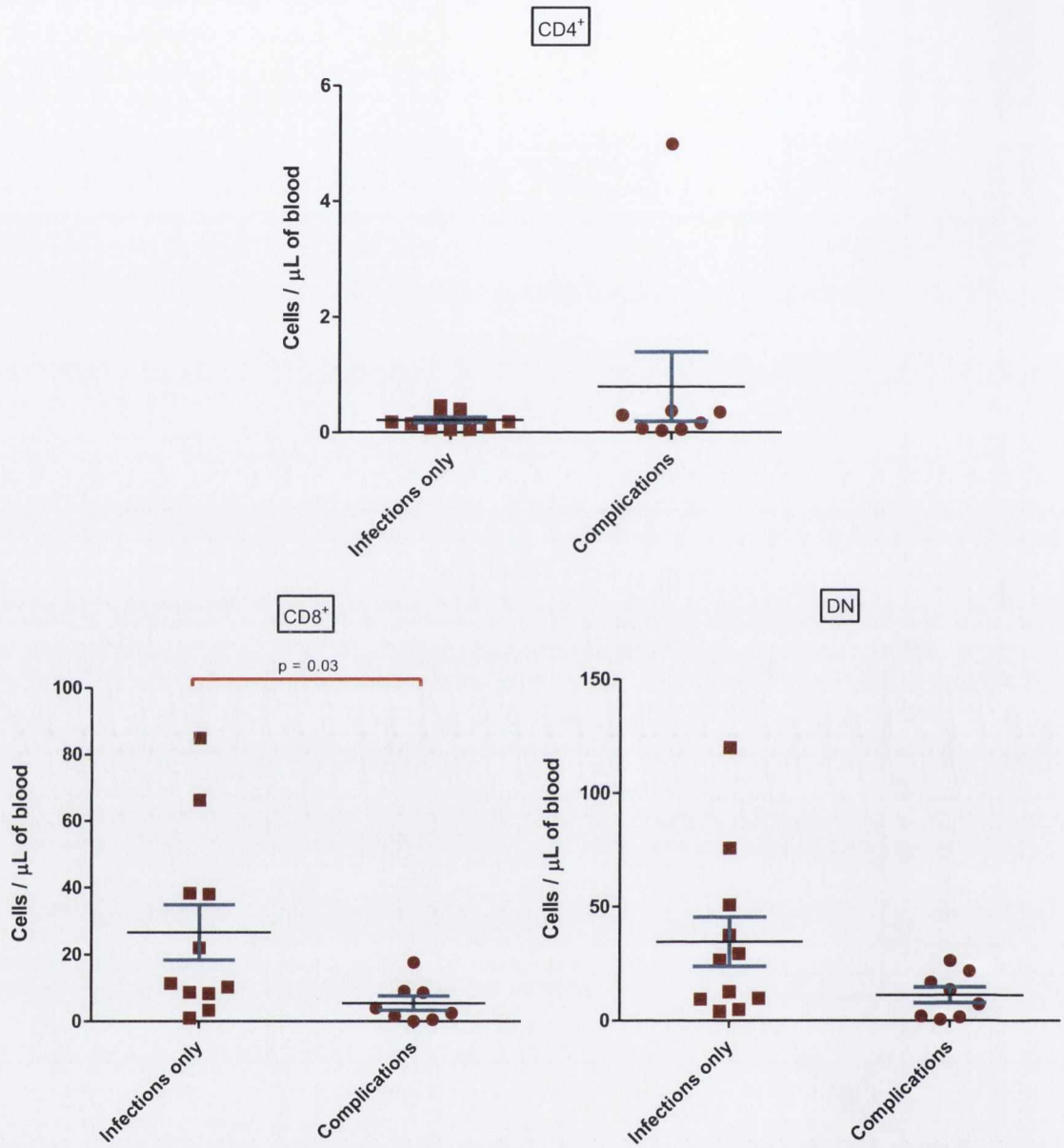


Figure 4.38. Absolute counts of $CD4^+$, $CD8^+$ and double negative Vδ2 γδ T cells in CVID patients with or without complications. The scatter plots show the absolute counts of $CD4^+$ (top), $CD8^+$ (bottom left) and double negative (DN, bottom right) Vδ2 γδ T cells, detected by flow cytometry as $CD3^+$ Vδ2 TCR^+ events, in whole blood from CVID patients with infections only (n = 11) or with infections and complications (Complications, n = 8). Statistical analysis was performed employing a two-tailed Mann-Whitney test.

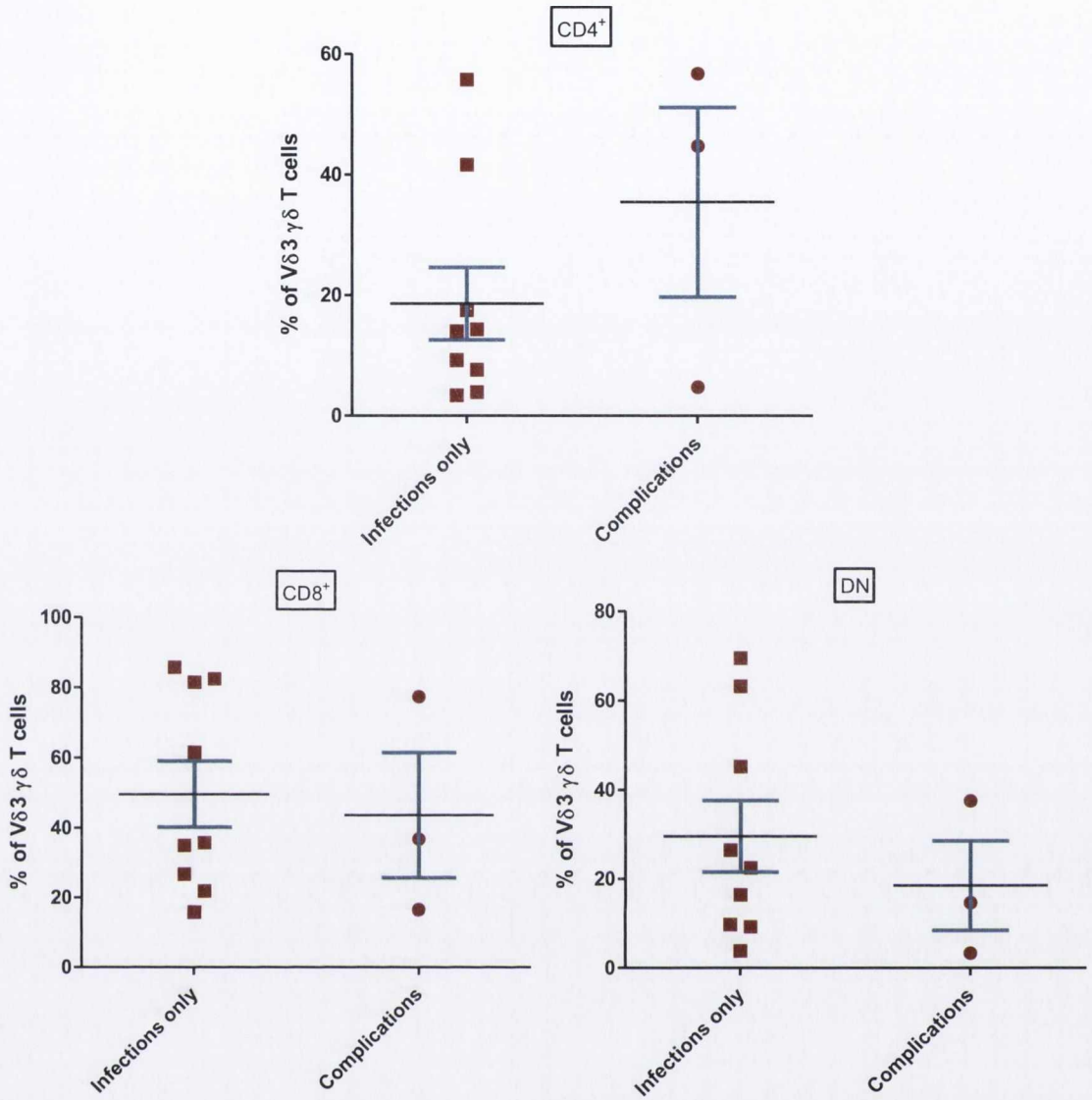


Figure 4.39. Frequencies of $CD4^+$, $CD8^+$ and double negative Vδ3 γδ T cells in CVID patients with or without complications. The scatter plots show the frequencies of $CD4^+$ (top), $CD8^+$ (bottom left) and double negative (DN, bottom right) Vδ3 γδ T cells, detected by flow cytometry as $CD3^+$ Vδ3 TCR^+ events, in whole blood from CVID patients with infections only (n = 9) or with infections and complications (Complications, n = 3). Statistical analysis was performed employing a two-tailed Mann-Whitney test.

4.6.3 – Associations between frequencies of iNKT cells and clinical phenotypes

Frequencies and absolute counts of circulating iNKT cells were previously found in this study to be significantly decreased in CVID patients in comparison to healthy donors (chapter 4.2.3). When associations between numbers of this population and the clinical status of CVID patients were probed, both frequencies and absolute counts of iNKT cells were

found to be significantly depleted in the peripheral blood of patients with complications in comparison to patients with infections only ($p = 0.04$ and $p = 0.02$, respectively; **Figure 4.40**). As shown in **Figure 4.41**, the significance of the associations between complications and low frequencies or absolute counts of iNKT cells was maintained when considering data from all patients recruited (CVID, SIgAD, IgG subclass deficiency, secondary antibody deficiency and query diagnosis; $p = 0.02$ for frequencies, $p = 0.007$ for absolute counts). It is worth noting that, in this same figure, the data point falling around 1.7 % in the "infections only" group represents the query diagnosis patient whose high iNKT cell frequencies were previously described in chapter 4.5. Importantly, the inclusion of this value does not significantly skew the analysis of the data set, as the significance of the association probed is maintained upon its removal ($p = 0.03$, data not shown).

When frequencies of iNKT cells from the whole cohort (i.e. all patients recruited) were broken up according to clinical phenotype, no complication type seemed uniquely linked to iNKT cell depletion (**Figure 4.42**). It must however be noted that this particular group of patients displayed a strong bias towards autoimmune conditions, so that only one patient with PLI was effectively representative of a distinct complication type.

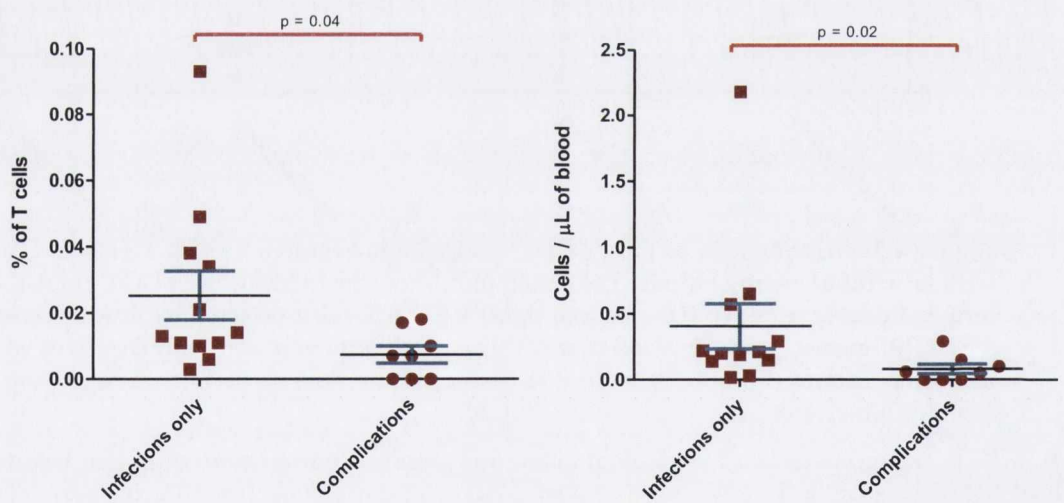


Figure 4.40. Frequencies and absolute counts of iNKT cells in CVID patients with or without complications. The scatter plots show the frequencies (left) and absolute counts (right) of iNKT cells, detected by flow cytometry as $CD3^+$ $V\alpha24\text{-}J\alpha18^+$ events, in whole blood from CVID patients with infections only ($n = 12$) or with infections and complications (Complications, $n = 8$). Statistical analysis was performed employing a two-tailed Mann-Whitney test.

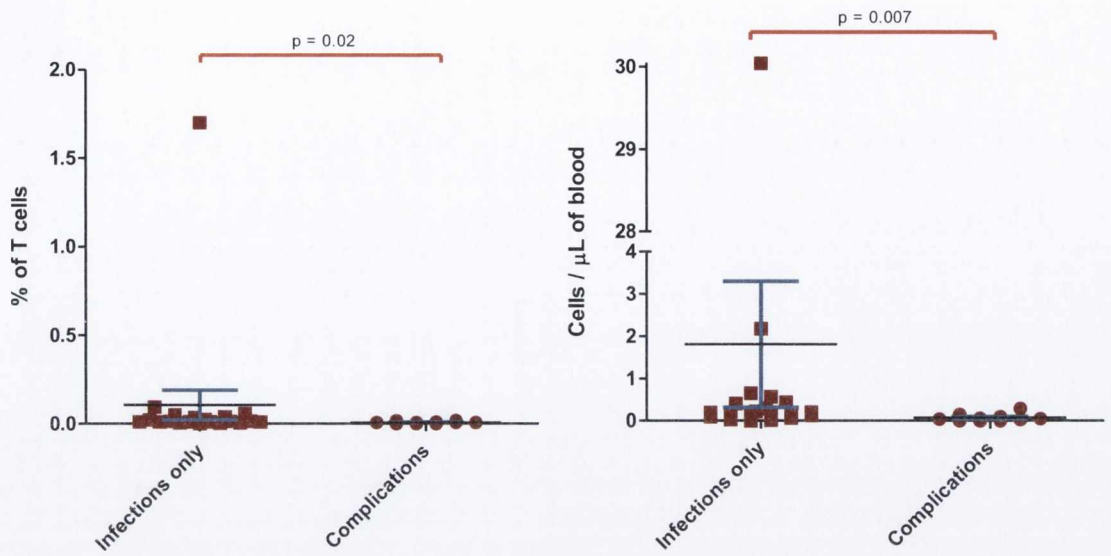


Figure 4.41. Frequencies and absolute counts of iNKT cells in patients with primary and secondary deficiencies, with or without complications. The scatter plot shows the frequencies (left) and absolute counts (right) of iNKT cells, detected by flow cytometry as $CD3^+$ $V\alpha24\text{-}J\alpha18^+$ events, in whole blood from patients with primary or secondary antibody deficiencies (i.e. CVID, SIgAD, IgG subclass deficiency, secondary antibody deficiency and query diagnosis) with infections only (n = 20) or with infections and complications (Complications, n = 10). Statistical analysis was performed employing a two-tailed Mann-Whitney test.

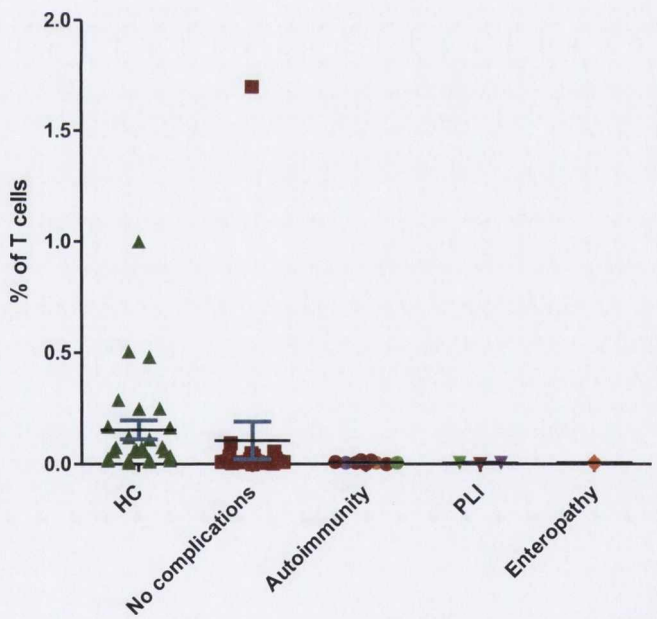


Figure 4.42. Frequencies of iNKT cells in the circulation of patients with primary and secondary antibody deficiencies, divided by clinical phenotype. The scatter plot shows the frequencies of iNKT cells, detected by flow cytometry as $CD3^+$ $V\alpha24\text{-}J\alpha18^+$ events, in whole blood from healthy controls (HC, dark green, n = 26) and patients with primary and secondary antibody deficiencies (i.e. CVID, SIgAD, IgG subclass deficiency, secondary antibody deficiency and query diagnosis), divided on the basis of their clinical phenotype: no complications (i.e. infections only, n = 20), autoimmunity (n = 9), PLI (polyclonal lymphocytic infiltration, n = 3), enteropathy (n = 1). The graph includes more data points than patients, as some patients belonged to more than one clinical phenotype: data points in orange, purple and leaf green mark out these individuals. No statistical analysis was performed on these data.

Thus, lower frequencies of circulating iNKT cells significantly associate with the complications of CVID, and more in general with the complications of primary and secondary immunodeficiencies. It was unfortunately not possible to investigate if the frequencies of CD4+, CD8+ and double negative iNKT cells associated with complications, as these phenotyping data were not available.

4.6.4 – Associations between frequencies of MAIT cells and clinical phenotypes

As shown in chapter 4.2.4, frequencies and absolute counts of MAIT cells were decreased in the circulation of CVID patients. Comparing frequencies of total MAIT cells in patients with infections only and in patients with infections and complications, significantly lower percentages and numbers of MAIT cells were detected in the circulation of the latter group ($p < 0.05$ and $p = 0.04$, respectively; **Figure 4.43**). The significance of these associations was maintained when data from all recruited patients (CVID, SIgAD, IgG subclass deficiency, secondary antibody deficiency and query diagnosis) were considered ($p = 0.03$ for frequencies and $p = 0.02$ for absolute counts; **Figure 4.44**). When frequencies from the whole cohort (i.e. all patients recruited) were broken up according to clinical phenotype, frequencies of MAIT cells appeared to be equally decreased in all complication groups (**Figure 4.45**). It must nonetheless be noted that this particular group of patients displayed a strong bias towards autoimmune conditions, so that only one patient with PLI was effectively representative of a distinct complication type.

We had previously found that frequencies of $CD4^+$ and $CD8^+$ MAIT cells, as well as absolute counts of $CD8^+$ and double negative MAIT cells, were altered in the peripheral blood of CVID patients (chapter 4.2.4). We therefore set out to determine if these alterations associated with the clinical status of patients. Frequencies of $CD4^+$, $CD8^+$ and double negative MAIT cells were similar in CVID patients with infections only or complications (**Figure 4.46**). As similar result was obtained when the whole patient cohort, i.e. all primary and secondary antibody deficiency patients, was considered (**Figure 4.47**).

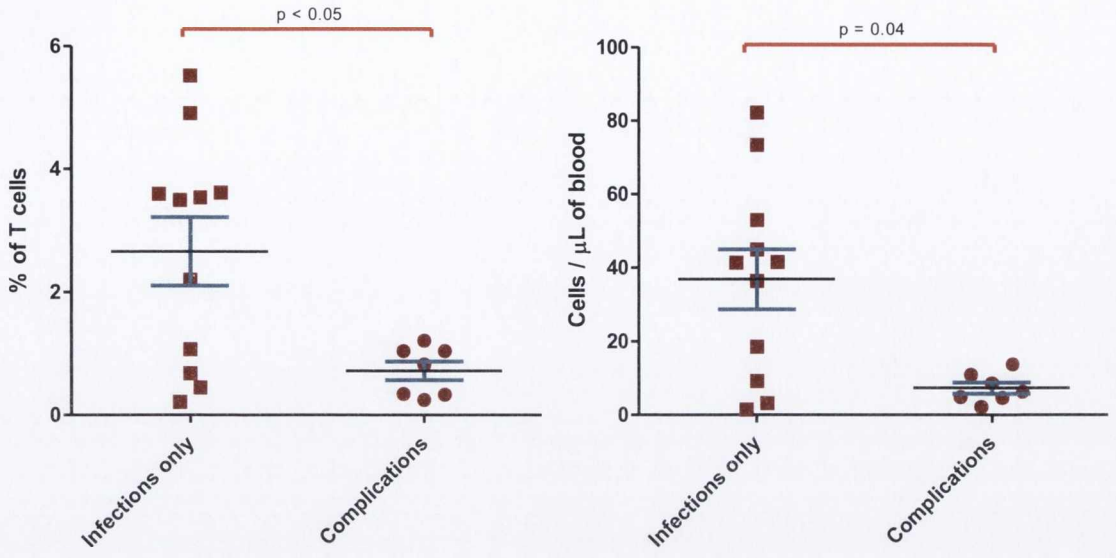


Figure 4.43. Frequencies and absolute counts of MAIT cells in CVID patients with or without complications. The scatter plots show the frequencies (left) and absolute counts (right) of MAIT cells, detected by flow cytometry as $CD3^+$ $V\alpha7.2^+$ $CD161^{high}$ events, in whole blood from CVID patients with infections only (n = 11) or with infections and complications (Complications, n = 7). Statistical analysis was performed employing a two-tailed Mann-Whitney test.

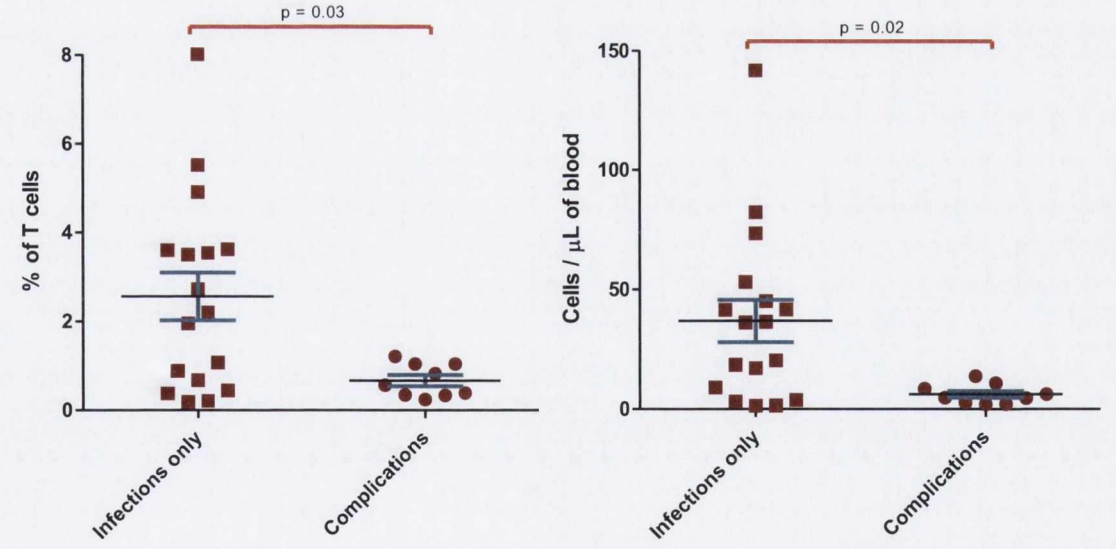


Figure 4.44. Frequencies and absolute counts of MAIT cells in patients with primary and secondary deficiencies, with or without complications. The scatter plot shows the frequencies (left) and absolute counts (right) of MAIT cells, detected by flow cytometry as $CD3^+$ $V\alpha7.2^+$ $CD161^{high}$ events, in whole blood from patients with primary or secondary antibody deficiencies (i.e. CVID, SIgAD, IgG subclass deficiency, secondary antibody deficiency and query diagnosis) with infections only (n = 17) or with infections and complications (Complications, n = 9). Statistical analysis was performed employing a two-tailed Mann-Whitney test.

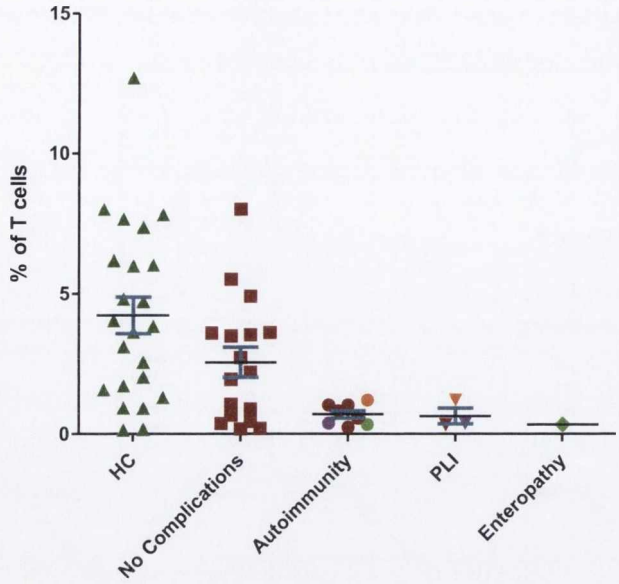


Figure 4.45. Frequencies of MAIT cells in the circulation of patients with primary and secondary antibody deficiencies, divided by clinical phenotype. The scatter plot shows the frequencies of MAIT cells, detected by flow cytometry as $CD3^+$ $V\alpha7.2^+$ $CD161^{high}$ events, in whole blood from healthy controls (HC, n = 23) and patients with primary and secondary antibody deficiencies (i.e. CVID, SIgAD, IgG subclass deficiency, secondary antibody deficiency and query diagnosis), divided on the basis of their clinical phenotype: no complications (i.e. infections only, n = 17), autoimmunity (n = 8), PLI (polyclonal lymphocytic infiltration, n = 3), enteropathy (n = 1). The graph includes more data points than patients, as some patients belonged to more than one clinical phenotype: data points in orange, purple and leaf green mark out these individuals. No statistical analysis was performed on these data.

We next analysed absolute count data for $CD4^+$, $CD8^+$ and double negative MAIT cells. As shown in **Figure 4.48**, counts of double negative MAIT cells were significantly lower in CVID patients with complications in comparison to patients with infections only ($p = 0.03$); counts of $CD8^+$ MAIT cells also appeared decreased in patients with complications, although not significantly so. A similar result was obtained when all patients with primary and secondary antibody deficiencies were considered (**Figure 4.49**), although in this instance a significant decrease of both $CD8^+$ and double negative MAIT cells was noted in patients with complications in comparison to patients with infections only ($p = 0.03$ for $CD8^+$ cells and $p = 0.01$ for double negative cells).

Thus, lower frequencies of circulating MAIT cells, as well as lower counts of $CD8^+$ and double negative MAIT cells, significantly associate with the complications of CVID, and more in general with the complications of primary and secondary immunodeficiencies.

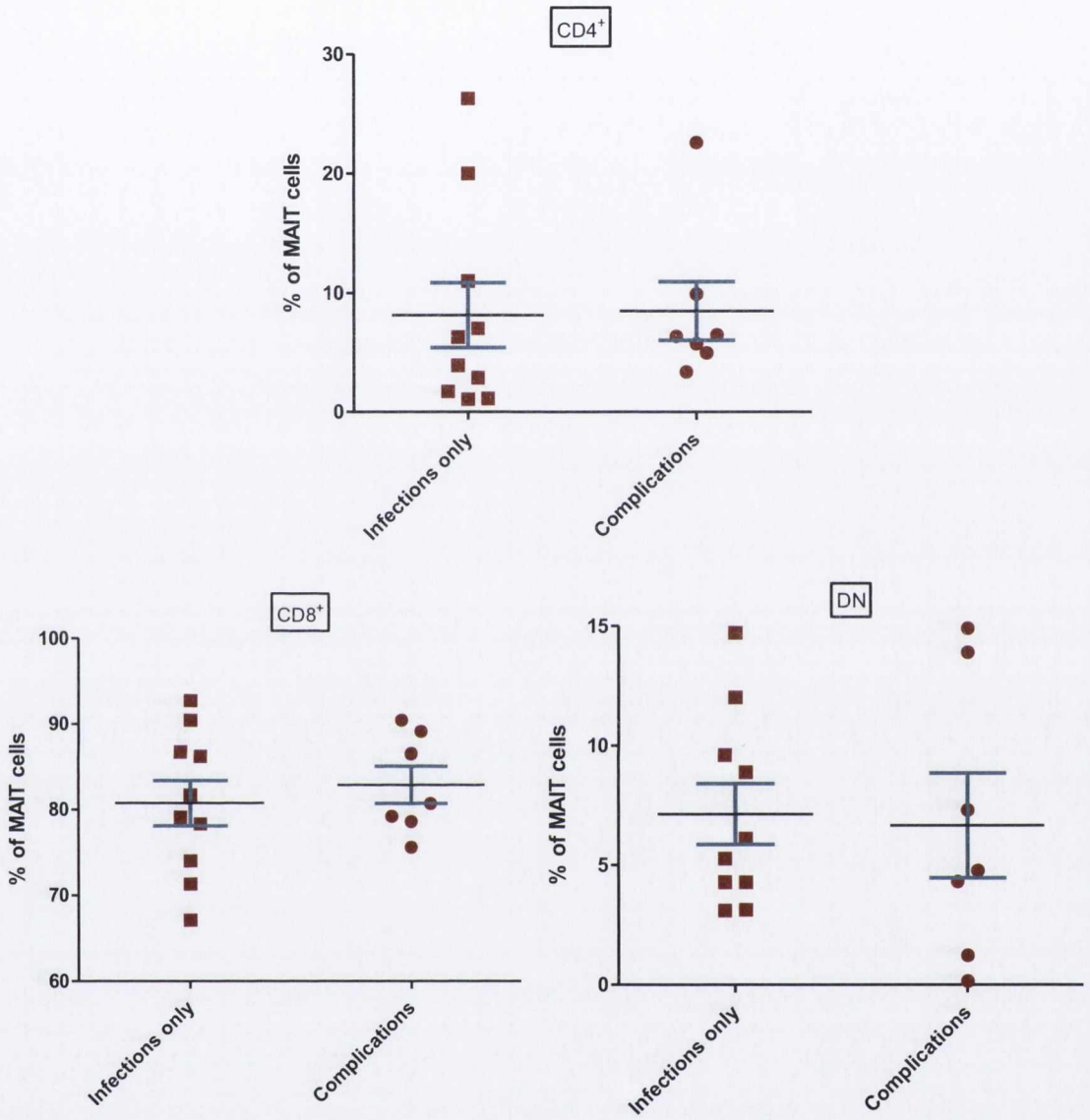


Figure 4.46. Frequencies of $CD4^+$, $CD8^+$ and double negative MAIT cells in CVID patients with or without complications. The scatter plots show the frequencies of $CD4^+$ (top), $CD8^+$ (bottom left) and double negative (DN, bottom right) MAIT cells, detected by flow cytometry as $CD3^+$ $V\alpha7.2^+$ $CD161^{high}$ events, in whole blood from CVID patients with infections only (n = 10) or with infections and complications (Complications, n = 7). Statistical analysis was performed employing a two-tailed Mann-Whitney test.

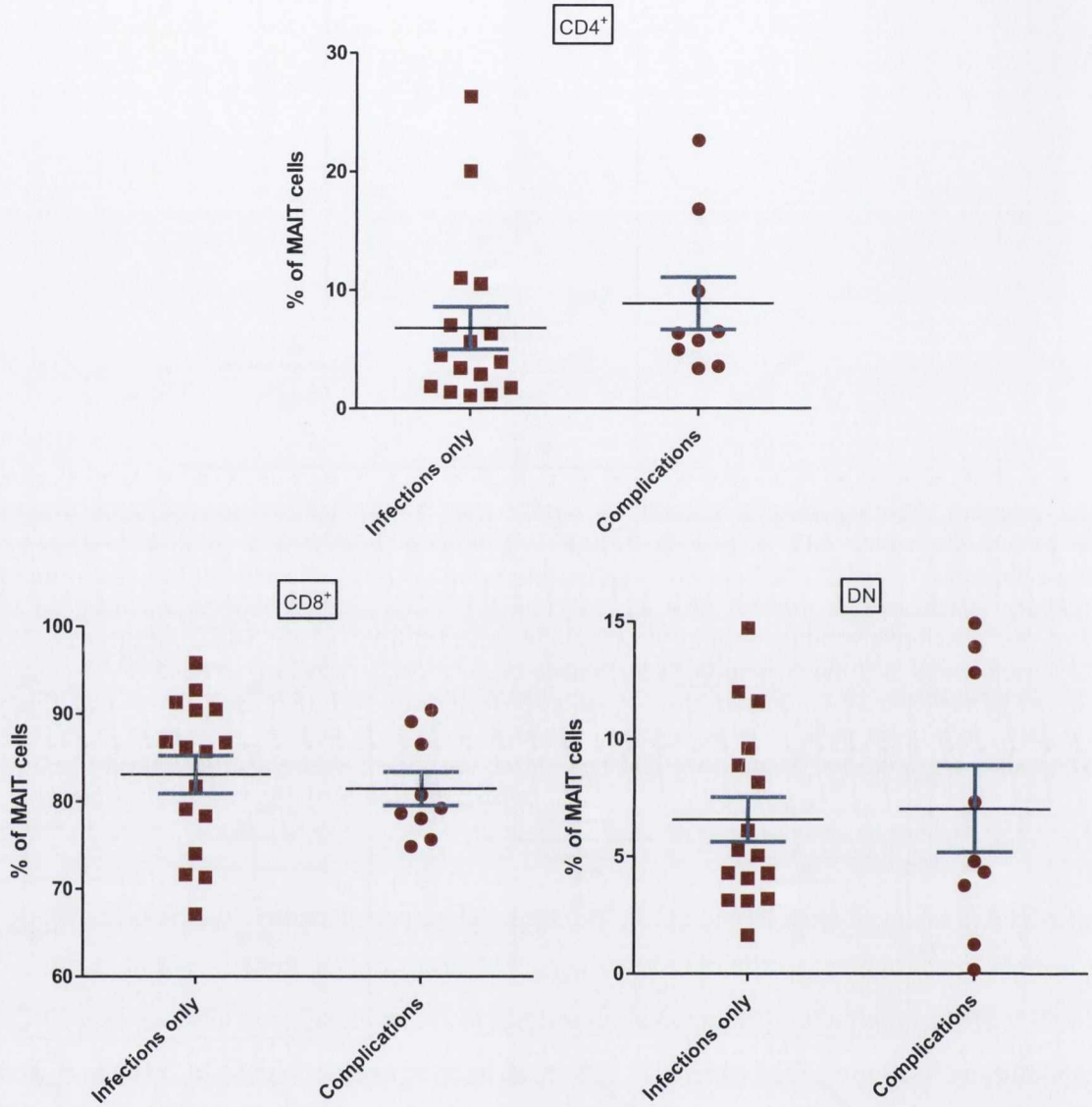


Figure 4.47. Frequencies of $CD4^+$, $CD8^+$ and double negative MAIT cells in patients with primary and secondary antibody deficiencies, with or without complications. The scatter plots show the frequencies of $CD4^+$ (top), $CD8^+$ (bottom left) and double negative (DN, bottom right) MAIT cells, detected by flow cytometry as $CD3^+$ $V\alpha7.2^+$ $CD161^{high}$ events, in whole blood from patients with primary and secondary antibody deficiencies (i.e. CVID, SIgAD, IgG subclass deficiency, secondary antibody deficiency and query diagnosis) with infections only (n = 16) or with infections and complications (Complications, n = 9). Statistical analysis was performed employing a two-tailed Mann-Whitney test.

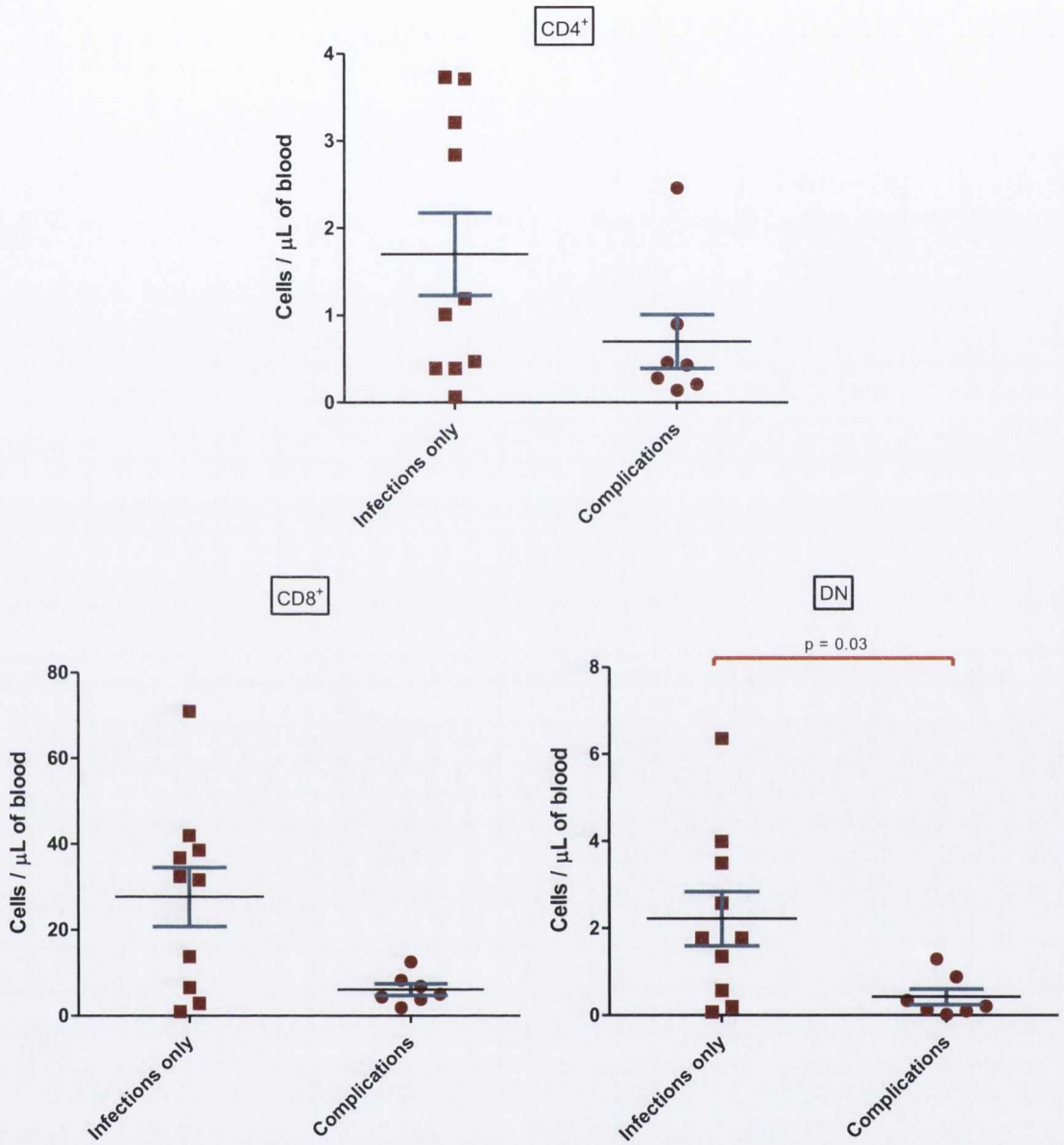


Figure 4.48. Absolute counts of $CD4^+$, $CD8^+$ and double negative MAIT cells in CVID patients with or without complications. The scatter plots show the frequencies of $CD4^+$ (top), $CD8^+$ (bottom left) and double negative (DN, bottom right) MAIT cells, detected by flow cytometry as $CD3^+$ $V\alpha7.2^+$ $CD161^{high}$ events, in whole blood from CVID patients with infections only (n = 10) or with infections and complications (Complications, n = 7). Statistical analysis was performed employing a two-tailed Mann-Whitney test.

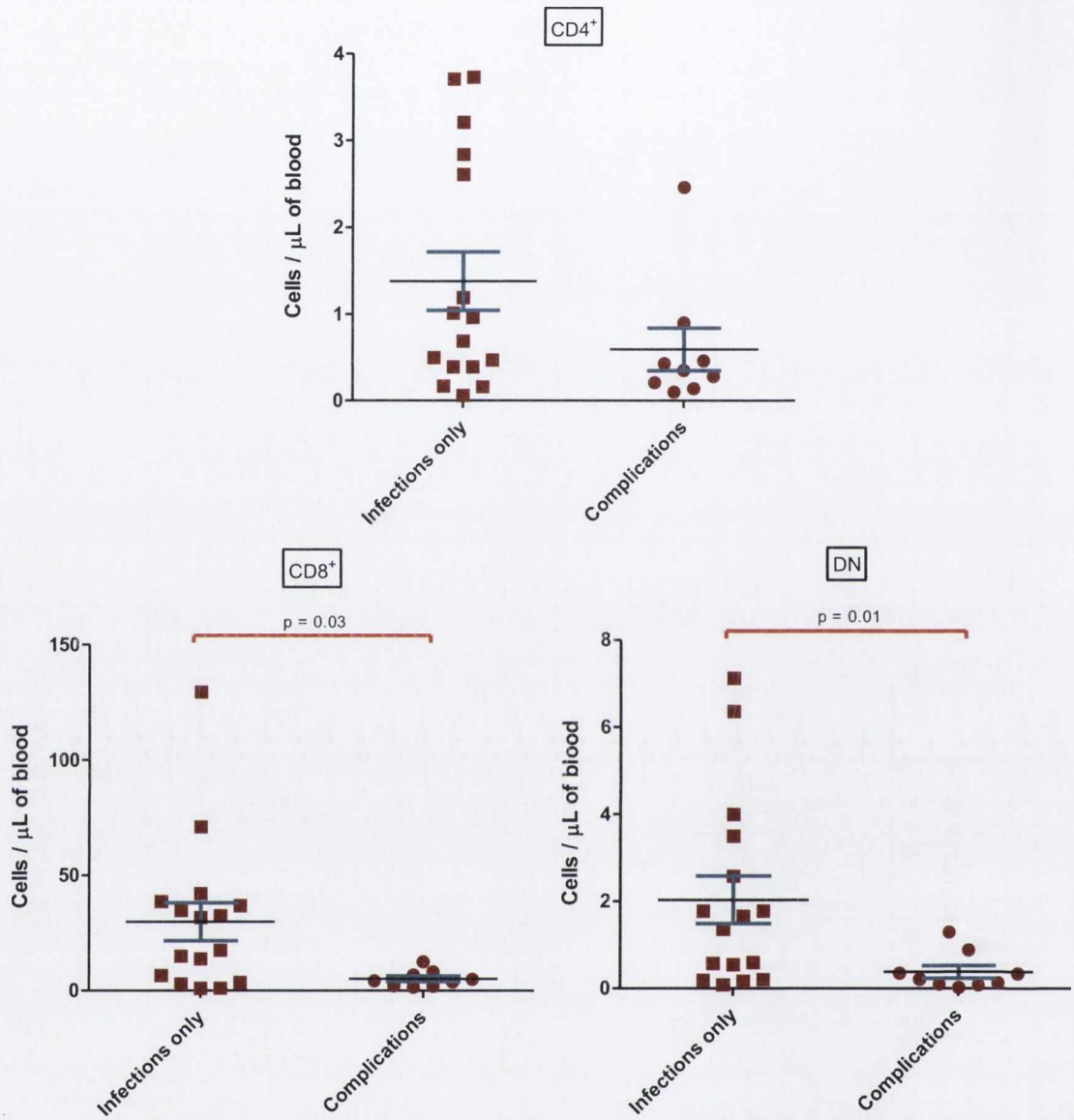


Figure 4.49. Absolute counts of $CD4^+$, $CD8^+$ and double negative MAIT cells in patients with primary and secondary antibody deficiencies, with or without complications. The scatter plots show the frequencies of $CD4^+$ (top), $CD8^+$ (bottom left) and double negative (DN, bottom right) MAIT cells, detected by flow cytometry as $CD3^+$ $V\alpha7.2^+$ $CD161^{high}$ events, in whole blood from patients with primary and secondary antibody deficiencies (i.e. CVID, SIgAD, IgG subclass deficiency, secondary antibody deficiency and query diagnosis) with infections only (n = 16) or with infections and complications (Complications, n = 9). Statistical analysis was performed employing a two-tailed Mann-Whitney test.

4.7 – Discussion

In addition to confirming and developing previous research on B cells, this study represents the first complete survey of innate T cell populations in CVID, resulting in considerable expansion of the knowledge available on the disease.

As described, frequencies and counts of circulating Vδ1, Vδ2 and Vδ3 γδ T cells, as well as NT cells, were found to be comparable in the circulation of CVID patients, secondary antibody deficiency patients and healthy donors. Frequencies and absolute counts of the $CD4^+$, $CD8^+$ and double negative subsets of these populations were also broadly similar to those of healthy controls, although significant decreases were noted in the numbers of $CD4^+$ and double negative Vδ1 γδ T cells and in those of $CD4^+$ Vδ2 γδ T cells. Conversely, iNKT cells and MAIT cells were found at significantly decreased frequencies and absolute counts in the circulation of CVID patients and secondary antibody deficiency patients in comparison to healthy controls. When compared to healthy donors, CVID patients also exhibited an abnormal distribution of circulating $CD4^+$, $CD8^+$ and double negative MAIT cells. More specifically, these individuals displayed significantly higher and lower frequencies of $CD4^+$ and $CD8^+$ MAIT cells, respectively, as well as lower absolute counts of $CD8^+$ and double negative cells. This distribution was not mirrored in the conventional T cell compartment, which featured significantly decreased $CD4^+$ and increased $CD8^+$ cell frequencies alongside depleted $CD4^+$ and double negative cell counts. Data from patients with SIgAD and IgG subclass deficiency suggest T cell numbers in the circulation of these donors are similar to those described for CVID patients; a single patient with query diagnosis, on the other hand, displayed extremely high frequencies of iNKT cells, as well as high-range frequencies of MAIT cells and Vδ2 γδ T cells.

When studying associations with clinical phenotypes, γδ T cells were detected at similar frequencies in the peripheral blood of CVID patients with infections only or with infections and complications, although non-significant decreases in the frequencies and absolute counts of Vδ1 and Vδ2 γδ T cells were noted in the latter. Frequencies and absolute counts of $CD4^+$, $CD8^+$ and double negative cells were comparable in CVID patients with infections only and patients with complications for all three γδ T cell subsets, with the exception of the frequencies of $CD4^+$ Vδ2 γδ T cells and the counts of $CD8^+$ Vδ2 γδ T cells, which were significantly increased and decreased, respectively, in patients with complications in comparison to patients with infections only.

With regard to associations between numbers of iNKT cells and MAIT cells and the clinical status of CVID patients, frequencies and counts of these two populations were

defined to be significantly decreased in the peripheral blood of CVID patients with complications in comparison to patients with infections only. These significant associations were maintained when data from other patients with primary and secondary antibody deficiencies (i.e. SIgAD, IgG subclass deficiency, secondary antibody deficiency and query diagnosis) were added to those obtained from the CVID cohort. The frequencies of $CD4^+$, $CD8^+$ and double negative MAIT cells in CVID and in the wider cohort of primary and secondary antibody deficiency patients showed them to be comparable in patients with infections only or with complications. Analysis of the absolute counts of these same MAIT cell subsets, on the other hand, pointed to a decrease in $CD8^+$ and double negative cells in patients with complications in comparison to patients with infections only.

Table 4.2 summarises the significant results obtained in this chapter.

Table 4.2 – Significant changes in the frequencies and counts of conventional and innate T cells in the circulation of CVID patients and associations with complications.

Population	Frequencies altered in CVID?	Counts altered in CVID?	CD4/CD8/DN cell frequencies altered in CVID?	CD4/CD8/DN cell counts altered in CVID?	Associations with complications? *
T cells	No	No	Yes: ↓ $CD4^+$ ↑ $CD8^+$	Yes: ↓ $CD4^+$ ↓ DN	/ §
Vδ1 γδ T cells	No	No	No	Yes: ↓ $CD4^+$ ↓ DN	No
Vδ2 γδ T cells	No	No	No	Yes: ↓ $CD4^+$	Yes: ↑ % $CD4^+$, ↓ counts $CD8^+$
Vδ3 γδ T cells	No	No	No	No	No
iNKT cells	Yes	Yes	/ §	/ §	Yes: ↓ total % and counts
MAIT cells	Yes	Yes	Yes: ↑ $CD4^+$ ↓ $CD8^+$	Yes: ↓ $CD8^+$ ↓ DN	Yes: ↓ total % and counts Yes: ↓ counts $CD8^+$ and DN
NT cells	No	No	No	No	/ §

* Associations with complications were defined by comparing data from patients with infections only and patients with infections and complications; all other results summarised in the table were obtained from comparisons of frequencies or counts of different T cell populations in CVID patients versus healthy controls. § Stands for "not performed".

Amongst the populations studied, Vδ1, Vδ2 and Vδ3 γδ T cells exhibited the mildest numerical alterations, suggesting a limited role in CVID and its complications. Abnormalities in these subsets appeared to affect the counts of $CD4^+$, $CD8^+$ and double negative cells, rather than the frequencies and counts of the parent populations as a whole.

This may be a consequence of the T cell lymphopenia reported for CVID patients in chapter 3.3.1.

Although our results support previously published data describing a significant decrease in iNKT cell frequencies in CVID,[169] it remains to be clarified whether this depletion in circulating iNKT cells is primary or secondary to the development of CVID itself. Numerical or functional abnormalities in this cell subset could play a key role in the development of the disease, as iNKT cells can support B cell maturation and antibody production, both through processes necessitating recognition of cognate antigen presented by B cells and through stimulation of follicular helper T cells via cytokine production.[99] Their depletion could therefore be involved in causing the B cell defects typical of CVID. *Vice versa*, B cell abnormalities could be the driving force behind the depletion of iNKT cells, as iNKT cell homeostasis has been found to depend on the availability of functional, CD1d-expressing B cells.[194] Certainly, whatever the cause of this subset's numerical decrease, a depleted pool of iNKT cells could influence bacterial clearance, as these cells exert anti-bacterial functions *in vivo*.[195,196]

A novel finding, previously undescribed in CVID, is the decrease in circulating MAIT cells identified in this cohort of patients. As for iNKT cells, it remains to be seen if this decrease is a cause, or rather a consequence, of CVID, its associated B cell differentiation defects, infection burden and complications. Determining the possible effects of a depletion of MAIT cells on B cells differentiation is currently impossible, as it is not known whether MAIT cell functions are conserved in CVID and even whether this innate T cell subset possesses any follicular helper abilities. We have begun exploring these research topics and present the results obtained in chapter 5 and 7 of this thesis, respectively. It should however be noted that the frequencies of several B cell populations, including naïve and class-switched memory B cells, were found here to be comparable in the peripheral blood of CVID patients displaying either high or low frequencies of circulating MAIT cells. This suggests that decreased availability of MAIT cells in the blood of CVID patients is not specifically linked to the decreased generation of certain B cell populations in CVID. Furthermore, it should be noted that a number of healthy individuals recruited to this study displayed frequencies and absolute counts of MAIT cells similar to those of CVID patients with very low or no MAIT cells. Therefore, low numbers of this innate T cell population are not, *per se*, the hallmark of an overt pathological state.

Although not as well studied as iNKT cells, MAIT cells are known to have important anti-bacterial and anti-fungal functions, carried out through production of cytokines and cytotoxic mediators such as granzyme.[106] In this respect, the most likely consequence of an

absolute depletion of this subset would be a lessened ability by patients to respond to infections. However, as MAIT cells have been observed to relocate from peripheral blood to bacterial and inflammatory lesions,[112,126] the numerical decrease identified in CVID could also be due to migratory behaviour in response to frequent infection and inflammation in peripheral tissues.

Confirming what has historically been described with regard to the phenotypes of total T cells in CVID,[161,162] we identified significantly increased frequencies of $CD8^+$ T cells and significantly decreased frequencies of $CD4^+$ T cells in the peripheral blood of patients with this disease. Cytomegalovirus infection, to which CVID patients appear to be susceptible, has previously been found to drive the expansion of $CD8^+$ T cells.[166] As for $CD4^+$ T cells, Perreau and colleagues have recently proposed that increased microbial translocation may be responsible in CVID for the decreases frequencies of anti-bacterial cells belonging to this subset, which display high levels of exhaustion marker PD-1 (programmed cell death-1), poor proliferative responsive and low secretion of IFNγ and IL-2.[165]

Interestingly, abnormalities in the distribution of $CD4^+$ and $CD8^+$ cells were not confined to T cells, but also affected MAIT cells. Contrary to what seen for T cells, these anomalies took the form of decreased frequencies of $CD8^+$ MAIT cells and increased frequencies of $CD4^+$ MAIT cells, which in absolute terms translated in significant decreases of $CD8^+$ and double negative MAIT cells numbers in circulation. It is worth noting that, in healthy controls, peripheral blood MAIT cells are overwhelmingly $CD8^+$ (80-90 %), while $CD4^+$ and double negative cells constitute only a minor part of their total (5-10 % each). The functional properties of the different subsets of MAIT cells have previously been assessed *in vitro*, following co-culture with DCs pulsed with bacteria.[112] These early experiments defined that $CD8^+$ and double negative MAIT cells responded to bacterial antigens by upregulating their surface expression of CD69, while $CD4^+$ MAIT cells remained unchanged. As a consequence of this, current literature on MAIT cells almost exclusively presents data on $CD8^+$ and double negative MAIT cells, while $CD4^+$ MAIT cells are, for all purposes, considered non-functional. This approach may prove controversial, as $CD4^+$ MAIT cells in the early stages of development have been identified in human thymus alongside $CD8^+$ and double negative cells,[111] suggesting they undergo a similar differentiation process. $CD4^+$ MAIT cells have also recently been detected using an MR-1 tetramer,[118] indicating that this subset is capable of binding cognate antigen. It is therefore possible that $CD4^+$ MAIT cells could have a role distinct from the effector functions of $CD8^+$ and double negative MAIT cells. This is for example the case for iNKT cells, which feature

a largely regulatory $CD4^+$ subset, a $CD8^+$ subset with potent effector functions, and double negative cells displaying characteristics of both other groups.[98]

Frequencies of MAIT cells in CVID had previously been investigated and described as normal in a review paper by the group of Olivier Lantz.[138] Unfortunately, this finding was reported in a review paper containing no data or information about the patient cohort recruited, making it difficult to explain the discrepancies with our own results. One possible explanation is that the number of patients enrolled in that study was not sufficient to achieve statistical significance. Alternatively, frequencies of $CD8^+$ and double negative MAIT cells, which as said are considered similar from a functional point of view, may have been agglomerated. This could have masked significances in the data, as we found frequencies of $CD8^+$ cells to be decreased in patients, while frequencies of double negative MAIT cells were increased.

Almost no data are available in the literature with regard to associations between numbers of innate T cells and the clinical status of CVID patients. In the only report published to date on this research topic, low iNKT cell frequencies were found to significantly associate in CVID with lymphoproliferative complications, particularly splenomegaly.[193] We show here that frequencies and absolute counts of iNKT cells are more generally decreased, in a significant manner, in all individuals with complicated CVID. As most of the patients with complications recruited to this study were affected by autoimmune conditions (7 out of 8), this datum is particularly suggestive of a link between decreased numbers of iNKT cells and autoimmunity. It is unclear at this time if the association identified is due to a causal link between a depletion in the iNKT cell pool and the development of complications, or rather if complications themselves could cause changes in the numbers of iNKT cells available in circulation. Certainly, iNKT cells are known to affect the development of autoimmunity both in mouse and in man, polarizing immune responses through the production of cytokines including IFNγ, IL-4, IL5, IL-10 and IL-13. A modified α-GalCer analogue favouring production of IL-4 by iNKT cells has for example been observed to induce T_H2-polarization, preventing the development of EAE in a murine model.[197] Numerical or functional defects in iNKT cells favour the development or accelerate the progression of disease in different mouse models of SLE, while CD1d deficiency alone can mediate a lupus-like syndrome in Balb/c mice.[198] Low frequencies of circulating iNKT cells have furthermore been detected in patients affected by autoimmune conditions including SLE, psoriasis, Crohn's disease, ulcerative colitis and rheumatoid arthritis.[199] Interestingly, frequencies of this cell subset were found to be at their lowest in

RA and SLE during active disease, and to increase following administration of anti-CD20 therapy.[194,200] Bosma *et al.* have shown that, upon treatment of SLE patients with anti-CD20, circulating B lymphocytes exhibiting defects in the cytoplasmic recycling and surface expression of CD1d are depleted and replaced by immature, healthy B cells.[194] At the beginning of this project, we briefly explored the idea that decreased iNKT cell frequencies in CVID patients may also be due to altered expression of CD1d by B cells. Preliminary data from 4 patients, not shown here, suggested this was not the case. That investigation, however, was limited to individuals with infections only, whom we have now shown to exhibit significantly higher frequencies of iNKT cells in comparison to patients with complications. We are therefore planning to further explore levels of CD1d expression in CVID patients with complications.

In the course of this study, we uncovered a second significant association between complications of CVID and low frequencies and absolute counts of MAIT cells. Analysis of the proportions of $CD4^+$, $CD8^+$ and double negative MAIT cells in patients with or without complications revealed that patients with complications were characterised by decreased absolute counts of $CD8^+$ and double negative MAIT cells in their peripheral blood. As already noted for iNKT cells, the associations identified do not give clues about causality, meaning that MAIT cells can not be assumed to participate in the development of the complications of CVID. In addition to this, the regulatory functions of MAIT cells are still very much a matter of debate, partly because conflicting results have been obtained in mouse models and in man. A role for this subset in the quenching of autoimmunity has previously been suggested in mouse models, as transgenically-induced high frequencies of MAIT cells have been shown to delay the onset of disease in non-obese diabetic animals[129] and inhibit the induction and progression of EAE.[130] In man, frequencies of circulating MAIT cells were found to be at their lowest during active phases of the disease in MS patients, and to recover upon remission.[131] This phenomenon was hypothesized by the authors to depend on the migration of MAIT cells from peripheral blood to sites of inflammation in peripheral tissues. This mechanism has recently been confirmed in patients affected by inflammatory bowel diseases (IBDs) such as Crohn's disease and ulcerative colitis, who exhibit similarly decreased frequencies of MAIT cells in peripheral blood as well as enriched frequencies of this cell subset in inflamed intestinal tissue.[132] Undoubtedly, the cytokine profile of MAIT cells is suggestive of a possible role in the development of autoimmunity, as these cells are abundant producers of TNFα and can secrete IFNγ, IL-17A and IL-22 upon stimulation but, differently from iNKT cells, do not normally generate IL-4 or IL-10.[106,132] While the pro-inflammatory properties of TNFα are well known, IL-17A and IL-22 are key both in the

resolution of bacterial infections and in the development of autoimmunity. STAT3-deficiency patients, for example, are highly susceptible to recurrent infections due to their inability to produce IL-17A, while overproduction of this cytokine contributes to the development of psoriasis, rheumatoid arthritis and multiple sclerosis.[201] Interestingly, MAIT cells from Crohn's disease and ulcerative colitis patients were found to secrete significantly more IL-17A and/or IL-22 upon *in vitro* stimulation,[132] possibly implicating these cytokines in the development of IBDs. In order to clarify if this cell subset could be capable of mediating a similar process in CVID, we explored the cytokine-producing abilities of MAIT cells from CVID patients and healthy donors, following *in vitro* stimulation of whole blood samples; the data obtained from these investigations are presented in Chapter 6 of this report.

It has to be stressed that the significant decreases noticed in the frequencies and in the absolute counts of total MAIT cells and iNKT cells, as well as decreased absolute counts of $CD8^+$ and double negative MAIT cells, were observed not only in complicated CVID, but also in other primary and secondary antibody deficiency patients affected by complications. This suggests that these phenomena are caused by processes common to antibody deficiencies with a CVID-like phenotype, such as low immunoglobulin levels and recurrent infections, regardless of their root causes. Importantly, some patients with infections only displayed levels of MAIT and/or iNKT cells similar to those of patients with complications. This could be due to confounding factors resulting from the strict criteria adopted for the categorisation of patients into clinical phenotypes. To make an example, patients were considered affected by complications in the presence of biopsy-proven enteropathy, but not when exhibiting enteropathy symptoms not confirmed by endoscopy data. Low levels of MAIT or iNKT cells in patients with infections only could also be a reflection of inter-patient variability, or depend on other currently unidentified factors.

As shown in chapter 4.5, a single query diagnosis patient enrolled in this study displayed strikingly high frequencies and counts of iNKT cells, as well as high frequencies and counts of MAIT cells and Vδ2 γδ T cells. This feature is uncommon, not only because it distinguishes this donor from all other patients with antibody deficiencies recruited, but also because disease states, including sarcoidosis,[202] atherosclerosis,[203] SLE,[194] and tumours,[204] are usually characterised by decreased frequencies of iNKT cells. Although it is currently unclear why this individual exhibits increased frequencies of this cell population, this anomaly could be rooted in the presumed genetic bases of his antibody deficiency. Interestingly, patients affected by myasthenia gravis (MG) with thymic hyperplasia exhibit increased frequencies of circulating iNKT cells; conversely, patients affected by MG with

thymoma, which can associate with hypogammaglobulinemia, display numbers of iNKT cells comparable to those of healthy controls.[205] It could therefore be worthwhile to investigate if this patient exhibits signs of thymic abnormalities.

Taken together, the data presented in this chapter support our hypothesis that T cells, and particularly innate T cell subsets, could play a role in CVID and its associated complications. More specifically, an involvement in the disease is possible for iNKT cells and MAIT cells, whose frequencies, absolute counts and CD4/CD8 phenotypes are notably altered in the circulation of CVID patients, particularly those affected by complications.

CHAPTER 5

ANALYSIS OF RELATIONSHIPS BETWEEN FREQUENCIES OR ABSOLUTE COUNTS OF INNATE T CELLS AND OTHER LYMPHOCYTE SUBSETS IN CVID

5.1 – Introduction

The immune system as a whole exists as a complex network of interactions between different cell types, which can take place by means of direct cell-to-cell contact or through the production of signalling mediators such as cytokines or chemokines. Collaboration between lymphocytes, as well as between lymphocytes and other immune populations, is essential in key immune processes, including antigen presentation to T cells, activation and differentiation of B cells and the modulation of immune responses. Amongst innate T cell populations, Vδ2 γδ T cells and iNKT cells have been shown to collaborate with a number of immune cell subsets, including monocytes, DCs, neutrophils, NK cells and T and B lymphocytes; less information is available about interactions involving MAIT cells, Vδ1 and Vδ3 γδ T cells.

Production of IFNγ and TNFα by Vδ2 γδ T cells induces the *in vitro* and *in vivo* differentiation of monocytes into IL-12-secreting DCs capable of stimulating T_H1-type responses.[58-60] IFNγ, TNFα and GM-CSF secreted by Vδ2 γδ T cells can also stimulate neutrophils to differentiate into APC-like cells able to sustain αβ T cell responses.[61] Vδ2 γδ T cells can furthermore recognise pathogen-derived antigens presented by macrophages,[51] and support B cells in their differentiation into APCs as well as in their maturation into antibody-producing plasma cells.[63,64,206]

iNKT cells can modulate immunity through the production of T_H1, T_H2 and T_H17-type cytokines;[97] early generation of IFNγ by iNKT cells upon administration of α-GalCer *in vivo* is for example known to induce expression of surface activation markers, IFNγ secretion and upregulation of proliferation and cytotoxicity by NK cells.[93,94] iNKT cells also collaborate with monocytes, which they induce to differentiate into tolerogenic DCs in the presence of GM-CSF and IL-13 *in vitro*.[91,92] Conversely, splenic administration of α-GalCer to mice alongside antigenic protein stimulates immunogenic DCs, inducing their upregulation of costimulatory markers CD80, CD86 and CD40L, secretion of IFNγ and TNFα and antigen presentation to naïve $CD4^+$ and $CD8^+$ T cells.[95,96] iNKT cells can furthermore sustain B cell responses, both directly and indirectly.[99] $iNKT_{FH}$, a subset of iNKT cells with follicular helper properties, respond to the presentation of lipid antigens by B cells, providing costimulatory signals and producing cytokines like IL-21 and IFNγ. Alternatively, iNKT cells can be activated by and cooperate with DCs in the secretion of mediators, including BAFF, APRIL (a proliferation-inducing ligand), IL-2 and IL-4, which in turn induce the activation of follicular helper T cell subsets. Finally, a role has been identified for iNKT cells in the suppression of immune responses. A particular subset of

iNKT cells resident in adipose tissues, termed regulatory iNKT ($iNKT_{REG}$) cells, can produce IL-10, promote the acquisition of an anti-inflammatory phenotype by macrophages and control the proliferation and suppressive functions of adipose T_{REG} cells.[207] iNKT cells may furthermore modulate immune responses by regulating the proliferation of certain B cell populations. Contact with $CD4^+$ iNKT cells has for example been shown to promote the *in vitro* expansion of $CD1d^{high}$ $CD5^+$ and $CD24^{high}$ $CD38^{high}$ B cell subsets, which include high frequencies of B_{REGS}.[208]

As previously said, little is known about the relationships existing between Vδ1 or Vδ3 γδ T cells and other immune cell subsets. These γδ T cell populations can however produce T_H1, T_H2 and T_H17 cytokines, which involve them in the regulation of immune responses.[68,75] A particular subset of Vδ1 γδ T cells expressing T_{REG} marker FoxP3 has also been identified, which can inhibit proliferation of $CD4^+$ T cells.[74]

With regard to MAIT cells, this population requires B cells for its expansion in peripheral tissues following selection by double positive, MR-1-expressing thymocytes and emigration from the thymus,[109] however it is currently not known exactly how B cells support MAIT cell proliferation and where this interaction takes place. Like Vδ2 γδ T cells, MAIT cells respond to bacterial antigens presented by neutrophils, generating GM-CSF, IFNγ and TNFα and promoting the differentiation of neutrophils themselves into APC-like cells.[61] Interestingly, frequencies of MAIT cells have been reported to correlate with those of $CD56^{bright}$ NK cells and $CD4^+$ iNKT cells in healthy donors, but not in patients with MS.[131] Interactions of MAIT cells with other cell types may therefore influence regulatory processes, for example in autoimmunity.

The data collected in chapter 3 of this thesis have shown that CVID patients exhibit significantly decreased frequencies and absolute counts of class-switched memory B cells, and significantly increased frequencies of naïve B cells, in comparison to healthy donors. These B cell anomalies existed alongside depleted frequencies and counts of circulating iNKT cells and MAIT cells (chapter 4). A significant statistical association has previously been observed in CVID between frequencies of iNKT cells and class-switched memory B cells, which was suggested to involve iNKT cells in the disease's aetiology. [169,193] No other correlations between lymphocytic populations have so far been defined in these patients, although it is known that defects in B cell/T cell interactions, such as the ones induced by mutations in the ICOS gene, can be a cause of CVID.[11]

5.2 – Hypothesis and aims of the chapter

In this chapter, we build on the phenotypic data previously presented, seeking to detect possible statistical correlations between numbers of circulating innate T cells (Vδ1, Vδ2 and Vδ3 γδ T cells, iNKT cells and MAIT cells) and those of other lymphocyte populations. More specifically, frequencies and absolute counts of each innate T cell subset were plotted against those of total B cells, transitional and naïve B cells, unswitched and class-switched memory B cells, $CD27^-$ IgD^- B cells, plasmablasts, total IgD^+ B cells, total NK cells, NT cells and the other innate T cell subsets. Our hypothesis was that CVID may be characterised by unusual interactions between B and innate T cell subsets, which in turn may hint at novel mechanisms of disease.

Because of the number of associations probed, this part of the study should be considered an exercise in exploratory data analysis. In this sense, the results provided here would necessitate a confirmatory study in a second patient and control cohort. Nonetheless, they lend some much-needed context for the study of innate T cells in CVID. They may also lay the foundation for further research on MAIT cells in healthy individuals. Due to the large amount of data produced for every innate T cell subset, only significant correlations of moderate strength and above are reported in this chapter, summarised in tables and visualised through graphs. The strength of correlations was expressed by a Spearman's correlation coefficient (r_S), while their significance was defined by a p value (p). Correlations were considered:

- Weak, for ($0 < r_S < 0.49$);
- Moderate, for ($0.50 < r_S < 0.69$);
- Strong, for ($0.70 < r_S < 0.89$);
- Very strong, for ($0.90 < r_S < 1.00$).

As recommended for exploratory analysis,[209,210] no Bonferroni correction was applied, meaning that all correlations with a p value lower than 0.05 were considered significant and included in this report. A corrected p value could however be calculated dividing the initial significance threshold of 0.05 by the number of correlations explored for each population, i.e. 15. This would result in an adjusted threshold of 0.003.

5.3 – Analysis of statistical correlations between frequencies or counts of Vδ1 γδ T cells and other lymphocyte subsets

Table 5.1 summarizes the correlations existing between frequencies of Vδ1 γδ T cells and those of other lymphocyte populations. No significant correlations were identified between frequencies of this cell subset and frequencies of other lymphocyte populations in healthy controls. Two significant correlations were however defined in CVID patients between frequencies of Vδ1 γδ T cells and iNKT cells ($r_S = 0.69$, $p = 0.001$) and MAIT cells ($r_S = 0.51$, $p = 0.003$); graphs for these are shown in **Figure 5.1**.

Table 5.1. Correlations between frequencies of Vδ1 γδ T cells and those of other lymphocyte populations in healthy controls and CVID patients

Cohort	Cell subset	P value	Moderate	Strong
Healthy controls	*No significant correlations identified.*			
CVID patients				
	iNKT cells	0.0006		0.73
	MAIT cells	0.003	0.51	

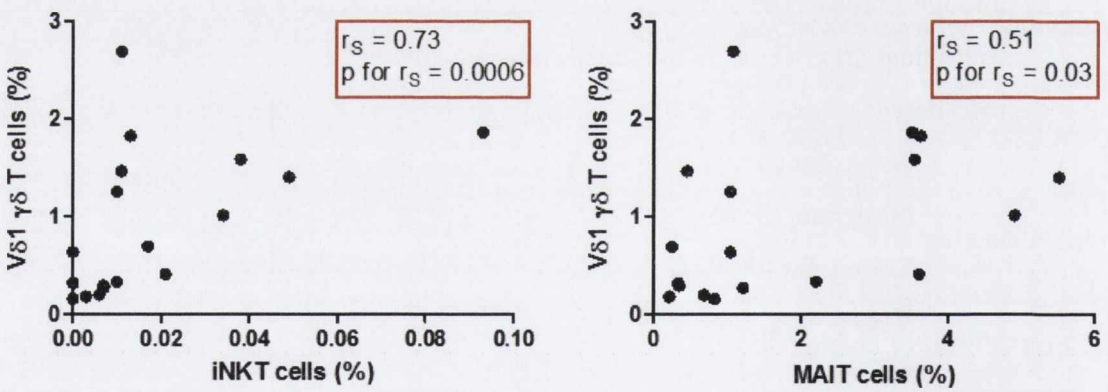


Figure 5.1. Significant correlations between frequencies of Vδ1 γδ T cells and frequencies of iNKT cells and MAIT cells in CVID patients. Vδ1 γδ T cells, iNKT cells and MAIT cells were detected by flow cytometry in whole blood samples from CVID patients as $CD3^+$ Vδ1 TCR^+, $CD3^+$ Vα24-Jα18$^+$ and $CD3^+$ Vα7.2$^+$ $CD161^{high}$ events, respectively. Frequencies of Vδ1 γδ T cells were then plotted against the frequencies of iNKT cells (left, n = 18) and MAIT cells (right, n = 18). The degree of correlation determined is expressed by a Spearman's correlation coefficient (r_S), defined by a p value (p for r_S).

Table 5.2 recapitulates the correlations detected between absolute counts of Vδ1 γδ T cells and those of other lymphocyte populations. Again, no significant correlations were detected between absolute counts of this cell subset and those of other lymphocyte

populations in healthy controls. Absolute counts of Vδ1 γδ T cells from CVID patients, on the other hand, appeared to correlate with those of a number of cell types, including both B and T cell subsets. Amongst B cell populations, absolute counts of Vδ1 γδ T cells correlated with those of total B cells, (r_S = 0.68, p = 0.002), naïve B cells, (r_S = 0.64, p = 0.006), class-switched memory B cells (r_S = 0.62, p = 0.007), $CD27^-$ IgD^- (double negative) B cells (r_S = 0.65, p = 0.005), plasmablasts (r_S = 0.74, p = 0.001) and total IgD^+ B cells (r_S = 0.68, p = 0.003). Graphs for these correlations are shown in **Figure 5.2**. A correlation was also identified between frequencies of Vδ1 γδ T cells and unswitched memory B cells, however this was weaker (r_S = 0.48) and not quite significant (p = 0.052). No correlation seemed to exist between levels of Vδ1 γδ T cells and transitional B cells.

Absolute counts of Vδ1 γδ T cells also correlated with those of several innate populations, i.e. iNKT cells (r_S = 0.68, p = 0.002), MAIT cells (r_S = 0.67, p = 0.002), Vδ3 γδ T cells (r_S = 0.54, p = 0.02) and NT cells (r_S = 0.52, p = 0.02). Graphs for these correlations are shown in **Figure 5.3.** Only weak and non-significant correlations were identified between counts of Vδ1 γδ T cells and those of NK cells and Vδ2 γδ T cells.

Table 5.2. Correlations between absolute counts of Vδ1 γδ T cells and those of other lymphocyte populations in healthy controls and CVID patients

Cohort	Cell subset	P value	Moderate	Strong
Healthy controls	*No significant correlations identified.*			
CVID patients				
	Total B cells	0.002	0.68	
	Naïve B cells	0.006	0.64	
	Class-sw. memory B cells	0.007	0.62	
	$CD27^-$ IgD^- B cells	0.005	0.65	
	Plasmablasts	0.001		0.74
	Total IgD^+ B cells	0.003	0.68	
	NT cells	0.02	0.52	
	iNKT cells	0.002	0.68	
	MAIT cells	0.002	0.67	
	Vδ3 γδ T cells	0.02	0.54	

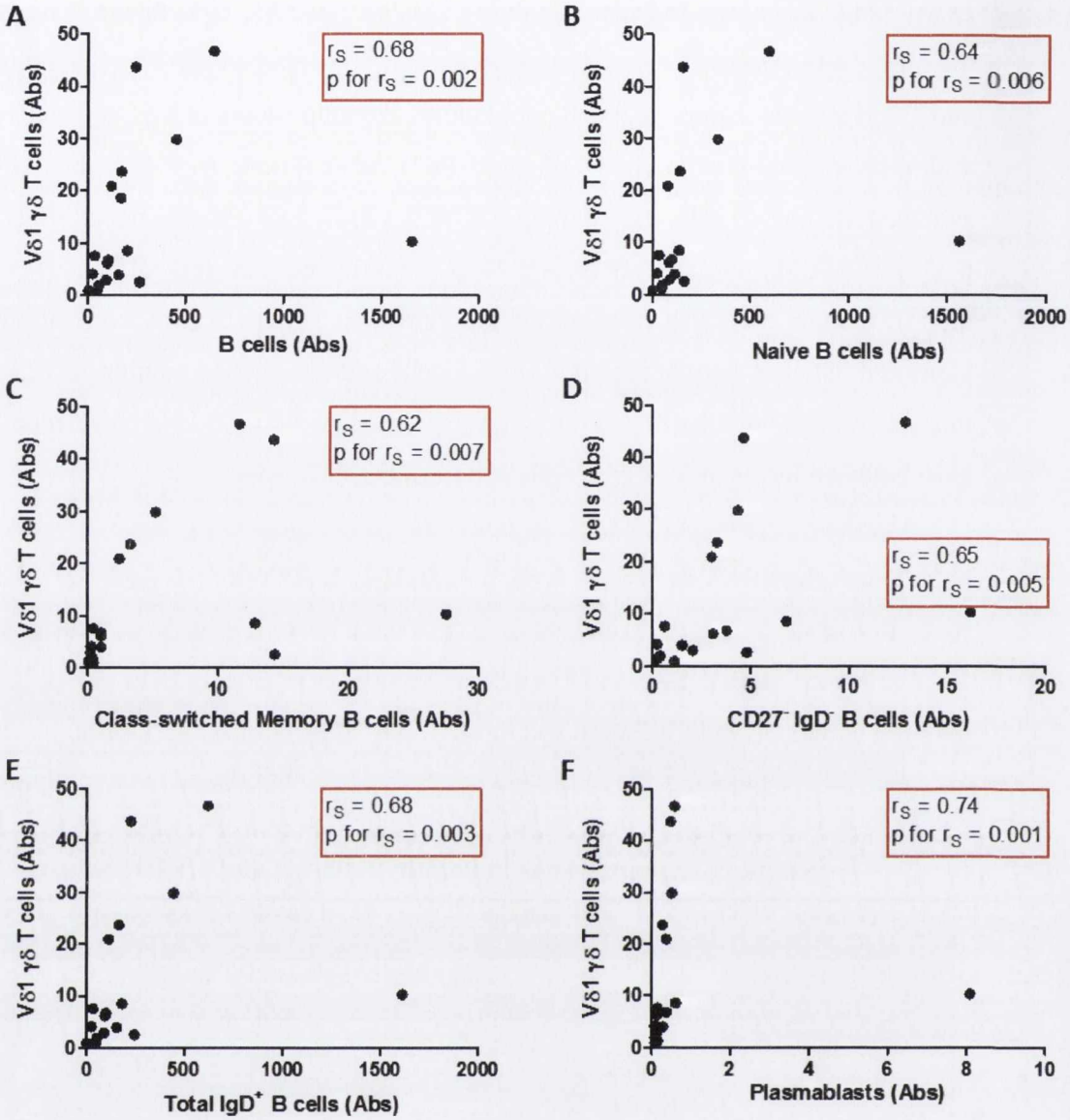


Figure 5.2. Significant correlations between absolute counts of Vδ1 γδ T cells and counts of B cell subsets in CVID patients. Absolute counts of Vδ1 γδ T cells ($CD3^+$ Vδ1 TCR^+ events) were determined by flow cytometry using whole blood samples from CVID patients. They were then plotted against similarly determined counts of total B cells (A, $CD45^+$ $CD19^+$phenotype, n = 18), naïve B cells (B, $CD19^+$ $CD27^-$ IgD^+ phenotype, n = 17), class-switched memory B cells (C, $CD19^+$ $CD27^+$ IgD^- phenotype, n = 17), $CD19^+$ $CD27^-$ IgD^- B cells (D, n = 17), total $CD19^+$ IgD^+ B cells (E, n = 17) and plasmablasts (F, $CD19^+$ $CD24^-$ $CD38^{high}$ phenotype, n = 16). The degree of correlation identified is expressed by a Spearman's correlation coefficient (r_S), defined by a p value (p for r_S).

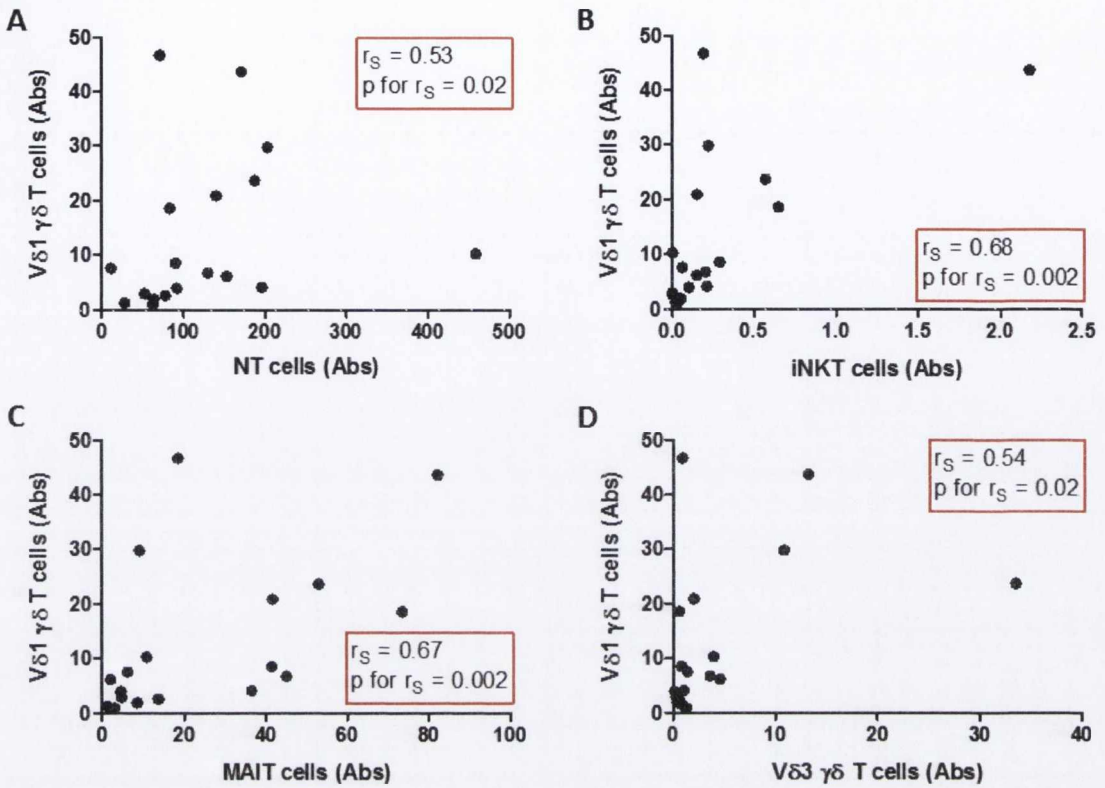


Figure 5.3. Significant correlations between absolute counts of Vδ1 γδ T cells and counts of other innate cell subsets in CVID patients. Absolute counts of Vδ1 γδ T cells ($CD3^+$ Vδ1 TCR^+ events) were determined by flow cytometry using whole blood samples from CVID patients. They were then plotted against similarly determined counts of NT cells (A, $CD3^+$ $CD56^+$ phenotype, n = 18), iNKT cells (B, $CD3^+$ Vα24-Jα18$^+$ phenotype, n = 18), MAIT cells (C, $CD3^+$, Vα7.2$^+$ $CD161^{high}$ phenotype, n = 18) and Vδ3 γδ T cells (D, $CD3^+$ Vδ3 TCR^+ phenotype, n = 18). The degree of correlation identified is expressed by a Spearman's correlation coefficient (r_S), defined by a p value (p for r_S).

5.4 – Analysis of statistical correlations between frequencies or counts of Vδ2 γδ T cells and other lymphocyte subsets

Table 5.3 recapitulates the correlations existing between frequencies of Vδ2 γδ T cells and those of other lymphocyte populations in healthy controls and CVID patients. As shown, frequencies of Vδ2 γδ T cells moderately correlate with those of only one population, i.e. MAIT cells, in both healthy controls (r_S = 0.57, p = 0.004) and CVID patients (r_S = 0.52, p = 0.003). Graphs for these correlations are shown in **Figure 5.4**.

Table 5.4 and Figure 5.5 summarize the correlations between absolute counts of Vδ2 γδ T cells and counts of other lymphocyte populations in healthy controls and CVID patients. Again, MAIT cells are the only lymphocyte population to display a moderate correlation

with Vδ2 γδ T cells in both healthy controls (r_S = 0.61, p = 0.003) and CVID patients (r_S = 0.63, p = 0.005).

Table 5.3. Correlations between frequencies of Vδ2 γδ T cells and those of other lymphocyte populations in healthy controls and CVID patients

Cohort	Cell subset	P value	Moderate	Strong
Healthy controls				
	MAIT cells	0.004	0.57	
CVID patients				
	MAIT cells	0.003	0.52	

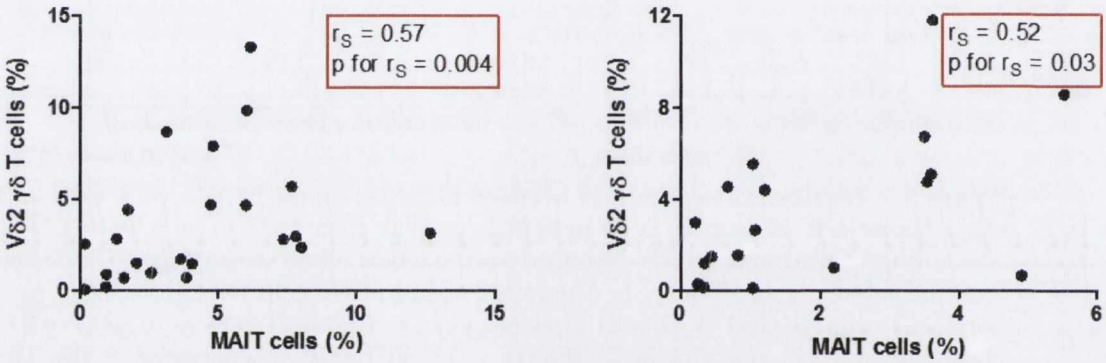


Figure 5.4. Significant correlations between frequencies of Vδ2 γδ T cells and frequencies of MAIT cells in healthy controls and CVID patients. Frequencies of Vδ2 γδ T cells ($CD3^+$ Vδ2 TCR^+ phenotype) and MAIT cells ($CD3^+$ $V\alpha7.2^+$ $CD161^{high}$ phenotype) were correlated following detection by flow cytometry in whole blood samples from healthy donors (left, n = 23) and CVID patients (right, n = 18). The degree of correlation determined is expressed by a Spearman's correlation coefficient (r_S), defined by a p value (p for r_S).

Table 5.4. Correlations between absolute counts of Vδ2 γδ T cells and those of other lymphocyte populations in healthy controls and CVID patients

Cohort	Cell subset	P value	Moderate	Strong
Healthy controls				
	MAIT cells	0.003	0.61	
CVID patients				
	MAIT cells	0.005	0.63	

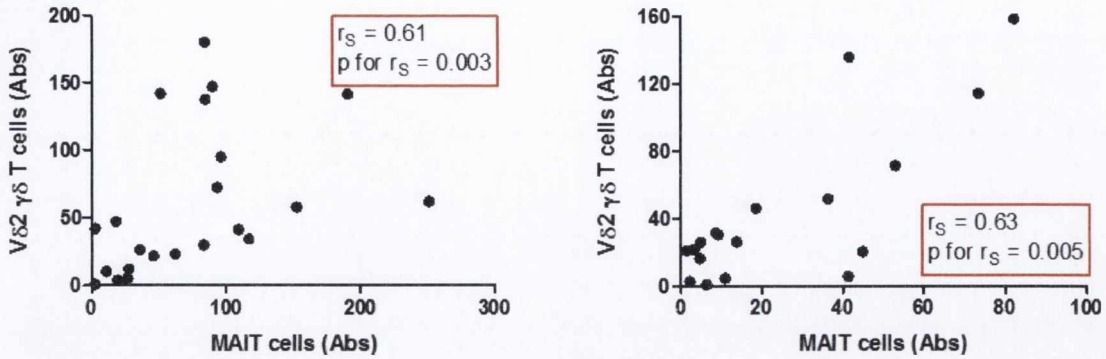


Figure 5.5. Significant correlations between absolute counts of Vδ2 γδ T cells and counts of MAIT cells in healthy controls and CVID patients. Absolute counts of Vδ2 γδ T cells ($CD3^+$ Vδ2 TCR^+ phenotype) and MAIT cells ($CD3^+$ $V\alpha7.2^+$ $CD161^{high}$ phenotype) were correlated following detection by flow cytometry in whole blood samples from healthy donors (left, n = 22) and CVID patients (right, n = 18). The degree of correlation determined is expressed by a Spearman's correlation coefficient (r_S), defined by a p value (p for r_S).

5.5 – Analysis of statistical correlations between frequencies or counts of Vδ3 γδ T cells and other lymphocyte subsets

Table 5.5 recapitulates the correlations between frequencies of Vδ3 γδ T cells and those of other lymphocyte populations in healthy controls and CVID patients. As shown, no significant moderate or strong correlations were identified for either group.

Table 5.6 summarises the correlations between absolute counts of Vδ3 γδ T cells and those of other lymphocyte populations in healthy controls and CVID patients respectively. No correlations were identified in the healthy control group, however absolute counts of Vδ3 γδ T cells appeared to correlate moderately with those of NT cells (r_S = 0.59, p = 0.006) and Vδ1 γδ T cells (r_S = 0.54, p = 0.02) in CVID patients. Graphs for the correlations between the absolute counts of Vδ3 γδ T cells and those of NT cells and Vδ3 γδ T cells are shown in **Figure 5.6**.

Table 5.5. Correlations between frequencies of Vδ3 γδ T cells and those of other lymphocyte populations in healthy controls and CVID patients

Cohort	Cell subset	P value	Moderate	Strong
Healthy controls	*No significant correlations identified.*			
CVID patients	*No significant correlations identified.*			

Table 5.6. Correlations between absolute counts of Vδ3 γδ T cells and those of other lymphocyte populations in healthy controls and CVID patients

Cohort	Cell subset	P value	Moderate	Strong
Healthy controls	*No significant correlations identified.*			
CVID patients				
	NT cells	0.006	0.59	
	Vδ1 γδ T cells	0.02	0.54	

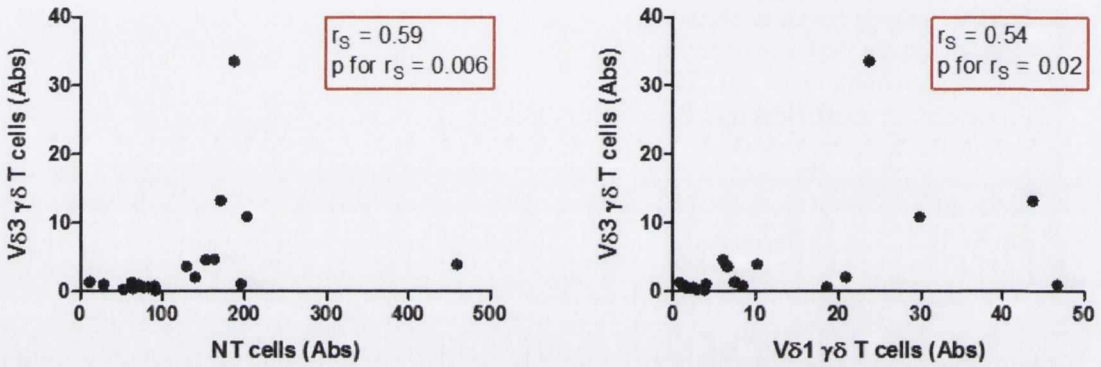


Figure 5.6. Significant correlations between absolute counts of Vδ3 γδ T cells and counts of other innate T cell subsets in CVID. Vδ3 γδ T cells, NT cells and Vδ1 γδ T cells were detected by flow cytometry in whole blood samples from CVID patients as $CD3^+$ Vδ3 TCR^+, $CD3^+$ $CD56^+$ and $CD3^+$ Vδ1 TCR^+ events, respectively. Absolute counts of Vδ3 γδ T cells were plotted against those of NT cells (left, n = 20) and Vδ1 γδ T cells (right, n = 18). The degree of correlation determined is expressed by a Spearman's correlation coefficient (r_S), defined by a p value (p for r_S).

5.6 – Analysis of statistical correlations between frequencies or counts of iNKT cells and other lymphocyte subsets

Table 5.7 summarises the correlations existing between frequencies of iNKT cells and those of other lymphocyte populations in healthy controls and CVID patients. No moderate or strong correlation was identified for healthy controls, however frequencies of iNKT cells correlated with those of MAIT cells ($r_S = 0.67$, $p = 0.002$) and Vδ1 γδ T cells ($r_S = 0.73$, $p = 0.0006$) in CVID patients. Graphs for these two correlations are shown in **Figure 5.7**.

Table 5.8 reports the correlations between absolute counts of iNKT cells and those of other lymphocyte populations in healthy controls and CVID patients. While no correlations were identified in the healthy control group, absolute counts of iNKT cells in the circulation

of CVID patients again correlate with those of MAIT cells ($r_S = 0.71$, $p = 0.0009$) and Vδ1 γδ T cells ($r_S = 0.68$, $p = 0.002$). Graphs for these correlations are shown in **Figure 5.8**.

Table 5.7. Correlations between frequencies of iNKT cells and those of other lymphocyte populations in healthy controls and CVID patients

Cohort	Cell subset	P value	Moderate	Strong
Healthy controls	*No significant correlations identified.*			
CVID patients				
	MAIT cells	0.002	0.67	
	Vδ1 γδ T cells	0.0006		0.73

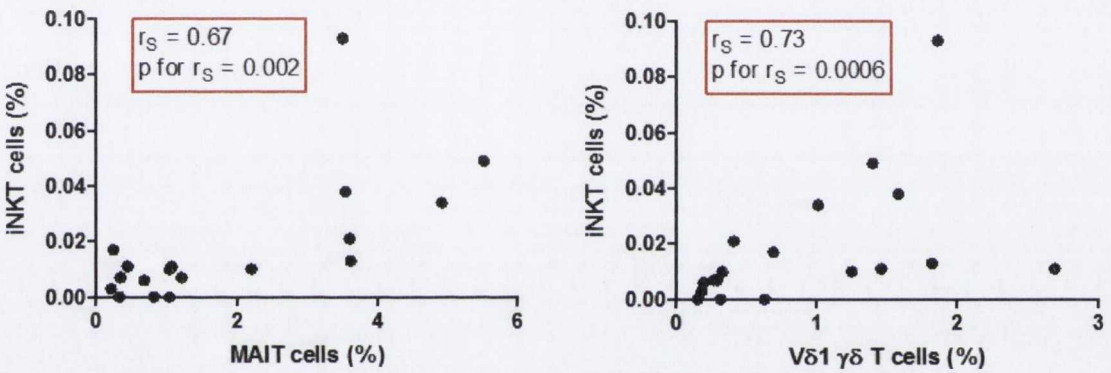


Figure 5.7. Significant correlations between frequencies of iNKT cells and frequencies of other innate T cell subsets in CVID. iNKT cells, MAIT cells and Vδ1 γδ T cells were detected by flow cytometry in whole blood samples from CVID patients as $CD3^+$ $Vα24\text{-}Jα18^+$, $CD3^+$ $Vα7.2^+$ $CD161^{high}$ and $CD3^+$ Vδ1 TCR^+ events, respectively. Frequencies of iNKT cells were then plotted against those of MAIT cells (left, n = 18) and Vδ1 γδ T cells (right, n = 18). The degree of correlation determined is expressed by a Spearman's correlation coefficient (r_S), defined by a p value (p for r_S).

Table 5.8. Correlations between absolute counts of iNKT cells and those of other lymphocyte populations in healthy controls and CVID patients

Cohort	Cell subset	P value	Moderate	Strong
Healthy controls	*No significant correlations identified.*			
CVID patients				
	MAIT cells	0.0009		0.71
	Vδ1 γδ T cells	0.002	0.68	

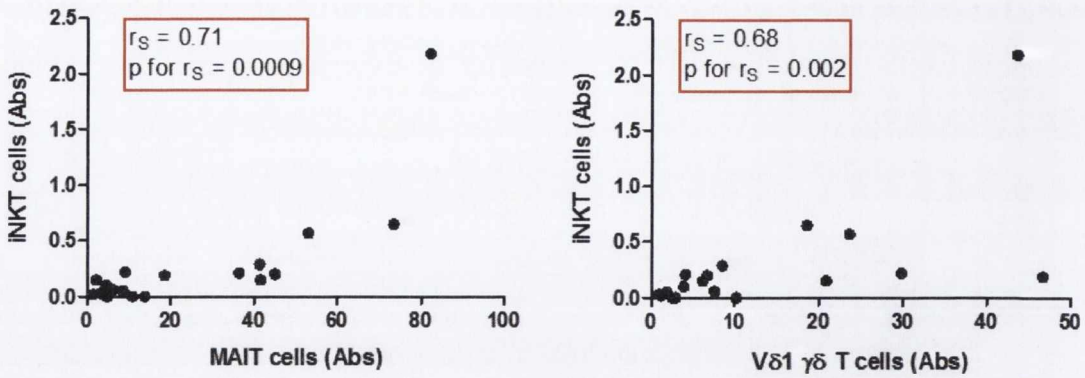


Figure 5.8. Significant correlations between absolute counts of iNKT cells and counts of other innate T cell subsets in CVID. iNKT cells, MAIT cells and Vδ1 γδ T cells were detected by flow cytometry in whole blood samples from CVID patients as $CD3^+$ $V\alpha24\text{-}J\alpha18^+$, $CD3^+$ $V\alpha7.2^+$ $CD161^{high}$ and $CD3^+$ Vδ1 TCR^+ events, respectively. Absolute counts of iNKT cells were then plotted against those of MAIT cells (left, n = 18) and Vδ1 γδ T cells (right, n =18). The degree of correlation determined is expressed by a Spearman's correlation coefficient (r_S), defined by a p value (p for r_S).

5.7 – Analysis of statistical correlations between frequencies or counts of MAIT cells and other lymphocyte subsets

Table 5.9 recapitulates the correlations existing between frequencies of MAIT cells and those of other lymphocyte populations in healthy controls and CVID patients. A moderate correlation was identified between frequencies of MAIT cells and Vδ2 γδ T cells in healthy controls ($r_S = 0.57$, $p = 0.004$). This correlation was maintained in CVID patients ($r_S = 0.52$, $p = 0.003$). Frequencies of MAIT cells from patients moreover correlated moderately with the frequencies of iNKT cells ($r_S = 0.67$, $p = 0.002$) and Vδ1 γδ T cells ($r_S = 0.51$, $p = 0.003$). Graphs for these correlations are shown in **Figure 5.9** for healthy controls and **Figure 5.10** for CVID patients.

Table 5.9. Correlations between frequencies of MAIT cells and those of other lymphocyte populations in healthy controls and CVID patients

Cohort	Cell subset	P value	Moderate	Strong
Healthy controls				
	Vδ2 γδ T cells	0.004	0.57	
CVID patients				
	iNKT cells	0.002	0.67	
	Vδ1 γδ T cells	0.003	0.51	
	Vδ2 γδ T cells	0.003	0.52	

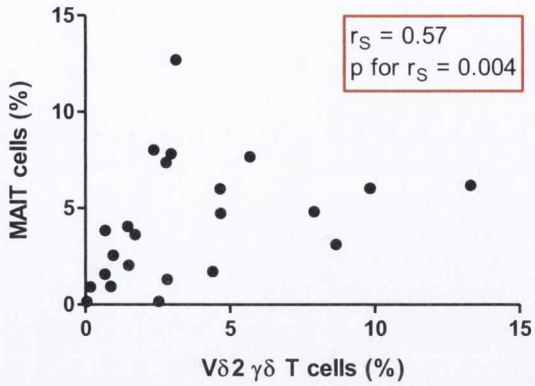


Figure 5.9. Significant correlation between frequencies of MAIT cells and Vδ2 γδ T cells in healthy controls. MAIT cells and Vδ2 γδ T cells were detected by flow cytometry in whole blood samples from healthy donors as $CD3^+$ $V\alpha7.2^+$ $CD161^{high}$ and $CD3^+$ Vδ2 TCR^+ events, respectively. Their frequencies were then plotted against one another (n = 23). The degree of correlation determined is expressed by a Spearman's correlation coefficient (r_S), defined by a p value (p for r_S).

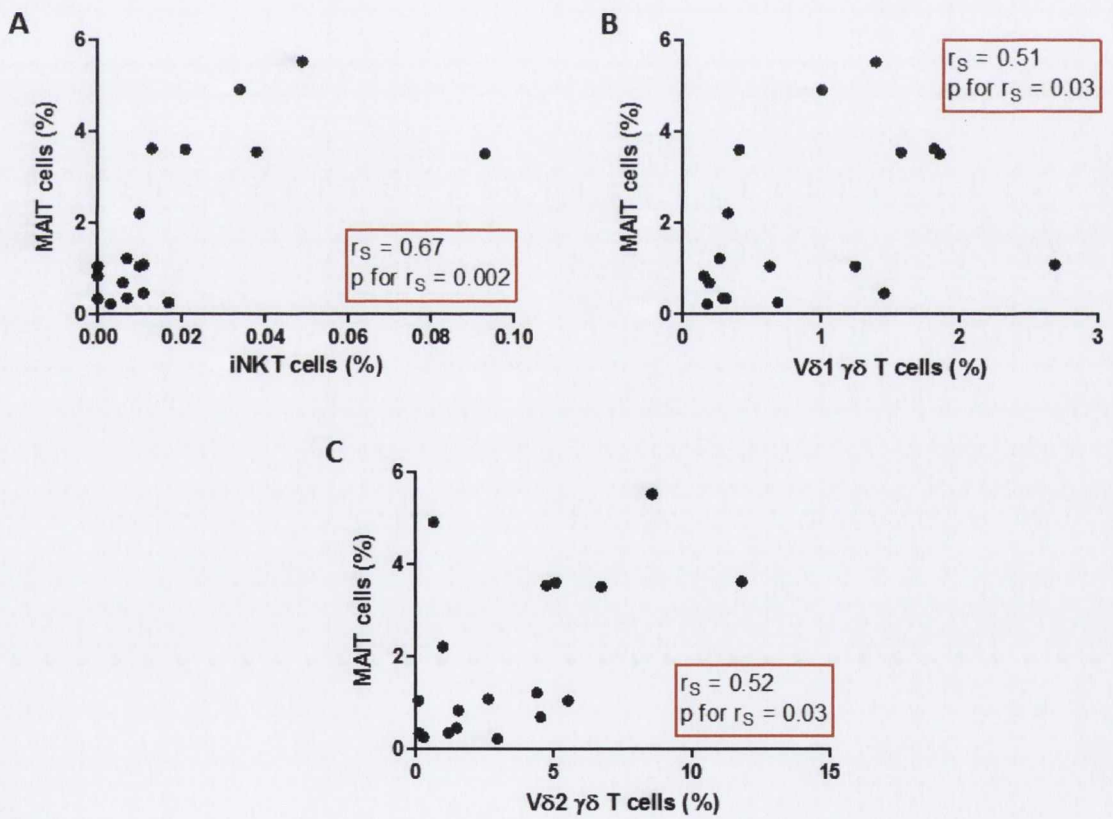


Figure 5.10. Significant correlations between frequencies of MAIT cells and frequencies of other innate T cell subsets in CVID. MAIT cells, INKT cells, and Vδ1 and Vδ2 γδ T cells were detected by flow cytometry in whole blood samples from CVID patients as $CD3^+$ $V\alpha7.2^+$ $CD161^{high}$, $CD3^+$ $V\alpha24\text{-}J\alpha18^+$, $CD3^+$ Vδ2 TCR^+ and $CD3^+$ Vδ2 TCR^+ events, respectively. Frequencies of MAIT cells were then plotted against those of iNKT cells (A, n = 18), Vδ1 γδ T cells (B, n = 18) and Vδ2 γδ T cells (C, n = 18). The degree of correlation determined is expressed by a Spearman's correlation coefficient (r_S), defined by a p value (p for r_S).

Table 5.10 summarizes the correlations between absolute counts of MAIT cells and those of other lymphocyte populations in healthy controls and CVID patients. As already seen for frequencies, absolute counts of Vδ2 γδ T cells moderately correlated with counts of MAIT cells in healthy controls ($r_S = 0.61$, $p = 0.003$). In a similar fashion, absolute counts of MAIT cells correlated in CVID patients with those of iNKT cells ($r_S = 0.71$, $p = 0.0009$), Vδ1 γδ T cells ($r_S = 0.67$, $p = 0.002$) and Vδ2 γδ T cells ($r_S = 0.63$, $p = 0.005$). In CVID, absolute counts of MAIT cells additionally correlated with those of class-switched memory B cells ($r_S = 0.55$, $p = 0.02$) and $CD27^-$ IgD^- B cells ($r_S = 0.50$, $p = 0.04$). Graphs for these correlations are shown in **Figure 5.11** for healthy controls and **Figure 5.12** for CVID patients.

Table 5.10. Correlations between absolute counts of MAIT cells and those of other lymphocyte populations in healthy controls and CVID patients

Cohort	Cell subset	P value	Moderate	Strong
Healthy controls				
	Vδ2 γδ T cells	0.003	0.61	
CVID patients				
	Class-sw. memory B cells	0.02	0.55	
	$CD27^-$ IgD^- B cells	0.04	0.50	
	iNKT cells	0.0009		0.71
	Vδ1 γδ T cells	0.002	0.67	
	Vδ2 γδ T cells	0.005	0.63	

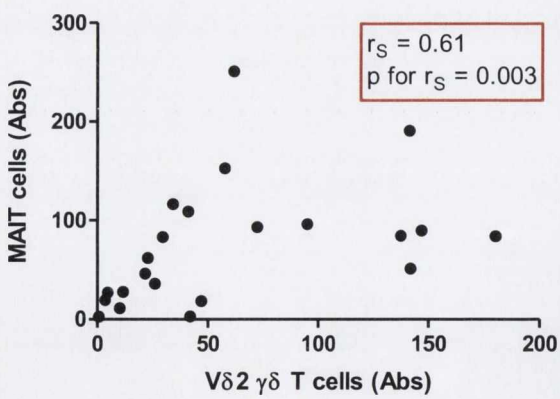


Figure 5.11. Significant correlation between absolute counts of MAIT cells and of Vδ2 γδ T cells in healthy controls. MAIT cells and Vδ2 γδ T cells were detected by flow cytometry in whole blood samples from healthy donors as $CD3^+$ $V\alpha7.2^+$ $CD161^{high}$ and $CD3^+$ Vδ2 TCR^+ events, respectively. Their absolute counts were then plotted against one another (n = 22). The degree of correlation is expressed by a Spearman's correlation coefficient (r_S), defined by a p value (p for r_S).

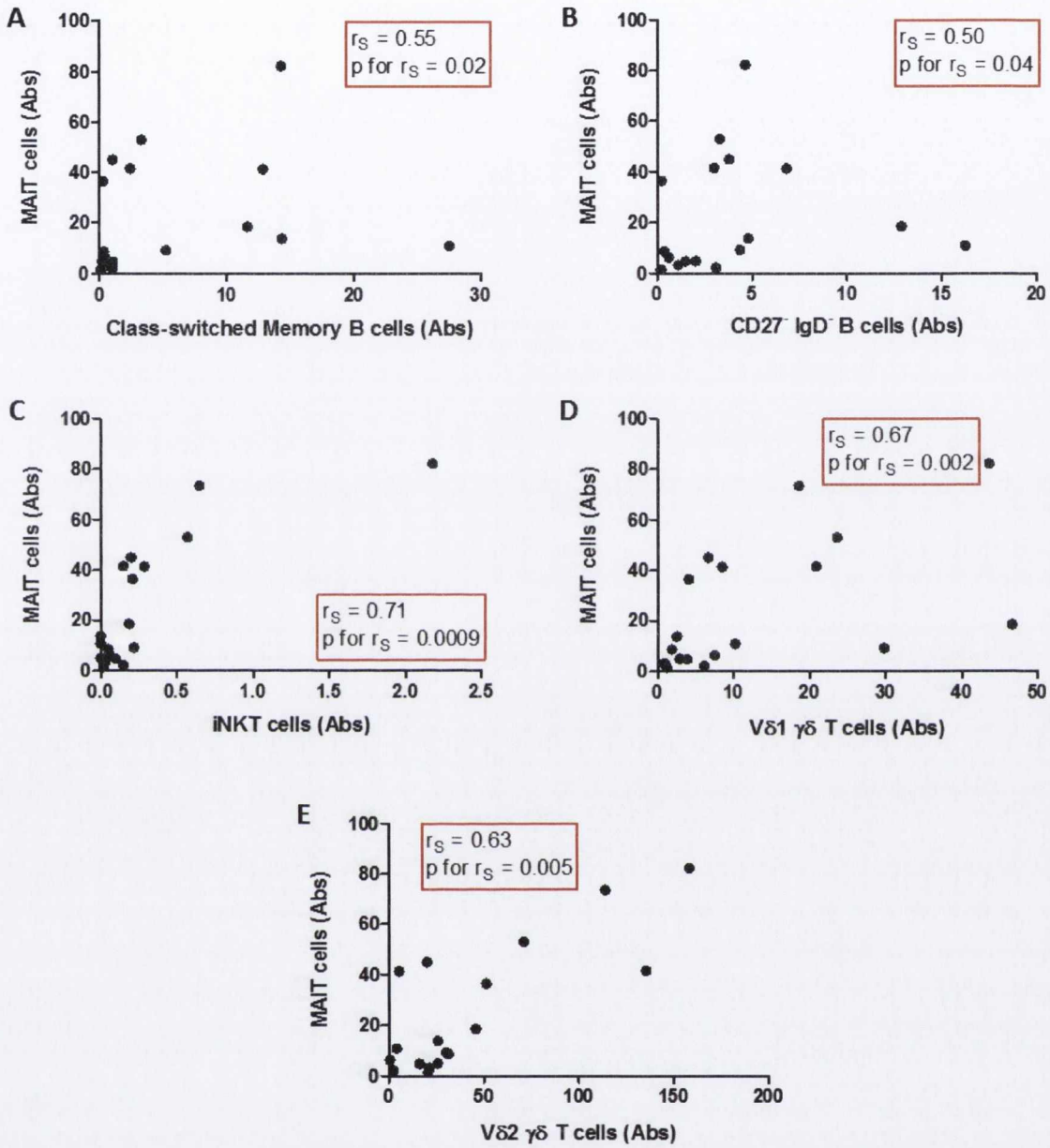


Figure 5.12. Significant correlations between absolute counts of MAIT cells and counts of B cell and innate T cell subsets in CVID. Absolute counts of MAIT cells ($CD3^+$ $V\alpha7.2^+$ $CD161^{high}$ events) were determined by flow cytometry using whole blood samples from CVID patients. They were then plotted against similarly determined counts of class-switched memory B cells (A, $CD19^+$ $CD27^+$ IgD^- phenotype, n = 17), $CD19^+$ $CD27^-$ IgD^- B cells (B, n = 17), iNKT cells (C, $CD3^+$ $V\alpha24$-$J\alpha18^+$ phenotype, n = 18), Vδ1 γδ T cells (D, $CD3^+$ Vδ1 TCR^+ phenotype, n = 18) and Vδ2 γδ T cells (E, $CD3^+$ Vδ2 TCR^+ phenotype, n = 18). The degree of correlation determined is expressed by a Spearman's correlation coefficient (r_S), defined by a p value (p for r_S).

5.8 – Diagrams of correlations between cell types

Due to the large amount of data contained in this chapter, it is difficult to form a complete view of the network of correlations intercurring between different lymphocyte subsets, in healthy controls and CVID patients alike. These data are therefore proposed here in the form of diagrams of interconnected populations.

Figure 5.13 represents correlations between frequencies of different lymphocyte subsets in healthy controls and CVID patients. As shown, correlations between frequencies in healthy controls only involve Vδ2 γδ T cells and MAIT cells. This relationship is maintained in CVID, but in this case frequencies of MAIT cells, Vδ1 γδ T cells and iNKT cells are also linked to each other.

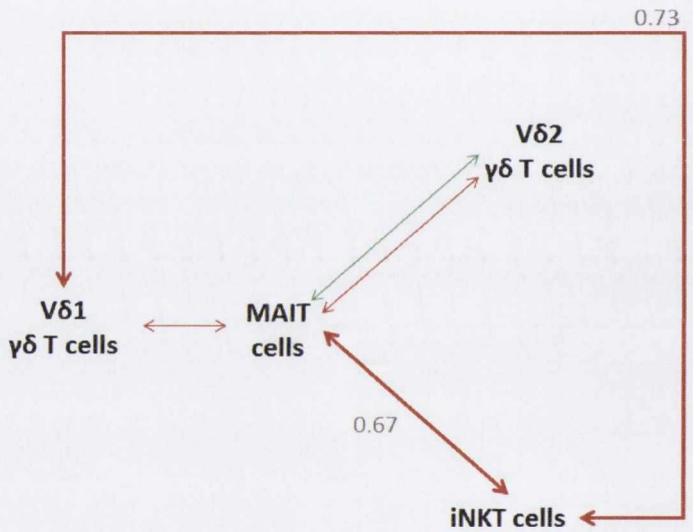


Figure 5.13. Summary of significant correlations between frequencies of lymphocyte subsets in healthy controls and CVID patients. Frequencies of B and innate T cell populations in the blood of healthy donors and CVID patients were determined by flow cytometry, then non-parametrically correlated, obtaining Spearman's correlation coefficients. Correlations detected in healthy controls are shown here as green lines, and correlations detected in CVID patients as red lines. Thicker lines stand for stronger correlations, with Spearman's correlation coefficients higher than 0.60; the coefficients for these correlations are indicated in grey beside the arrows.

Figure 5.14 shows correlations between absolute counts of lymphocyte subsets in healthy controls and CVID patients. The correlations already seen for frequencies are all maintained. In addition to this, Vδ1 γδ T cells counts correlate with those of a number of B cell populations, as well as NT and Vδ3 γδ T cells. Absolute counts of MAIT cells also correlate with those of class-switched memory B cells and $CD27^-$ IgD^- B cells.

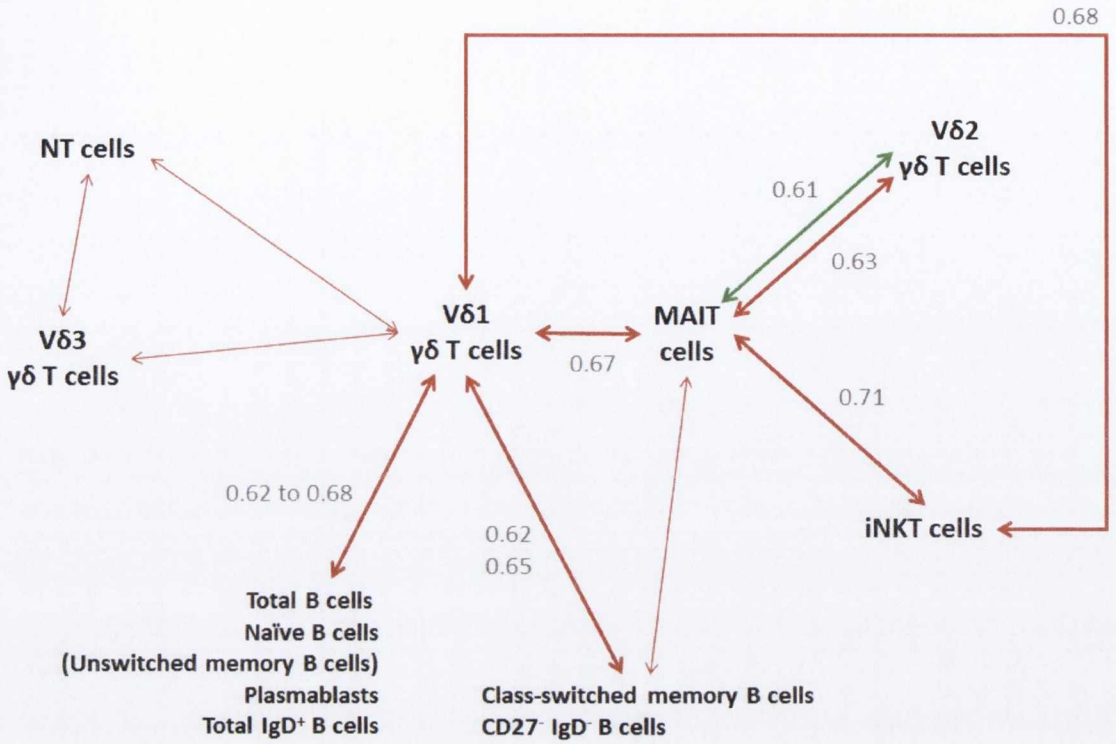


Figure 5.14. Summary of significant correlations between absolute counts of lymphocyte subsets in healthy controls and CVID patients. Absolute counts of B and innate T cell populations in the blood of healthy donors and CVID patients were determined by flow cytometry, then non-parametrically correlated, obtaining Spearman's correlation coefficients. Correlations detected in healthy controls are shown here as green lines, and correlations in CVID patients as red lines. Thicker lines stand for stronger correlations, with Spearman's correlation coefficients (r_S) higher than 0.60; the coefficients for these correlations are indicated in grey beside the arrows. Unswitched memory B cells are shown in brackets as their correlation with Vδ1 γδ T cells is weaker ($r_S = 0.48$) and not quite significant ($p = 0.052$).

5.9 – Discussion

In chapters 3 and 4 we showed that CVID manifests with abnormalities in the frequencies and absolute counts of several circulating B and T cell subsets. The data presented in this fifth chapter suggest that this primary immunodeficiency also alters the links between innate T cell subsets and other immune cell populations. The only significant correlation identified in this study in healthy donors was between frequencies and absolute counts of MAIT cells and Vδ2 γδ T cells. Although this relationship was maintained in CVID patients, a number of further connections were uncovered in CVID. Moderate to strong correlations were for example detected between frequencies and absolute counts of MAIT cells and iNKT cells; absolute counts of MAIT cells correlated with those of class-switched memory B cells and $CD27^-$ IgD^-. Vδ1 γδ T cells also appeared to be involved in CVID in a host of novel interactions. Frequencies and absolute counts of this population correlated with those of iNKT cells and MAIT cells. In addition to this, when absolute counts alone were investigated, Vδ1 γδ T cells displayed moderate correlations with total B cells, naïve B cells, class-switched memory B cells, plasmablasts and $CD27^-$ IgD^- B cells. Correlations of moderate strength were furthermore identified between absolute counts of Vδ1 γδ T cells, Vδ3 γδ T cells and NT cells.

As already noted in subchapter 5.2, the sheer number of associations probed make this part of the study an exercise in exploratory data analysis. As a direct consequence of this, before any kind of conclusion can be reached about the data presented, a confirmatory study would be needed in a second patient and control cohort. This is particularly important as no multiple testing correction was applied to the results presented, meaning that at least some of the significant correlations identified are likely to be false positives dependent on type I errors. Any datum found to be still significant in the second cohort would then have to be interrogated for biological relevance in a robust experimental way. Surely, the first necessary step would be to define if the correlations identified by statistical means mirror actual, direct interactions between the cell types involved, keeping in mind that any of the correlations described could easily depend on ulterior factors not considered in this thesis. This would mean, at the very least, creating *in vitro* systems of the populations of interest, and investigating their expression of activation markers, cytokine and chemokine production, direct cell-to-cell interactions as well as other applicable outputs, such as their ability to lyse target cells or produce antibodies. Knock-out or transgenic animal models could also be useful, providing for example confirmation that an absence or hypergeneration of a certain population can results in direct numerical alterations of a correlated cell subset. Ultimately,

a biologically relevant mechanism, able to account for the link between the different cell types, would have to be identified at a molecular level. In this respect, CVID could be useful as a disease control, offering clues as to why some correlation may not be apparent in healthy controls. It is however important to remember that CVID is not a monogenic disease, and that CVID patients constitute an extremely heterogeneous population. As such, its use as a disease control would be particularly challenging.

The correlation between MAIT cells and Vδ2 γδ T cells described in this chapter is unique amongst those probed because it was detected in both healthy controls and CVID patients. This finding is notable for two reasons: first of all, it suggests that interactions between MAIT cells and Vδ2 γδ T cells could play an important physiological role; secondly, it indicates that the relationship between these two subsets is not affected by the pathogenic mechanisms at work in CVID. As such mechanisms heavily involve B cells, the correlation is unlikely to be explained by interactions between these T cell subsets and B cell populations. A link may however exist between MAIT cells and Vδ2 γδ T cells on the basis of shared functions. These two cell populations certainly play an anti-microbial role and recognize some of the same pathogens, including *Escherichia coli*, *Pseudomonas aeruginosa* and *Mycobacterium tuberculosis*.[211,52,112] Davey and colleagues have also shown that GM-CSF, IFNγ and TNFα secreted by MAIT cells and Vδ2 γδ T cells in response to activation by their cognate antigens can induce differentiation of neutrophils into APC-like cells able to support both $CD4^+$ and $CD8^+$ T cell responses.[61] In both CVID and healthy individuals, MAIT cells and Vδ2 γδ T cells could therefore promote the development of adaptive immune responses, and possibly each other's proliferation, through the early production of cytokines at infection sites.

Previous research has identified correlations between frequencies of MAIT cells, $CD4^+$ iNKT cells and $CD56^{bright}$ NK cells in healthy donors.[131] These correlations, which were lost in MS patients, were suggestive of the existence of a network of innate T cells with regulatory abilities, of which both MAIT cells and iNKT cells would be part. Due to the rarity of iNKT cells, we unfortunately could not probe the relationship between MAIT cells and $CD4^+$ iNKT cells. We have however identified a novel correlation between MAIT cells and total iNKT cells in CVID. As shown in chapter 4, the frequencies and absolute counts of these innate T cell populations are significantly decreased in the circulation of CVID patients, and lower frequencies of both cell types were found to associate with the complications of the disease. MAIT cells and iNKT cells also share several important features: both subsets develop in the thymus in the presence of a population of double

positive thymocytes[81,108], express transcription factor PLZF[82,111] and are found at high frequencies in the liver.[82,106] They moreover participate in anti-microbial responses[212,112] and produce IFNγ, TNFα and IL-17A.[98,106] The correlation between these innate T cell subsets could therefore be due to factors influencing their biological functions, such as the high number of infections experienced by patients with CVID.

Another possibility is that MAIT cells and iNKT cells could be linked by their ability to interact with B cells. It is widely accepted that iNKT cells can support B cell proliferation and antibody production,[99,194] while MAIT cells require B cells for their expansion after birth.[109] Interestingly, lower frequencies of iNKT cells have been found to associate in CVID with lower frequencies of class-switched memory B cells,[169,193] however no link had been identified so far between MAIT cells and specific B cell subsets in health or disease states. Here, we show that absolute counts of circulating MAIT cells correlate with those of class-switched memory B cells and $CD27^-$ IgD^- B cells in the circulation of CVID patients, but not in healthy controls. This finding may reflect a negative effect of defective B cell differentiation on the numbers of MAIT cells available in the circulation patients with CVID, indicating a specific involvement of class-switched B cell subsets in the expansion of MAIT cells. The correlation could also point to an effect of MAIT cells on B cell differentiation. On the basis of these correlation data, and of the functional similarities between MAIT cells and innate T cell subsets with follicular helper-like functions (i.e. iNKT cells and Vδ2 γδ T cells), we have begun to investigate the effect of MAIT cells on B cell phenotype and functions. The results obtained are presented in chapter 7 of this thesis.

Speculating about the possible role of Vδ1 γδ T cells in CVID is not easy, first and foremost because little is known about the functions of this population in healthy donors. The correlations identified in CVID between absolute counts of this cell subset and those of numerous B cell populations, from undifferentiated to fully differentiated, suggest that Vδ1 γδ T cells could affect B cell numbers, or *vice versa*. As shown in chapter 4, however, frequencies and absolute counts of Vδ1 γδ T cells are similar in healthy controls and CVID patients, indicating that this population is not numerically affected by the defective B cell differentiation observed in CVID. The correlations observed could therefore involve Vδ1 γδ T cells in the homeostasis of B lymphocytes. Interestingly, recent research shows that about 50 % of Vδ1 γδ T cells can recognise both peptide antigens presented by HLA molecules and lipid antigens presented by CD1d.[213] Although their specificity for lipid antigens differs from that of iNKT cells, they can respond to α-GalCer. It is therefore possible that Vδ1 γδ T cells could share the ability of iNKT cells to promote B cell maturation and antibody production.[99,194] The prospect of a link between B cells and Vδ1 γδ T cells has so far gone

largely unexplored. Only two reports exists on this topic, one detailing interactions between Vδ1 γδ T cells and non-virally infected activated B cells *in vitro*, through an unidentified ligand,[214] the other describing IL-4 generation and weak T_H2-like B cell helper activity of $CD4^+$ Vδ1 γδ T cells obtained from the nasal mucosa of allergic individuals, promoting production of IgE antibodies.[215] B cells have however been shown to interact with Vδ2 γδ T cells,[63] demonstrating that cells belonging to the γδ T cell lineage are capable of supporting B cell functions. Notably, tissue homing properties are one of the main differences detected so far between Vδ1 and Vδ2 γδ T cells: Vδ2 cells are found in peripheral blood, while Vδ1 cells are intraepithelial lymphocytes highly represented in visceral organs, including the intestine, the spleen and the liver.[45,46] Putative interactions between Vδ1 γδ T cells and B cells *in vivo* could therefore involve resident B cell subsets such as marginal zone B cells or intestinal subsets responsible for the production of IgA.

In addition to their links to B cells, frequencies and absolute counts of Vδ1 γδ T cells appeared to firmly correlate in CVID with those of MAIT cells and iNKT cells. Although no clear link between these population has come to light so far, Vδ1 γδ T cells are similar to MAIT cells and iNKT cells in their ability to produce pro-inflammatory cytokines IFNγ, TNFα and IL-17A.[216] It could be speculated that Vδ1 γδ T cells, whose numbers in the peripheral blood of CVID patients are not altered, may functionally compensate for the diminished frequencies and counts of circulating iNKT cells and MAIT cells. It is also possible that, conversely, iNKT cells and MAIT cells could compensate for functional abnormalities or decreased intraepithelial numbers of Vδ1 γδ T cells, migrating to peripheral tissues.

Taken together, the results presented in this chapter support our hypothesis that CVID could be characterised by unusual interactions between B and innate T cell subsets. Although the interpretation of the correlations identified is complex, the data obtained could guide new investigations in the field of immune cell biology. Using co-culture systems, we have for example begun to explore if MAIT cells can affect the differentiation status of B cells and their antibody production (see chapter 7 of this thesis). Similar methods could be applied to study putative interactions between Vδ1 γδ T cells and B cell subsets, as well as between MAIT cells and Vδ2 γδ T cells.

CHAPTER 6

FUNCTIONAL PROPERTIES OF MAIT CELLS FROM HEALTHY DONORS AND CVID PATIENTS

6.1 – Introduction

As shown in chapter 4, the frequencies and absolute numbers of MAIT cells and iNKT cells, but not of Vδ1, Vδ2 or Vδ3 γδ T cells, were found in this study to be lower in the circulation of CVID patients than in healthy subjects. Within the MAIT cell population, frequencies of $CD4^+$ cells were significantly increased and those of $CD8^+$ cells significantly decreased in the peripheral blood of patients affected by CVID in comparison to healthy donors, while counts of circulating $CD8^+$ and double negative MAIT cells were significantly depleted. The depletion in total MAIT cells and iNKT cells was particularly prominent in patients with complications, the vast majority of whom presented with autoimmune conditions. In addition to these findings from immunophenotyping, novel statistical correlations not observed in healthy controls appeared to become established in CVID between the frequencies and absolute counts of MAIT cells and iNKT cells, and between the numbers of MAIT cells and those of class-switched memory B cells (chapter 5). We previously speculated that the decreased numbers of both innate T cell subsets could be due to impaired proliferation or to their recruitment and migration to sites of infection or inflammation in peripheral tissues. We also suggested that the correlations identified for MAIT cells could indicate the existence of a relationship between this T cell population and differentiated B cells, and that, similar to iNKT cells, MAIT cells could sustain B cell proliferation and antibody production.

Innate T cells can produce a range of cytokines. iNKT cells are versatile in this respect, secreting both T_H1- and T_H2-type cytokines, including IFNγ, TNFα, IL-4, IL-5, IL-13, as well as IL-10 and IL-17.[98] Their ability to generate all these different mediators makes iNKT cells a key regulatory subset, able to polarise the immune response and influence the behaviour of a number of other cell types, including monocytes, DCs, NK cells and B cells.[91,93,95,99] MAIT cells appear to generate a more restricted spectrum of T_H1 and T_H17 cytokines. They certainly secrete abundant quantities of TNFα following stimulation with anti-CD3 and anti-CD28 antibodies *in vitro*; stronger stimulation with PMA and ionomycin in culture elicits the production of IFNγ, IL-2, IL-17 and IL-22.[106,132] These same mediators are produced by MAIT cells in the presence of antigen presenting cells pulsed with bacteria or fungi able to produce this population's antigens.[106,112,116] Early activation of MAIT cells following stimulation by pulsed APCs *in vitro* has previously been defined by measuring surface expression of CD69.[112]

Almost nothing is known about the functional characteristics of MAIT cells and iNKT cells in the context of CVID. In the only report produced to date on this subject, iNKT cells

from CVID patients, but not from healthy donors, failed to expand *in vitro* following stimulation with α-GalCer.[193] It has therefore been proposed that this cell subset may be functionally stunted and unable to proliferate normally in CVID. Because of the reciprocal relationship known to exist between iNKT cells and B cells,[99] this may in turn affect B cell differentiation and antibody production.

6.2 – Hypothesis and aims of the chapter

Taken together, the findings presented in chapters 4 and 5 of this thesis were suggestive of an involvement of MAIT cells and iNKT cells in the workings of CVID. MAIT cells were of particular interest, not only for their relative novelty, but also because our previous observations hinted at a potential, undescribed relationship between this population and differentiated B cell subsets. The T_H1/T_H17-type cytokine profile of MAIT cells could moreover implicate this subset in anti-microbial responses and in the development of autoimmunity, both key processes in CVID. As mentioned in chapter 6.1, previous research showed that iNKT cells from CVID patients would not readily proliferate in culture.[193] Although a protocol for the *in vitro* expansion of MAIT cells is yet to be developed, this innate T cell population is relatively abundant in human blood, allowing us to directly determine the functional status of this cell subset and avoiding potential culturing issues.

We therefore elected to focus on MAIT cells, hypothesising that this population could play a role in the complications of CVID, as well as be linked to the extensive defects in B cell differentiation and maturation seen in patients. In order to investigate these aspects, we decided to examine the functional capabilities of MAIT cells from healthy controls and donors affected by CVID. Our specific aims for this chapter were:

1. to define in what measure MAIT cells from CVID patients and healthy individuals reacted to *in vitro* stimulation, in the form of anti-CD3 and anti-CD28 antibodies or PMA and ionomycin, by upregulating their expression of surface markers CD69 and CD40L. As noted in the introduction to this chapter, CD69 has previously been employed to study the activation status of MAIT cells *in vitro*.[112] It is a short-term activation molecule, whose surface expression increases up to 4 hours following stimulation and is then maintained at upregulated levels for a time. CD40L (also known as CD154) is the ligand of CD40, a signalling molecule expressed on the

surface of antigen presenting cells, including B cells. The binding of CD40L to CD40 is involved in events such as B cell activation and maturation, as well as isotype class-switching;

2. to determine if MAIT cells from CVID patients and healthy donors exhibited comparable cytokine profiles. These data could supply clues about a possible role of MAIT cells in the development of CVID or its complications, as well as suggest new therapeutic avenues for the treatment of patients. The panel of cytokines detected in these experiments comprised:
    - TNFα and IFNγ, pro-inflammatory mediators abundantly produced by MAIT cells[106] and important in the fight against microbial infections as well as in inflammatory processes;
    - IL-10 and IL-4, cytokines not normally produced by this cell type[106] but involved in B cell proliferation, maturation and class-switching;[217-219]
    - IL-17A and IL-22, implicated in infection resolution and in the development of autoimmunity.[201,220]

As described in chapter 2.8.4, these determinations were carried out using a whole blood protocol that offered several advantages over PBMC preparation-based ones. The results of the experiments on MAIT cells are reported here alongside those of T cells, their parent population. As conventional T cells produce all the cytokines detected and also upregulate CD69 and CD40L upon stimulation, they constitute useful experiment controls. They moreover supply a framework of reference for the interpretation of the results obtained from MAIT cells.

6.3 – Upregulation of activation markers by T cells and MAIT cells following *in vitro* stimulation

6.3.1 – CD69 expression by T cells and MAIT cells following *in vitro* stimulation

Whole blood from healthy donors and CVID patients was left unstimulated or stimulated with either anti-CD3 and anti-CD28 antibodies or PMA and ionomycin. **Figures 6.1 and 6.2** show representative flow cytometry dot plots of unstimulated and stimulated T

cells and MAIT cells, respectively, obtained following 4 hours of incubation and staining with an anti-CD69 antibody. The experiments presented in this chapter report measurements of total CD69, i.e. of both the surface and intracellular forms of this marker.

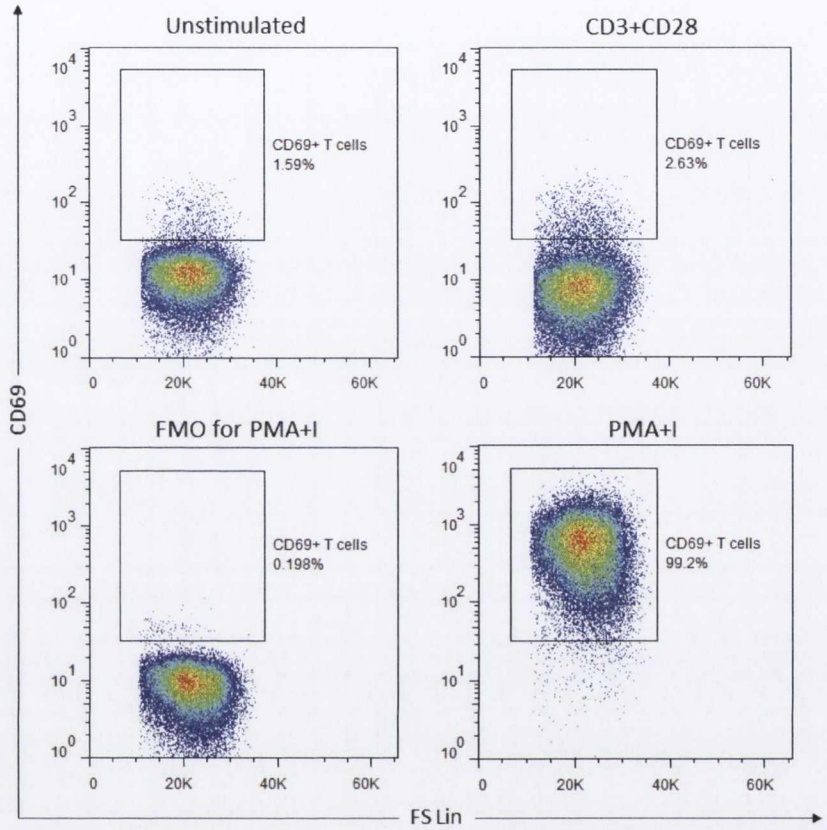


Figure 6.1. Flow cytometry dot plots representative of CD69 expression by T cells. Whole blood samples were left unstimulated or stimulated for 4 hours with anti-CD3 and anti-CD28 antibodies (CD3+CD28) or PMA and ionomycin (PMA+I). Fluorescence minus one (FMO) controls were used to aid the gating of both unstimulated and stimulated samples; an example is shown here of an FMO obtained following stimulation with PMA and ionomycin (FMO for PMA+I). The gates in the dot plots define the frequencies of CD69-expressing T cells, following gating on $CD3^+$ cells. This image is representative of the staining pattern observed for 6 healthy donors and 12 CVID patients.

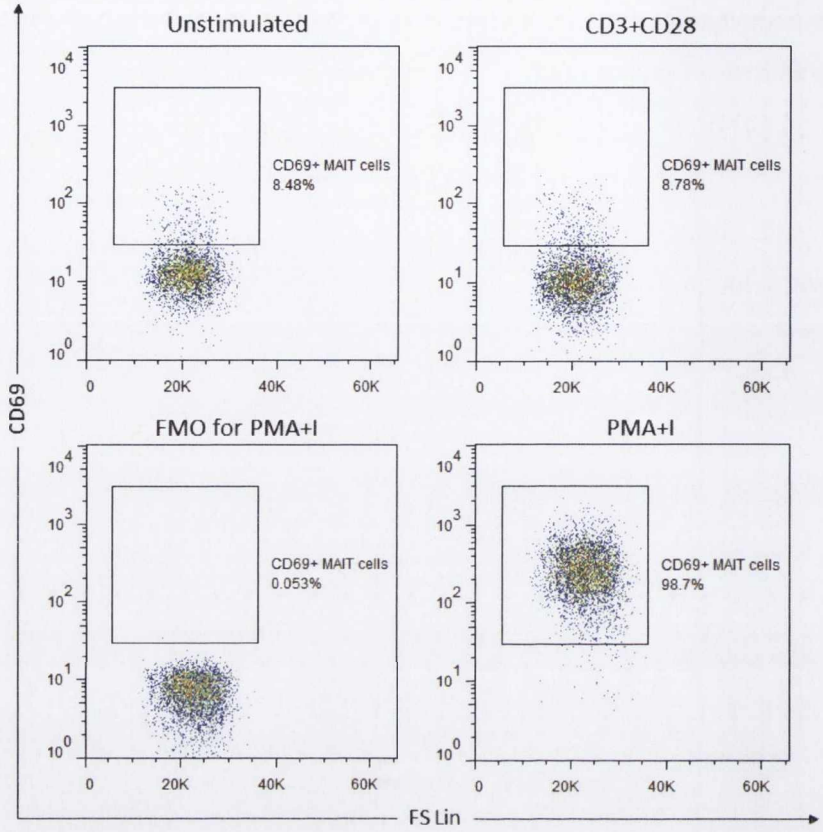


Figure 6.2. Flow cytometry dot plots representative of CD69 expression by MAIT cells. Whole blood samples were left unstimulated or stimulated for 4 hours with anti-CD3 and anti-CD28 antibodies (CD3+CD28) or PMA and ionomycin (PMA+I). Fluorescence minus one (FMO) controls were used to aid the gating of both unstimulated and stimulated samples; an example is shown here of an FMO obtained following stimulation with PMA and ionomycin (FMO for PMA+I). The gates in the dot plots define the frequencies of CD69-expressing MAIT cells, following gating on $CD3^+$ $V\alpha7.2^+$ $CD161^{high}$ events. This image is representative of the staining pattern observed for 6 healthy donors and 12 CVID patients.

As shown in **Figure 6.3**, the frequencies of T cells expressing CD69 were comparable in unstimulated blood samples from healthy controls and CVID patients, as well as in samples stimulated with anti-CD3 and anti-CD28 antibodies. Significantly lower frequencies of $CD69^+$ T cells were detected in blood from CVID patients stimulated with PMA and ionomycin in comparison to healthy controls ($p = 0.04$). After separating data from CVID patients with infections only and patients with infections and complications, the significant decrease previously identified in samples stimulated with PMA and ionomycin was found to depend on patients with complications ($p < 0.05$). This is most likely due to the results obtained for a single patient with complications, for which expression of CD69 by T cells following stimulation with PMA and ionomycin was not universal. $CD69^+$ T cells were further found at significantly higher frequencies in unstimulated blood from CVID patients with infections only in comparison to patients with complications ($p < 0.05$).

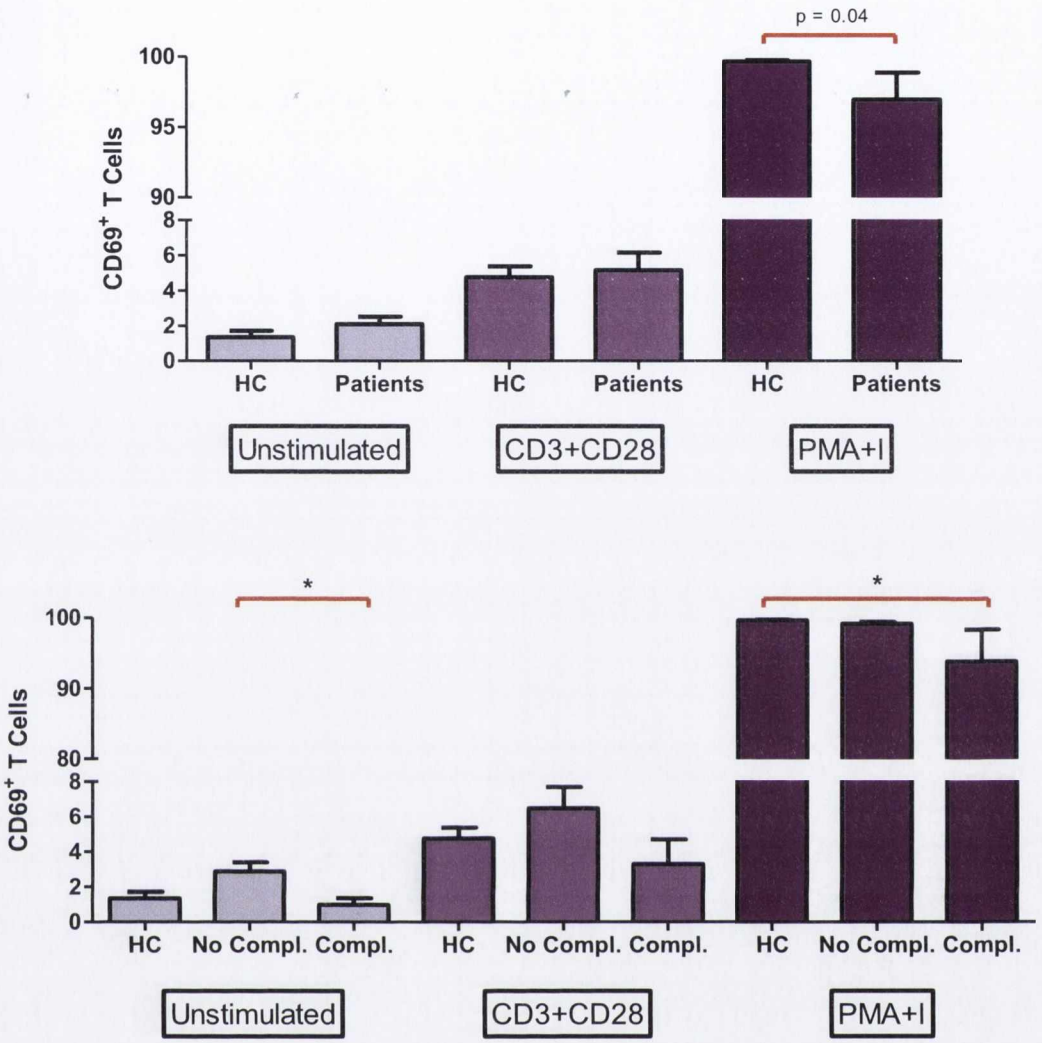


Figure 6.3. Frequencies of CD69$^+$ T cells in unstimulated and stimulated blood from healthy controls and CVID patients. Whole blood was left unstimulated or stimulated for 4 hours with anti-CD3 and anti-CD28 antibodies (CD3+CD28) or PMA and ionomycin (PMA+I). Unstimulated and stimulated samples were then analysed by flow cytometry, detecting T cells as CD3$^+$ events. In the top graph, frequencies of T cells expressing CD69 were assessed in samples from healthy controls (HC, n = 6) and CVID patients (Patients, n = 12). In the bottom graph, CVID patients were divided on the basis of their complication status, in a group affected by infections only (No Compl., n = 7) and one affected by infections and complications (Compl., n = 5). Results are expressed as means ± SEM. Statistical analysis was performed using a two-tailed Mann-Whitney test (top) or a Kruskal-Wallis test plus Dunn's post hoc test (bottom). * $p < 0.05$

Similar percentages of CD69$^+$ MAIT cells were noted in the blood of healthy donors and CVID patients following stimulation with PMA and ionomycin, which resulted in universal expression of CD69 expression by this population (**Figure 6.4**). CD69$^+$ MAIT cells were however detected at significantly higher frequencies in the blood of CVID patients than in that of healthy controls when samples were left unstimulated and when they were stimulated with anti-CD3 and anti-CD28 antibodies (both $p = 0.03$). Indeed, when data

obtained from these conditions was visualised by scatter plot, a number of CVID patients manifested extremely high frequencies of $CD69^+$ MAIT cells even in the absence of any stimulation (**Figure 6.5**).

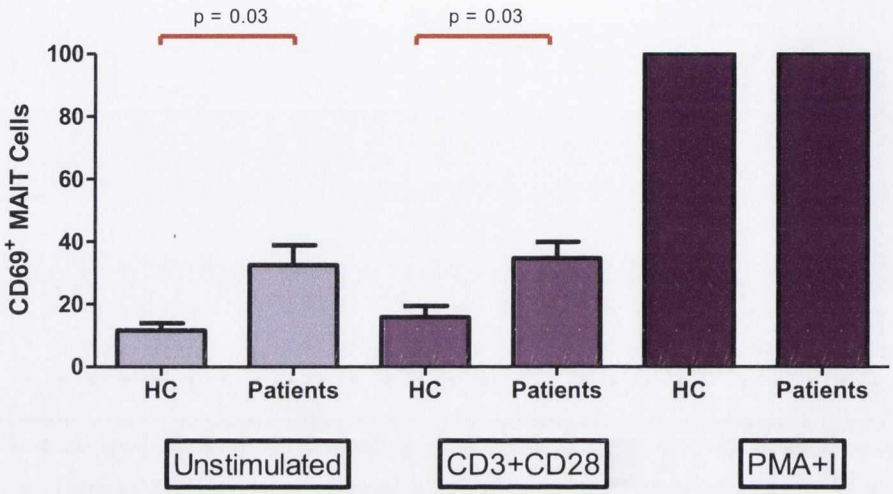


Figure 6.4. Frequencies of $CD69^+$ MAIT cells in unstimulated and stimulated blood from healthy controls and CVID patients. Whole blood was left unstimulated or stimulated for 4 hours with anti-CD3 and anti-CD28 antibodies (CD3+CD28) or PMA and ionomycin (PMA+I). Unstimulated and stimulated samples were then analysed by flow cytometry, detecting MAIT cells as $CD3^+$ $V\alpha7.2^+$ $CD161^{high}$ events. Frequencies of CD69-expressing MAIT cells were assessed in samples from healthy controls (HC, n = 6) and CVID patients (Patients, n = 12). Results are expressed as means ± SEM. Statistical analysis was performed using a two-tailed Mann-Whitney test.

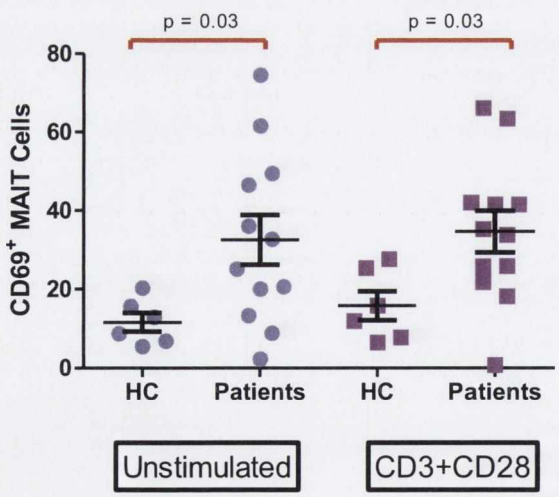


Figure 6.5. Frequencies of $CD69^+$ MAIT cells in unstimulated and stimulated blood from healthy controls and CVID patients. Whole blood was left unstimulated or stimulated for 4 hours with anti-CD3 and anti-CD28 antibodies (CD3+CD28); Unstimulated and stimulated samples were then analysed by flow cytometry, detecting MAIT cells as $CD3^+$ $V\alpha7.2^+$ $CD161^{high}$ events. Frequencies of CD69-expressing MAIT cells were assessed in samples from healthy controls (HC, n = 6) and CVID patients (Patients, n = 12). Results are expressed as means ± SEM. Statistical analysis was performed using a two-tailed Mann-Whitney test.

Subdivision of CVID patients according to their complication status, in patients with infections only and patients with infections and complications, did not reveal any significant differences in the frequencies of $CD69^+$ MAIT cells in the unstimulated or stimulated blood of the two groups (**Figure 6.6**). Unstimulated blood from CVID patients with infections only was however found to contain significantly higher frequencies of these cells in comparison to healthy controls ($p < 0.05$).

Thus, frequencies of $CD69^+$ T cells are essentially comparable in unstimulated and stimulated samples from healthy donors and CVID patients, while frequencies of $CD69^+$ MAIT cells are significantly higher in unstimulated and antibody-stimulated samples from CVID patients, regardless of their complication status, thank in healthy controls.

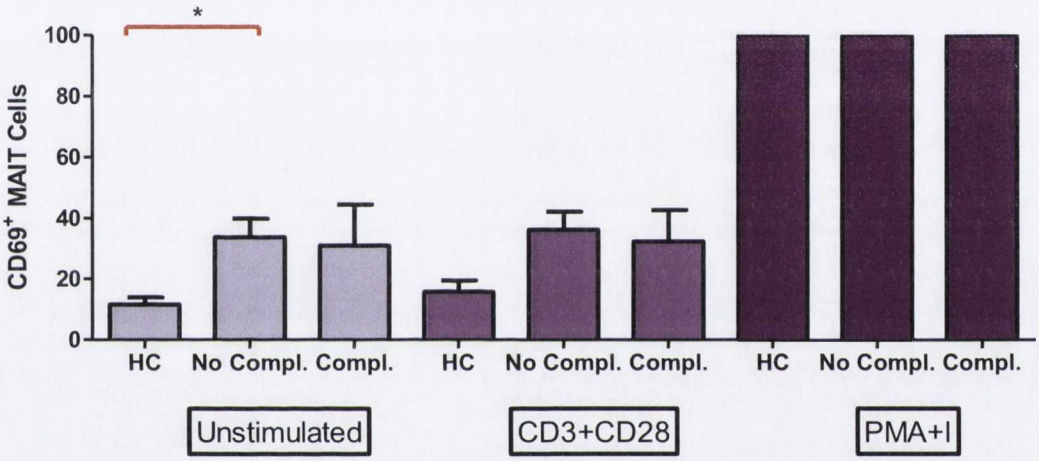


Figure 6.6. Frequencies of $CD69^+$ MAIT cells in unstimulated and stimulated blood from healthy controls and CVID patients with or without complications. Whole blood was left unstimulated or stimulated for 4 hours with anti-CD3 and anti-CD28 antibodies (CD3+CD28) or PMA and ionomycin (PMA+I). Unstimulated and stimulated samples were then analysed by flow cytometry, detecting MAIT cells as $CD3^+$ $V\alpha7.2^+$ $CD161^{high}$ events. Frequencies of CD69-expressing MAIT cells were assessed in samples from healthy controls (HC, n = 6), CVID patients with infections only (No Compl., n = 7) and CVID patients with infections and complications (Compl., n = 5). Results are expressed as means ± SEM. Statistical analysis was performed using a Kruskal-Wallis test plus Dunn's post hoc test. * $p < 0.05$.

6.3.2 – CD40L expression by T cells and MAIT cells following *in vitro* stimulation

Whole blood from healthy donors and CVID patients was left unstimulated or stimulated with either anti-CD3 and anti-CD28 antibodies or PMA and ionomycin. After 4 hours of incubation in the presence of monensin and anti-CD40L antibody, T cells and MAIT cells were detected by staining with an appropriate panel of fluorochrome-conjugated

antibodies. **Figure 6.7** shows flow cytometry dot plots representative of CD40L expression by unstimulated and stimulated T cells and MAIT cells; see chapter 6.3.1 for examples of the FMOs used in these experiments.

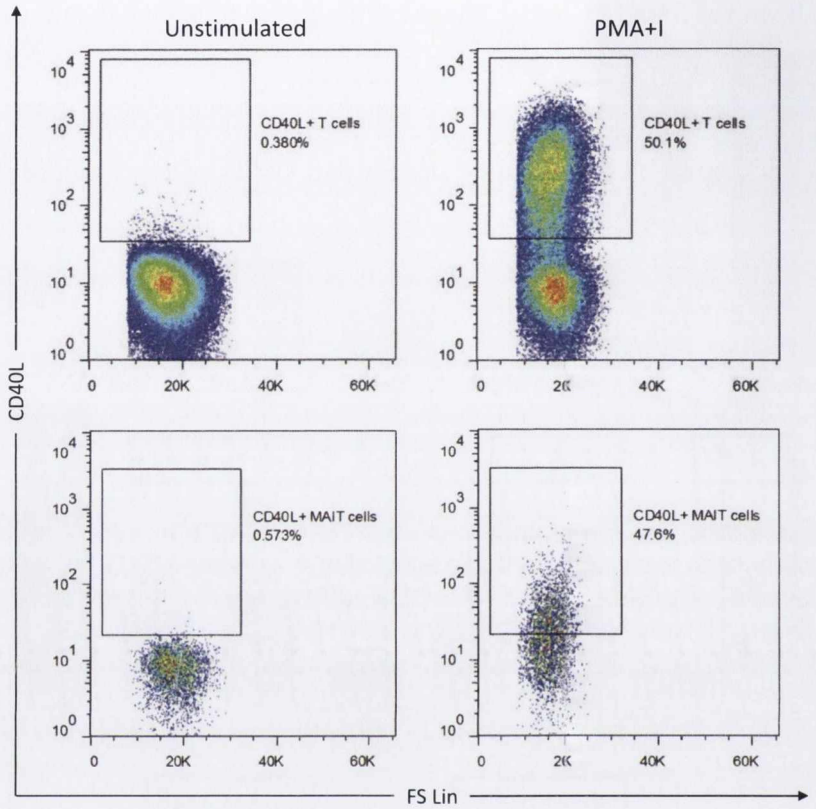


Figure 6.7. Flow cytometry dot plots representative of CD40L expression by T and MAIT cells. Whole blood samples were left unstimulated (left) or stimulated for 4 hours with PMA and ionomycin (PMA+I, right), in the presence of monensin and ani-CD40L antibody. The gates in the plots define the frequencies of CD40L-expressing T cells (top, following gating on $CD3^+$ cells) and MAIT cells (bottom, following gating on $CD3^+$ $V\alpha7.2^+$ $CD161^{high}$ events). This image is representative of the staining pattern observed for 6 healthy donors and 12 CVID patients.

No significant differences were noted between CVID patients and healthy controls with regard to the frequencies of $CD40L^+$ T cells, either in unstimulated or stimulated blood; their frequencies were also found to be comparable when CVID patients were divided according to their complication status (**Figure 6.8**).

Similarly, no significant differences were noted between healthy controls and CVID patients with regard to their frequencies of $CD40L^+$ MAIT cells; percentages of these cells were also similar in all groups assessed when CVID patients were divided according to their complication status (**Figure 6.9**).

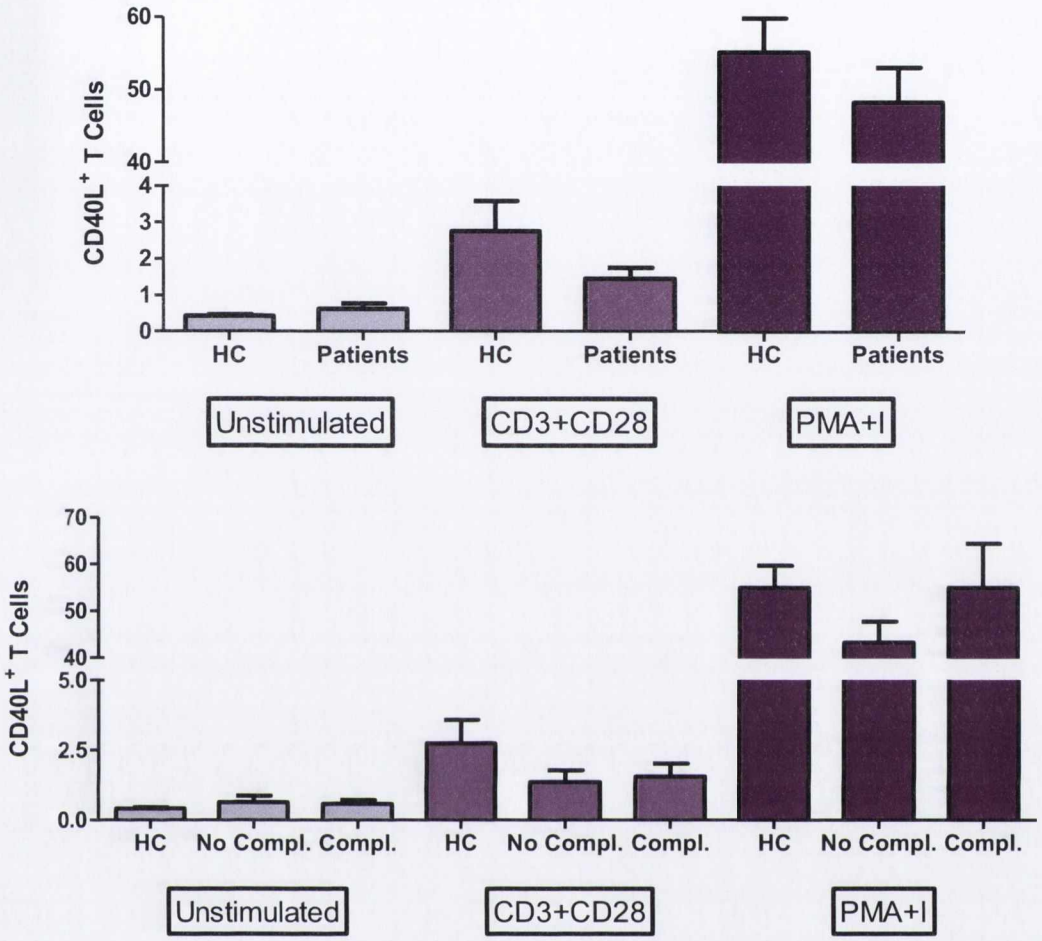


Figure 6.8. Frequencies of CD40L$^+$ T cells in unstimulated and stimulated blood from healthy controls and CVID patients. Whole blood was left unstimulated or stimulated for 4 hours with anti-CD3 and anti-CD28 antibodies (CD3+CD28) or PMA and ionomycin (PMA+I), in the presence of monensin and anti-CD40L antibody. Unstimulated and stimulated samples were then analysed by flow cytometry, detecting T cells as CD3$^+$ events. In the top graph, frequencies of T cells expressing CD69 were assessed in samples from healthy controls (HC, n = 6) and CVID patients (Patients, n = 12). In the bottom graph, CVID patients were divided on the basis of their complication status, in a group affected by infections only (No Compl., n = 7) and one affected by infections and complications (Compl., n = 5). Results are expressed as means ± SEM. Statistical analysis was performed using a two-tailed Mann-Whitney test (top) or a Kruskal-Wallis test plus Dunn's post hoc test (bottom).

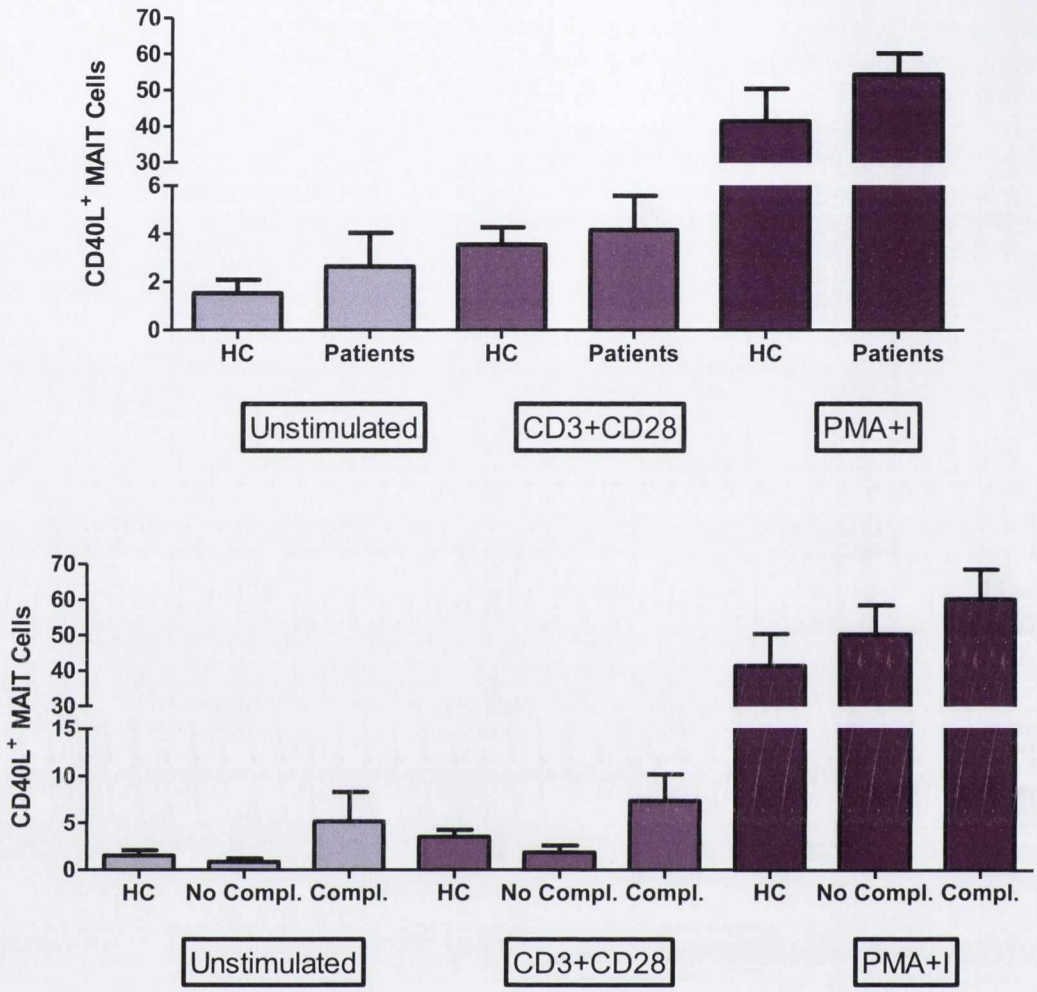


Figure 6.9. Frequencies of CD40L$^+$ MAIT cells in unstimulated and stimulated blood from healthy controls and CVID patients. Whole blood was left unstimulated or stimulated for 4 hours with anti-CD3 and anti-CD28 antibodies (CD3+CD28) or PMA and ionomycin (PMA+I), in the presence of monensin and anti-CD40L antibody. Unstimulated and stimulated samples were then analysed by flow cytometry, detecting MAIT cells as CD3$^+$ Vα7.2$^+$ CD161^{high} events. In the top graph, frequencies of MAIT cells expressing CD69 were assessed in healthy controls (HC, n = 6) and CVID patients (Patients, n = 12). In the bottom graph, CVID patients were divided on the basis of their complication status, in a group affected by infections only (No Compl., n = 7) and one affected by infections and complications (Compl., n = 5). Results are expressed as means ± SEM. Statistical analysis was performed using a two-tailed Mann-Whitney test (top) or a Kruskal-Wallis test plus Dunn's post hoc test (bottom).

6.4 – Cytokine production by T cells and MAIT cells following *in vitro* stimulation

6.4.1 – Production of TNFα by T cells and MAIT cells following *in vitro* stimulation

Whole blood from healthy donors and CVID patients was left unstimulated or stimulated with either anti-CD3 and anti-CD28 antibodies or PMA and ionomycin. After 8 hours of incubation in the presence of brefeldin A and staining with an appropriate panel of antibodies, TNFα was detected intracellularly by flow cytometry. **Figures 6.10 and 6.11** show flow cytometry dot plots representative of TNFα production by unstimulated and stimulated T cells and MAIT cells, respectively, as well as examples of the FMOs used throughout the experiments presented in chapter 6.4.

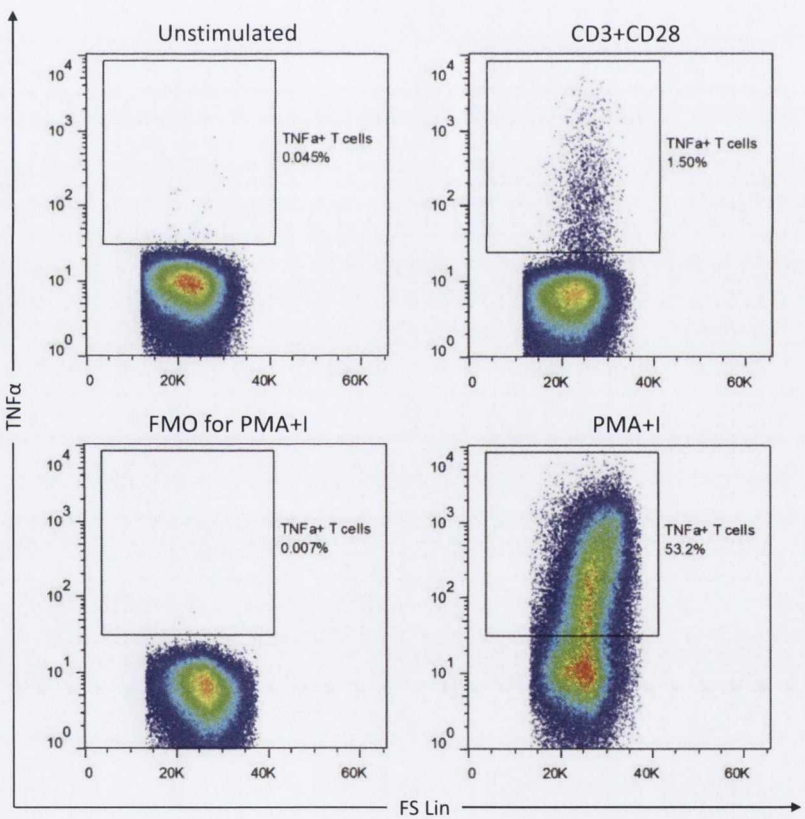


Figure 6.10. Flow cytometry dot plots representative of TNFα production by T cells. Whole blood samples were left unstimulated or stimulated for 8 hours with anti-CD3 and anti-CD28 antibodies (CD3+CD28) or PMA and ionomycin (PMA+I), in the presence of brefeldin A. Fluorescence minus one (FMO) controls were used to aid the gating of both unstimulated and stimulated samples; an example is shown here of an FMO obtained following stimulation with PMA and ionomycin (FMO for PMA+I). The gates in the dot plots define the frequencies of $TNF\alpha^+$ T cells, following gating on $CD3^+$ cells. This image is representative of the staining pattern observed for 6 healthy donors and 12 CVID patients.

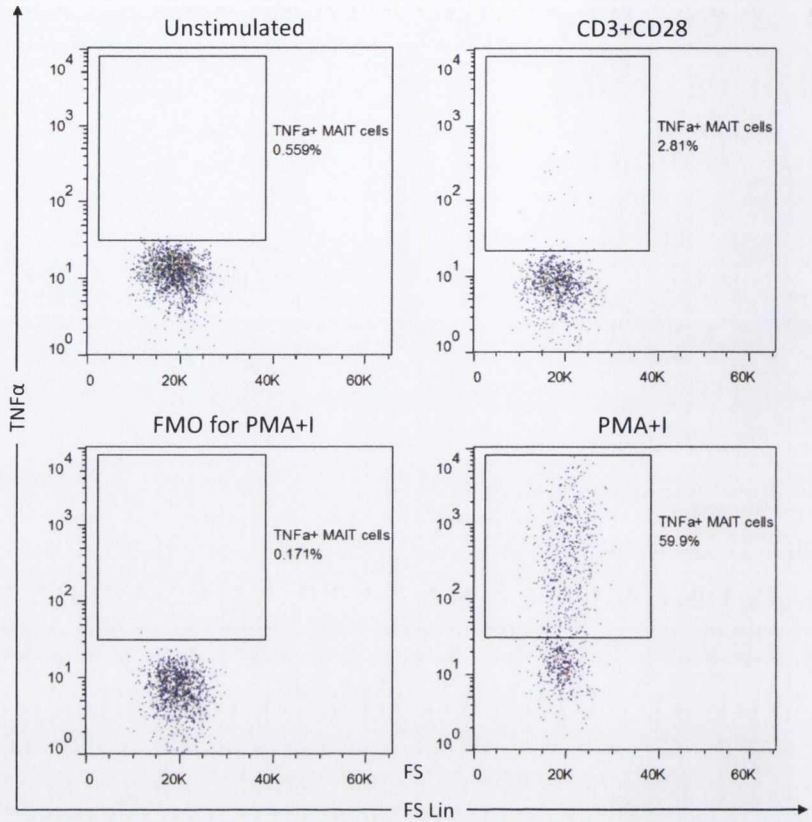


Figure 6.11. Flow cytometry dot plots representative of TNFα production by MAIT cells. Whole blood samples were left unstimulated or stimulated for 8 hours with anti-CD3 and anti-CD28 antibodies (CD3+CD28) or PMA and ionomycin (PMA+I), in the presence of brefeldin A. Fluorescence minus one (FMO) controls were used to aid the gating of both unstimulated and stimulated samples; an example is shown here of an FMO obtained following stimulation with PMA and ionomycin (FMO for PMA+I). The gates in the dot plots define the frequencies of $TNF\alpha^+$ MAIT cells, following gating on $CD3^+$ $V\alpha7.2^+$ $CD161^{high}$ events. This image is representative of the staining pattern observed for 6 healthy donors and 12 CVID patients.

Frequencies of $TNF\alpha^+$ T cells were found to be similar in unstimulated blood, as well as in blood stimulated with PMA and ionomycin, from healthy controls and CVID patients; their percentages were however significantly higher in the blood of patients following stimulation with anti-CD3 and anti–CD28 antibodies ($p = 0.04$, **Figure 6.12**). No significant differences were noted in the frequencies of $TNF\alpha^+$ T cells when results from CVID patients with infections only and patients with complications were considered separately.

Similar to total T cells, frequencies of $TNF\alpha^+$ MAIT cells were comparable in blood from healthy controls and CVID patients that had been left unstimulated or stimulated with PMA and ionomycin, but significantly increased in patient blood following stimulation with anti-CD3 and anti–CD28 antibodies ($p = 0.02$, **Figure 6.13**). Again, no significant differences were detected when results from patients with only infections were considered separately from those of patients with infections and complications.

Thus, frequencies of TNFα$^+$ T cells and MAIT cells were found to be significantly higher in CVID patients in comparison with controls following stimulation with anti-CD3 and anti-CD28 antibodies, regardless of their complication status.

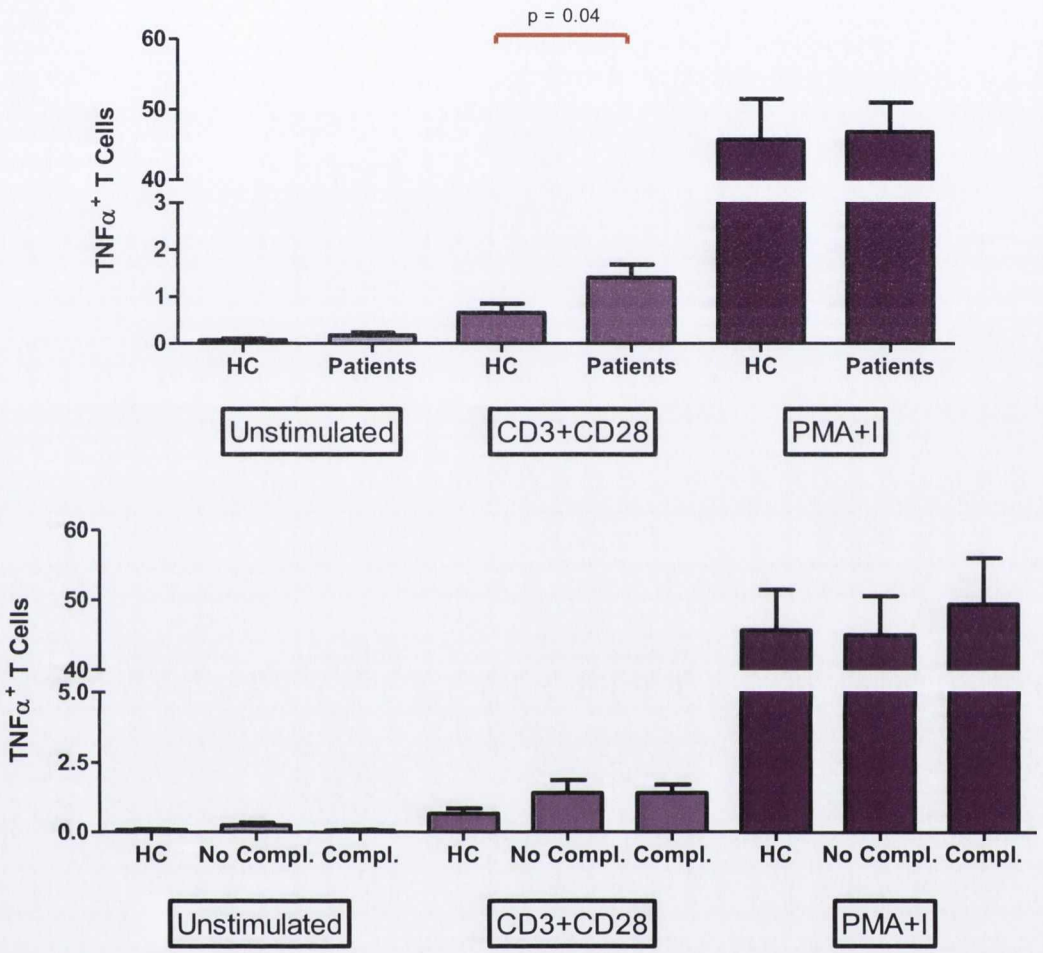


Figure 6.12. Frequencies of TNFα$^+$ T cells in unstimulated and stimulated blood from healthy controls and CVID patients. Whole blood was left unstimulated or stimulated for 8 hours with anti-CD3 and anti-CD28 antibodies (CD3+CD28) or PMA and ionomycin (PMA+I), in the presence of brefeldin A. Unstimulated and stimulated samples were then analysed by flow cytometry, detecting MAIT cells as CD3$^+$ events. In the top graph, frequencies of TNFα-producing T cells were assessed in samples from healthy controls (HC, n = 6) and CVID patients (Patients, n = 12). In the bottom graph, CVID patients were divided on the basis of their complication status, in a group affected by infections only (No Compl., n = 7) and one affected by infections and complications (Compl., n = 5). Results are expressed as means ± SEM. Statistical analysis was performed using a two-tailed Mann-Whitney test (top) or a Kruskal-Wallis test plus Dunn's post hoc test (bottom).

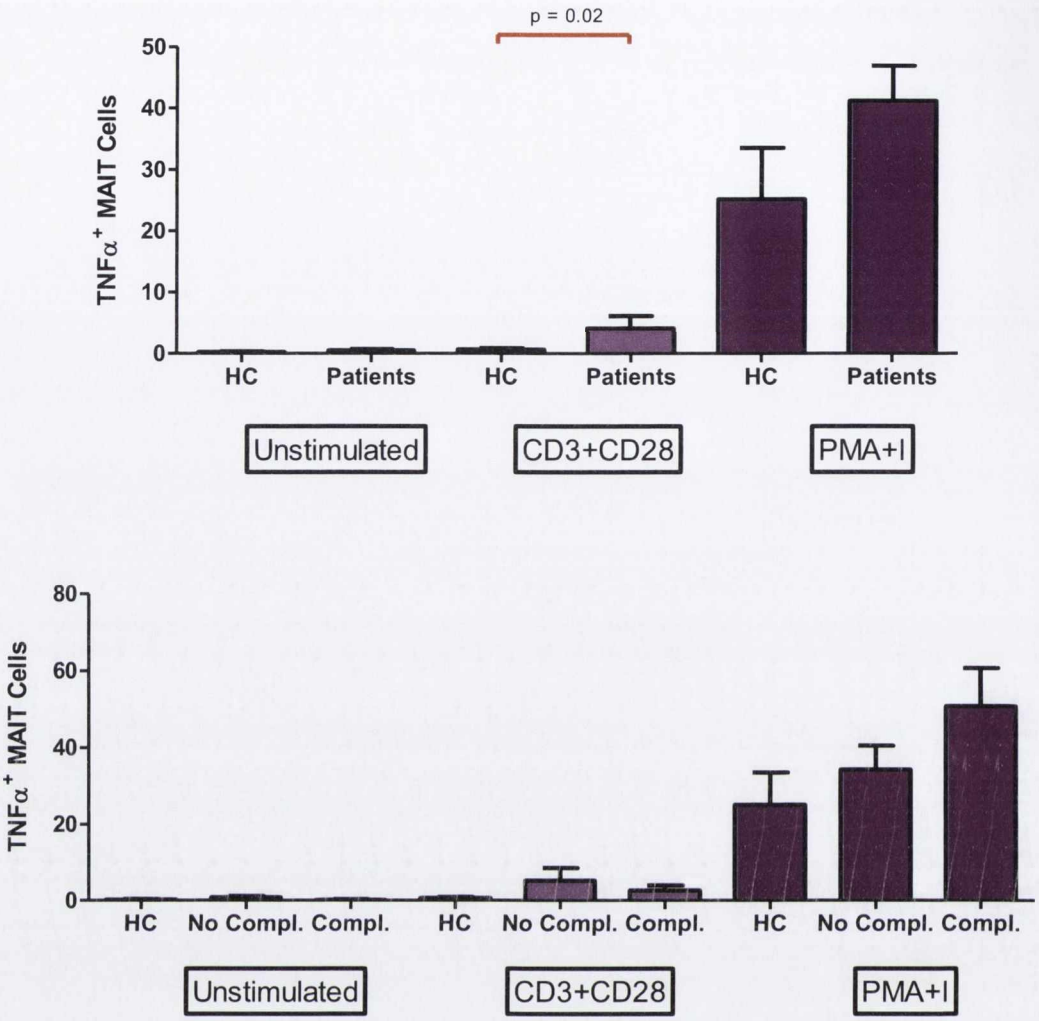


Figure 6.13. Frequencies of TNFα$^+$ MAIT cells in unstimulated and stimulated blood from healthy controls and CVID patients. Whole blood was left unstimulated or stimulated for 8 hours with anti-CD3 and anti-CD28 antibodies (CD3+CD28) or PMA and ionomycin (PMA+I), in the presence of brefeldin A. Unstimulated and stimulated samples were then analysed by flow cytometry, detecting MAIT cells as CD3$^+$ Vα7.2$^+$ CD161^{high} events. In the top graph, frequencies of TNFα-producing MAIT cells were assessed in samples from healthy controls (HC, n = 6) and CVID patients (Patients, n = 12). In the bottom graph, CVID patients were divided on the basis of their complication status, in a group affected by infections only (No Compl., n = 7) and one affected by infections and complications (Compl., n = 5). Results are expressed as means ± SEM. Statistical analysis was performed using a two-tailed Mann-Whitney test (top) or a Kruskal-Wallis test plus Dunn's post hoc test (bottom).

6.4.2 – Production of IFNγ by T cells and MAIT cells following *in vitro* stimulation

In order to produce the data presented here, whole blood from healthy donors and CVID patients was left unstimulated or stimulated with either anti-CD3 and anti-CD28 antibodies or PMA and ionomycin. After 8 hours of incubation in the presence of brefeldin A and

staining with an appropriate panel of antibodies, IFNγ was detected intracellularly by flow cytometry. **Figure 6.14** shows flow cytometry dot plots representative of IFNγ production by unstimulated and stimulated T cells and MAIT cells. See chapter 6.4.1 for examples of the FMOs used in this series of experiments.

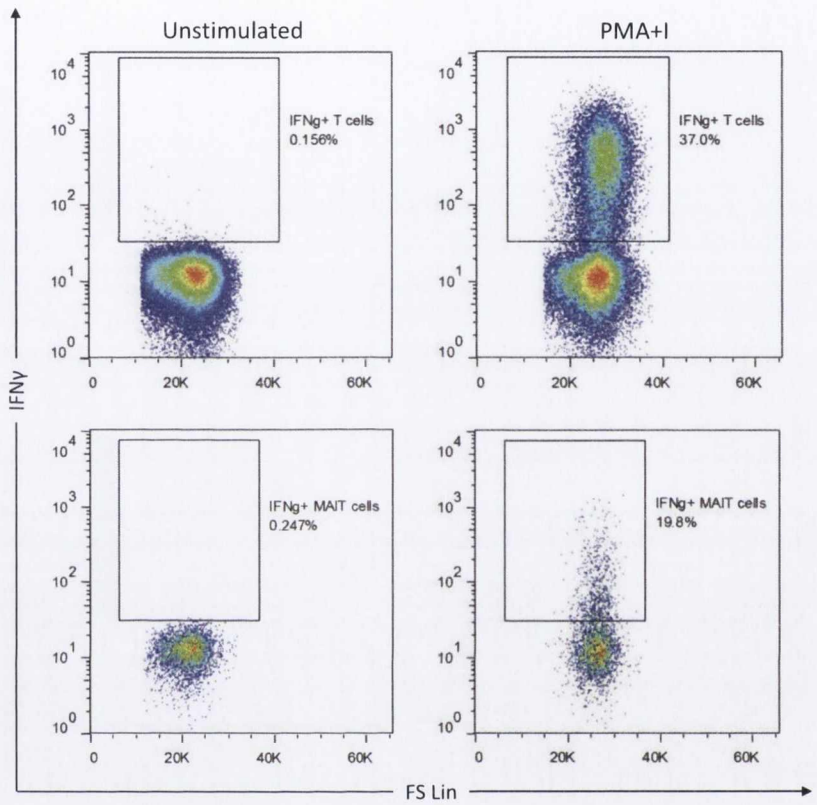


Figure 6.14. Flow cytometry dot plots representative of IFNγ production by T and MAIT cells. Whole blood samples were left unstimulated or stimulated for 8 hours with anti-CD3 and anti-CD28 antibodies or PMA and ionomycin (PMA+I), in the presence of brefeldin A. The gates in the dot plots define the frequencies of $IFN\gamma^+$ T cells (top, following gating on $CD3^+$ cells) and MAIT cells (bottom, following gating on $CD3^+$ $V\alpha7.2^+$ $CD161^{high}$ events). This image is representative of the staining pattern observed for 6 healthy donors and 12 CVID patients.

No significant differences were observed in the frequencies of T cells producing IFNγ in unstimulated and stimulated blood from healthy controls and CVID patients, neither when patients were considered as one group, nor when they were divided by complication status (**Figure 6.15**).

Likewise, frequencies of $IFN\gamma^+$ MAIT cells were comparable in unstimulated and stimulated blood from healthy controls and CVID patients, both when patients were considered as one cohort and after their separation according to complication status (**Figure 6.16**).

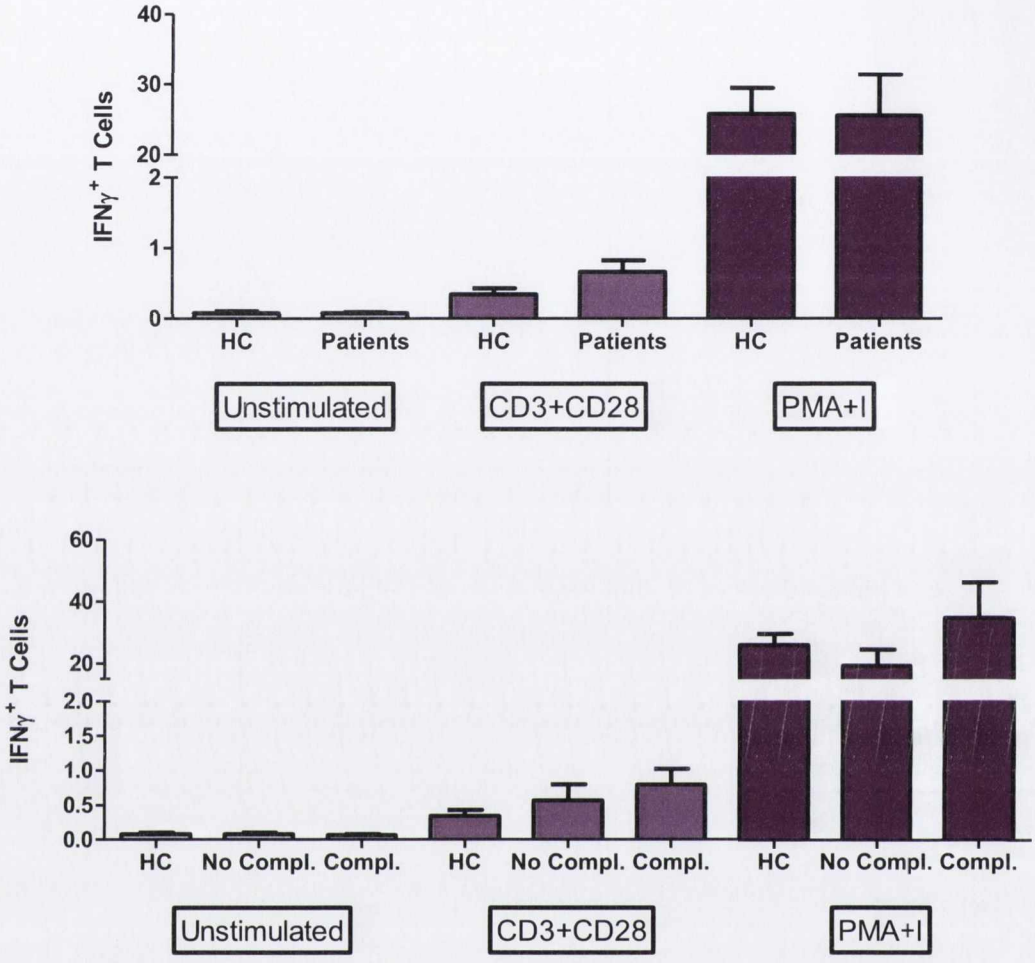


Figure 6.15. Frequencies of IFNγ$^+$ T cells in unstimulated and stimulated blood from healthy controls and CVID patients. Whole blood was left unstimulated or stimulated for 8 hours with anti-CD3 and anti-CD28 antibodies (CD3+CD28) or PMA and ionomycin (PMA+I), in the presence of brefeldin A. Unstimulated and stimulated samples were then analysed by flow cytometry, detecting MAIT cells as CD3$^+$ events. In the top graph, frequencies of IFNγ-producing T cells were assessed in samples from healthy controls (HC, n = 6) and CVID patients (Patients, n = 12). In the bottom graph, CVID patients were divided on the basis of their complication status, in a group affected by infections only (No Compl., n = 7) and one affected by infections and complications (Compl., n = 5). Results are expressed as means ± SEM. Statistical analysis was performed using a two-tailed Mann-Whitney test (top) or a Kruskal-Wallis test plus Dunn's post hoc test (bottom).

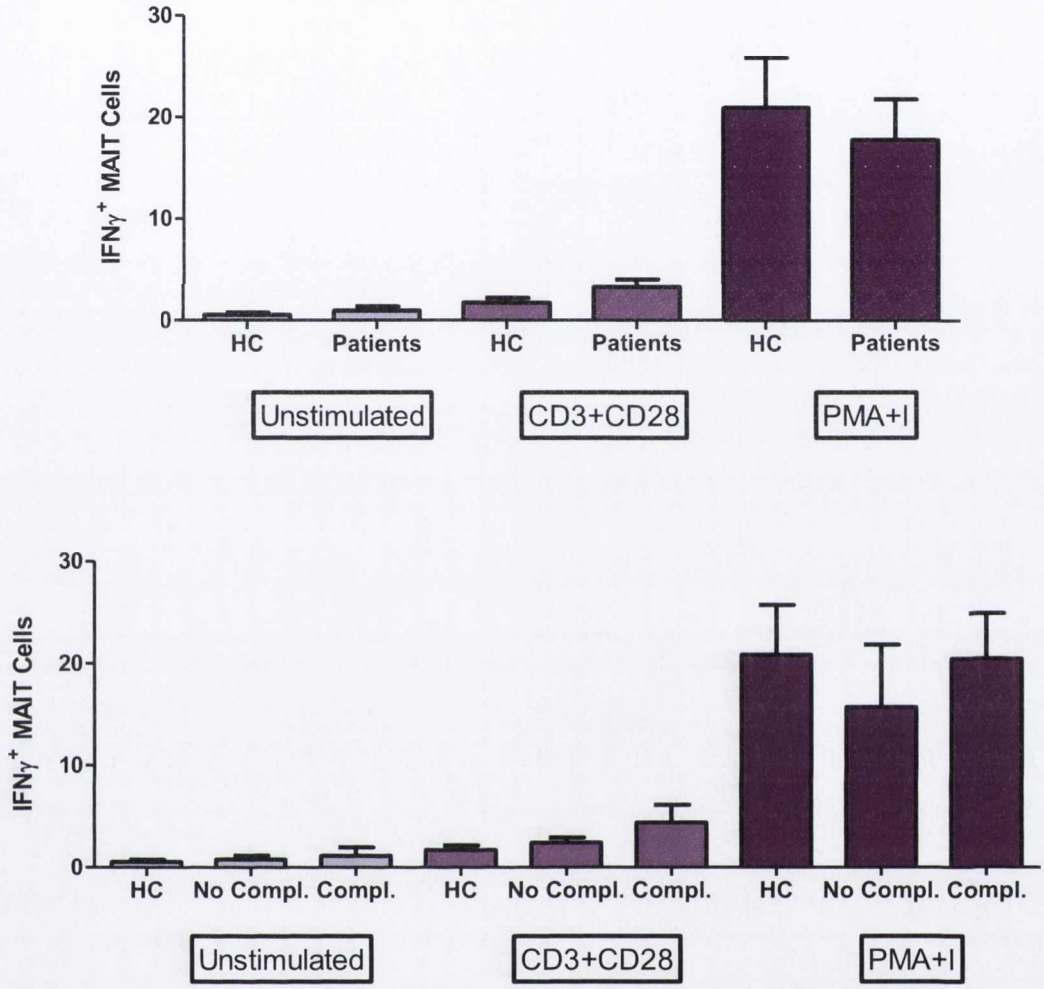


Figure 6.16. Frequencies of IFNγ$^+$ MAIT cells in unstimulated and stimulated blood from healthy controls and CVID patients. Whole blood was left unstimulated or stimulated for 8 hours with anti-CD3 and anti-CD28 antibodies (CD3+CD28) or PMA and ionomycin (PMA+I), in the presence of brefeldin A. Unstimulated and stimulated samples were then analysed by flow cytometry, detecting MAIT cells as CD3$^+$ Vα7.2$^+$ CD161^{high} events. In the top graph, frequencies of IFNγ-producing MAIT cells were assessed in samples from healthy controls (HC, n = 6) and CVID patients (Patients, n = 12). In the bottom graph, CVID patients were divided on the basis of their complication status, in a group affected by infections only (No Compl., n = 7) and one affected by infections and complications (Compl., n = 5). Results are expressed as means ± SEM. Statistical analysis was performed using a two-tailed Mann-Whitney test (top) or a Kruskal-Wallis test plus Dunn's post hoc test (bottom).

6.4.3 – Production of IL-4 by T cells and MAIT cells following *in vitro* stimulation

The data presented here were produced by leaving whole blood from healthy donors and CVID patients unstimulated or by stimulating it with either anti-CD3 and anti-CD28 antibodies or PMA and ionomycin. After 8 hours of incubation in the presence of brefeldin A and staining with an appropriate panel of antibodies, IL-4 was detected intracellularly by flow cytometry. **Figure 6.17** shows flow cytometry dot plots representative of IL-4 production by unstimulated and stimulated T cells and MAIT cells; see chapter 6.4.1 for examples of the FMOs used in this series of experiments.

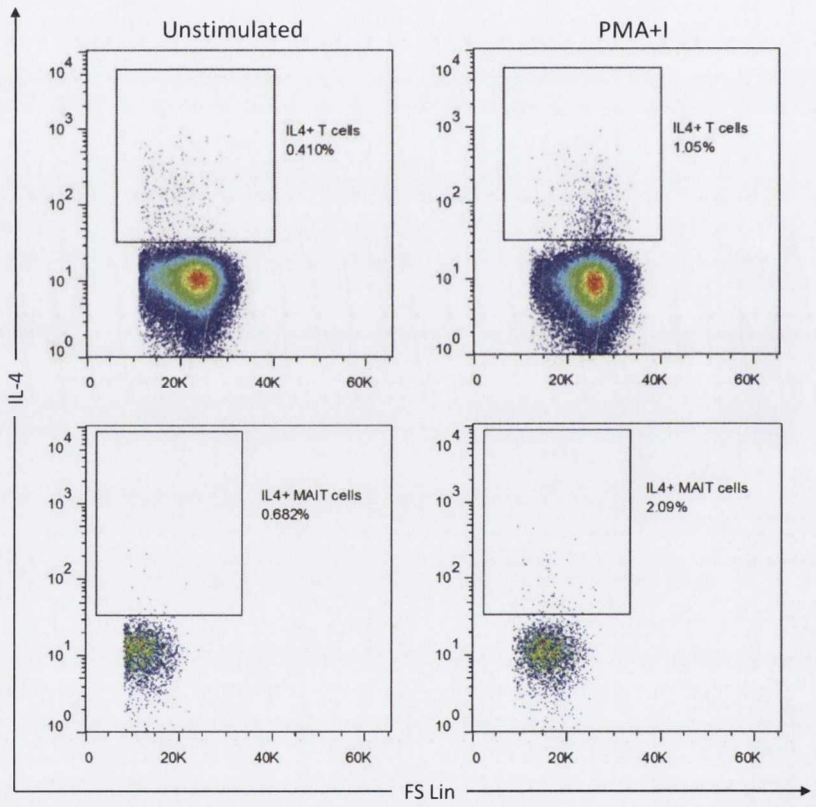


Figure 6.17. Flow cytometry dot plots representative of IL-4 production by T and MAIT cells. Whole blood samples were left unstimulated or stimulated for 8 hours with anti-CD3 and anti-CD28 antibodies or PMA and ionomycin (PMA+I), in the presence of brefeldin A. The gates in the dot plots define the frequencies of IL-4$^+$ T cells (top, following gating on CD3$^+$ cells) and MAIT cells (bottom, following gating on CD3$^+$ Vα7.2$^+$ CD161^{high} events). This image is representative of the staining pattern observed for 6 healthy donors and 12 CVID patients.

Frequencies of T cells producing IL-4 in unstimulated and stimulated blood from healthy controls and CVID patients were similar, both when patients were considered as a single group, and when they were divided according to complication status (**Figure 6.18**).

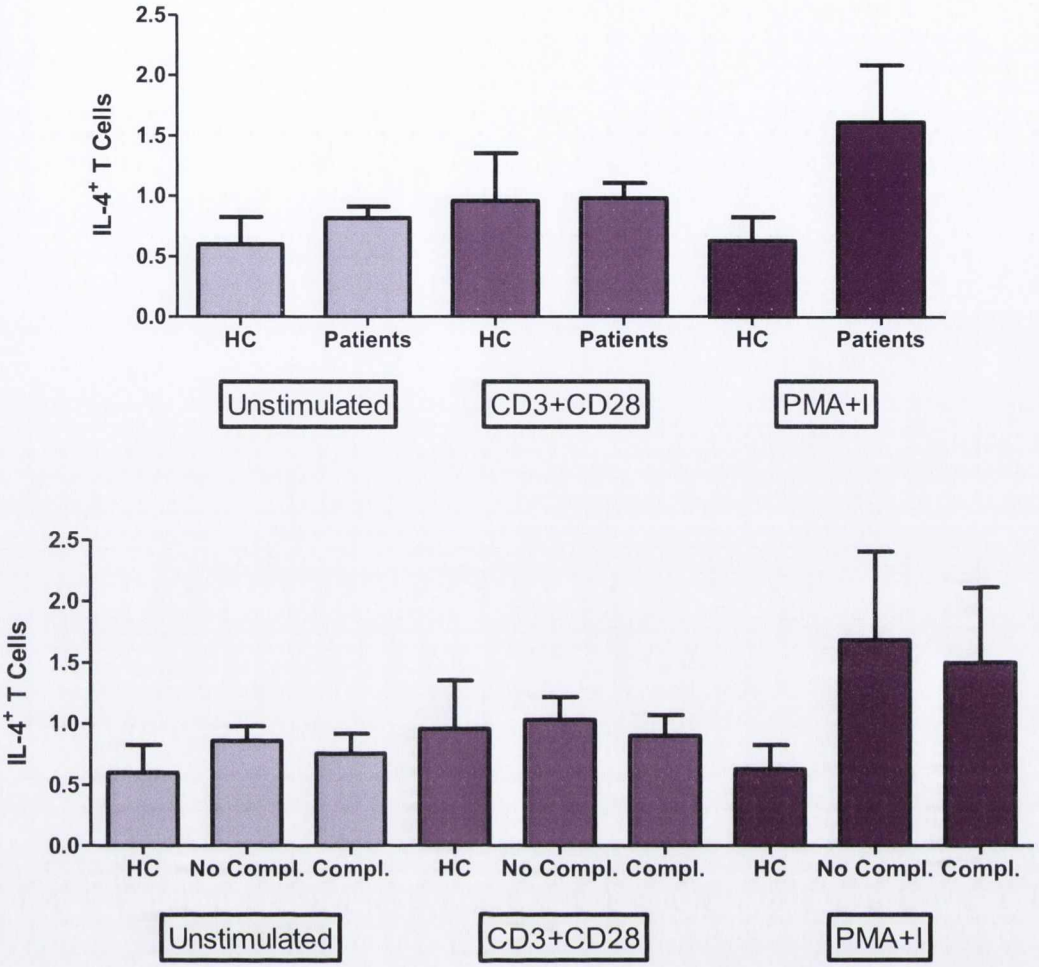


Figure 6.18. Frequencies of IL-4$^+$ T cells in unstimulated and stimulated blood from healthy controls and CVID patients. Whole blood was left unstimulated or stimulated for 8 hours with anti-CD3 and anti-CD28 antibodies (CD3+CD28) or PMA and ionomycin (PMA+I), in the presence of brefeldin A. Unstimulated and stimulated samples were then analysed by flow cytometry, detecting MAIT cells as CD3$^+$ events. In the top graph, frequencies of IL-4-producing T cells were assessed in samples from healthy controls (HC, n = 6) and CVID patients (Patients, n = 12). In the bottom graph, CVID patients were divided on the basis of their complication status, in a group affected by infections only (No Compl., n = 7) and one affected by infections and complications (Compl., n = 5). Results are expressed as means ± SEM. Statistical analysis was performed using a two-tailed Mann-Whitney test (top) or a Kruskal-Wallis test plus Dunn's post hoc test (bottom).

Frequencies of IL4$^+$ MAIT cells were comparable in blood from healthy controls and CVID patients left unstimulated or stimulated with anti-CD3 and anti-CD28 antibodies; they were however found to be significantly increased ($p = 0.001$) in blood from CVID patients treated with PMA and ionomycin in comparison to healthy controls (**Figure 6.19**). After separation of the CVID cohort in patients with and without complications, both groups of patients seemed to be responsible for this effect ($p < 0.01$ for patients without complications, $p < 0.05$ for patients with complications).

Thus, frequencies of IL-4$^+$ T cells were comparable in blood samples from CVID patients and healthy donors, while those of IL-4$^+$ MAIT cells appeared to be increased in samples from CVID patients, and were in particular significantly increased in samples stimulated with PMA and ionomycin.

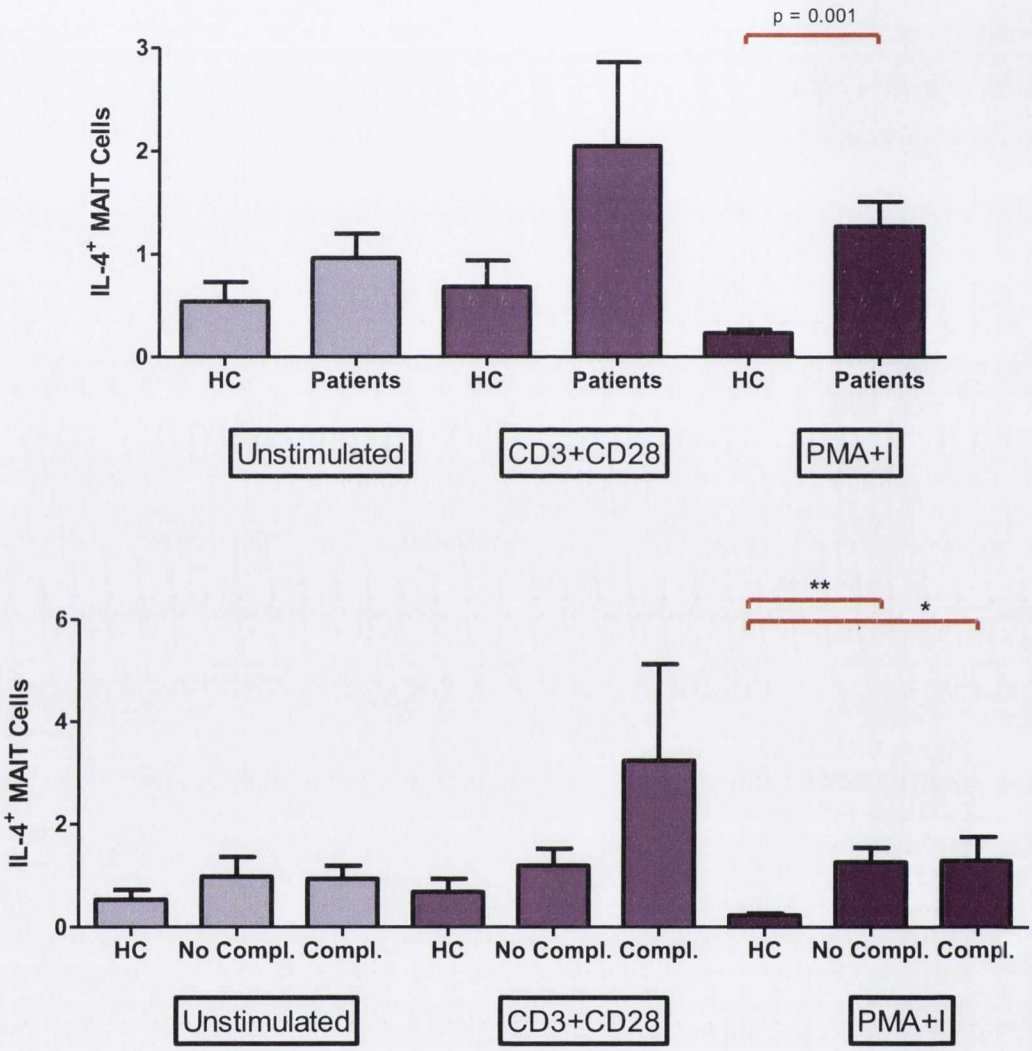


Figure 6.19. Frequencies of IL-4$^+$ MAIT cells in unstimulated and stimulated blood from healthy controls and CVID patients. Whole blood was left unstimulated or stimulated for 8 hours with anti-CD3 and anti-CD28 antibodies (CD3+CD28) or PMA and ionomycin (PMA+I), in the presence of brefeldin A. Unstimulated and stimulated samples were then analysed by flow cytometry, detecting MAIT cells as CD3$^+$ Vα7.2$^+$ CD161^{high} events. In the top graph, frequencies of IL-4-producing MAIT cells were assessed in samples from healthy controls (HC, n = 6) and CVID patients (Patients, n = 12). In the bottom graph, CVID patients were divided on the basis of their complication status, in a group affected by infections only (No Compl., n = 7) and one affected by infections and complications (Compl., n = 5). Results are expressed as means ± SEM. Statistical analysis was performed using a two-tailed Mann-Whitney test (top) or a Kruskal-Wallis test plus Dunn's post hoc test (bottom). * $p < 0.05$; ** $p < 0.01$.

6.4.4 – Production of IL-10 by T cells and MAIT cells following *in vitro* stimulation

These experiments were performed by leaving whole blood from healthy donors and CVID patients unstimulated or by stimulating it with either anti-CD3 and anti-CD28 antibodies or PMA and ionomycin. After 8 hours of incubation in the presence of brefeldin A and staining with an appropriate panel of antibodies, IL-10 was detected intracellularly by flow cytometry. **Figure 6.20** shows flow cytometry dot plots representative of IL-10 production by unstimulated and stimulated T cells and MAIT cells; see chapter 6.4.1 for examples of the FMOs used in this series of experiments.

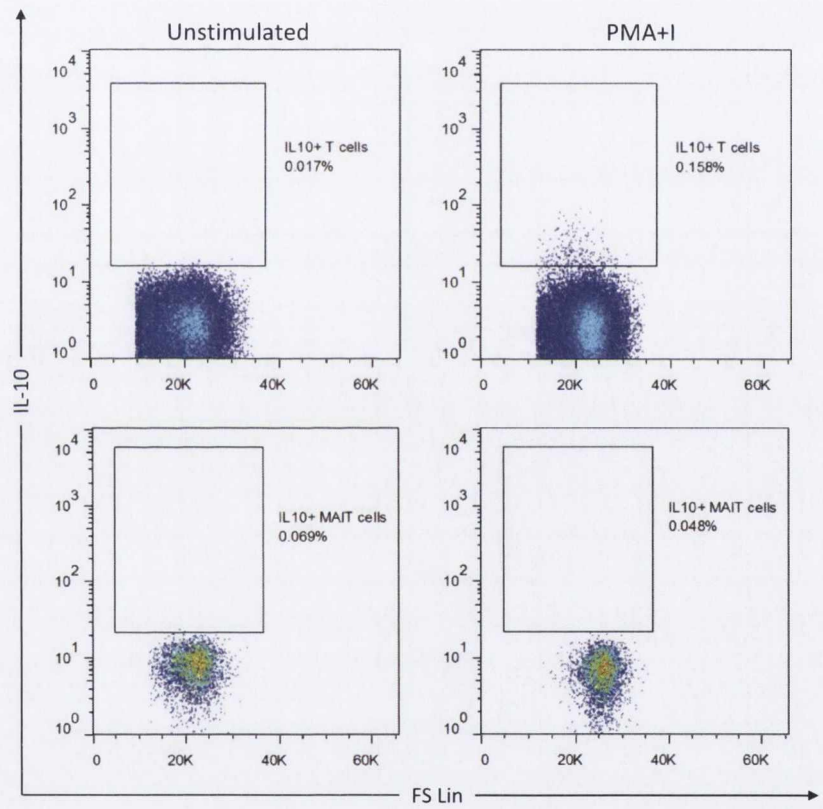


Figure 6.20. Flow cytometry dot plots representative of IL-10 production by T and MAIT cells. Whole blood samples were left unstimulated or stimulated for 8 hours with anti-CD3 and anti-CD28 antibodies or PMA and ionomycin (PMA+I), in the presence of brefeldin A. The gates in the dot plots define the frequencies of IL-10$^+$ T cells (top, following gating on CD3$^+$ cells) and MAIT cells (bottom, following gating on CD3$^+$ Vα7.2$^+$ CD161^{high} events). This image is representative of the staining pattern observed for 6 healthy donors and 12 CVID patients.

IL-10-producing T cells were found at comparable low frequencies in the unstimulated and stimulated blood of healthy controls and CVID patients; no significant differences were

uncovered when the results for CVID patients with infections only were considered separately from those for patients with complications (**Figure 6.21**).

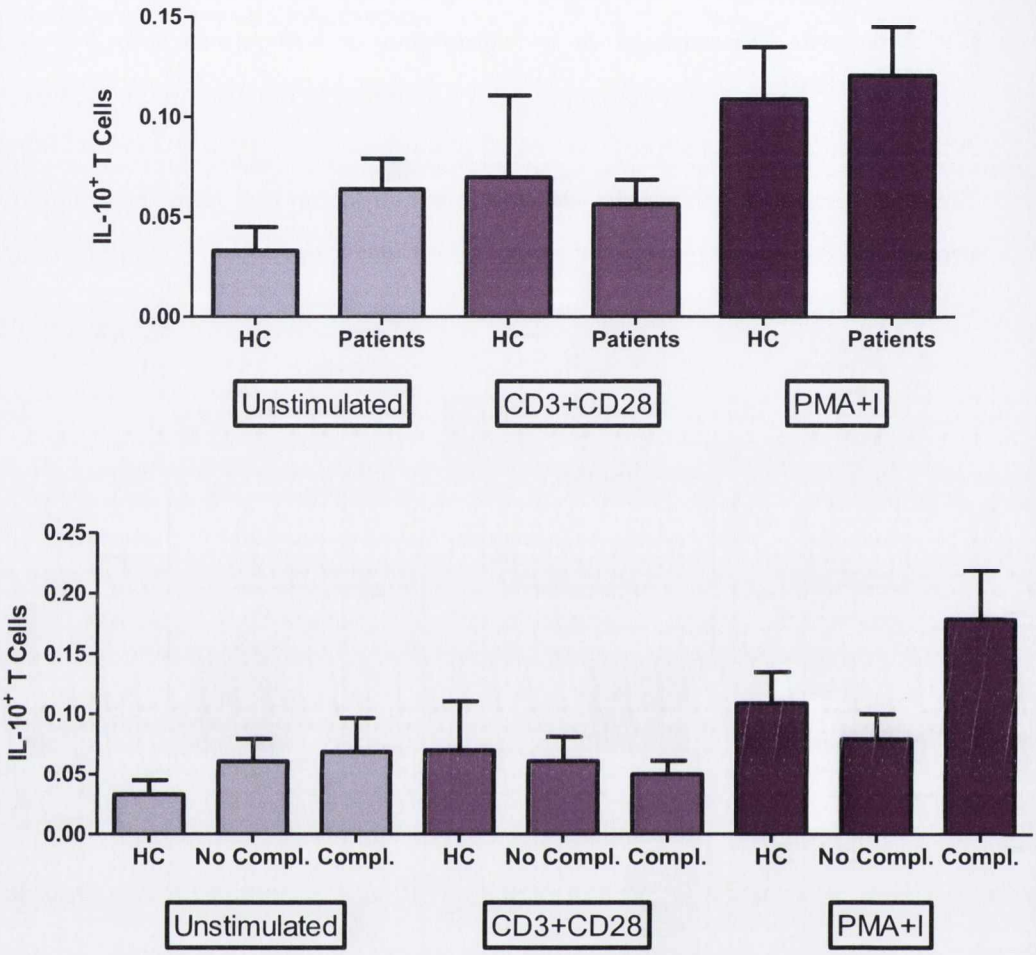


Figure 6.21. Frequencies of IL-10$^+$ T cells in unstimulated and stimulated blood from healthy controls and CVID patients. Whole blood was left unstimulated or stimulated for 8 hours with anti-CD3 and anti-CD28 antibodies (CD3+CD28) or PMA and ionomycin (PMA+I), in the presence of brefeldin A. Unstimulated and stimulated samples were then analysed by flow cytometry, detecting MAIT cells as CD3$^+$ events. In the top graph, frequencies of IL-10-producing T cells were assessed in samples from healthy controls (HC, n = 6) and CVID patients (Patients, n = 12). In the bottom graph, CVID patients were divided on the basis of their complication status, in a group affected by infections only (No Compl., n = 7) and one affected by infections and complications (Compl., n = 5). Results are expressed as means ± SEM. Statistical analysis was performed using a two-tailed Mann-Whitney test (top) or a Kruskal-Wallis test plus Dunn's post hoc test (bottom).

Frequencies of IL-10$^+$ MAIT cells were also low and not significantly different between healthy controls and CVID patients in any of the conditions studied, however cells producing this cytokine seemed to be detected at higher percentages in patient blood stimulated with anti-CD3 and anti-CD28 antibodies (**Figure 6.22**). Division of the CVID cohort in two groups, one for patients with infections only and the second for patients with infections and

complications, revealed a significant increase in the frequencies of IL-10$^+$ MAIT cells only in the latter ($p < 0.05$ in comparison to both patients with infections and to healthy controls).

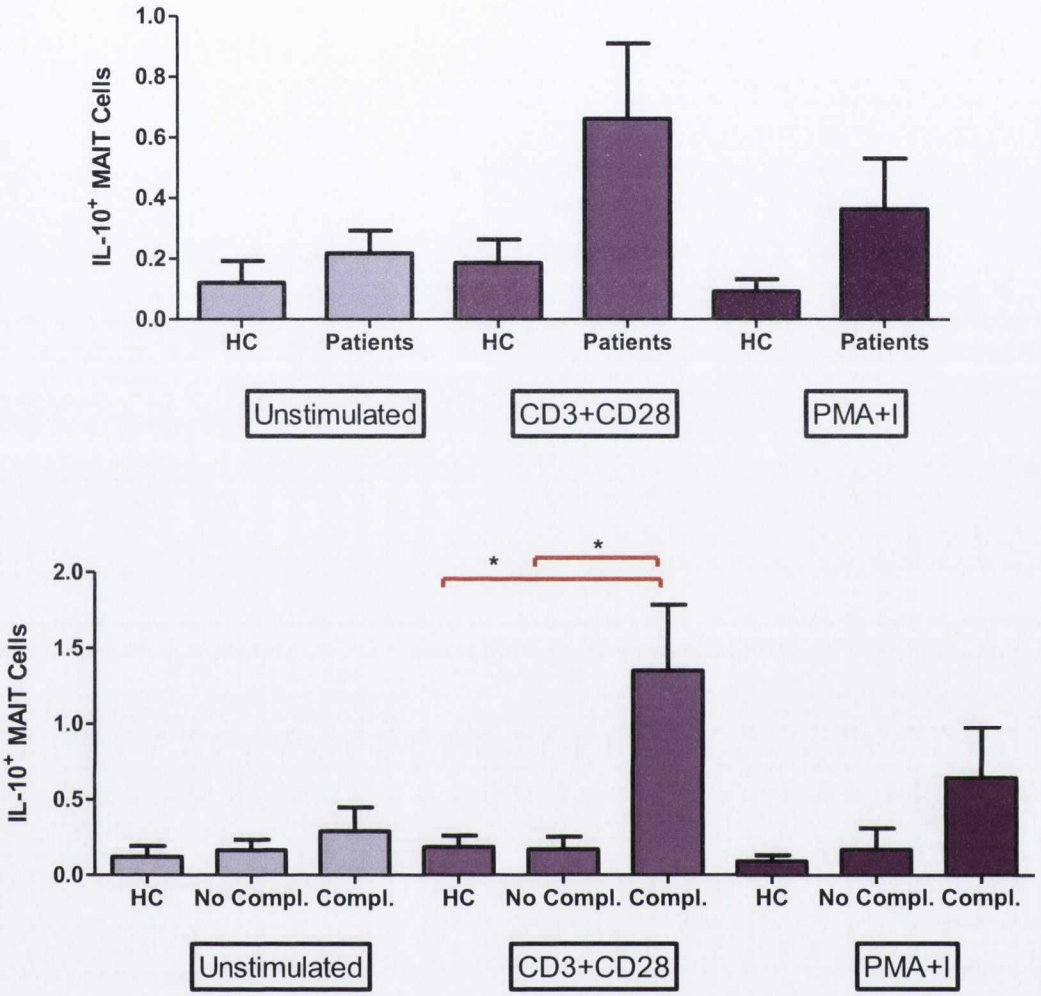


Figure 6.22. Frequencies of IL-10$^+$ MAIT cells in unstimulated and stimulated blood from healthy controls and CVID patients. Whole blood was left unstimulated or stimulated for 8 hours with anti-CD3 and anti-CD28 antibodies (CD3+CD28) or PMA and ionomycin (PMA+I), in the presence of brefeldin A. Unstimulated and stimulated samples were then analysed by flow cytometry, detecting MAIT cells as CD3$^+$ Vα7.2$^+$ CD161^{high} events. In the top graph, frequencies of IL-10-producing MAIT cells were assessed in samples from healthy controls (HC, n = 6) and CVID patients (Patients, n = 12). In the bottom graph, CVID patients were divided on the basis of their complication status, in a group affected by infections only (No Compl., n = 7) and one affected by infections and complications (Compl., n = 5). Results are expressed as means ± SEM. Statistical analysis was performed using a two-tailed Mann-Whitney test (top) or a Kruskal-Wallis test plus Dunn's post hoc test (bottom). * $p < 0.05$.

6.4.5 – Production of IL-17A by T cells and MAIT cells following *in vitro* stimulation

In these experiments, whole blood from healthy donors and CVID patients was left unstimulated or stimulated with either anti-CD3 and anti-CD28 antibodies or PMA and ionomycin. After 8 hours of incubation in the presence of brefeldin A and staining with an appropriate panel of antibodies, IL-17A was detected intracellularly by flow cytometry. **Figure 6.23** shows flow cytometry dot plots representative of IL-17A production by unstimulated and stimulated T cells and MAIT cells; see chapter 6.4.1 for examples of the FMOs used in this series of experiments.

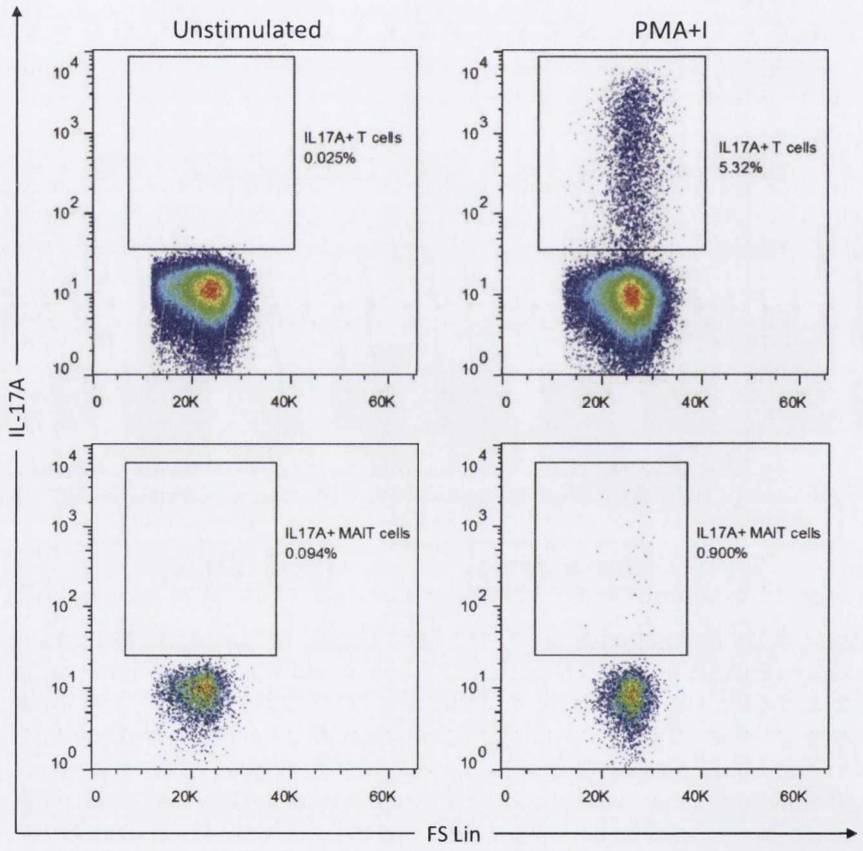


Figure 6.23. Flow cytometry dot plots representative of IL-17A production by T and MAIT cells. Whole blood samples were left unstimulated or stimulated for 8 hours with anti-CD3 and anti-CD28 antibodies or PMA and ionomycin (PMA+I), in the presence of brefeldin A. The gates in the dot plots define the frequencies of IL-17A$^+$ T cells (top, following gating on CD3$^+$ cells) and MAIT cells (bottom, following gating on CD3$^+$ Vα7.2$^+$ CD161^{high} events). This image is representative of the staining pattern observed for 6 healthy donors and 12 CVID patients.

Frequencies of IL-17A$^+$ T cells were significantly higher in unstimulated blood from CVID patients than in blood from controls ($p = 0.03$), but similar between the two groups

when blood was stimulated with either anti-CD3 and anti-CD28 antibodies or PMA and ionomycin (**Figure 6.24**). When considering CVID patients with only infections separately from patients with complications, higher frequencies of these cells were noted in the former, but not in the latter, in comparison to healthy controls ($p < 0.05$).

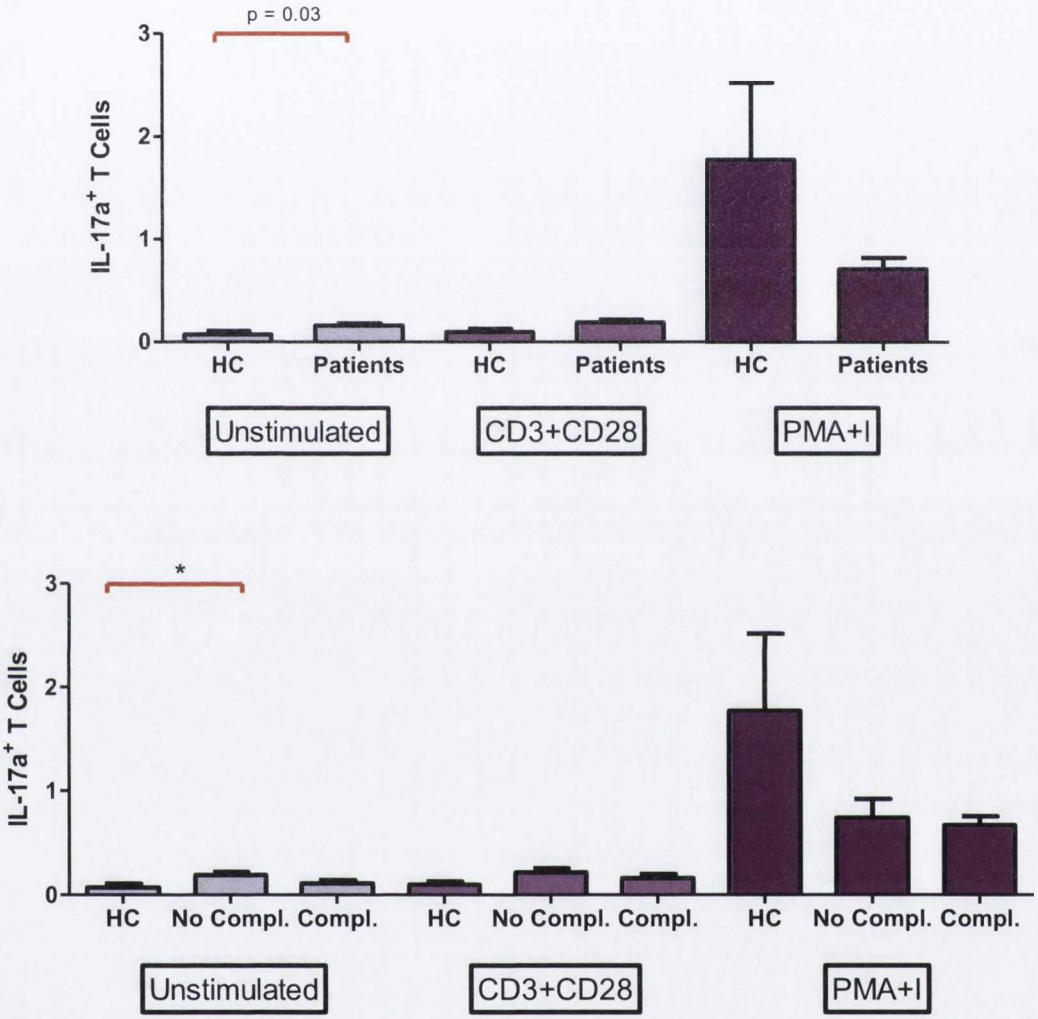


Figure 6.24. Frequencies of IL-17A$^+$ T cells in unstimulated and stimulated blood from healthy controls and CVID patients. Whole blood was left unstimulated or stimulated for 8 hours with anti-CD3 and anti-CD28 antibodies (CD3+CD28) or PMA and ionomycin (PMA+I), in the presence of brefeldin A. Unstimulated and stimulated samples were then analysed by flow cytometry, detecting MAIT cells as CD3$^+$ events. In the top graph, frequencies of IL-17A-producing T cells were assessed in samples from healthy controls (HC, n = 6) and CVID patients (Patients, n = 12). In the bottom graph, CVID patients were divided on the basis of their complication status, in a group affected by infections only (No Compl., n = 7) and one affected by infections and complications (Compl., n = 5). Results are expressed as means ± SEM. Statistical analysis was performed using a two-tailed Mann-Whitney test (top) or a Kruskal-Wallis test plus Dunn's post hoc test (bottom). * $p < 0.05$.

When IL-17A$^+$ MAIT cells were investigated, it was found that their frequencies were significantly raised in blood from CVID patients stimulated with anti-CD3 and anti-CD28

antibodies in comparison to similarly treated blood from healthy controls ($p = 0.01$); in fact, IL-17A$^+$ MAIT cells also seemed more frequent, although not significantly so, in unstimulated and PMA and ionomycin-stimulated patient blood (**Figure 6.25**). Categorization of patients as infections only or infections plus complications revealed that both patient groups exhibited higher frequencies of IL-17A-producing MAIT cells following antibody-mediated stimulation, although this increase was only significant for patients with complicated CVID ($p < 0.05$).

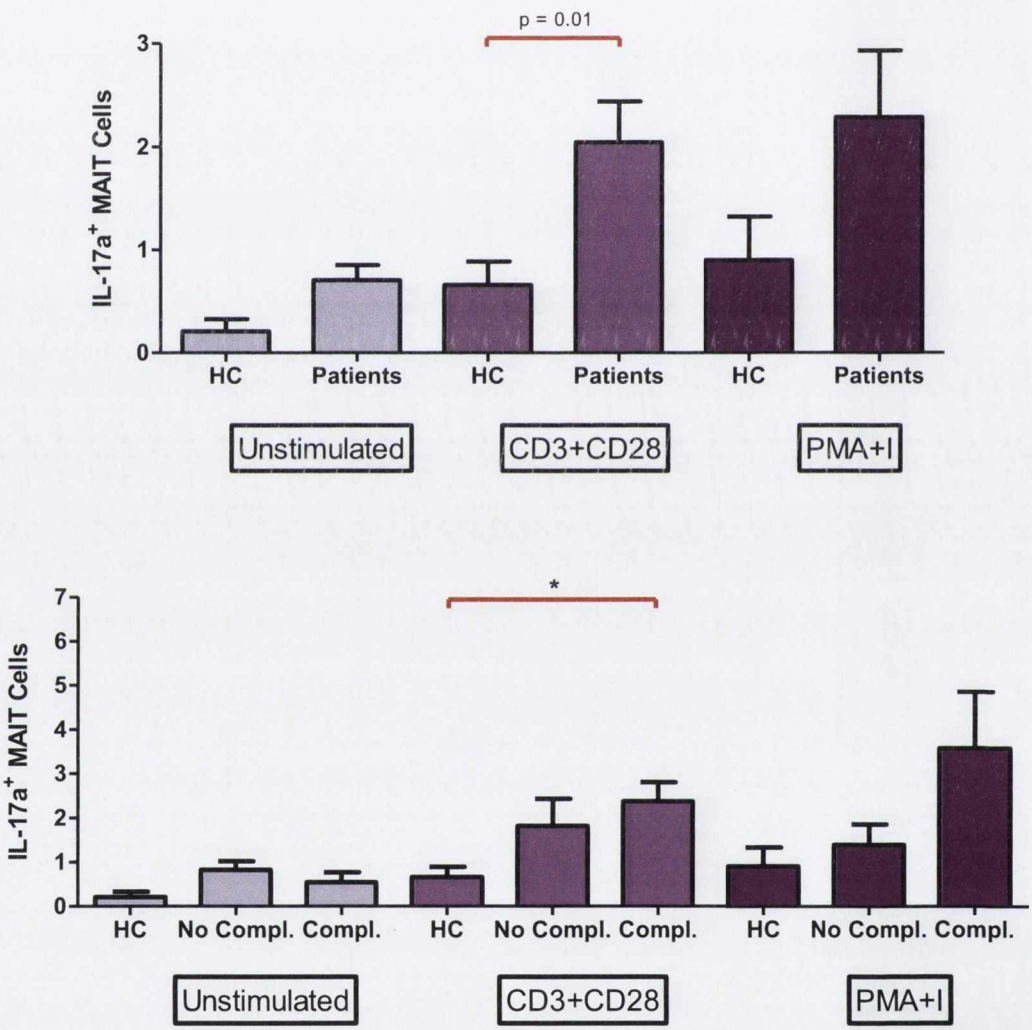


Figure 6.25. Frequencies of IL-17A$^+$ MAIT cells in unstimulated and stimulated blood from healthy controls and CVID patients. Whole blood was left unstimulated or stimulated for 8 hours with anti-CD3 and anti-CD28 antibodies (CD3+CD28) or PMA and ionomycin (PMA+I), in the presence of brefeldin A. Unstimulated and stimulated samples were then analysed by flow cytometry, detecting MAIT cells as CD3$^+$ Vα7.2$^+$ CD161^{high} events. In the top graph, frequencies of IL-17A-producing MAIT cells were assessed in samples from healthy controls (HC, n = 6) and CVID patients (Patients, n = 12). In the bottom graph, CVID patients were divided on the basis of their complication status, in a group affected by infections only (No Compl., n = 7) and one affected by infections and complications (Compl., n = 5). Results are expressed as means ± SEM. Statistical analysis was performed using a two-tailed Mann-Whitney test (top) or a Kruskal-Wallis test plus Dunn's post hoc test (bottom). * $p < 0.05$.

Thus, frequencies of IL-17A$^+$ T cells were slightly but significantly increased in blood samples from CVID patients in comparison to healthy donors. Frequencies of IL-17A$^+$ MAIT cells were significantly higher in blood from CVID patients stimulated with anti-CD3 and anti-CD28 antibodies in comparison to healthy control, and generally appeared increased in all conditions tested.

6.4.6 – Production of IL-22 by T cells and MAIT cells following *in vitro* stimulation

The data collected here were produced by leaving whole blood from healthy donors and CVID patients unstimulated or stimulating it with either anti-CD3 and anti-CD28 antibodies or PMA and ionomycin. After 8 hours of incubation in the presence of brefeldin A and staining with an appropriate panel of antibodies, IL-22 was detected intracellularly by flow cytometry. **Figure 6.26** shows flow cytometry dot plots representative of IL-22 production by unstimulated and stimulated T cells and MAIT cells; see chapter 6.4.1 for examples of the FMOs used in this series of experiments. As noticeable, staining for IL-22 could only detect low numbers of positive events; additionally, these positive events did not manifest at high fluorescence intensities in flow cytometry plots.

When considering the frequencies of IL-22-producing T cells, no differences were observed between healthy controls and CVID patients in samples of unstimulated or stimulated blood, regardless of the stimuli used (**Figure 6.27**). No additional significances were observed when patients were divided on the basis of their complication status in patients with infections only and patients with complications.

As shown in **Figure 6.28**, frequencies of IL-22$^+$ MAIT cells were comparable in unstimulated blood from healthy controls and CVID patients, however they were found at significantly higher frequencies in blood from CVID patients stimulated with either anti-CD3 and anti-CD28 antibodies ($p = 0.01$) or PMA and ionomycin ($p = 0.005$). When CVID patients with infections only and with complications were considered separately, both groups displayed high frequencies of IL-22$^+$ MAIT cells following antibody-mediated stimulation, although not significantly higher than those found in healthy controls. On the other hand, only patients with complications exhibited significantly higher percentages of this population in comparison to healthy controls upon stimulation with PMA and ionomycin ($p < 0.01$).

Thus, frequencies of IL-22$^+$ T cells were comparable in CVID patients and healthy controls in all conditions tested. Frequencies of IL-22$^+$ MAIT cells, on the other hand, were significantly increased in the blood of CVID patients in comparison to healthy donors following stimulation with anti-CD3 and anti-CD28 antibodies and PMA and ionomycin.

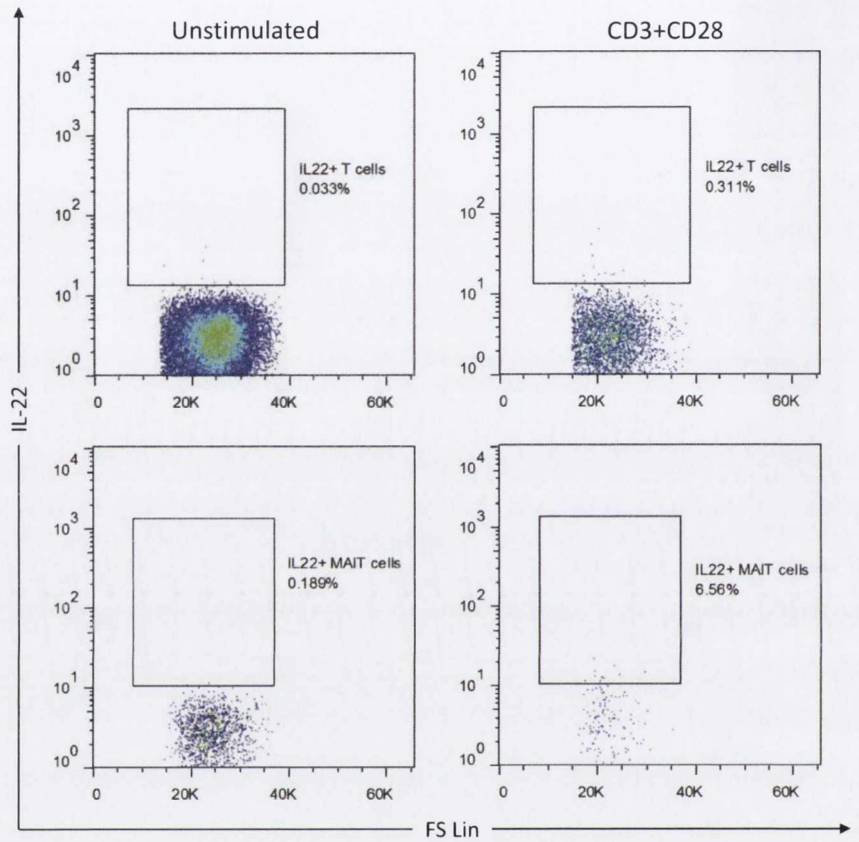


Figure 6.26. Flow cytometry dot plots representative of IL-22 production by T and MAIT cells. Whole blood samples were left unstimulated or stimulated for 8 hours with anti-CD3 and anti-CD28 antibodies or PMA and ionomycin (PMA+I), in the presence of brefeldin A. The gates in the dot plots define the frequencies of IL-22$^+$ T cells (top, following gating on CD3$^+$ cells) and MAIT cells (bottom, following gating on CD3$^+$ Vα7.2$^+$ CD161^{high} events). This image is representative of the staining pattern observed for 6 healthy donors and 12 CVID patients.

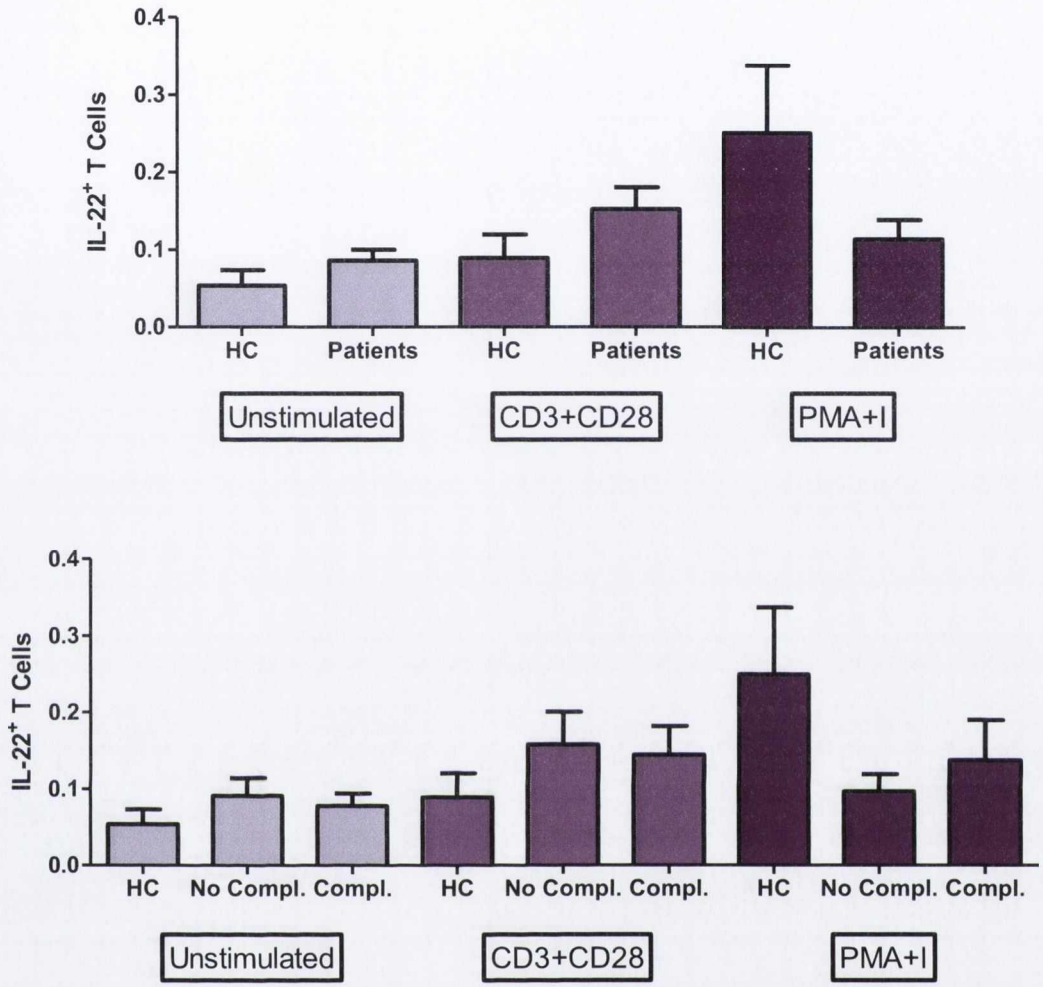


Figure 6.27. Frequencies of IL-22$^+$ T cells in unstimulated and stimulated blood from healthy controls and CVID patients. Whole blood was left unstimulated or stimulated for 8 hours with anti-CD3 and anti-CD28 antibodies (CD3+CD28) or PMA and ionomycin (PMA+I), in the presence of brefeldin A. Unstimulated and stimulated samples were then analysed by flow cytometry, detecting MAIT cells as CD3$^+$ events. In the top graph, frequencies of IL-22-producing T cells were assessed in samples from healthy controls (HC, n = 6) and CVID patients (Patients, n = 12). In the bottom graph, CVID patients were divided on the basis of their complication status, in a group affected by infections only (No Compl., n = 7) and one affected by infections and complications (Compl., n = 5). Results are expressed as means ± SEM. Statistical analysis was performed using a two-tailed Mann-Whitney test (top) or a Kruskal-Wallis test plus Dunn's post hoc test (bottom).

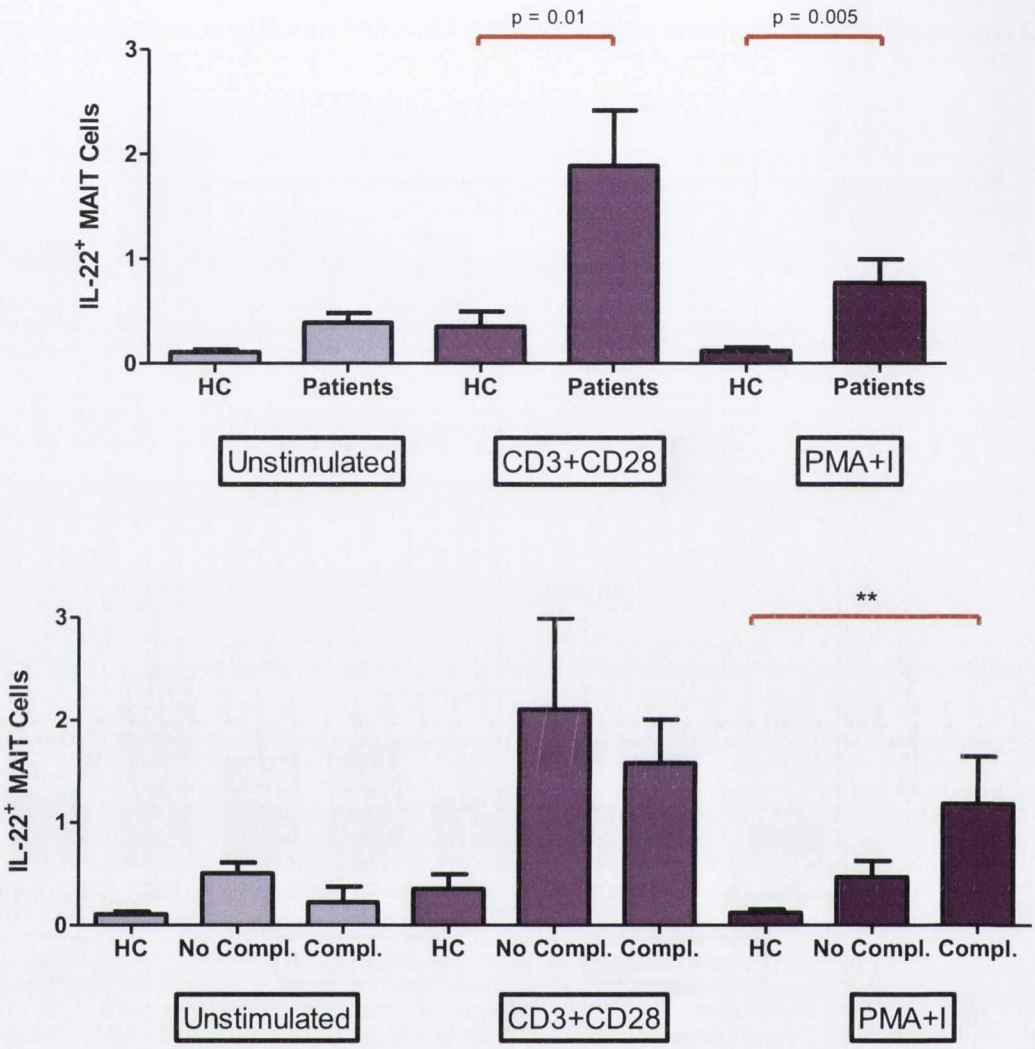


Figure 6.28. Frequencies of IL-22$^+$ MAIT cells in unstimulated and stimulated blood from healthy controls and CVID patients. Whole blood was left unstimulated or stimulated for 8 hours with anti-CD3 and anti-CD28 antibodies (CD3+CD28) or PMA and ionomycin (PMA+I), in the presence of brefeldin A. Unstimulated and stimulated samples were then analysed by flow cytometry, detecting MAIT cells as CD3$^+$ Vα7.2$^+$ CD161^{high} events. In the top graph, frequencies of IL-22-producing MAIT cells were assessed in samples from healthy controls (HC, n = 6) and CVID patients (Patients, n = 12). In the bottom graph, CVID patients were divided on the basis of their complication status, in a group affected by infections only (No Compl., n = 7) and one affected by infections and complications (Compl., n = 5). Results are expressed as means ± SEM. Statistical analysis was performed using a two-tailed Mann-Whitney test (top) or a Kruskal-Wallis test plus Dunn's post hoc test (bottom). ** $p < 0.01$.

6.5 – Discussion

Previously in this study, we found MAIT cell frequencies and absolute counts to be significantly decreased in the peripheral blood of CVID patients in comparison to controls; this was particularly noticeable in patients affected by complications (chapter 4). A study of the correlations of MAIT cell counts with those of other B and T cell subsets also suggested that numbers of this innate T cell subset correlated with those of circulating class-switched memory B cells and $CD27^-$ IgD^- B cells in CVID patients, but not in healthy donors (chapter 5). On the basis of these data, we expanded our investigation to the functional characteristics of MAIT cells from CVID patients and healthy controls, hypothesizing that this population could be involved in the development of CVID and/or its complications. More particularly, we sampled upregulation of activation markers CD69 and CD40L and production of cytokines by MAIT cells left unstimulated or stimulated *in vitro* with anti-CD3 and anti-CD28 antibodies or PMA and ionomycin. Incubation with anti-CD3 and anti-CD28 antibodies was employed in an attempt to simulate the physiological activation of MAIT cells, while PMA and ionomycin were used to induce maximal responses. In order to supply a frame of reference, our findings were presented alongside data for total T cell, the larger population of which MAIT cells are part. All results included in this chapter were produced employing a whole blood protocol, previously described in detail in chapter 2.8.4. Its use had several advantages over PBMC-based ones, including shorter preparation times, better overall cell yields and the ability to analyse unmanipulated samples.

With regard to activation markers, expression of CD40L by T cells and MAIT cells from CVID patients was found to be similar to that exhibited by healthy controls both in unstimulated and stimulated blood, regardless of the stimulus used. Expression of total (i.e. surface and intracellular) CD69 by T cells was similarly comparable in the patient and healthy donor groups. Frequencies of $CD69^+$ MAIT cells, however, were significantly increased in both unstimulated and anti-CD3/anti-CD28-stimulated blood from CVID patients in comparison to healthy controls.

As for cytokines, generation of IFNγ by T cells and MAIT cells was comparable in CVID patients and healthy controls in all conditions tested, however $TNF\alpha^+$ T cells and MAIT cells were found at significantly higher frequencies in blood from CVID patients than from healthy donors following stimulation with anti-CD3 and anti-CD28 antibodies. This increase did not appear to be specifically linked to the complication status of patients, as patients with infections only and patients with complications displayed similar frequencies of these cells. CVID patients and healthy controls exhibited similar frequencies of $IL\text{-}4^+$ T cells in both

unstimulated and unstimulated blood. Frequencies of IL-4$^+$ MAIT cells, on the contrary, were noted to be significantly increased in blood from CVID patients following stimulation with PMA and ionomycin; this was accompanied by a non-significant increase in the frequencies of MAIT cells generating IL-4 following antibody-mediated stimulation. Patients with infections only and patients with complications appeared to be equally responsible for these phenomena. IL-10$^+$ T and MAIT cells were found at similar frequencies in unstimulated and stimulated blood from CVID patients and healthy donors. Despite this, blood from patients with complications contained significantly higher frequencies of IL-10$^+$ MAIT cells than either healthy controls or patients with infections only following stimulation with anti-CD3 and anti-CD28 antibodies. Frequencies of IL-17A$^+$ and IL-22$^+$ T cells were generally similar in healthy controls and CVID patients, although unstimulated patient blood displayed a small but significant increase in the percentages of IL-17A$^+$ events. In comparison to healthy controls, percentages of IL-17A-producing MAIT cells appeared elevated in patient samples in all conditions tested, however they were found to be significantly increased only upon stimulation with anti-CD3 and anti-CD28 antibodies. After subdividing patients according to their complication status, patients with complications were largely responsible for this finding. Finally, significantly higher frequencies of IL-22$^+$ MAIT cells were noticed in blood from CVID patients stimulated with both anti-CD3 and anti-CD28 and PMA and ionomycin in comparison to healthy donors. No particular association was noted between high frequencies of IL-22-producing MAIT cells and complication status in samples treated with anti-CD3 and anti-CD28, however patients with complications exhibited significantly higher percentages of this population than healthy controls following treatment with PMA and ionomycin.

CD40L, which is expressed by activated T cells, binds to CD40, a molecule found on the surface of antigen presenting cells, including B cells. B cells respond to CD40 binding by differentiating, producing antibodies and undergoing isotype class-switching; CD40/CD40L interactions are also involved in the formation of GCs.[221] Our data suggest that CD40L expression by MAIT cells in CVID is normal, however the intensity of surface expression of CD40L and its mRNA (messenger RNA) levels have previously been found decreased in activated lymphocytes of a subgroup of CVID patients.[222] These aspects should therefore be investigated before definitively concluding that MAIT cells from these individuals are capable of normal interactions through CD40L. Additionally, surface expression of CD40 by B cells of CVID patients should be assessed.

CD69 is a short term activation marker which is normally expressed on the surface of 5-10 % of unstimulated peripheral blood lymphocytes.[223] Following stimulation of T cells, cytoplasmic stocks of this protein are rapidly translocated to the cell membrane and CD69 becomes detectable on the cell surface within 1 hour; transcription of the CD69 gene is concurrently activated, presumably to replenish intracellular reservoirs of the molecule and sustain surface presentation.[224,225] Decreased upregulation of CD69, both in terms of MFI and of mRNA production, has previously been reported for B cells from CVID patients following activation with CpG.[226] On the contrary, upregulation of CD69 by $CD4^+$ and $CD8^+$ T cells from CVID patients was previously defined to be normal after treatment with anti-CD3 and anti-CD28 antibodies.[227] A similar result was obtained upon stimulation of total $CD3^+$ cells from paediatric CVID patients with anti-CD3 antibody.[228] The data we present are based on intracellular staining of CD69, and as such include both surface and cytoplasmic CD69 expression. Due to this, any increase in the frequencies of CD69-expressing cells following stimulation reflects both the presentation of cytosolic, pre-formed CD69 and the *de novo* production of the molecule. Noticeably higher frequencies of $CD69^+$ MAIT cells, but not T cells, were however detected in unstimulated peripheral blood from CVID patients. Due to the short incubation time employed in these experiments, this points to increased availability of CD69 in these cells *in vivo*, suggesting that they are found in CVID in a state of constitutive, chronic activation.

Of all the antibodies employed for the experiments presented in this chapter, the anti-IL-22 antibody gave the least convincing staining. Indeed, not only it detected low numbers of positive events, but these positive events also did not manifest at high fluorescence intensities. As such, the data concerning the increased frequencies of IL-22^+ MAIT cells in whole blood from CVID patients stimulated with anti-CD3 and anti-CD28 antibodies should be treated with caution; this is even more so as frequencies and counts of MAIT cells as a whole have previously been shown in this thesis to be decreased in the blood of this patient population. In order to obtain more convincing data, the experiments concerned could be repeated using larger quantities of blood. Lengthening the incubation time or increasing the intensity of the antibody-mediated stimulation performed could prove challenging, as incubation of whole blood with soluble anti-CD3 antibody appeared to induce down-regulation of the TCR of MAIT cells already at concentrations of 1 μg/mL and 8 hours of stimulation. It is however possible that other stimulation methods, for example Dynabeads, could give better results.

Keeping in mind the possible shortfalls of the results obtained for IL-22, it is nonetheless interesting that significantly increased frequencies of T and MAIT cells producing pro-inflammatory cytokines, including IL-22 as well as TNFα and IL-17A, were detected in samples from CVID patients, particularly following stimulation with anti-CD3 and anti-CD28 antibodies. The involvement of TNFα in inflammatory and autoimmune processes has been thoroughly dissected over the years.[229] IL-17A and IL-22, on the other hand, are known to play a role in the resolution of bacterial infections as well as in the development of autoimmunity.[201,220] The fact that relatively weak antibody-mediated stimulation could induce a significantly higher proportion of MAIT cells from patients to produce these cytokines suggests this cell subset is found in patient blood in a primed state, supporting the findings obtained for CD69. As MAIT cells, IL-17A and IL-22 are all involved in anti-bacterial responses, it is easy to envision how this could be part of a response to the recurrent infections seen in CVID. Notably, 25 to 50 % of CVID patients go on to develop autoimmune comorbidities, in which IL-17A and IL-22 could play a role. Of particular interest in this respect is the fact that the CVID cohort recruited for this study comprised a number of patients affected by psoriasis, in which both mediators have been implicated.[201,220] Still, the possibility remains that the functional changes observed in MAIT cells are a consequence, rather than a cause, of the complications seen in CVID. MAIT cells could for example be induced to activation, and possibly to the production of pro-inflammatory cytokines, by the existence of an already established cytokine milieu. In this sense, they could still participate in the development of complications, but they would not be their cause. Future studies should certainly address the question of whether MAIT cells are enriched in sites of infection and/or inflammation in the peripheral tissues of CVID patients, and whether MAIT cells isolated from these tissues are truly characterised by an enhanced ability to produce pro-inflammatory mediators.

T_H2 mediators in general are not considered part of MAIT cells' cytokine portfolio.[106] IL-4 can however be generated by this cell subset in certain pathophysiological conditions, e.g. in older individuals.[121] Notably, this cytokine is involved in the induction of isotype class-switching processes, favouring the production of IgG1, IgG4 and IgE antibodies.[230,38] It is therefore possible that the small but significant increases we identified in the frequencies of IL-4^+ MAIT cells in the blood of CVID patients could reflect a response mechanism of this population cells to the pervasive defects in B cell class-switching common in the disease.

Our detection of IL-10^+ MAIT cells, although at low frequencies, is controversial, in that production of IL-10 by this cell subset has been excluded in the past.[106] This finding is however supported by the observation that MAIT cells isolated from the omentum, an

abdominal tissue rich in lipids and innate T cells, can also produce IL-10.[231] In addition to this, cell subsets previously considered unable to generate this cytokine have been found in recent years to possess this ability. Examples are IL-10-secreting B cells, often referred to as B_{REG},[30] as well as iNKT cells from adipose tissue.[207]

It is unclear at this time why IL-10 production by circulating MAIT cells has gone unrecognised. A possible explanation is that MAIT cell responses could be influenced by the surrounding environment to a higher degree than currently expected. As previously noted, the experiments presented in this chapter were performed using whole blood, rather than isolated PBMCs or sorted MAIT cells. This would have allowed MAIT cells to interact with components of blood that are usually not represented in experimental conditions, such as the complement, granulocytes, monocytes and circulating DCs. Interactions between MAIT cells and these elements, which are not well studied at present, could affect their ability to generate cytokines. This idea is strengthened by the disparity in the frequencies of IL-17$^+$ and IL-22$^+$ MAIT cells described in this thesis and in a previous report by Walker and colleagues on CD161^{high} CD8αα cells, of which MAIT cells constitute the majority.[116] In that study, stimulation of total PBMCs from healthy donors with PMA and ionomycin resulted in average frequencies of 5 % IL-17$^+$ cells and 2.5 % of IL-22$^+$ cells, versus median frequencies of about 1 % and 0.2 % reported here in whole blood samples.

As IL-10 can supports isotype class-switching and the generation of IgG1 and IgG3 antibodies,[232] this cytokine could potentially play a role similar to that hypothesised for IL-4. It should nonetheless be noted that slightly but significantly increased frequencies of IL-10$^+$ MAIT cells were specifically detected in this study in patients with complications, the majority of whom were affected by autoimmune conditions. Thus, IL-10 would be more likely to participate in this context in the suppression of immune responses. This would be of particular interest when considering the homing profile of MAIT cells, which are known to preferentially migrate to areas of inflammation.

Taken together, the data collected in this chapter support our hypothesis that MAIT cells are functionally altered in CVID. In particular, our findings suggest that MAIT cells from CVID patients have a highly activated phenotype, and are primed to the secretion of mediators including T_H2 cytokine IL-4 and pro-inflammatory cytokines TNFα, IL-17A and IL-22. T cells from these patients, too, exhibit higher production of mediators with inflammatory properties, being more frequent producers of IL-17A$^+$ in the absence of stimulation, and of TNFα$^+$ following antibody-mediated stimulation. T cells and MAIT cells

could therefore promote in CVID the establishment of a pro-inflammatory environment, which may predispose patients to the development of autoimmune conditions.

CHAPTER 7

EFFECTS OF MAIT CELLS ON B CELL MATURATION AND ANTIBODY PRODUCTION

7.1 – Introduction

The differentiation of B cells in antibody-producing cells can be sustained by different cell types. Amongst these, the best studied are follicular helper T (T_{FH}) cells, a specialised subset of $CD4^+$ T cells characterised by the expression of transcriptional master regulator Bcl-6 and by surface expression of chemokine receptor CXCR5, ICOS and activation markers CD40L and PD-1.[233] T_{FH} cells secrete IL-21, whose autocrine signalling can support their follicular helper functions, and are necessary for the formation of GCs, in which B cell somatic hypermutation, affinity maturation and isotype class-switching take place.[234]

In recent years, unexpectedly, B cell-helping functions have also been identified for two innate T cell populations, Vδ2 γδ T cells and iNKT cells. Vδ2 γδ T cells with a follicular helper-like phenotype, characterised by expression of CXCR5, ICOS and CD40L, have been identified in tonsillar tissue.[63] *In vitro*, this cell subset can promote differentiation of naïve B cells and antibody generation through secretion of IL-4 and IL-10. IL-21, as said a key cytokine for T_{FH} cells, promotes differentiation of Vδ2 γδ T cells towards a follicular helper phenotype.[64]

Follicular helper iNKT ($iNKT_{FH}$) cells express Bcl6, PD-1 and CXCR5; they moreover respond to the presence of lipid antigens, presented by B cells through CD1d, by secreting IL-21.[100] Like T_{FH} cells, they can promote early GC formation and antibody responses, although they do not induce the generation of long-lived plasma cells. iNKT cells not displaying a follicular helper-like phenotype can also indirectly support antibody production by B cells, through their interactions with antigen presenting DCs and the secretion of cytokines that activate T_{FH} cells.[99] Interestingly, the relationship between iNKT cells and B cells is reciprocal, in that not only iNKT cells can promote B cells maturation and antibody production, but CD1d-expressing B cells are required to maintain the homeostasis and proliferative abilities of circulating iNKT cells.[169]

We have previously shown that CVID is characterised by B cell defects that impede normal B cell differentiation, isotype class-switching and therefore antibody production (chapter 3). CVID patients furthermore exhibit decreased frequencies and absolute numbers of circulating iNKT cells (chapter 4.2.3). Interestingly, low frequencies of circulating iNKT cells have been shown to significantly associate in CVID with low frequencies of class-switched memory B cells.[169,193] As a consequence of this, it has been suggested that a defect in iNKT cell functions could underlie the inability of B cells from CVID patients to normally produce antibodies. So far, it has however proved impossible to study the functional abilities of iNKT cells from CVID patients, has this cell subset could not be expanded *in vitro*.[193]

7.2 – Hypothesis and aims of the chapter

iNKT cells and MAIT cells share a number of important phenotypic and functional features, including an invariant TCR and anti-microbial properties.[112] Similar to iNKT cells, MAIT cells are also known to interact with B cells, whose presence they necessitate for their expansion after birth.[109] Earlier in this project, we uncovered a significant decrease in the frequencies and absolute counts of MAIT cells in the peripheral blood of CVID patients (chapter 4.2.4). A statistically significant, moderate correlation was later identified between absolute counts of MAIT cells and counts of differentiated B cell subsets, namely class-switched memory B cells and $CD27^-$ IgD^- B cells (chapter 5.6). Finally, *in vitro* analysis of cytokine production by MAIT cells from CVID patients and healthy controls suggested that cells from patients were more likely to produce IL-4 and IL-10, cytokines involved in the induction of class-switching, following stimulation with anti-CD3 and anti-CD28 antibodies or PMA and ionomycin (chapters 6.4.3 and 6.4.4).

On the basis of the known similarities between iNKT cells and MAIT cells, as well as the data presented in the previous chapters of this thesis, we hypothesised that, like iNKT cells, MAIT cells can promote the maturation of B cells, and/or induce antibody production. In order to investigate this possibility, in this chapter we aimed:

1. to define if MAIT cells can affect B cell differentiation and antibody production in healthy individuals. At this time, MAIT cells cannot easily be expanded in culture,[106] however they can be isolated from blood. We therefore set up co-cultures of autologous B cells and MAIT cells obtained from blood packs donated by the Irish Blood Transfusion Service. This part of the study relied on the use of non-activated MAIT cells, as cognate antigen for this population was not readily available at the time these experiments were performed. In these early investigations, we also decided against using PMA and ionomycin or PHA as stimulants, as these compounds can induce TCR-independent activation of T cells, making the interpretation of the resulting data difficult. Previous experiments carried out in our laboratory using co-cultures of B cells and autologous iNKT cells or Vδ2 γδ T cells had previously demonstrated increased antibody production by B cells in the absence of α-GalCer and HMB-PP, respectively, as well as other exogenous stimuli;[206,208]

2. to determine if MAIT cells may affect antibody production in CVID. We chose not to set up co-cultures of B cells and MAIT cells from CVID patients, as large volumes of blood would have been required for the isolation of sufficient numbers of MAIT cells. We did however attempt to explore the possible effects of MAIT cells on antibody production in these individuals, by correlating the levels of IgM, IgG and IgA antibodies measured in their blood at diagnosis with their frequencies and absolute counts of circulating MAIT cells.

7.3 – Effects of MAIT cells on the differentiation of autologous B cells *in vitro*

The effects of MAIT cells on B cell differentiation were studied using autologous co-cultures. MAIT cells were sorted from PBMC preparations enriched in $CD3^+$ cells, while B cells were negatively selected from the remaining $CD3^-$ fraction using magnetic beads; MAIT cell-depleted T cells were also recovered during the sorting of MAIT cells, and retained for use as a control. B cells were seeded in 96-well plates in a 1:1 ratio with either MAIT cells or MAIT cell-depleted T cells and incubated at 37 °C for 3 or 7 days. Using an appropriate panel of fluorochrome-conjugated antibodies, we stained for differentiation markers CD27 and IgD at 0, 3 or 7 days of co-culture. This allowed us to simultaneously identify four cell subsets, i.e. naïve B cells ($CD27^-$ IgD^+), unswitched memory B cells ($CD27^+$ IgD^+), class-switched memory B cells ($CD27^+$ IgD^-) and double negative B cells ($CD27^-$ IgD^-).

Figures 7.1 to 7.4 display the results obtained for all four B cell populations at the three time points assessed. As shown, no significant differences were identified at 3 or 7 days between the differentiation status of B cells cultured alone, with MAIT cells or with MAIT cell-depleted T cells. The co-culturing process itself seemed to be accompanied by a progressive decrease in the frequencies of naïve B cells and a parallel increase in the frequencies of the other three cell subsets, however statistical analysis comparing data from B cells cultured alone at 0, 3 and 7 days showed this trend not to be significant.

No proliferation and similar frequencies of cell death were detected for B cells in all conditions tested, indicating that the results obtained were not differentially influenced by these processes (data not shown).

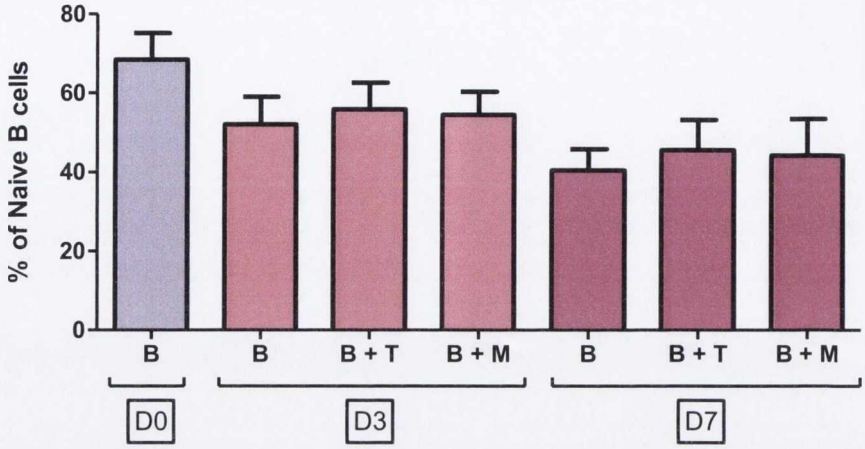


Figure 7.1. Frequencies of naïve B cells following co-culture with MAIT cells. Negatively-selected, total B cells (B) were phenotyped by flow cytometry at day 0 (D0) or following 3 days (D3) or 7 days (D7) of co-culture with sorted MAIT cells (B+M) or MAIT cell-depleted T cells (B+T). Frequencies of naïve B cells, defined as $CD19^+$ $CD27^-$ IgD^+ events, were expressed as a percentage of total B cells. Statistical analysis was performed employing a Kruskal-Wallis test plus Dunn's post hoc test. The results, obtained from 5 healthy donors, are displayed as means with SEMs.

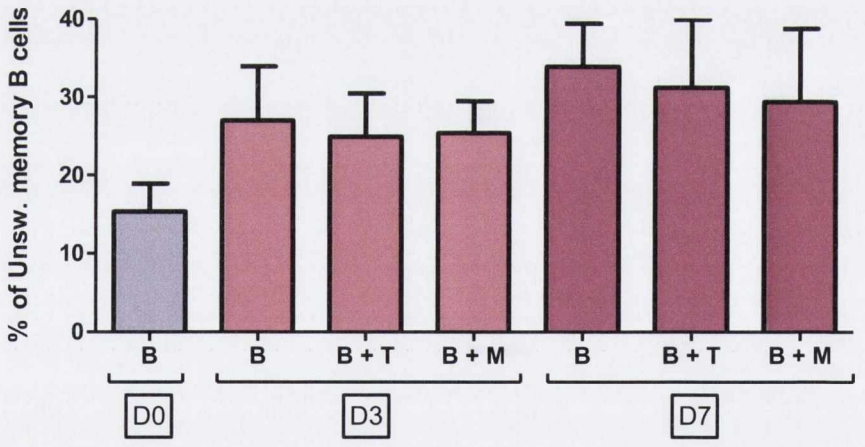


Figure 7.2. Frequencies of unswitched memory B cells following co-culture with MAIT cells. Negatively-selected, total B cells (B) were phenotyped by flow cytometry at day 0 (D0) or following 3 days (D3) or 7 days (D7) of co-culture with sorted MAIT cells (B+M) or MAIT cell-depleted T cells (B+T). Frequencies of unswitched memory B cells, defined as $CD19^+$ $CD27^+$ IgD^+ events, were expressed as a percentage of total B cells. Statistical analysis was performed employing a Kruskal-Wallis test plus Dunn's post hoc test. The results, obtained from 5 healthy donors, are displayed as means with SEMs.

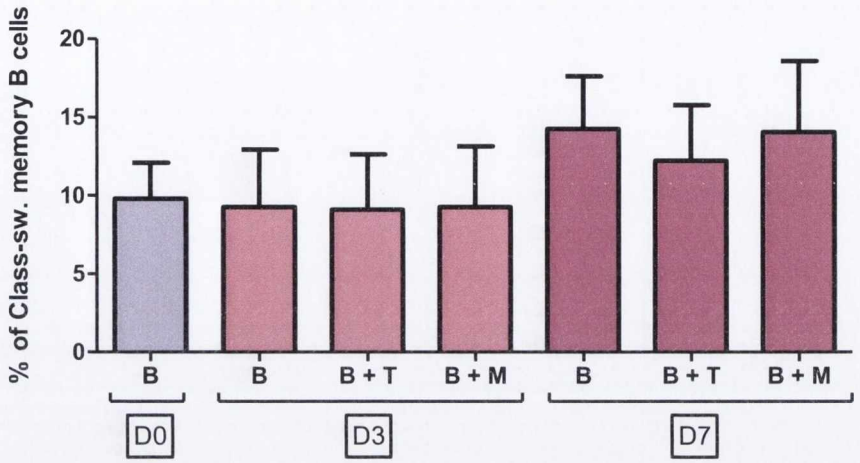


Figure 7.3. Frequencies of class-switched memory B cells following co-culture with MAIT cells. Negatively-selected, total B cells (B) were phenotyped by flow cytometry at day 0 (D0) or following 3 days (D3) or 7 days (D7) of co-culture with sorted MAIT cells (B+M) or MAIT cell-depleted T cells (B+T). Frequencies of class-switched memory B cells, defined as $CD19^+$ $CD27^+$ IgD^- events, were expressed as a percentage of total B cells. Statistical analysis was performed employing a Kruskal-Wallis test plus Dunn's post hoc test. The results, obtained from 5 healthy donors, are displayed as means with SEMs.

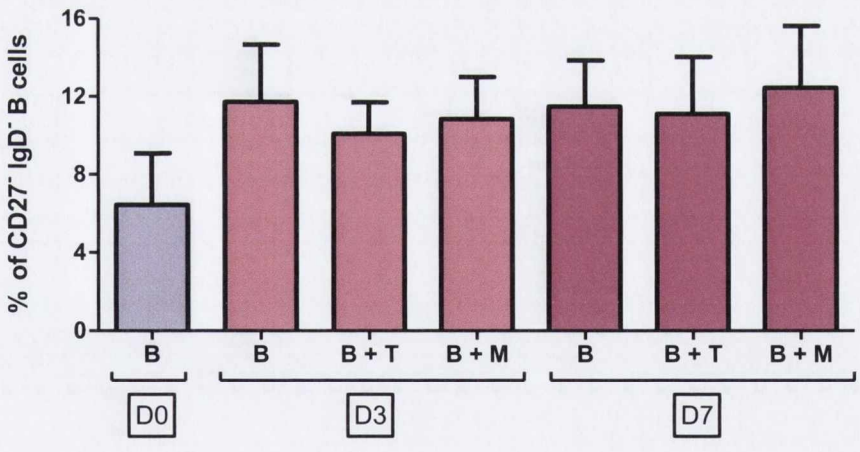


Figure 7.4. Frequencies of $CD27^-$ IgD^- B cells following co-culture with MAIT cells. Negatively-selected, total B cells (B) were phenotyped by flow cytometry at day 0 (D0) or following 3 days (D3) or 7 days (D7) of co-culture with sorted MAIT cells (B+M) or MAIT cell-depleted T cells (B+T). Frequencies of double negative B cells, defined as $CD19^+$ $CD27^-$ IgD^- events, were expressed as a percentage of total B cells. Statistical analysis was performed employing a Kruskal-Wallis test plus Dunn's post hoc test. The results, obtained from 5 healthy donors, are displayed as means with SEMs.

7.4 – Effects of MAIT cells on antibody production by autologous B cells *in vitro*

7.4.1 – Quantification of IgM antibodies in co-cultures of autologous MAIT cells and B cells

MAIT cells were sorted from PBMC preparations enriched for $CD3^+$ cells, while B cells were negatively selected from the remaining $CD3^-$ fraction using magnetic beads; MAIT cell-depleted T cells were also recovered during the sorting of MAIT cells, and retained for use as a control. B cells were seeded in 96-well plates in a 1:1 ratio with either MAIT cells or MAIT cell-depleted T cells and incubated at 37 °C for 3 or 7 days. Supernatants from the co-cultures were removed at the end of each incubation period, stored and later used to perform a cytometric bead array (CBA) assay, a proprietary method which allows to quantify IgM, IgG and IgA antibodies by flow cytometry.

Figures 7.5 and 7.6 display the concentrations of IgM antibodies detected in supernatants harvested at 3 or 7 days, respectively, from cultures of B cells alone or co-cultures of B cells and either MAIT cells or MAIT cell-depleted T cells. As shown, no overall significant difference was identified between the culture conditions surveyed with regard to the quantities of IgM antibodies produced at 3 or 7 days.

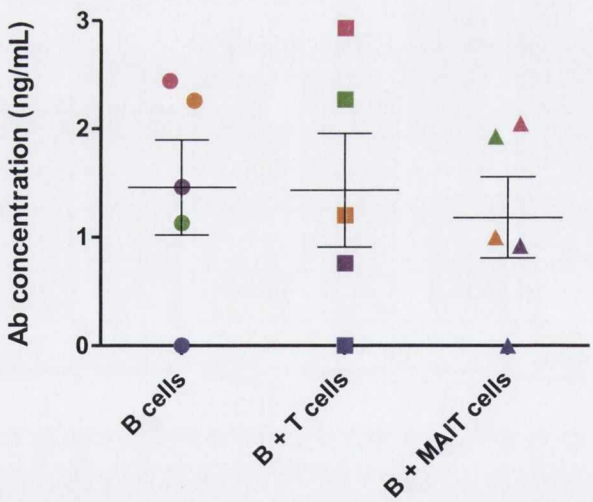


Figure 7.5. Quantification of IgM antibodies in 3 day co-culture supernatants. Total B cells were obtained by negative selection, while MAIT cells and MAIT cell-depleted T cells were isolated by fluorescence-assisted cell sorting. Supernatants were obtained at 3 days from cultures of B cells alone (B cells) or co-cultures of B cells and MAIT cells (B+MAIT cells) or MAIT cell-depleted T cells (B + T cells). IgM antibodies were quantified by CBA assay. Data points of the same colour refer to a single patient. Statistical analysis was performed employing a Kruskal-Wallis test plus Dunn's post hoc test. The results, obtained from 5 healthy donors, are displayed as means with SEMs.

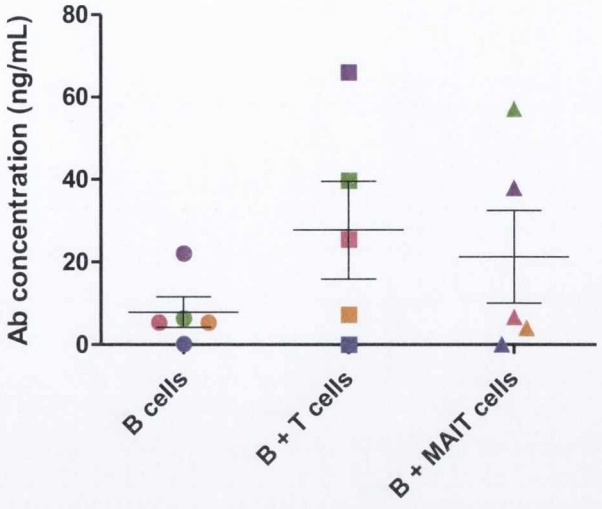


Figure 7.6. Quantification of IgM antibodies in 7 day co-culture supernatants. Total B cells were obtained by negative selection, while MAIT cells and MAIT cell-depleted T cells were isolated by fluorescence-assisted cell sorting. Supernatants were obtained at 7 days from cultures of B cells alone (B cells) or co-cultures of B cells and MAIT cells (B+MAIT cells) or MAIT cell-depleted T cells (B + T cells). IgM antibodies were quantified by CBA assay. Data points of the same colour refer to a single patient. Statistical analysis was performed employing a Kruskal-Wallis test plus Dunn's post hoc test. The results, obtained from 5 healthy donors, are displayed as means with SEMs.

During the analysis of the data, however, it became apparent that 3 out of the 5 donors displayed an increase in the levels of IgM antibodies produced by B cells cultured for 7 days in the presence of MAIT cells and/or T cells in comparison to B cells cultured alone. **Figure 7.7** shows fluorescence intensity plots relating to these individuals.

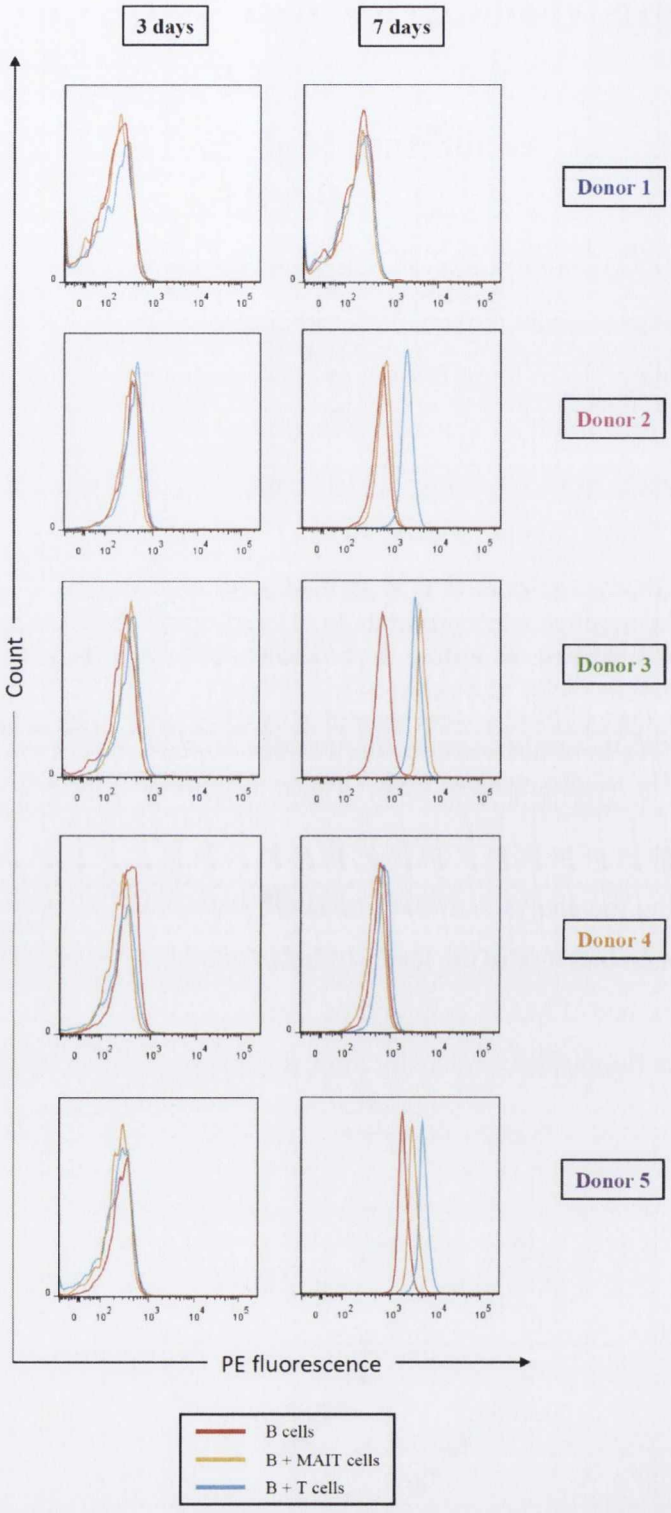


Figure 7.7. Production of IgM antibodies in the presence of MAIT cells and/or T cells at 3 and 7 days of co-culture. The antibody content of culture supernatants was assessed using a quantitative cytometric bead array assay after culturing negatively-selected B cells alone or with sorted MAIT cells or MAIT cell-depleted T cells. The results of the assay are visualised as histograms, whose fluorescence intensity in the PE channel is directly proportional to the quantity antibody produced at 3 days (left) or 7 days (right) of culture in the presence of B cells alone (red lines), B cells and MAIT cells (orange lines) or B cells and MAIT cell-depleted T cells (blue lines). The colour of each donor's name recalls that of the data points in Figures 7.5 and 7.6. Antibody production in the presence of MAIT cells and/or MAIT cell-depleted T cells was observed at 7 days in donors 2, 3 and 5.

7.4.2 – Quantification of IgG antibodies in co-cultures of autologous MAIT cells and B cells

As described in chapter 2.7.7, negatively-selected B cells were seeded in 96-well plates in a 1:1 ratio with sorted MAIT cells or MAIT cell-depleted T cells and incubated at 37 °C for 3 or 7 days. Supernatants from the co-cultures were removed at the end of each incubation period, stored and later used to perform a CBA assay, a proprietary method which allows to quantify IgM, IgG and IgA antibodies by flow cytometry.

Figures 7.8 and 7.9 show the concentrations of IgG antibodies detected in supernatants harvested at 3 or 7 days, respectively, from cultures of B cells alone or co-cultures of B cells and either MAIT cells or MAIT cell-depleted T cells. No overall significant differences were identified between the culture conditions surveyed with regard to the quantities of IgG antibodies produced at 3 or 7 days; antibody production also appeared weaker in comparison to IgM antibodies. Donors 2, 3 and 5, however, displayed small increases in the levels of IgG antibodies produced at 7 days of co-culture in the presence of T cells and, in one case, of MAIT cells, in comparison to those seen in cultures of B cells alone; fluorescence intensity plots relating to these individuals are shown in **Figure 7.10**.

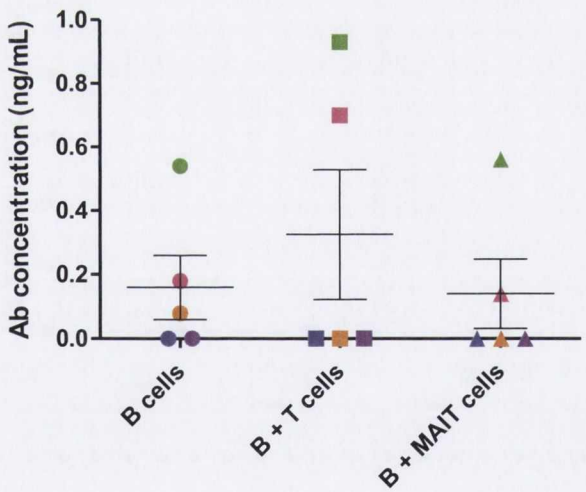


Figure 7.8. Quantification of IgG antibodies in 3 day co-culture supernatants. Total B cells were obtained by negative selection, while MAIT cells and MAIT cell-depleted T cells were isolated by fluorescence-assisted cell sorting. Supernatants were obtained at 3 days from cultures of B cells alone (B cells) or co-cultures of B cells and MAIT cells (B+MAIT cells) or MAIT cell-depleted T cells (B + T cells). IgG antibodies were quantified by CBA assay. Data points of the same colour refer to a single patient. Statistical analysis was performed employing a Kruskal-Wallis test plus Dunn's post hoc test. The results, obtained from 5 healthy donors, are displayed as means with SEMs.

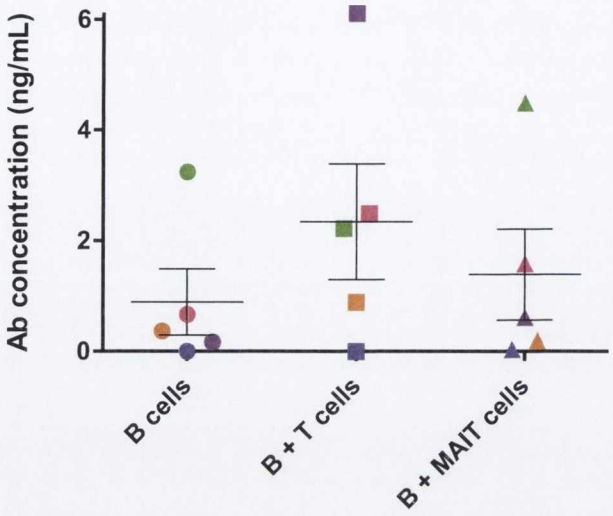


Figure 7.9. Quantification of IgG antibodies in 7 day co-culture supernatants. Total B cells were obtained by negative selection, while MAIT cells and MAIT cell-depleted T cells were isolated by fluorescence-assisted cell sorting. Supernatants were obtained at 7 days from cultures of B cells alone (B cells) or co-cultures of B cells and MAIT cells (B+MAIT cells) or MAIT cell-depleted T cells (B + T cells). IgG antibodies were quantified by CBA assay. Data points of the same colour refer to a single patient. Statistical analysis was performed employing a Kruskal-Wallis test plus Dunn's post hoc test. The results, obtained from 5 healthy donors, are displayed as means with SEMs.

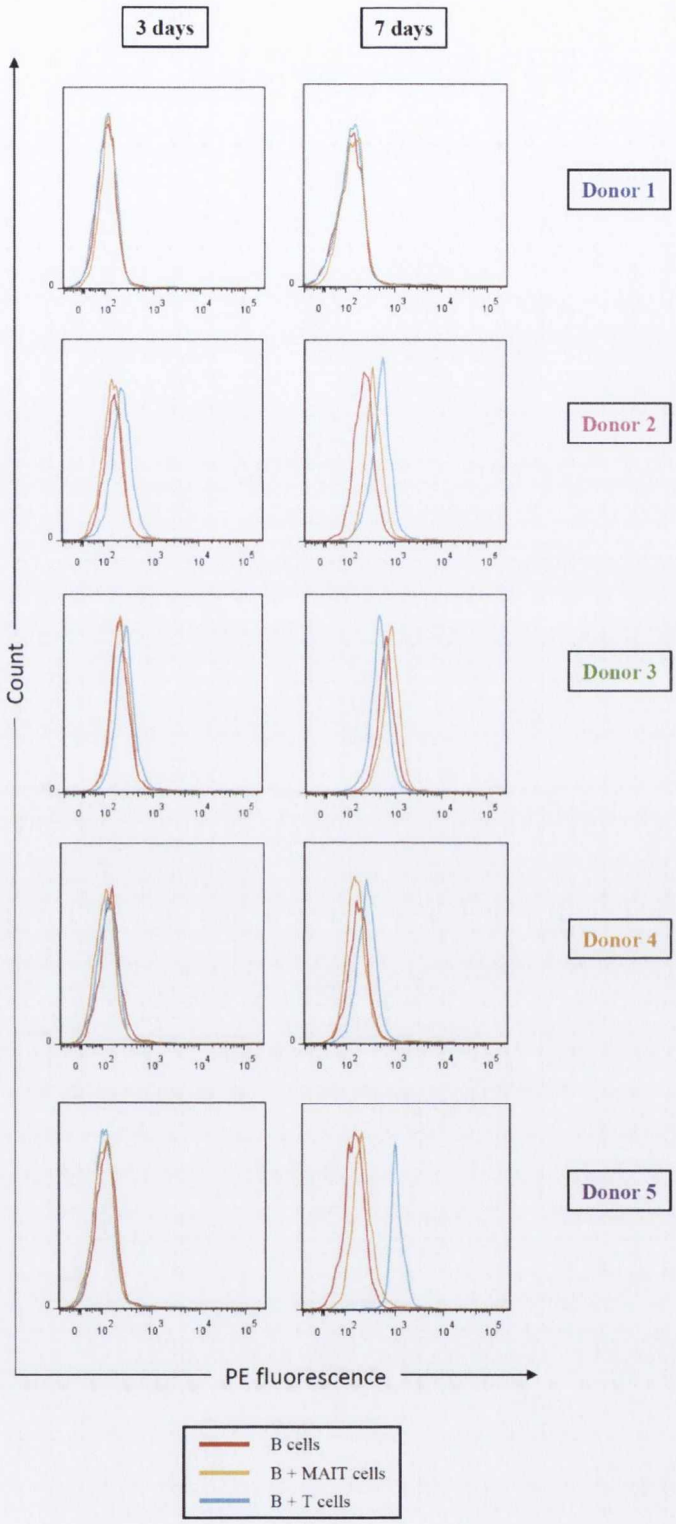


Figure 7.10. Production of IgG antibodies in the presence of T cells or MAIT cells at 3 and 7 days of co-culture. The antibody content of culture supernatants was assessed using a quantitative cytometric bead array assay after culturing negatively-selected B cells alone or with sorted MAIT cells or MAIT cell-depleted T cells. The results of the assay are visualised as histograms, whose fluorescence intensity in the PE channel is directly proportional to the quantity antibody produced at 3 days (left) or 7 days (right) of culture in the presence of B cells alone (red lines), B cells and MAIT cells (orange lines) or B cells and MAIT cell-depleted T cells (blue lines). The colour of each donor's name recalls that of the data points in Figures 7.8 and 7.9. Antibody production in the presence of MAIT cells and/or MAIT cell-depleted T cells was observed at 7 days in donors 2, 3 and 5.

7.4.3 – Quantification of IgA antibodies in co-cultures of autologous MAIT cells and B cells

As described in chapter 2.7.7, B cells were seeded in 96-well plates in a 1:1 ratio with sorted MAIT cells or MAIT cell-depleted T cells and incubated at 37 °C for 3 or 7 days. Supernatants from the co-cultures were removed at the end of each incubation period, stored and later used to perform a CBA assay, a proprietary method which allows to quantify IgM, IgG and IgA antibodies by flow cytometry.

Figures 7.11 and 7.12 display the concentrations of IgA antibodies detected in supernatants harvested at 3 or 7 days, respectively, from cultures of B cells alone or co-cultures of B cells and either MAIT cells or other T cells. In general, production of IgA antibodies seemed weaker in comparison to IgM antibodies, although it was more sustained in comparison to IgG antibodies. Similar to IgM and IgG antibodies, no overall significant difference was identified between the culture conditions surveyed with regard to the quantities of IgA antibodies produced at the two time points. However, B cells from donors 3 and 4 appeared to produce higher concentrations of IgA antibodies after 7 days of incubation with MAIT cell-depleted T cells than they did when cultured alone; in donor 3, increased production of IgA antibodies was also observed in co-cultures of B cells and MAIT cells. **Figure 7.13** shows fluorescence intensity plots relating to these 2 responders.

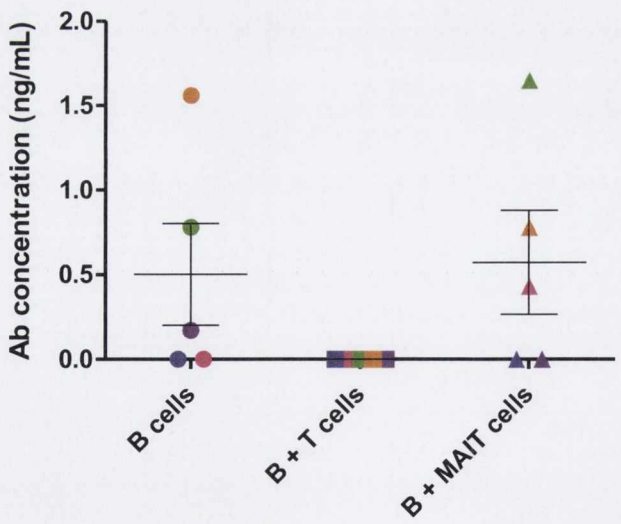


Figure 7.11. Quantification of IgA antibodies in 3 day co-culture supernatants. Total B cells were obtained by negative selection, while MAIT cells and MAIT cell-depleted T cells were isolated by fluorescence-assisted cell sorting. Supernatants were obtained at 3 days from cultures of B cells alone (B cells) or co-cultures of B cells and MAIT cells (B+MAIT cells) or MAIT cell-depleted T cells (B + T cells). IgA antibodies were quantified by CBA assay. Data points of the same colour refer to a single patient. Statistical analysis was performed employing a Kruskal-Wallis test plus Dunn's post hoc test. The results, obtained from 5 healthy donors, are displayed as means with SEMs.

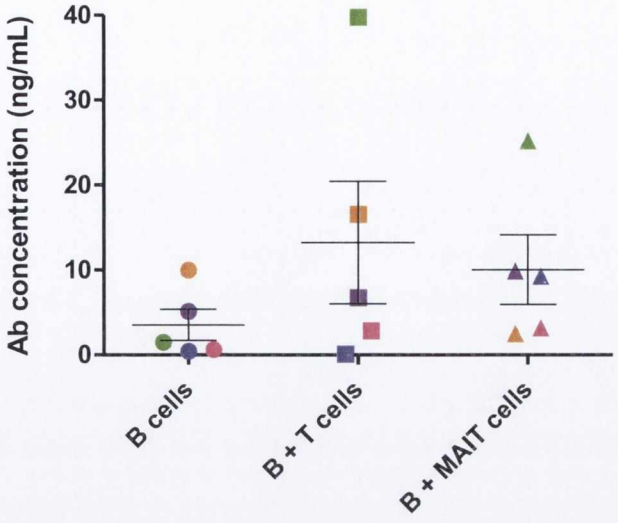


Figure 7.12. Quantification of IgA antibodies in 7 day co-culture supernatants. Total B cells were obtained by negative selection, while MAIT cells and MAIT cell-depleted T cells were isolated by fluorescence-assisted cell sorting. Supernatants were obtained at 7 days from cultures of B cells alone (B cells) or co-cultures of B cells and MAIT cells (B+MAIT cells) or MAIT cell-depleted T cells (B + T cells). IgA antibodies were quantified by CBA assay. Data points of the same colour refer to a single patient. Statistical analysis was performed employing a Kruskal-Wallis test plus Dunn's post hoc test. The results, obtained from 5 healthy donors, are displayed as means with SEMs.

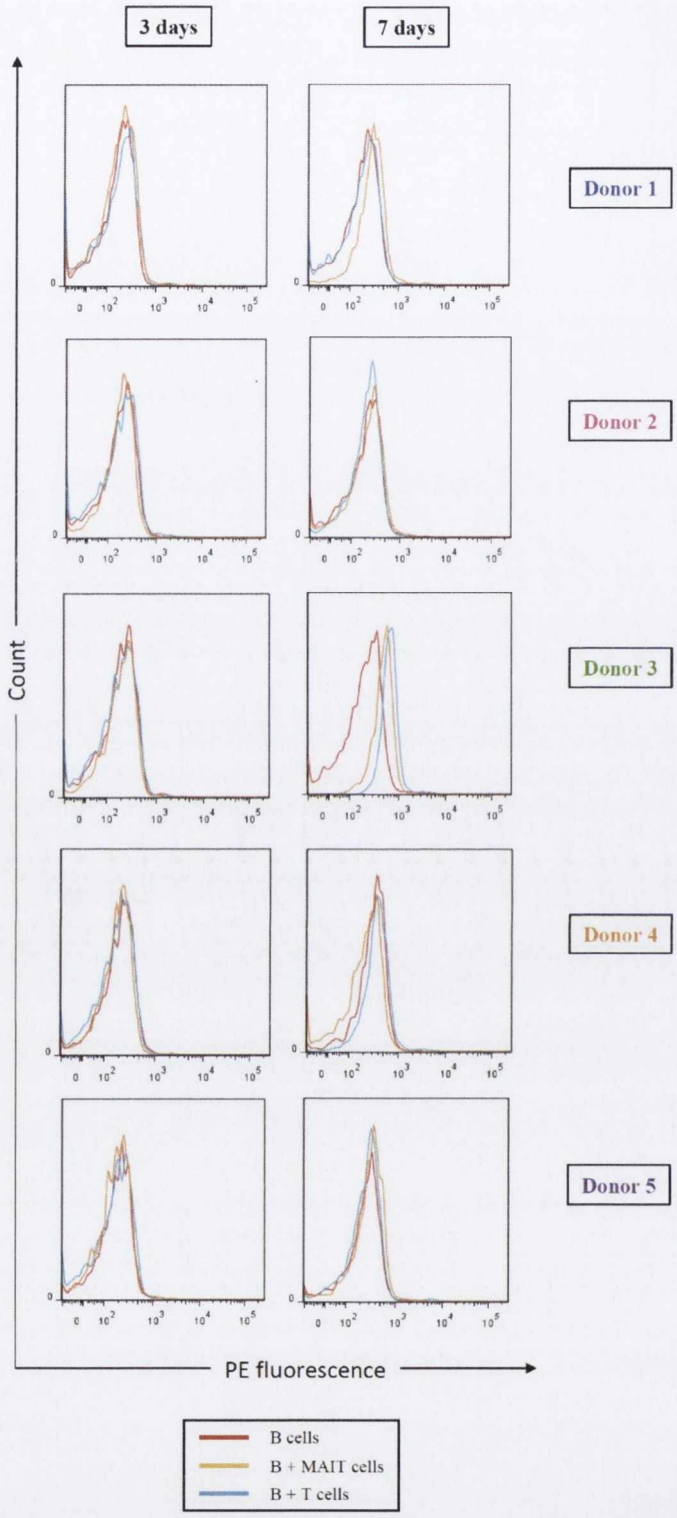


Figure 7.13. Production of IgA antibodies in the presence of T cells or MAIT cells at 3 and 7 days of co-culture. The antibody content of culture supernatants was assessed using a quantitative cytometric bead array assay after culturing negatively-selected B cells alone or with sorted MAIT cells or MAIT cell-depleted T cells. The results of the assay are visualised as histograms, whose fluorescence intensity in the PE channel is directly proportional to the quantity antibody produced at 3 days (left) or 7 days (right) of culture in the presence of B cells alone (red lines), B cells and MAIT cells (orange lines) or B cells and MAIT cell-depleted T cells (blue lines). The colour of each donor's name recalls that of the data points in Figures 7.11 and 7.12. Antibody production in the presence of MAIT cells and/or MAIT cell-depleted T cells was observed at 7 days in donors 3 and 4.

7.5 – Analysis of correlations between MAIT cell frequencies and circulating antibody levels at diagnosis in CVID patients

Earlier in this study, we determined the frequencies and absolute counts of MAIT cells in the circulation of CVID patients and healthy controls (4.2.4), defining that this population was significantly depleted in the former. In order to explore a possible role for MAIT cells in antibody production, we made further use of these phenotyping data by testing for correlations between numbers of MAIT cells and the levels of IgM, IgG or IgA antibodies exhibited by CVID patients at diagnosis. As frequencies and absolute counts of MAIT cells were each tested for three correlations (with IgM, IgG and IgA levels), an appropriate Bonferroni correction was applied, dividing the initial significance threshold (0.05) by 3. This resulted in an adjusted p value of 0.02. The strength of these correlations was expressed using a Spearman's correlation coefficient (r_S), whose significance was defined by a p value.

As shown in **Figure 7.14**, no significant correlations were identified when frequencies of MAIT cells were plotted against the levels of IgG and IgA antibodies measured in the blood of patients at diagnosis. A moderate correlation between frequencies of this population and levels of IgM antibodies ($r_S = -0.52$, $p = 0.03$) was defined as significant before the Bonferroni correction was applied, and close to significance according to the corrected p value. No significant associations were detected between absolute counts of MAIT cells and the levels of any antibody classes at diagnosis (**Figure 7.15**).

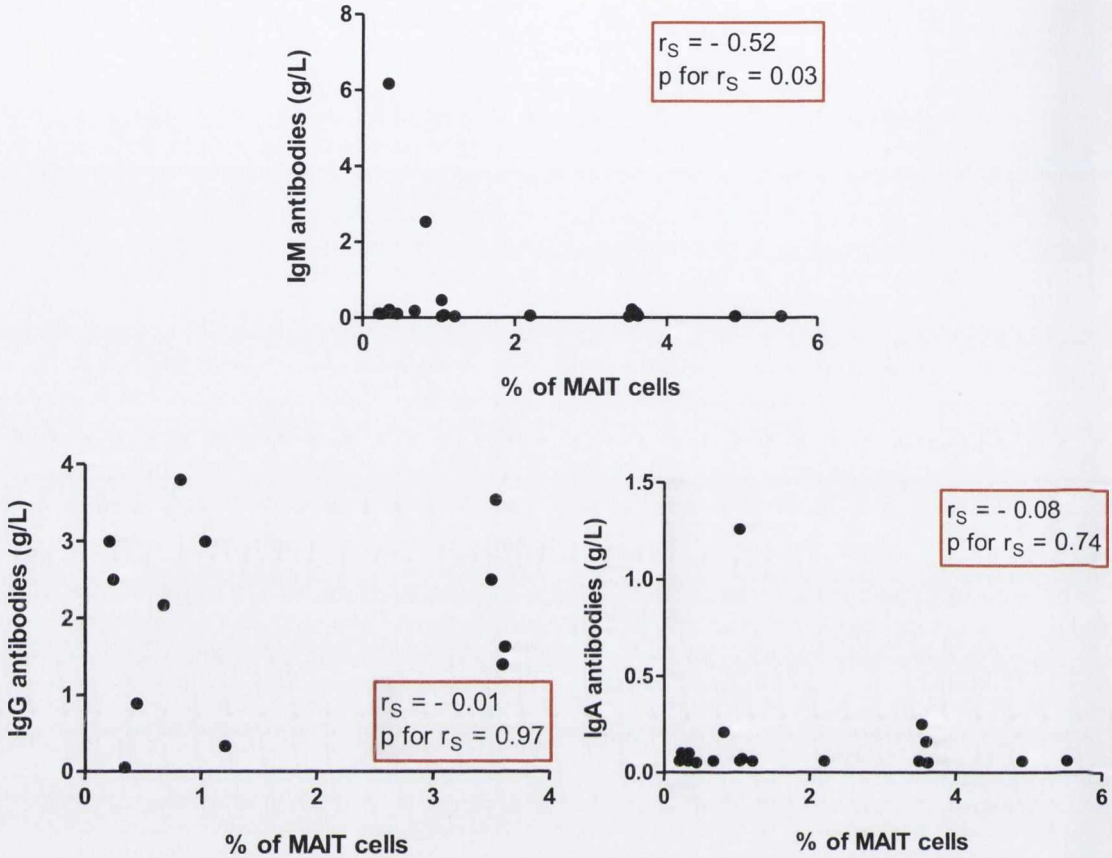


Figure 7.14. Correlations of circulating MAIT cell frequencies and IgM, IgG and IgA antibody levels at diagnosis. Frequencies of MAIT cells, previously detected by flow cytometry as $CD3^+$ $V\alpha7.2^+$ $CD161^{high}$ events, were expressed as percentages of total T cells and plotted against the levels of IgM (top, n = 18), IgG (bottom left, n = 12) or IgA (bottom right, n = 18) antibodies measured in the blood of CVID patients at diagnosis. The strength of the correlations tested is expressed by a Spearman's correlation coefficient (r_S), defined by a p value.

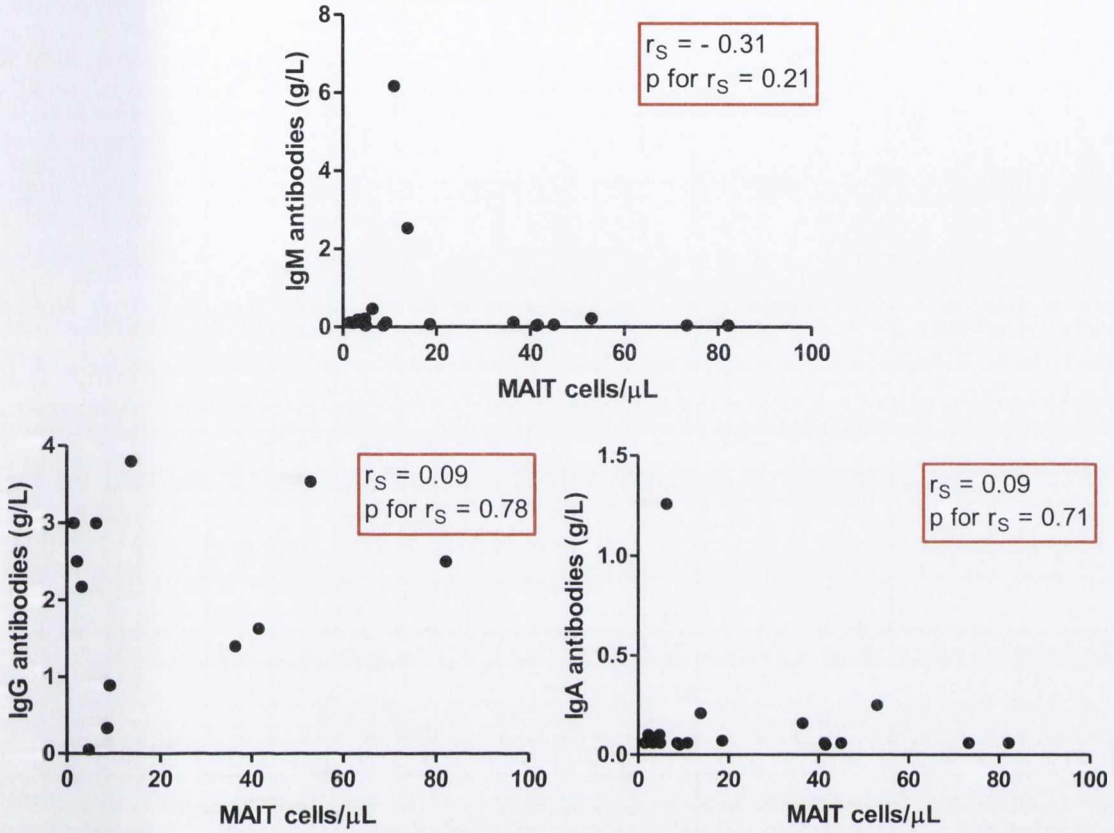


Figure 7.15. Correlations of circulating MAIT cell counts and IgM, IgG and IgA antibody levels at diagnosis. Absolute numbers of MAIT cells, previously detected by flow cytometry as $CD3^+$ $V\alpha7.2^+$ $CD161^{high}$ events, were expressed as cells/μL and plotted against the levels of IgM (top, n = 18), IgG (bottom left, n = 12) or IgA (bottom right, n = 18) antibodies measured in the blood of CVID patients at diagnosis. The strength of the correlations tested is expressed by a Spearman's correlation coefficient (r_S), defined by a p value.

7.6 – Discussion

The expression of follicular helper-like qualities by MAIT cells could provide a potential explanation for the observed depletion of this innate T cell population in CVID, and a target for therapeutic intervention. We therefore explored the possibility that MAIT cells could sustain B cell differentiation and/or antibody production. To this end, we cultured B cells alone, with MAIT cells or MAIT cell-depleted T cells for 3 or 7 days and then used flow cytometry to evaluate the expression of CD27 and IgD markers by B cells, as well as the concentration of IgM, IgG and IgA antibodies in culture supernatants. No significant differences in the frequencies of naïve B cells, unswitched memory B cells, class-switched memory B cells or $CD27^-$ IgD^- B cells were noted when B cells were cultured alone, with MAIT cells or with MAIT cell-depleted T cells. Similarly, no significant differences were noted in the concentrations of IgM, IgG or IgA antibodies produced in the three culture conditions. Increased antibody production was however noticed at 7 days when B cells from certain donors were cultured with MAIT cells and/or MAIT cell-depleted T cells, in comparison to when they were incubated alone. This was particularly evident for IgM antibodies, which were produced in the highest quantities in this *in vitro* system. Finally, a moderate inverse correlation was identified between frequencies of MAIT cells and levels of IgM antibodies measured in the blood of CVID patients at diagnosis; this correlation was significant before a Bonferroni correction was applied, and remained close to significance after its application.

As MAIT cells did not appear to influence B cell maturation in these experiments, it is difficult at this time to envision a defect in MAIT cell functions as being the source of the impaired B cell differentiation process seen in CVID. It should however be noted that the experiments described here utilised non-activated MAIT cells and T cells. The decision to use unstimulated cells was based on the results of previous research carried out in our laboratory on the interactions between B cells and two innate T cell populations, i.e. iNKT cells and Vδ2 γδ T cells. In those experiments, B cells were induced by iNKT cells and Vδ2 γδ T cells to secrete IgM, IgG and IgA antibodies in the absence of α-GalCer, HMB-PP or other exogenous stimuli.[206, 208] MAIT cells display functional similarities to iNKT cells and Vδ2 γδ T cells, nonetheless the potential expression of follicular helper-like functions by MAIT cells could be subject to different requirements; the results obtained in this study should therefore be confirmed using activated MAIT cells.

Activation of MAIT cells *in vitro* has previously been achieved by using synthetic cognate antigens, PMA, PHA or incubation with DCs. rRL-6-CH_2OH, a MAIT cell antigen

recently synthesised by the Rossjohn group,[107] would be an ideal stimulant, however the compound is not commercially available. PMA can freely diffuse through the cell membrane, promoting TCR-independent activation through the protein kinase C (PKC) pathway. PHA, on the other hand, acts by indiscriminately cross-linking and activating glycosylated surface proteins, including the TCR and co-stimulatory receptors, and causing the activation of multiple downstream signalling pathway. Thus, both PMA and PHA can induce potent but non-TCR-specific cell activation. As such, neither would allow to mimic the physiological interactions between MAIT cells and B cells, making them less than ideal for our purposes. Incubation with DCs pulsed with fixed bacterial or fungal species able to produce vitamin B2 has been shown in the past to consistently activate MAIT cells.[112] Unfortunately, reliance on mixed co-cultures of MAIT cells, B cells and DCs would create extensive problems in the interpretation of results, as DCs can directly interact with B cells and influence B cell survival, proliferation, isotype class-switching and antibody production.[235,236] As a consequence of this, MAIT cells should first be activated with DCs, then isolated and transferred into co-cultures with B cells; this would in turn pose further technical problems, decreasing the final yield of MAIT cells available for use. These issues could be avoided by activating MAIT cells with superantigens, compounds which act by simultaneously binding outside of the antigen-presenting groove of MHC class II molecules and to the β chain of the TCR. Superantigens could be used in the presence of B cells and MAIT cells alone, forgoing the need for other exogenous stimuli, cognate antigen or DCs. As the specificity of superantigen-mediated activation of T cells depends on the β chain of the TCR, an appropriate agent should be selected on the basis of its ability to bind to Vβ2 and/or Vβ13 chains, the most expressed by MAIT cells. Possible candidates could for example be TSST-1 (toxic shock syndrome toxin-1) and SPE-C (streptococcal pyrogenic exotoxin-C), Vβ2-binding proteins produced by *Staphylococcus aureus* and *Streptococcus pyogenes*, respectively.[237,238]

The five donors whose cells were used in these experiments exhibited widely different responses with regard to antibody production. B cells from donor 3 appeared to generate higher concentrations of IgM, IgG and IgA antibodies after 7 days in the presence of T cells and/or MAIT cells than when cultured alone. When considered in the same conditions, B cells from donors 2 and 5 generated IgM and IgG antibodies, while donor 4 produced IgA antibodies. Finally, donor 1 did not produce appreciable levels of antibodies belonging to any of the three isotype classes. This suggests a high degree of inter-donor variability in the responses of B cells in culture, which sees some individuals (e.g. donor 3) respond better than others (e.g. donor 1). These differences did not appear to be the results of disparities in

cell viability. They could however depend on subclinical infections experienced by donors at the time of their blood donation; some blood packs provided by the transfusion service for use in research may also be fresher than others. It is impossible to establish if and how these factors impact the performance of B cells in culture, as the blood packs from which they were harvested were totally anonymised and not traceable. Future experiments, using fresh blood from a larger cohort of known donors, may help in clarifying these aspects. Sorted populations of naïve B cells, rather than total B cells, could also be used as starting culture material, thus eliminating the introduction of biases depending on the presence of different subpopulations of memory B cells in samples from distinct donors. Alternatively, responses by specific B cell subsets could be studied separately, by sorting B cells on the basis of their expression of CD27 and IgD.

B cells from two out of five donors surveyed in this study exhibited an ability to produce IgM antibodies, at concentrations between 40 to 60 ng/mL, when cultured with MAIT cells over the course of 7 days. An inverse correlation was also identified between frequencies of circulating MAIT cells and levels of IgM antibodies, but not IgG or IgA antibodies, measured in the blood of CVID patients at diagnosis. Taken together, these findings may indicate a possible effect of MAIT cells on the production of IgM antibodies. The inverse correlation identified in CVID could be explained by the fact that decreased frequencies of MAIT cells in circulation could be linked to increased contact with IgM-producing B cells in the periphery. At this time, it is unclear where such interactions between MAIT cells and antibody producing B cells could take place. Small populations of MAIT cells have previously been detected in the spleen as well as in the mediastinal and mesenteric lymph nodes of mice 14 days post-infection with live *Francisella tularensis*;[126] MAIT cells have also been observed in the spleen and in mesenteric lymph nodes of human foetuses.[111] Adult human MAIT cells, however, are generally $CCR7^-$ and do not preferentially home to lymphoid tissues,[106] which suggests they do not play a major role in immune interactions within GCs. It is nonetheless possible that MAIT cells could interact with B cells at other sites, for example inflammatory sites at intestinal level, to which they are typically drawn.

More research is needed about the effects of MAIT cells on B cell maturation and IgM antibody production. The use of higher numbers of fresh blood samples would help to minimise the effects of inter-donor variability encountered in this study. As almost no antibody secretion was observed at 3 days of co-culture, incubations of at least 7 days should be considered, using both unstimulated and stimulated MAIT cells. As noted, although the experiments presented here have assessed antibody production by total B cells, future experiments could make use of naïve B cells only, or of populations of B cells sorted on the

basis of their expression of CD27 and IgD. The effects of MAIT cells on antibody production by $CD27^+$ IgD^+ unswitched memory B cells would be of particular interest, as this B cell subset can generate IgM-producing plasmablasts and plasma cells upon second contact with its cognate antigen. A positive finding would be notable in that it could open an immunotherapeutic avenue for the treatment of CVID patients. As shown in chapter 3 and in previous literature, frequencies of circulating unswitched memory B cells are usually normal in CVID, which is mostly characterised by defects in class-switching. About 50 % of CVID patients also exhibit levels of IgM antibodies comparable to those of healthy individuals, suggesting a preservation of the functions of IgM-producing cells. MAIT cell-targeted interventions aimed at boosting the levels of protective IgM antibodies in circulation may therefore reduce reliance on IgG infusions in a significant proportion of patients.

Future work could also explore the expression of follicular helper-like markers and cytokines by MAIT cells. As shown in chapter 6, this population expresses CD40L and is capable of secreting IL-4 in certain conditions; ICOS has also been detected on the surface of murine MAIT cells,[130] although this finding has yet to be confirmed in man. On the other hand, secretion of IL-21 and expression of CXCR5 and Bcl-6 by MAIT cells have not been investigated. It is possible that, regardless of the T_H17-type profile of the majority of the population, a small subset of MAIT cells may have follicular helper-like activities and phenotype.

Taken together, the data collected in this chapter do not provide conclusive evidence that MAIT cells can promote B cell maturation and/or induce antibody production. Results from some of the donors analysed, however, suggest that this innate T cell population may support IgM antibody secretion. This should be investigated further, using blood samples from healthy controls and, eventually, CVID patients. Should MAIT cells be confirmed to sustain production of IgM antibodies, this could eventually allow their use for therapeutic purposes in CVID.

CHAPTER 8

DISCUSSION

Although relatively common, CVID is still poorly understood. A small number of familial cases have been attributed to monogenic mutations in genes involved in B cell differentiation and interactions between B cells and T cells, such as CD19, ICOS, TACI and BAFF-R.[10-13] No cause of disease is however identified in about 90 % of patients. In addition to being characterised by recurrent infections, CVID is associated with a higher than normal risk of developing complications such as autoimmunity, enteropathy, granulomatous disease, lymphadenopathy and malignancy; autoimmunity is particularly frequent, affecting 25 to 50 % of patients. All comorbidities are treated symptomatically and, as for CVID itself, the reasons for their occurrence are obscure.

Abnormal numbers of B, T and NK lymphocytes and their subsets have previously been identified in the circulation of CVID patients. These individuals usually present with decreased frequencies of class-switched memory B cells and plasmablasts, as well as increased frequencies of naïve B cells and, sometimes, transitional B cells.[157] T_{REG} cells, $CD4^+$ T cells and NK cells have been detected in low numbers, while frequencies of $CD8^+$ T cells are generally increased in their blood in comparison to healthy donors.[161,162,168,170] Amongst innate T cell subsets, only iNKT cells have been the object of some study, having been found to be depleted in the peripheral blood of patients.[169]

As CVID is first and foremost a B cell-mediated disease, the initial part of this study was dedicated to the B cell compartment of the immune system. The detailed B cell phenotyping performed allowed us to track B lymphocytes throughout their differentiation, from the transitional through to the plasmablast stage. The data collected confirm previous research, showing that CVID features a depletion of mature B cell subsets, such as class-switched memory B cells and plasmablasts, and a parallel increase in immature phenotypes, specifically naïve B cells. Frequencies of unswitched memory B cells, which lay at the hinge between undifferentiated and class-switched phenotypes, were unaltered. These results strengthen the idea that CVID could largely depend on defects in GC output rather than GC formation, in line with previous observations of GCs, although ill-defined and hyperplastic ones, in patient biopsies.[188] Conversely, secondary antibody deficiency patients were found to display frequencies of immature and differentiated B cell subsets similar to those of healthy donors, suggesting that hypogammaglobulinemia may be caused in these individuals by functional defects of terminally differentiated B cell subsets or by a reduction in total B cell numbers, manifesting as B cell lymphopenia.

In addition to using combinations of cell-surface markers previously employed for the phenotyping of B cell subsets, we determined the frequencies and absolute counts of total

IgD^+ B cells. IgD is commonly used alongside CD27 for the definition of naïve, unswitched memory and class-switched memory B cell subsets by flow cytometry. However, our data suggest that IgD could also be valuable when used alone, allowing to discriminate between patients affected by certain primary antibody deficiencies, i.e. CVID and SIgAD, and healthy subjects or individuals affected by secondary antibody deficiencies. Recent studies in primary immunodeficiencies (PIDs) have focussed on TRECs (T cell receptor excision circles) and KRECs (K-deleting recombination excision circles), non-replicating episomal DNA structures that are produced in the thymus and in the bone marrow during V(D)J recombination and the generation of T and B lymphocytes, respectively.[239,240] Since TRECs and KRECs can be quantified in peripheral blood by real time PCR, their measurement has been used to distinguish between healthy donors and subjects with PID. This has proven of huge value in neonatal screening, allowing to identify babies with life-threatening SCIDs (severe combined immunodeficiencies) using dried blood samples stored on Guthrie cards.[241,242] Unfortunately, the technique is ineffectual for the early detection of CVID and SIgAD, as patients affected by these diseases exhibit levels of TRECs and KRECs similar to those of healthy donors (**Figure 8.1**).[243] Determination of IgD by flow cytometry could therefore be advantageous in a screening context, particularly as both the marker and the technique are already widely established in routine laboratories. It remains however to be seen if IgD could be used for early diagnosis, e.g. to distinguish paediatric patients with transient antibody deficiencies from children who will go on to develop full-blown CVID. It should furthermore be noted that determination of IgD^+ B cell frequencies could not be employed in neonates, due to the wide variability and high pace of development of the immune system in the first months of life. Use of this marker in older children, possibly from 5-6 years of age, would additionally require fresh blood samples and the prior determination of age-matched reference ranges in healthy individuals.

Several T cell populations have been shown to support antibody production by B cells. Follicular helper T (T_{FH}) cells, the best known, are a subset of conventional $CD4^+$ T cells characterised by expression of CXCR5, CD40L, ICOS and Bcl-6 and by the secretion of IL-21.[234,235] Follicular helper-like qualities have also been defined for two innate T cell populations, i.e. iNKT cells and Vδ2 γδ T cells, which can promote B cell maturation and antibody production.[63,100,101] As reviewed in chapter 1.5.2.2, innate T cells are furthermore involved in the mediation of immunity against infections, both directly and through their interactions with other cell types including DCs and neutrophils, as well as in the development of autoimmunity. Since CVID is characterised by altered B cell functionality,

recurrent infections and frequent autoimmune complications, we hypothesized that innate T cells could contribute to its pathogenesis.

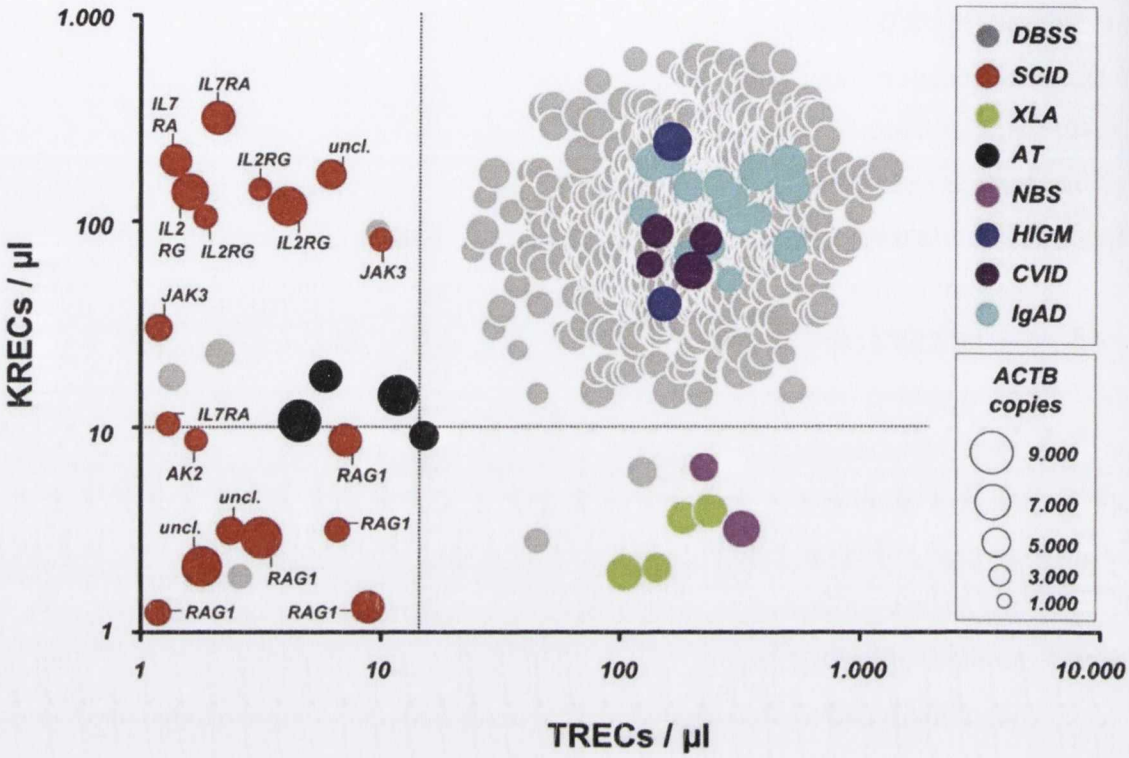


Figure 8.1. Identification of individuals with primary immunodeficiencies by TREC and KREC quantification. TRECs (T cell receptor excision circles) and KRECs (K-deleting recombination excision circles) were quantified in dried blood spot samples (DBSS) from Guthrie cards, using a multiplex real time quantitative PCR assay. The analysis allowed to identify individuals with primary immunodeficiencies (coloured dots) affected by severe combined immunodeficiency (SCID), XLA, ataxia-telangiectasia (AT), Nijmegen-breakage-syndrome (NBS), X-chromosome linked hyper-IgM syndrome (HIGM), CVID and SIgAD. The size of the dots refers to the number of β-actin (ACTB) copies detected, which were used as markers of successful DNA extraction from samples. Image from Borte S. *et al.*[243]

The second part of this thesis was therefore dedicated to innate T cells and their possible role in CVID. Whereas the status of B cells in CVID is by now well understood, this study largely represents the first attempt to catalogue the numbers, phenotype, and in some cases the function, of innate T cells in this disease.

As shown in chapter 4, CVID patients were found to exhibit frequencies and counts of circulating iNKT cells that were significantly lower than those detected in healthy controls. This population was particularly depleted in patients with complications in comparison to patients with infections only. A previous study had reported iNKT cell frequencies to be decreased in CVID, and noted an association between low frequencies of iNKT cells and of

class-switched memory B cells in the disease.[169] Our data reinforced and further expanded on these findings, showing that low frequencies of iNKT cells associate with complications, particularly of an autoimmune type. This was recently confirmed by Gao and colleagues, who found iNKT cell frequencies to be particularly low in patients with lymphoproliferative complications.[193] Taken together, these results highlight a possible involvement of iNKT cells in CVID.

iNKT cells are a multifunctional immune population with strong regulatory properties. They can for example influence the functions of cell subsets involved in anti-microbial responses, polarizing immunity in a T_H1 or T_H2 sense through their ability to produce a range of cytokines,[97,98] activating hepatic and splenic NK cells and sustaining their cytotoxic abilities[93,94] as well as inducing antigen presentation by DCs to $CD4^+$ and $CD8^+$ T cells *in vivo*.[96] iNKT cells can moreover prevent autoimmunity in mouse models of multiple sclerosis, uveitis and diabetes,[197,244-246] and have been found at low frequencies in the circulation of patients affected by SLE, psoriasis, Crohn's disease, ulcerative colitis and rheumatoid arthritis.[199] Finally, this innate T cell subset can sustain B cell maturation and antibody production, both through direct interactions with B cells and through the stimulation of DCs and T_{FH} cells.[100,101]

It is unclear at this time if the lower frequencies of iNKT cells observed in the blood of CVID patients are due to a loss or failed expansion of this population or rather to its migration to peripheral tissues. The fact that CD1d-expressing B cells are required to maintain the proliferative and cytokine-producing abilities of iNKT cells[194] certainly suggests that this innate T cell population could be affected by the B cell differentiation defects so common in CVID. On the other hand, iNKT cells have themselves been found to affect B cell homeostasis, sustaining B cell proliferation, maturation and function.[99,208] It therefore remains to be defined if the depletion of iNKT cells observed in the peripheral blood of CVID patients is primary or secondary to the development of the B cell defects of CVID. Certainly, the inability of iNKT cells from CVID patients to expand *in vitro* following stimulation with α-GalCer and IL-2 indicates that this population is not simply numerically depleted but likely functionally altered.[193] Due to the versatility of iNKT cells and their wide-ranging effects, numerical losses or functional anomalies affecting this population could influence many aspects of immune responses in CVID. Indeed, they could translate in the development of recurrent infections and autoimmune complications, as well as affect B cell maturation and the secretion of antibodies.

Prior to this study, no description of the phenotype of MAIT cells from CVID patients existed in the literature. As shown in chapter 4, MAIT cells were detected at significantly lower frequencies in the blood of CVID patients than in healthy donors. Anomalously distributed frequencies of $CD4^+$ and $CD8^+$ MAIT cells furthermore translated into decreased absolute numbers of $CD8^+$ and double negative MAIT cells in the circulation of patients. Frequencies of $CD69^+$ MAIT cells were significantly higher in unstimulated blood samples from CVID patients than in samples from healthy donors, while frequencies of $CD69^+$ T cells were comparable.

Similar to iNKT cells, it has not been defined in this study whether the numerical decrease in MAIT cells noted in the circulation of CVID patients is a cause or a consequence of CVID. It is unclear at this time if MAIT cells may have any effect on B cell differentiation, and our own experiments employing unstimulated MAIT cells co-cultured with B cells have failed to produce any conclusive observation in this respect. However, previous experiments in germ-free mice and mice lacking the immunoglobulin heavy chain joining region ($J_H^{-/-}$), which are completely devoid of B cells, have shown that MAIT cells necessitate B cells and a commensal microbiome for their expansion after birth.[109] It is therefore possible that this cell population may be vulnerable in its development to defects in B cell differentiation, and fail to expand in a widely abnormal B cell environment such as the one found in CVID. As MAIT cells have well recognised anti-bacterial and anti-fungal functions,[112] their depletion could then predispose CVID patients to recurrent microbial infections, mirroring the higher bacterial loads found in mouse models lacking this subset.[124] It should however be noted that normal or only partially decreased levels of MAIT cell TCR transcripts have been identified in the blood of two out of four patient with XLA, a condition which causes a total or almost total lack of B cells.[109] This indicates that, similar to mouse models, minimal residual populations of B cells, possibly presenting bacterial antigens to MAIT cells at the intestinal level, are sufficient to allow for the expansion and maintenance of this innate T cell population in man. In addition to this, significantly different frequencies of MAIT cells were observed in this study in the circulation of groups of CVID patients displaying comparable frequencies of both immature and differentiated B cell populations. Taken together, these observations suggests that the depletion of circulating MAIT cells observed in this study is unlikely to be rooted in a B cell defect.

MAIT cells exhibit a well-known propensity to migrating to inflammatory and bacterial lesions. Their frequencies were for example found to be decreased in the peripheral blood of patients with inflammatory bowel diseases and increased in their inflamed intestinal

tissue.[132] This cell subset was also enriched in the pulmonary lesions and depleted in the circulation of tuberculosis patients.[112] An alternative explanation for the decreased numbers of MAIT cells seen in the blood of CVID patients is therefore that this subset may not be depleted, but rather redistributed. It is worth noting that the pathogens most commonly involved in infectious events in CVID, such as *H. influenzae*, *S. pneumoniae* and *S. aureus*, all possess the *ex novo* riboflavin synthesis pathway required for production of MAIT cell antigens (**Table 8.1**). A recall of MAIT cells to the periphery would be further facilitated by their expression of chemokine receptors mediating preferential homing not only to areas of inflammation, but also specifically to lung and intestinal epithelia, frequent sites of infection in CVID (**Table 8.2**).[106,110]

Table 8.1. Riboflavin production by microorganisms commonly isolated from CVID patients.

Microorganism	Ex novo riboflavin production pathway*
Haemophilus influenzae	Yes
Streptococcus pneumoniae	Yes
Streptococcus pyogenes	No
Staphylococcus aureus	Yes
Neisseria meningitidis	Yes
Bordetella pertussis	Yes
Giardia lamblia	No
Campylobacter (jejuni)	Yes
Candida (albicans)	Yes

* Information collected from www.genome.jp/kegg/pathway.html

Table 8.2. MAIT cell-expressed chemokine receptors and tissue specificity.

Chemokine receptor	Expression	Tissue specificity
CCR5	High	Inflamed tissues[216]
CCR6	High	Lung and intestinal epithelia and mucosae[217]
CXCR6	High	Liver, lung[218]
CCR9	Intermediate	*Lamina propria* of the small bowel[219]

Taken together, these observations suggest that recurrent infections, and high antigen availability at the infected sites, may summon MAIT cells from the circulation of CVID patients to peripheral tissues. Of particular interest, in this respect, is the observation that $CD8^+$ and double negative MAIT cells, but not $CD4^+$ MAIT cells, respond *in vitro* to DCs

loaded with bacteria by upregulating CD69.[112] This finding appears to exactly mirror the selective depletion of $CD8^+$ and double negative MAIT cells we observed in the peripheral blood of CVID patients, as well as the high frequencies of CD69-expressing MAIT cells detected in otherwise unstimulated patient blood.

In addition to frequently expressing CD69 prior to stimulation, MAIT cells from CVID patients were found in this study to display an altered pattern of cytokine secretion, producing TNFα, IL-17A and IL-22 significantly more frequently than controls after stimulation with anti-CD3 and anti-CD28 antibodies. No differences were noted with regard to the production of these mediators following stimulation of cells from CVID patients with or without complications, however lower numbers of MAIT cells were detected during this study in the circulation of CVID patients affected by complications in comparison to patients with infections only. These observations suggest that MAIT cells from patients are predisposed to the secretion of pro-inflammatory cytokines *in vivo*, and hint at a possible involvement of this innate T cell population in the comorbidities that accompany CVID.

It is unclear at this time to what degree MAIT cells could participate in the complications of CVID, especially as, like the disease itself, the comorbidities accompanying CVID are highly heterogeneous. Interestingly, however, the cytokines produced by MAIT cells are involved both in anti-microbial responses and in the occurrence of inflammatory and autoimmune conditions. TNFα is for example overproduced in Crohn's disease,[229] while IL-17A and IL-22 are involved in the development of rheumatoid arthritis and psoriasis.[201,220] MAIT cells have additionally been reported to produce IL-17A in psoriatic plaques,[133] and IL-17A and IL-22 in the intestinal tissue of patients with inflammatory bowel diseases.[132] It is therefore possible that MAIT cells, recalled from the bloodstream by recurrent infections, may be triggered in the tissues of CVID patients to chronically overproduce pro-inflammatory cytokines, which would over time participate in the development of autoimmunity and inflammation in susceptible individuals. This hypothesis should be tested further, e.g. investigating whether MAIT cells are enriched and/or functionally altered in peripheral tissues samples obtained from CVID patients in the presence of inflammation or autoimmune lesions. It is however notable that, while the B cell anomalies reported in this study appeared to be specific to CVID, MAIT cells were detected at altered frequencies in the circulation of all patient groups considered, including secondary antibody deficiency patients. This supports the idea that the MAIT cell abnormalities observed may be rooted in pathogenic mechanisms shared by all these antibody deficiencies, such as recurrent infections.

With regard to the complications specifically exhibited by the CVID patients recruited for this study, the vast majority presented with psoriasis, either alone or accompanied by other autoimmune displays. For some time now, psoriatic plaques have been known to host $CD4^+$ and $CD8^+$ T cells able to produce T_H1 and T_H17 mediators, including IL-17 as well as IL-22, IFNγ and TNFα. Amongst these cytokines, IL-17 in particular has been shown to be critical for the development of the disease, and as such as been identified as a viable therapeutic target.[201,247,248] It has recently been confirmed that, although the $CD8^+$ cell population involved comprises mostly conventional T cells, activated MAIT cells are enriched in psoriatic skin in comparison to healthy tissue and constitute an alternative source of IL-17A.[133] It remains to be seen if the immune composition of psoriatic lesions described in immunocompetent subjects is maintained in CVID, as a consequence of the numerous immune abnormalities displayed by these patients.

In addition to frequent autoimmune complications, CVID is often accompanied by a particular brand of enteropathy, often similar in presentation to coeliac sprue but refractory to a gluten-free diet and characterised by an absence of plasma cells in the gastrointestinal tract and by autoimmune-like features.[249-251] Indeed, multivariate analysis carried out during a recent study on data from 22012 patients belonging to the ESID database has defined that CVID patients most often present with both autoimmunity and enteropathy, or on the other hand with both splenomegaly and granulomatous disease.[252]

Data on the microenvironment found in the intestine of CVID patients with enteropathy is not abundant. It is however known that these patients display intraepithelial lymphocytiosis and enrichment in $CD3^+$ $CD8^+$ cells in the *lamina propria*.[250,253] Additionally, it has been reported that *lamina propria* mononuclear cells (LPMCs) isolated from the intestine of these patients produce high levels of T_H1 cytokine IL-12, as well as IFNγ in quantities similar to those of LPMCs isolated from patients with Crohn's disease. Production of IL-23, IL-17 and TNFα by LPMCs from CVID patients was also investigated, however this study did not include data on healthy donors, making a direct comparison with the results presented in this thesis impossible.[253] It has nonetheless been observed that MAIT cells express receptors for IL-12R, IL-23R and IL-18Rα,[116] and that TCR-independent activation and increased production of IFNγ by this population take place *in vitro* in the presence of IL-12.[122] In consideration of this and of their tissue homing properties, MAIT cells could therefore play a role in CVID enteropathy.

The cross-sectional and mostly descriptive character of the analysis performed in this study means it was not possible to definitively determine whether the alterations observed in CVID patients with regard to innate T cells were primary or secondary to the development of CVID itself, its hallmark infections and/or its complications. This should be clarified in future studies, for example by:

- collecting longitudinal data, which would allow to track the frequencies and absolute counts of innate T cell populations in patients and healthy donors over a period of time. This kind of investigation would first of all serve the purpose to confirm if the decreased frequencies of circulating MAIT cells and iNKT cells observed in CVID are stably maintained during the course of the disease. Such determinations could moreover be useful if carried out in individuals belonging to families characterised by a predisposition to the development of SIgAD and CVID. As noted in chapter 4, the frequencies of MAIT cells detected in this study in the circulation of patients affected by SIgAD were found to be low but still comparable to those of healthy donors. It would therefore be interesting to determine if they would decrease over time, possibly alongside serum antibody levels, as SIgAD morphs into CVID. Similarly, frequencies of MAIT cells and iNKT cells could be tracked in patients newly diagnosed with CVID, observing any changes taking place as the patients are placed on IgG replacement therapy or develop complications secondary to the disease;
- performing further *in vitro* experiments, involving isolated MAIT cells and iNKT cells from CVID patients. This would allow an in depth investigation of the functionality of these cell subsets, including their ability to secrete cytokines and other signalling mediators, lyse target cells or stimulate other cell types through direct cell-to-cell contact, and the molecular interactions involved in these processes;
- developing *in vivo* models, for example mouse models characterised by specific B cell defects, in order to define if these defects associate with T cell anomalies similar to those observed in this study;
- studying disease controls, to determine whether anomalies similar to those observed in the innate T cell compartment of CVID patients are also found in other patient populations sharing one or more of their pathological characteristics. Interestingly, several studies have already shown that decreased frequencies of circulating MAIT cells are a feature of inflammatory enteropathies, such as Crohn's disease and ulcerative colitis, as well as autoimmune conditions like SLE, rheumatoid arthritis and coeliac disease.[132,254,255] A parallel enrichment of MAIT cells in inflamed tissues has

furthermore been identified in Crohn's disease, ulcerative colitis and rheumatoid arthritis.[132,254];

- observing MAIT and iNKT cell behaviour in monogenic diseases. A recent study by Wilson and colleagues[256] has for example described decreased frequencies of circulating MAIT cells and iNKT cells, but not γδ T cells, in patients affected by autosomal dominant hyper-IgE syndrome (AD-HIES), a disease characterised by heterozygous loss of function mutations in the STAT3 gene and susceptibility to infections by particular pathogens, such as *C. Albicans* and *S. aureus*. Functional anomalies in the MAIT cell population in AD-HIES, and specifically this subset's inability to produce anti-microbial cytokine IL-17, suggests that a lack of functionality of MAIT cells can predispose to the development of infections. As previously noted in this thesis, increased frequencies of IL-17A$^+$ MAIT cells were detected in the blood of CVID patients following TCR-mediated stimulation; additionally, none of the patients recruited for the study presented with fungal infections, usually considered to be a hallmark of T cell dysfunctionality. A comparison of the data obtained from the two studies therefore suggests that MAIT cells remain largely functional in CVID, and that their decrease in the circulation of patients may be a consequence, rather than a cause, of recurrent infections.

Once the mechanisms through which iNKT cells and MAIT cells come to be depleted in CVID are well understood, these innate T cell populations could be considered for immunotherapeutic uses.

Interest in the clinical applications of iNKT cells has been high since promotion of T_H1 responses and IFNγ production by this subset was shown to be critical for the rejection of certain sarcomas and melanomas in murine models.[257, 258] Notably, in addition to their promotion of T_H1 immunity, iNKT cells can sustain T_H2-type responses. In mouse models, they have for example been found to perform B cell-helping functions similar to those normally carried out by T cells, sustaining the production of antibodies against protein antigens administered alongside α-GalCer.[259,260] Chemically-modified analogues of α-GalCer have furthermore shown an ability to steer iNKT cells away from IFNγ generation and towards IL-4 production, possibly paving the way for the use of this population in the treatment of autoimmunity and in the induction of antibody responses.[197] Assuming that iNKT cell functionality is maintained in CVID, an application could therefore be envisioned for this cell subset in vaccination. Unfortunately, while no data are currently available on the functional status of iNKT cells in CVID, a previous attempt to obtain iNKT cell lines from

CVID patients has failed,[193] suggesting a loss of function of this subset. Their use in CVID would also be hindered by the pervasive B cell defects characterising the disease, which impede humoral responses to both polysaccharide and protein-based vaccines.

MAIT cell frequencies in peripheral blood are constitutively higher than those of iNKT, and our results suggest that this population is dysregulated but functional in CVID. Because of this, they could potentially constitute an attractive target for the treatment of infections or the prevention of complications associated with the disease. Biologicals known to interfere with the action of TNFα, IL-17A or IL-22 could for example be employed if cytokine production by MAIT cells is confirmed to mediate the development of complications in patients. However, in light of the important anti-microbial functions of these pro-inflammatory cytokines, and of the immunocompromised state and recurrent infections already suffered by CVID patients, the effects of any compound targeting these pathways would have to be carefully considered. Increased numbers of infections have already been widely reported as a side effect of treatment with TNFα antagonists and IL-17A blockers in immunocompetent patients.[261-263]

An alternative therapeutic approach may involve the expansion of MAIT cells, which could help patients fight infections. Several obstacles would have to be overtaken before such a scenario can be considered, first and foremost the fact that no culturing method has so far been established that allows appreciable, long-term expansion of this population. In addition to this, as previously discussed, the reintroduction of successfully expanded MAIT cells in the circulation of CVID patients could result in an exacerbation of their complications, following their migration to peripheral tissues, activation and production of pro-inflammatory cytokines.

As noted, it is unclear at this time if MAIT cells can positively affect antibody secretion, and if their putative follicular helper-like qualities of MAIT cells would be maintained in CVID. Some evidence collected during this study suggested that this innate T cell population may affect the production of IgM antibodies, which, importantly, are found at normal levels in the circulation of about 50% of CVID patients. A use may therefore be envisaged for this innate T cell subset in boosting protective humoral responses in this subgroup of individuals.

This study generates a number of opportunities for future research. The data collected during B cell phenotyping may be further analysed to determine if the frequencies and/or absolute counts of B cell populations associate with complications. Patients could additionally be grouped according to the stage of B cell differentiation at which they display a block, to determine if specific defects in B cell maturation associate with altered numbers

of innate T cells. This may for example reveal a role in CVID for γδ T cells, which were detected at similar frequencies and counts in the blood of patients and healthy controls. Analysis of the data collected for Vδ1 γδ T cells could be of particular interest, as counts of this population have been shown in chapter 5 of this study to correlate in CVID with those of a number of B cell subsets.

As mentioned earlier in this discussion, IgD may constitute a valuable marker, allowing to identify patients with CVID-like primary immunodeficiencies. As well as confirming its sensitivity and specificity in a larger cohort of donors, further study is required to determine if it could be used for the early diagnosis of paediatric patients, and for the development of suitable age-matched reference ranges. The coupling of IgD with markers other than CD27 may also prove informative. Panels combining antibodies against CD19, IgD, CD3 and Vα24-Jα18 or Vα7.2, for example, would allow to simultaneously interrogate both the T cell and B cell arms of the immune system, defining the frequencies of total IgD^+ T cells alongside those of iNKT cells or MAIT cells. As lower frequencies of iNKT cells and MAIT cells have been identified in this study in patients with complications than in patients with infections only, these panels may have a prognostic value, allowing to recognise individuals with more severe disease forms.

Coming to MAIT cells, the novel correlation identified in both healthy controls and CVID patients between frequencies and absolute counts of this population and Vδ2 γδ T cells should be investigated further, as it is potentially very significant. Co-cultures of the two cell types would allow to determine if they can functionally synergize, to produce, for example, higher quantities of anti-bacterial cytokines. With regard to the role of MAIT cells in CVID, further work will be needed to determine if this cell subset cells indeed migrates from the circulation to the peripheral tissues of patients, and if so, what role they play *in loco*, for example in the complications of CVID. Patient-derived material, such as broncho-alveolar lavages and intestinal biopsies paired with blood samples, would be required to this end. Analysis of a bigger cohort of CVID patients would allow to determine if lower frequencies of MAIT cells are mostly associated with autoimmune complications, or if they are also consistently observed in patients affected by other types of comorbidities.

The possible interactions between MAIT cells and B cells demand additional study, both in healthy controls and in CVID patients. At present, no information is available on where these interactions could take place, whether MAIT cells are capable of stimulating B cell differentiation and antibody production, and even whether they express follicular helper markers. Functional study of these aspects would require the sourcing of either appropriately fixed MAIT cell-activating microorganisms,[107,112] synthetic purified antigen or, possibly,

an appropriate superantigen. If this cell population is ultimately found to affect B cell maturation and/or the generation of antibodies in healthy subjects, the mechanisms underlying this effect, which could be due to cell to cell contact and/or cytokine production, should be determined. The properties of MAIT cells from CVID patients should also be tested in co-cultures with B cells from healthy subjects, to investigate if their B cell-helping functions are maintained. Experiments requiring the isolation and co-culturing of MAIT cells could encounter difficulties due to the quantity of blood required; this would particularly affect investigations employing samples from CVID patients, as frequencies and absolute counts of MAIT cells are lower in the circulation of these subjects. Further studies could therefore investigate and refine methods for the expansion of MAIT cells *in vitro*.

The role of iNKT cells in CVID remains to be dissected. It is not clear at this stage if defective iNKT cell functions may be the cause, or the consequence, of faulty B cell differentiation, and how this cell subset is involved in the complications of CVID. As said, although methods exist to culture this population *in vitro*, recent efforts to expand iNKT cells from CVID patients failed,[193] suggesting an underlying functional defect but complicating future research efforts. Certainly, data already collected during this study should be further analysed, to determine if B cells from CVID patients, particularly with complications, express normal levels of CD1d. A defect in the recycling and surface presentation of this marker has already been shown to affect iNKT cell homeostasis and proliferation in systemic lupus erythematosus, and to be resolved by treatment with Rituximab.[194]

The data presented in this thesis suggest that, in addition to iNKT cells and MAIT cells, the pathogenic mechanisms of CVID could also involve Vδ1 γδ T cells, another innate T cell subset with anti-bacterial functions. The frequencies and absolute counts of this population were found to be unaltered in blood samples from CVID patients. However, frequencies and absolute counts of Vδ1 γδ T cells strongly correlated with those of MAIT cells and iNKT cells; their absolute counts also correlated with those of a number of B cell subsets, from naïve B cells through to plasmablasts. It is unclear at this time what role, if any, Vδ1 γδ T cells may play in the disease, in particular because their functions are not well studied. The relationship of this innate T cell subset with undifferentiated and differentiated B cell populations in CVID nevertheless suggests that it could possess B cell-helping functions, or sustain B cell proliferation. This could be investigated applying a co-culturing protocol similar to the one employed in this thesis for the exploration of the effects of MAIT cells on B cells.

Finally, the phenotypic characteristics of the B and T cell subsets of a query diagnosis patient were described in this study. This donor's medical history set him apart from the other patients recruited. He had for example been placed on IgG replacement therapy very early in life, before 1 year of age; a strong history of meningitis in his mother's family indicated that his condition could have genetic causes, and possibly be X-linked. BTK and PI3K-δ mutations, as well as CD40, CD40L and properdin deficiency, had all been previously excluded. Through phenotyping, we determined that the B cell profile of this donor differed from that of patients with other primary antibody deficiencies, being characterised by low frequencies of naïve B cells and high frequencies of class-switched memory B cells; frequencies and counts of total B cells were also raised in his blood. Amongst T cell populations, frequencies and counts of circulating MAIT cells and Vδ2 γδ T cells were high, while those of iNKT cells were extremely high. This was particularly notable as it confirmed the observation of correlations between these three innate T cell subsets in healthy controls and/or CVID patients. Interestingly, high numbers of innate T cell may partly explain why this donor could remain infection-free when IgG infusions were administered at longer than normal intervals, up to 6 weeks. As patients affected by thymic hyperplasia associated with myasthenia gravis can display increased frequencies of circulating iNKT cells,[205] further investigations for thymic abnormalities could be carried out for this patient. It is however possible that the numerical anomalies noted in this thesis with regard to innate T cell subsets may have genetic bases. In that case, this could be the first description of a novel antibody deficiency.

In conclusion, this study numerically, phenotypically and functionally characterized innate T cells in CVID, with particular attention to MAIT cells, a poorly known population currently of great interest. In doing so, it:

- confirmed that, in a majority of patients, CVID is associated with a defect in B cell isotype class-switching;
- proposed that IgD may be used as a novel marker allowing to identify patients with CVID-like antibody deficiencies;
- greatly expanded our knowledge of innate T cells in CVID, providing an overview of which populations are numerically and phenotypically altered in the disease;
- uncovered the existence of a novel link between low frequencies of MAIT cells and iNKT cells and complications of CVID. Taken together, these data suggest a role for innate T cells in the disease;

- revealed that MAIT cells from CVID patients conserve the ability to respond to antigen presenting cells and produce cytokines, but that some of their properties are dysregulated. In particular, they appear to be highly activated and more prone to producing pro-inflammatory cytokines such as TNFα, IL-17A and IL-22. This could in turn implicate MAIT cells in the pathogenesis of the complications of CVID;
- determined that unstimulated MAIT cells do not have the ability to affect B cell maturation and antibody production *in vitro*, while at the same time suggesting the follicular-helper properties of this population should be the subject of further study;
- suggested that, once the role played by iNKT cells and MAIT cells in CVID is better understood, these innate T cell subsets could constitute attractive immunotherapy targets, to be used for the treatment of the infections and/or of the complications that characterize the disease;
- laid out an outline of future research that could be undertaken on the basis of the results obtained, with regard to the basic biology of MAIT cells and the role of innate T cell subsets in CVID.

REFERENCES

[1] Rosen FS, Eibl M, Roifman C, Fischer A, Volanakis J, Aiuti F, Notarangelo L, Kishimoto T, Resnick IB, Hammarstrom L, Seger R, Chapel H, Cooper MD, Geha RS, Good RA, Waldmann TA, Wedgwood RJP. Primary Immunodeficiency Diseases Report of an IUIS Scientific Committee. Clinical & Experimental Immunology. 1999;118: 1–28.

[2] Salzer U, Warnatz K, Peter HH. Common variable immunodeficiency - an update. Arthritis Res Ther. 2012;14(5):223.

[3] Janeway CA, Apt L, Gitlin D. Agammaglobulinemia. Trans Assoc Am Physicians. 1953;66:200-2.

[4] Oksenhendler E, Gérard L, Fieschi C, Malphettes M, Mouillot G, Jaussaud R, Viallard JF, Gardembas M, Galicier L, Schleinitz N, Suarez F, Soulas-Sprauel P, Hachulla E, Jaccard A, Gardeur A, Théodorou I, Rabian C, Debré P; DEFI Study Group. Infections in 252 patients with common variable immunodeficiency. Clin Infect Dis. 2008;46(10):1547-54.

[5] Cunningham-Rundles C, Bodian C. Common variable immunodeficiency: clinical and immunological features of 248 patients. Clin Immunol. 1999;92:34–48.

[6] Cunningham-Rundles C, Siegal FP, Cunningham-Rundles S, Lieberman P. Incidence of cancer in 98 patients with common varied immunodeficiency. J Clin Immunol. 1987;7(4):294-9.

[7] Espanol T, Catala M, Hernandez M, Caragol I, Bertran JM. Development of a common variable immunodeficiency in IgA deficient patients. Clin Immunol Immunopathol. 1996;80:333 5.

[8] Gutierrez MG, Kirkpatrick CH. Progressive immunodeficiency in a patient with IgA deficiency. Ann Allergy Asthma Allergy. 1997;79:297 301.

[9] Vorechovský I, Zetterquist H, Paganelli R, Koskinen S, Webster AD, Björkander J, Smith CI, Hammarström L. Family and linkage study of selective IgA deficiency and common variable immunodeficiency. Clin Immunol Immunopathol. 1995;77(2):185-92.

[10] van Zelm MC, Reisli I, van der Burg M, Castaño D, van Noesel CJ, van Tol MJ, Woellner C, Grimbacher B, Patiño PJ, van Dongen JJ, Franco JL. An antibody-deficiency syndrome due to mutations in the CD19 gene. N Engl J Med. 2006;354(18):1901-12.

[11] Salzer U, Maul-Pavicic A, Cunningham-Rundles C, Urschel S, Belohradsky BH, Litzman J, Holm A, Franco JL, Plebani A, Hammarstrom L, Skrabl A, Schwinger W, Grimbacher B. ICOS deficiency in patients with common variable immunodeficiency. Clin Immunol. 2004;113:234–40.

[12] Castigli E, Wilson SA, Garibyan L, Rachid R, Bonilla F, Schneider L, Geha RS. TACI is mutant in common variable immunodeficiency and IgA deficiency. *Nat Genet*. 2005;37(8):829-34.

[13] Warnatz K, Salzer U, Rizzi M, Fischer B, Gutenberger S, Böhm J, Kienzler AK, Pan-Hammarström Q, Hammarström L, Rakhmanov M, Schlesier M, Grimbacher B, Peter HH, Eibel H. B-cell activating factor receptor deficiency is associated with an adult-onset antibody deficiency syndrome in humans. Proc Natl Acad Sci U S A. 2009;106(33):13945-50.

[14] Kralovicova J, Hammarström L, Plebani A, Webster AD, Vorechovsky I. Fine-scale mapping at IGAD1 and genome-wide genetic linkage analysis implicate HLA-DQ/DR as a major susceptibility locus in selective IgA deficiency and common variable immunodeficiency. J Immunol. 2003;170(5):2765-75.

[15] Olerup O, Smith CI, Björkander J, Hammarström L. Shared HLA class II-associated genetic susceptibility and resistance, related to the HLA-DQB1 gene, in IgA deficiency and common variable immunodeficiency. Proc Natl Acad Sci U S A. 1992;89(22):10653-7.

[16] Volanakis JE, Zhu ZB, Schaffer FM, Macon KJ, Palermos J, Barger BO, Go R, Campbell RD, Schroeder HW, Cooper MD. Major histocompatibility complex class III genes and susceptibility to immunoglobulin A deficiency and common variable immunodeficiency. J. Clin. Invest. 1992;89(6):1914.

[17] Schroeder HW Jr, Zhu ZB, March RE, Campbell RD, Berney SM, Nedospasov SA, Turetskaya RL, Atkinson TP, Go RC, Cooper MD, Volanakis JE. Susceptibility locus for IgA deficiency and common variable immunodeficiency in the HLA-DR3, -B8, -A1 haplotypes. Mol Med. 1998;4(2):72-86.

[18] Liu J, Marino MW, Wong G, Grail D, Dunn A, Bettadapura J, Slavin AJ, Old L, Bernard CC. TNF is a potent anti-inflammatory cytokine in autoimmune-mediated demyelination. Nat Med. 1998;4(1):78-83.

[19] Chatzantoni K, Mouzaki A. Anti-TNF-alpha antibody therapies in autoimmune diseases. Curr Top Med Chem. 2006;6(16):1707-14.

[20] Yel L. Selective IgA deficiency. J Clin Immunol. 2010;30(1):10-6.

[21] Ammann AJ, Hong R. Selective IgA deficiency: presentation of 30 cases and a review of the literature. Medicine (Baltimore). 1971;50(3):223-36.

[22] Edwards E, Razvi S, Cunningham-Rundles C. IgA deficiency: clinical correlates and responses to pneumococcal vaccine. Clin Immunol. 2004;111(1):93-7.

[23] Mellemkjaer L, Hammarstrom L, Andersen V, Yuen J, Heilmann C, Barington T, Bjorkander J, Olsen JH. Cancer risk among patients with IgA deficiency or common variable immunodeficiency and their relatives: a combined Danish and Swedish study. Clin Exp Immunol. 2002;130(3):495-500.

[24] Cataldo F, Marino V, Ventura A, Bottaro G, Corazza GR. Prevalence and clinical features of selective immunoglobulin A deficiency in coeliac disease: an Italian multicentre study. Italian Society of Paediatric Gastroenterology and Hepatology (SIGEP) and "Club del Tenue" Working Groups on Coeliac Disease. Gut. 1998;42(3):362-5.

[25] Chow MA, Lebwohl B, Reilly NR, Green PH. Immunoglobulin A deficiency in celiac disease. J Clin Gastroenterol. 2012;46(10):850-4.

[26] Plebani A, Carbonara AO, Bottaro A, Gallina R, Boccazzi C, Crispino P, Ruggeri L, Salvioni F, Duina M, Negrini A, et al. Gene deletion as a cause of associated deficiency of IgA1, IgG2, IgG4 and IgE. Immunodeficiency. 1993;4(1-4):245-8.

[27] Geisberger R, Lamers M, Achatz G. The riddle of the dual expression of IgM and IgD. Immunology. 2006;118(4):429-37.

[28] Maecker HT, McCoy JP, Nussenblatt R. Standardizing immunophenotyping for the Human Immunology Project. Nat Rev Immunol. 2012;12(3):191-200.

[29] Agrawal S, Smith SA, Tangye SG, Sewell WA. Transitional B cell subsets in human bone marrow. Clin Exp Immunol. 2013;174(1):53-9.

[30] Blair PA, Noreña LY, Flores-Borja F, Rawlings DJ, Isenberg DA, Ehrenstein MR, Mauri C. CD19(+) CD24(hi) CD38(hi) B cells exhibit regulatory capacity in healthy individuals but are functionally impaired in systemic Lupus Erythematosus patients. Immunity. 2010;32(1):129-40.

[31] Yanaba K, Bouaziz JD, Haas KM, Poe JC, Fujimoto M, Tedder TF. A regulatory B cell subset with a unique CD1d^{hi} CD5^{+} phenotype controls T cell-dependent inflammatory responses. Immunity. 2008;28(5):639-50.

[32] Chung JB, Silverman M, Monroe JG. Transitional B cells: step by step towards immune competence. Trends Immunol. 2003;24(6):343-9.

[33] Weill JC, Weller S, Reynaud CA. Human marginal zone B cells. Annu Rev Immunol. 2009;27:267-85.

[34] Weller S, Reynaud CA, Weill JC. Splenic marginal zone B cells in humans: where do they mutate their Ig receptor? Eur J Immunol. 2005;35(10):2789-92.

[35] Garraud O, Borhis G, Badr G, Degrelle S, Pozzetto B, Cognasse F, Richard Y. Revisiting the B-cell compartment in mouse and humans: more than one B-cell subset exists in the marginal zone and beyond. BMC Immunol. 2012;13:63.

[36] Cerutti A, Cols M, Puga I. Marginal zone B cells: virtues of innate-like antibody-producing lymphocytes. Nat Rev Immunol. 2013;13(2):118-32.

[37] Klein U, Rajewsky K, Küppers R. Human immunoglobulin (Ig)M+IgD+ peripheral blood B cells expressing the CD27 cell surface antigen carry somatically mutated variable region genes: CD27 as a general marker for somatically mutated (memory) B cells. J Exp Med. 1998;188(9):1679-89.

[38] Gascan H, Gauchat JF, Aversa G, Van Vlasselaer P, de Vries JE. Anti-CD40 monoclonal antibodies or CD4+ T cell clones and IL-4 induce IgG4 and IgE switching in purified human B cells via different signaling pathways. J Immunol. 1991;147(1):8-13

[39] Sonoda E, Matsumoto R, Hitoshi Y, Ishii T, Sugimoto M, Araki S, Tominaga A, Yamaguchi N, Takatsu K. Transforming growth factor β induces IgA production and acts additively with interleukin 5 for IgA production. J. Exp. Med. 1989;170:1415-1420.

[40] Fairfax KA, Kallies A, Nutt SL, Tarlinton DM. Plasma cell development: from B-cell subsets to long-term survival niches. Semin Immunol. 2008;20(1):49-58.

[41] Colonna-Romano G, Bulati M, Aquino A, Pellicanò M, Vitello S, Lio D, Candore G, Caruso C. A double-negative (IgD-CD27-) B cell population is increased in the peripheral blood of elderly people. Mech Ageing Dev. 2009;130(10):681-90.

[42] Peine M, Rausch S, Helmstetter C, Fröhlich A, Hegazy AN, Kühl AA, Grevelding CG, Höfer T, Hartmann S, Löhning M. Stable T-bet(+)GATA-3(+) Th1/Th2 hybrid cells arise in vivo, can develop directly from naive precursors, and limit immunopathologic inflammation. PLoS Biol. 2013;11(8):e1001633.

[43] Xiong N, Raulet DH. Development and selection of gammadelta T cells. Immunol Rev. 2007;215:15-31.

[44] Carding SR, Egan PJ. Gammadelta T cells: functional plasticity and heterogeneity. Nat Rev Immunol. 2002;2(5):336-45.

[45] Hayday A, Theodoridis E, Ramsburg E, Shires J. Intraepithelial lymphocytes: exploring the Third Way in immunology. Nat Immunol. 2001;2(11):997-1003.

[46] Bonneville M, O'Brien RL, Born WK. Gammadelta T cell effector functions: a blend of innate programming and acquired plasticity. Nat Rev Immunol. 2010;10(7):467-78

[47] Hintz M, Reichenberg A, Altincicek B, Bahr U, Gschwind RM, Kollas AK, Beck E, Wiesner E, Eberl M, Jomaa H. Identification of (E)-4-hydroxy-3-methyl-but-2-enyl pyrophosphate as a major activator for human gammadelta T cells in Escherichia coli. FEBS Lett. 2001;509(2):317-22.

[48] Vavassori S, Kumar A, Wan GS, Ramanjaneyulu GS, Cavallari M, El Daker S, Beddoe T, Theodossis A, Williams NK, Gostick E, Price DA, Soudamini DU, Voon KK, Olivo M, Rossjohn J, Mori L, De Libero G. Butyrophilin 3A1 binds phosphorylated antigens and stimulates human γδ T cells. Nat Immunol. 2013;14(9):908-16.

[49] Bukowski JF, Morita CT, Tanaka Y, Bloom BR, Brenner MB, Band H. V gamma 2V delta 2 TCR-dependent recognition of non-peptide antigens and Daudi cells analyzed by TCR gene transfer. J Immunol. 1995;154(3):998-1006.

[50] Carvalho AC, Matteelli A, Airò P, Tedoldi S, Casalini C, Imberti L, Cadeo GP, Beltrame A, Carosi G. gammadelta T lymphocytes in the peripheral blood of patients with tuberculosis with and without HIV co-infection. Thorax. 2002;57(4):357-60

[51] Qin G, Mao H, Zheng J, Sia SF, Liu Y, Chan PL, Lam KT, Peiris JS, Lau YL, Tu W. Phosphoantigen-expanded human gammadelta T cells display potent cytotoxicity against monocyte-derived macrophages infected with human and avian influenza viruses. J Infect Dis. 2009;200(6):858-65.

[52] Dieli F, Troye-Blomberg M, Ivanyi J, Fournié JJ, Krensky AM, Bonneville M, Peyrat MA, Caccamo N, Sireci G, Salerno A. Granulysin-dependent killing of intracellular and extracellular Mycobacterium tuberculosis by Vgamma9/Vdelta2 T lymphocytes. J Infect Dis. 2001;184(8):1082-5.

[53] Dunne MR, Mangan BA, Madrigal-Estebas L, Doherty DG. Preferential Th1 Cytokine Profile of Phosphoantigen-Stimulated Human Vγ9Vδ2 T Cells. Mediators Inflamm. 2010:704941.

[54] Girardi M. Immunosurveillance and immunoregulation by gammadelta T cells. J Invest Dermatol. 2006;126(1):25-31.

[55] Halary F, Pitard V, Dlubek D, Krzysiek R, de la Salle H, Merville P, Dromer C, Emilie D, Moreau JF, Déchanet-Merville J. Shared reactivity of V{delta}2(neg){gamma}{delta} T cells against cytomegalovirus-infected cells and tumor intestinal epithelial cells. J Exp Med. 2005;201(10):1567-78.

[56] Kabelitz D, Wesch D, He W. Perspectives of gammadelta T cells in tumor immunology. Cancer Res. 2007;67(1):5-8.

[57] Zocchi MR, Poggi A. Role of gammadelta T lymphocytes in tumor defense. Front Biosci. 2004;9:2588-604.

[58] Dunne MR, Madrigal-Estebas L, Tobin LM, Doherty DG. (E)-4-hydroxy-3-methyl-but-2 enyl pyrophosphate-stimulated Vgamma9Vdelta2 T cells possess T helper type 1-promoting adjuvant activity for human monocyte-derived dendritic cells. Cancer Immunol Immunother. 2010;59(7):1109-20.

[59] Eberl M, Roberts GW, Meuter S, Williams JD, Topley N, Moser B. A rapid crosstalk of human gammadelta T cells and monocytes drives the acute inflammation in bacterial infections. PLoS Pathog. 2009;5(2):e1000308.

[60] Caccamo N, Sireci G, Meraviglia S, Dieli F, Ivanyi J, Salerno A. gammadelta T cells condition dendritic cells in vivo for priming pulmonary CD8 T cell responses against Mycobacterium tuberculosis. Eur J Immunol. 2006;36(10):2681-90.

[61] Davey MS, Morgan MP, Liuzzi AR, Tyler CJ, Khan MW, Szakmany T, Hall JE, Moser B, Eberl M. Microbe-specific unconventional T cells induce human neutrophil differentiation into antigen cross-presenting cells. J Immunol. 2014;193(7):3704-16.

[62] Davey MS, Lin CY, Roberts GW, Heuston S, Brown AC, Chess JA, Toleman MA, Gahan CG, Hill C, Parish T, Williams JD, Davies SJ, Johnson DW, Topley N, Moser B, Eberl M. Human neutrophil clearance of bacterial pathogens triggers anti-microbial γδ T cell responses in early infection. PLoS Pathog. 2011;7(5):e1002040.

[63] Caccamo N, Battistini L, Bonneville M, Poccia F, Fournié JJ, Meraviglia S, Borsellino G, Kroczek RA, La Mendola C, Scotet E, Dieli F, Salerno A. CXCR5 identifies a subset of Vgamma9Vdelta2 T cells which secrete IL-4 and IL-10 and help B cells for antibody production. J Immunol. 2006;177(8):5290-5.

[64] Caccamo N, Todaro M, La Manna MP, Sireci G, Stassi G, Dieli F. IL-21 regulates the differentiation of a human γδ T cell subset equipped with B cell helper activity. PLoS One. 2012;7(7):e41940.

[65] Dieli F, Poccia F, Lipp M, Sireci G, Caccamo N, Di Sano C, Salerno A. Differentiation of effector/memory Vdelta2 T cells and migratory routes in lymph nodes or inflammatory sites. J Exp Med. 2003;198(3):391-7.

[66] Brandes M, Willimann K, Lang AB, Nam KH, Jin C, Brenner MB, Morita CT, Moser B. Flexible migration program regulates gamma delta T-cell involvement in humoral immunity. Blood. 2003;102(10):3693-701.

[67] Wen L, Pao W, Wong FS, Peng Q, Craft J, Zheng B, Kelsoe G, Dianda L, Owen MJ, Hayday AC. Germinal center formation, immunoglobulin class switching, and autoantibody production driven by "non alpha/beta" T cells. J Exp Med. 1996;183(5):2271-82.

[68] Spada FM, Grant EP, Peters PJ, Sugita M, Melián A, Leslie DS, Lee HK, van Donselaar E, Hanson DA, Krensky AM, Majdic O, Porcelli SA, Morita CT, Brenner MB. Self-recognition of CD1 by gamma/delta T cells: implications for innate immunity. J Exp Med. 2000;191(6):937-48.

[69] Bai L, Picard D, Anderson B, Chaudhary V, Luoma A, Jabri B, Adams EJ, Savage PB, Bendelac A. The majority of CD1d-sulfatide-specific T cells in human blood use a semiinvariant Vδ1 TCR. Eur J Immunol. 2012;42(9):2505-10.

[70] Griffith E, Ramsburg E, Hayday A. Recognition by human gut gamma delta cells of stress inducible major histocompatibility molecules on enterocytes. Gut. 1998;43(2):166-7.

[71] Kabelitz D, Kalyan S, Oberg HH, Wesch D. Human Vδ2 versus non-Vδ2 γδ T cells in antitumor immunity. Oncoimmunology. 2013;2(3):e23304.

[72] Poggi A, Catellani S, Musso A, Zocchi MR. Gammadelta T lymphocytes producing IFNgamma and IL-17 in response to Candida albicans or mycobacterial antigens: possible implications for acute and chronic inflammation. Curr Med Chem. 2009;16(35):4743-9.

[73] Pitard V, Roumanes D, Lafarge X, Couzi L, Garrigue I, Lafon ME, Merville P, Moreau JF, Déchanet-Merville J. Long-term expansion of effector/memory Vdelta2- gammadelta T cells is a specific blood signature of CMV infection. Blood. 2008;112(4):1317-24.

[74] Li X, Kang N, Zhang X, Dong X, Wei W, Cui L, Ba D, He W. Generation of human regulatory gammadelta T cells by TCRgammadelta stimulation in the presence of TGF-beta and their involvement in the pathogenesis of systemic lupus erythematosus. J Immunol. 2011;186(12):6693-700.

[75] Mangan BA, Dunne MR, O'Reilly VP, Dunne PJ, Exley MA, O'Shea D, Scotet E, Hogan AE, Doherty DG. Cutting edge: CD1d restriction and Th1/Th2/Th17 cytokine secretion by human Vδ3 T cells. J Immunol. 2013;191(1):30-4.

[76] Déchanet J, Merville P, Lim A, Retière C, Pitard V, Lafarge X, Michelson S, Méric C, Hallet MM, Kourilsky P, Potaux L, Bonneville M, Moreau JF. Implication of gammadelta T cells in the human immune response to cytomegalovirus. J Clin Invest. 1999;103(10):1437-49.

[77] Bartkowiak J, Kulczyck-Wojdala D, Blonski JZ, Robak T. Molecular diversity of gammadelta T cells in peripheral blood from patients with B-cell chronic lymphocytic leukaemia. Neoplasma. 2002;49(2):86-90.

[78] Kabelitz D, Hinz T, Dobmeyer T, Mentzel U, Marx S, Böhme A, Arden B, Rossol R, Hoelzer D. Clonal expansion of Vgamma3/Vdelta3-expressing gammadelta T cells in an HIV-1/2-negative patient with CD4 T-cell deficiency. Br J Haematol. 1997;96(2):266-71.

[79] Godfrey DI, MacDonald HR, Kronenberg M, Smyth MJ, Van Kaer L. NKT cells: what's in a name? Nat Rev Immunol. 2004;4(3):231-7.

[80] Bendelac A. Positive selection of mouse $NK1^+$ T cells by CD1-expressing cortical thymocytes. J. Exp. Med. 1995;182, 2091–2096.

[81] Kovalovsky D, Uche OU, Eladad S, Hobbs RM, Yi W, Alonzo E, Chua K, Eidson M,Kim HJ, Im JS, Pandolfi PP, Sant'Angelo DB. The BTB-zinc finger transcriptional regulator PLZF controls the development of invariant natural killer T cell effector functions. Nat Immunol. 2008;9(9):1055-64.

[82] Savage AK, Constantinides MG, Han J, Picard D, Martin E, Li B, Lantz O, Bendelac A. The transcription factor PLZF directs the effector program of the NKT cell lineage. Immunity. 2008;29(3):391-403.

[83] Matsuda JL, Zhang Q, Ndonye R, Richardson SK, Howell AR, Gapin L. T-bet concomitantly controls migration, survival, and effector functions during the development of Valpha14i NKT cells. Blood. 2006;107(7):2797-805.

[84] Kawano T, Cui J, Koezuka Y, Toura I, Kaneko Y, Motoki K, Ueno H, Nakagawa R, Sato H, Kondo E, Koseki H, Taniguchi M. CD1d-restricted and TCR-mediated activation of valpha14 NKT cells by glycosylceramides. Science. 1997;278(5343):1626-9.

[85] Jerud ES, Bricard G, Porcelli SA. CD1d-Restricted Natural Killer T Cells: Roles in Tumor immunosurveillance and tolerance. Transfus Med Hemother. 2006;33:18–36.

[86] Nakagawa R, Motoki K, Nakamura H, Ueno H, Iijima R, Yamauchi A, Tsuyuki S, Inamoto T, Koezuka Y. Antitumor activity of alpha-galactosylceramide, KRN7000, in mice with EL-4 hepatic metastasis and its cytokine production. Oncol Res. 1998;10(11-12):561-8.

[87] Hayakawa Y, Takeda K, Yagita H, Smyth MJ, Van Kaer L, Okumura K, Saiki I. IFN-gamma-mediated inhibition of tumor angiogenesis by natural killer T-cell ligand, alpha-galactosylceramide. Blood. 2002;100(5):1728-33.

[88] Metelitsa LS, Weinberg KI, Emanuel PD, Seeger RC. Expression of CD1d by myelomonocytic leukemias provides a target for cytotoxic NKT cells. Leukemia. 2003;17(6):1068-77.

[89] Fais F, Morabito F, Stelitano C, Callea V, Zanardi S, Scudeletti M, Varese P, Ciccone E, Grossi CE. CD1d is expressed on B-chronic lymphocytic leukemia cells and mediates alpha-galactosylceramide presentation to natural killer T lymphocytes. Int J Cancer. 2004;109(3):402-11.

[90] Gansert JL, Kiessler V, Engele M, Wittke F, Röllinghoff M, Krensky AM, Porcelli SA, Modlin RL, Stenger S. Human NKT cells express granulysin and exhibit antimycobacterial activity. J Immunol. 2003;170(6):3154-61.

[91] Hegde S, Jankowska-Gan E, Roenneburg DA, Torrealba J, Burlingham WJ, Gumperz JE. Human NKT cells promote monocyte differentiation into suppressive myeloid antigen-presenting cells. J Leukoc Biol. 2009;86(4):757-68.

[92] Hegde S, Lockridge JL, Becker YA, Ma S, Kenney SC, Gumperz JE. Human NKT cells direct the differentiation of myeloid APCs that regulate T cell responses via expression of programmed cell death ligands. J Autoimmun. 2011;37(1):28-38.

[93] Carnaud C, Lee D, Donnars O, Park SH, Beavis A, Koezuka Y, Bendelac A. Cutting edge: Cross-talk between cells of the innate immune system: NKT cells rapidly activate NK cells. J Immunol. 1999;163(9):4647-50.

[94] Eberl G, MacDonald HR. Selective induction of NK cell proliferation and cytotoxicity by activated NKT cells. Eur J Immunol. 2000;30(4):985-92.

[95] Fujii S, Liu K, Smith C, Bonito AJ, Steinman RM. The linkage of innate to adaptive immunity via maturing dendritic cells in vivo requires CD40 ligation in addition to antigen presentation and CD80/86 costimulation. J Exp Med. 2004;199(12):1607-18.

[96] Hermans IF, Silk JD, Gileadi U, Salio M, Mathew B, Ritter G, Schmidt R, Harris AL, Old L, Cerundolo V. NKT cells enhance CD4+ and CD8+ T cell responses to soluble antigen in vivo through direct interaction with dendritic cells. J Immunol. 2003;171(10):5140-7.

[97] Godfrey DI, Kronenberg M. Going both ways: immune regulation via CD1d-dependent NKT cells. J Clin Invest. 2004;114(10):1379-88.

[98] O'Reilly V, Zeng SG, Bricard G, Atzberger A, Hogan AE, Jackson J, Feighery C, Porcelli SA, Doherty DG. Distinct and overlapping effector functions of expanded human CD4+, CD8α+ and CD4-CD8α- invariant natural killer T cells. PLoS One. 2011;6(12):e28648.

[99] Vomhof-DeKrey EE, Yates J, Leadbetter EA. Invariant NKT cells provide innate and adaptive help for B cells. Curr Opin Immunol. 2014;28C:12-17.

[100] Chang PP, Barral P, Fitch J, Pratama A, Ma CS, Kallies A, Hogan JJ, Cerundolo V, Tangye SG, Bittman R, Nutt SL, Brink R, Godfrey DI, Batista FD, Vinuesa CG. Identification of Bcl-6-dependent follicular helper NKT cells that provide cognate help for B cell responses. Nat Immunol. 2011;13(1):35-43.

[101] Leadbetter EA, Brigl M, Illarionov P, Cohen N, Luteran MC, Pillai S, Besra GS, Brenner MB. NK T cells provide lipid antigen-specific cognate help for B cells. Proc Natl Acad Sci U S A. 2008;105(24):8339-44.

[102] Tonti E, Galli G, Malzone C, Abrignani S, Casorati G, Dellabona P. NKT-cell help to B lymphocytes can occur independently of cognate interaction. Blood. 2009;113(2):370-6.

[103] Bai L, Deng S, Reboulet R, Mathew R, Teyton L, Savage PB, Bendelac A. Natural killer T (NKT)-B-cell interactions promote prolonged antibody responses and long-term memory to pneumococcal capsular polysaccharides. Proc Natl Acad Sci U S A. 2013;110(40):16097-102.

[104] Lehuen A, Fazilleau N. Innate iNKT cell help to B cells: fast but does not last. Nat Immunol. 2011;13(1):11-3.

[105] Tilloy F, Treiner E, Park SH, Garcia C, Lemonnier F, de la Salle H, Bendelac A, Bonneville M, Lantz O. An invariant T cell receptor alpha chain defines a novel TAP-independent major histocompatibility complex class Ib-restricted alpha/beta T cell subpopulation in mammals. J Exp Med. 1999;189(12):1907-21.

[106] Dusseaux M, Martin E, Serriari N, Péguillet I, Premel V, Louis D, Milder M, Le Bourhis L, Soudais C, Treiner E, Lantz O. Human MAIT cells are xenobiotic-resistant, tissue-targeted, $CD161^{hi}$ IL-17-secreting T cells. Blood. 2011;117(4):1250-9

[107] Kjer-Nielsen L, Patel O, Corbett AJ, Le Nours J, Meehan B, Liu L, Bhati M, Chen Z, Kostenko L, Reantragoon R, Williamson NA, Purcell AW, Dudek NL, McConville MJ, O'Hair RA, Khairallah GN, Godfrey DI, Fairlie DP, Rossjohn J, McCluskey J. MR1 presents microbial vitamin B metabolites to MAIT cells. Nature. 2012;491(7426):717-23.

[108] Seach N, Guerri L, Le Bourhis L, Mburu Y, Cui Y, Bessoles S, Soudais C, Lantz O. Double-positive thymocytes select mucosal-associated invariant T cells. J Immunol. 2013;191(12):6002-9.

[109] Treiner E, Duban L, Bahram S, Radosavljevic M, Wanner V, Tilloy F, Affaticati P, Gilfillan S, Lantz O. Selection of evolutionarily conserved mucosal-associated invariant T cells by MR1. Nature. 2003;422(6928):164-9. Erratum in: Nature. 2003;423(6943):1018.

[110] Martin E, Treiner E, Duban L, Guerri L, Laude H, Toly C, Premel V, Devys A, Moura IC, Tilloy F, Cherif S, Vera G, Latour S, Soudais C, Lantz O. Stepwise development of MAIT cells in mouse and human. PLoS Biol. 2009;7(3):e54.

[111] Leeansyah E, Loh L, Nixon DF, Sandberg JK. Acquisition of innate-like microbial reactivity in mucosal tissues during human fetal MAIT-cell development. Nat Commun. 2014;5:3143.

[112] Le Bourhis L, Martin E, Péguillet I, Guihot A, Froux N, Coré M, Lévy E, Dusseaux M, Meyssonnier V, Premel V, Ngo C, Riteau B, Duban L, Robert D, Huang S, Rottman M, Soudais C, Lantz O. Antimicrobial activity of mucosal-associated invariant T cells. Nat Immunol. 2010;11(8):701-8. Erratum in: Nat Immunol. 2010;11(10):969. Huang, Xhouxiong [added].

[113] Gérart S, Sibéril S, Martin E, Lenoir C, Aguilar C, Picard C, Lantz O, Fischer A, Latour S. Human iNKT and MAIT cells exhibit a PLZF-dependent proapoptotic propensity that is counterbalanced by XIAP. Blood. 2013;121(4):614-23.

[114] Le Bourhis L, Guerri L, Dusseaux M, Martin E, Soudais C, Lantz O. Mucosal-associated invariant T cells: unconventional development and function.Trends Immunol. 2011;32(5):212-8.

[115] Miley MJ, Truscott SM, Yu YY, Gilfillan S, Fremont DH, Hansen TH, Lybarger L. Biochemical features of the MHC-related protein 1 consistent with an immunological function. J Immunol. 2003;170(12):6090-8.

[116] Walker LJ, Kang YH, Smith MO, Tharmalingham H, Ramamurthy N, Fleming VM, Sahgal N, Leslie A, Oo Y, Geremia A, Scriba TJ, Hanekom WA, Lauer GM, Lantz O, Adams DH, Powrie F, Barnes E, Klenerman P. Human MAIT and CD8αα cells develop from a pool of type-17 precommitted $CD8^+$ T cells. Blood. 2012;119(2):422-33.

[117] Billerbeck E, Kang YH, Walker L, Lockstone H, Grafmueller S, Fleming V, Flint J, Willberg CB, Bengsch B, Seigel B, Ramamurthy N, Zitzmann N, Barnes EJ, Thevanayagam J, Bhagwanani A, Leslie A, Oo YH, Kollnberger S, Bowness P, Drognitz O, Adams DH, Blum HE, Thimme R, Klenerman P. Analysis of CD161 expression on human $CD8^+$ T cells defines a distinct functional subset with tissue-homing properties. Proc Natl Acad Sci U S A. 2010;107(7):3006-11.

[118] Reantragoon R, Corbett AJ, Sakala IG, Gherardin NA, Furness JB, Chen Z, Eckle SB, Uldrich AP, Birkinshaw RW, Patel O, Kostenko L, Meehan B, Kedzierska K, Liu L, Fairlie DP, Hansen TH,

Godfrey DI, Rossjohn J, McCluskey J, Kjer-Nielsen L. Antigen-loaded MR1 tetramers define T cell receptor heterogeneity in mucosal-associated invariant T cells. J Exp Med. 2013;210(11):2305-20.

[119] Walker LJ, Marrinan E, Muenchhoff M, Ferguson J, Kloverpris H, Cheroutre H, Barnes E, Goulder P, Klenerman P. CD8αα Expression Marks Terminally Differentiated Human CD8+ T Cells Expanded in Chronic Viral Infection. Front Immunol. 2013;4:223.

[120] Le Bourhis L, Dusseaux M, Bohineust A, Bessoles S, Martin E, Premel V, Coré M, Sleurs D, Serriari NE, Treiner E, Hivroz C, Sansonetti P, Gougeon ML, Soudais C, Lantz O. MAIT cells detect and efficiently lyse bacterially-infected epithelial cells. PLoS Pathog. 2013;9(10):e1003681.

[121] Lee OJ, Cho YN, Kee SJ, Kim MJ, Jin HM, Lee SJ, Park KJ, Kim TJ, Lee SS, Kwon YS, Kim N, Shin MG, Shin JH, Suh SP, Ryang DW, Park YW. Circulating mucosal-associated invariant T cell levels and their cytokine levels in healthy adults. Exp Gerontol. 2014;49:47-54.

[122] Ussher JE, Bilton M, Attwod E, Shadwell J, Richardson R, de Lara C, Mettke E, Kurioka A, Hansen TH, Klenerman P, Willberg CB. CD161++ CD8+ T cells, including the MAIT cell subset, are specifically activated by IL-12+IL-18 in a TCR-independent manner. Eur J Immunol. 2014;44(1):195-203.

[123] Gold MC, Cerri S, Smyk-Pearson S, Cansler ME, Vogt TM, Delepine J, Winata E, Swarbrick GM, Chua WJ, Yu YY, Lantz O, Cook MS, Null MD, Jacoby DB, Harriff MJ, Lewinsohn DA, Hansen TH, Lewinsohn DM. Human mucosal associated invariant T cells detect bacterially infected cells. PLoS Biol. 2010;8(6):e1000407.

[124] Chua WJ, Truscott SM, Eickhoff CS, Blazevic A, Hoft DF, Hansen TH. Polyclonal mucosa-associated invariant T cells have unique innate functions in bacterial infection. Infect Immun. 2012;80(9):3256-67.

[125] Grimaldi D, Le Bourhis L, Sauneuf B, Dechartres A, Rousseau C, Ouaaz F, Milder M, Louis D, Chiche JD, Mira JP, Lantz O, Pène F. Specific MAIT cell behaviour among innate-like T lymphocytes in critically ill patients with severe infections. Intensive Care Med. 2014;40(2):192-201.

[126] Meierovics A, Yankelevich WJ, Cowley SC. MAIT cells are critical for optimal mucosal immune responses during in vivo pulmonary bacterial infection. Proc Natl Acad Sci U S A. 2013;110(33):E3119-28.

[127] Georgel P, Radosavljevic M, Macquin C, Bahram S. The non-conventional MHC class I MR1 molecule controls infection by Klebsiella pneumoniae in mice. Mol Immunol. 2011;48(5):769-75.

[128] Chiba A, Tajima R, Tomi C, Miyazaki Y, Yamamura T, Miyake S. Mucosal-associated invariant T cells promote inflammation and exacerbate disease in murine models of arthritis. Arthritis Rheum. 2012;64(1):153-61.

[129] Shimamura M, Huang YY, Goji H, Endo S, Migishima R, Yokoyama M. Regulation of immunological disorders by invariant Vα19-Jα33 TCR-bearing cells. Immunobiology. 2011;216(3):374-8.

[130] Croxford JL, Miyake S, Huang YY, Shimamura M, Yamamura T. Invariant V(alpha)19i T cells regulate autoimmune inflammation. Nat Immunol. 2006;7(9):987-94.

[131] Miyazaki Y, Miyake S, Chiba A, Lantz O, Yamamura T. Mucosal-associated invariant T cells regulate Th1 response in multiple sclerosis. Int Immunol. 2011;23(9):529-35.

[132] Serriari NE, Eoche M, Lamotte L, Lion J, Fumery M, Marcelo P, Chatelain D, Barre A, Nguyen-Khac E, Lantz O, Dupas JL, Treiner E. Innate mucosal-associated invariant T (MAIT) cells are activated in inflammatory bowel diseases. Clin Exp Immunol. 2014;176(2):266-74.

[133] Teunissen MB, Yeremenko NG, Baeten DL, Chielie S, Spuls PI, de Rie MA, Lantz O, Res PC. The IL-17A-producing CD8+ T-cell population in psoriatic lesional skin comprises mucosa-associated invariant T cells and conventional T cells. J Invest Dermatol. 2014;134(12):2898-907.

[134] Cosgrove C, Ussher JE, Rauch A, Gärtner K, Kurioka A, Hühn MH, Adelmann K, Kang YH, Fergusson JR, Simmonds P, Goulder P, Hansen TH, Fox J, Günthard HF, Khanna N, Powrie F, Steel A, Gazzard B, Phillips RE, Frater J, Uhlig H, Klenerman P. Early and nonreversible decrease of CD161++ /MAIT cells in HIV infection. Blood. 2013;121(6):951-61.

[135] Leeansyah E, Ganesh A, Quigley MF, Sönnerborg A, Andersson J, Hunt PW, Somsouk M, Deeks SG, Martin JN, Moll M, Shacklett BL, Sandberg JK. Activation, exhaustion, and persistent decline of the antimicrobial MR1-restricted MAIT-cell population in chronic HIV-1 infection. Blood. 2013;121(7):1124-35.

[136] Wong EB, Akilimali NA, Govender P, Sullivan ZA, Cosgrove C, Pillay M, Lewinsohn DM, Bishai WR, Walker BD, Ndung'u T, Klenerman P, Kasprowicz VO. Low levels of peripheral CD161++CD8+ mucosal associated invariant T (MAIT) cells are found in HIV and HIV/TB co-infection. PLoS One. 2013;8(12):e83474.

[137] Thompson FM, van Wilgenburg B, Ramamurthy N, Willberg C, Oo YH, Fabris P, Klenerman P. Hepatitis C virus potently activates human CD161++/MAIT (Mucosal Associated Invariant T) cells. 49th annual meeting of the European association for the study of the liver, April 9-13, 2014 - London, United Kingdom.

[138] Treiner E, Duban L, Moura IC, Hansen T, Gilfillan S, Lantz O. Mucosal-associated invariant T (MAIT) cells: an evolutionarily conserved T cell subset. Microbes Infect. 2005;7(3):552-9.

[139] Wakao H, Yoshikiyo K, Koshimizu U, Furukawa T, Enomoto K, Matsunaga T, Tanaka T, Yasutomi Y, Yamada T, Minakami H, Tanaka J, Oda A, Sasaki T, Wakao R, Lantz O, Udagawa T, Sekiya Y, Higuchi K, Harada N, Nishimura K, Ohtaka M, Nakanishi M, Fujita H. Expansion of functional human mucosal-associated invariant T cells via reprogramming to pluripotency and redifferentiation. Cell Stem Cell. 2013;12(5):546-58.

[140] Takeda K, Cretney E, Hayakawa Y, Ota T, Akiba H, Ogasawara K, Yagita H, Kinoshita K, Okumura K, Smyth MJ. TRAIL identifies immature natural killer cells in newborn mice and adult mouse liver. Blood. 2005;105(5):2082-9.

[141] Zamai L, Ahmad M, Bennett IM, Azzoni L, Alnemri ES, Perussia B. Natural killer (NK) cell-mediated cytotoxicity: differential use of TRAIL and Fas ligand by immature and mature primary human NK cells. J Exp Med. 1998;188(12):2375-80.

[142] Ranson T, Vosshenrich CA, Corcuff E, Richard O, Müller W, Di Santo JP. IL-15 is an essential mediator of peripheral NK-cell homeostasis. Blood. 2003;101(12):4887-93.

[143] Marcoe JP, Lim JR, Schaubert KL, Fodil-Cornu N, Matka M, McCubbrey AL, Farr AR, Vidal SM, Laouar Y. TGF-β is responsible for NK cell immaturity during ontogeny and increased susceptibility to infection during mouse infancy. Nat Immunol. 2012;13(9):843-50.

[144] Cooper MA, Fehniger TA, Turner SC, Chen KS, Ghaheri BA, Ghayur T, Carson WE, Caligiuri MA. Human natural killer cells: a unique innate immunoregulatory role for the CD56(bright) subset. Blood. 2001;97(10):3146-51.

[145] Maeda N, Izumiya C, Taniguchi K, Matsushima S, Fukaya T. Role of NK cells and HLA-G in endometriosis. Front Biosci (Schol Ed). 2012;4:1568-81.

[146] Jacobs R, Hintzen G, Kemper A, Beul K, Kempf S, Behrens G, Sykora KW, Schmidt RE. CD56bright cells differ in their KIR repertoire and cytotoxic features from CD56dim NK cells. Eur J Immunol. 2001;31(10):3121-7.

[147] Fehniger TA, Cooper MA, Nuovo GJ, Cella M, Facchetti F, Colonna M, Caligiuri MA. 2003. $CD56^{bright}$ natural killer cells are present in human lymph nodes and are activated by T cell-derived IL-2: a potential new link between adaptive and innate immunity. Blood. 101(8):3052-7.

[148] Di Santo JP. Natural killer cell developmental pathways: a question of balance. Annu Rev Immunol. 2006;24:257-86.

[149] Sun JC, Beilke JN, Lanier LL. Adaptive immune features of natural killer cells. Nature. 2009;457(7229):557-61. Erratum in:Nature. 457(7233):1168.

[150] Sun JC, Lopez-Verges S, Kim CC, DeRisi JL, Lanier LL. NK cells and immune "memory". J Immunol. 2011;186(4):1891-7.

[151] Satoh M, Seki S, Hashimoto W, Ogasawara K, Kobayashi T, Kumagai K, Matsuno S, Takeda K. Cytotoxic gammadelta or alphabeta T cells with a natural killer cell marker, CD56, induced from human peripheral blood lymphocytes by a combination of IL-12 and IL-2. J Immunol. 1996;157(9):3886-92

[152] Lu PH, Negrin RS. A novel population of expanded human CD3+CD56+ cells derived from T cells with potent in vivo antitumor activity in mice with severe combined immunodeficiency. J Immunol. 1994;153(4):1687-96.

[153] Kelly-Rogers J, Madrigal-Estebas L, O'Connor T, Doherty DG. Activation-induced expression of CD56 by T cells is associated with a reprogramming of cytolytic activity and cytokine secretion profile in vitro. Hum Immunol. 2006;67(11):863-73.

[154] Linn YC, Hui KM. Cytokine-induced killer cells: NK-like T cells with cytotolytic specificity against leukemia. Leuk Lymphoma. 2003;44(9):1457-62.

[155] Doherty DG, Norris S, Madrigal-Estebas L, McEntee G, Traynor O, Hegarty JE, O'Farrelly C. The human liver contains multiple populations of NK cells, T cells, and CD3+CD56+ natural T cells with distinct cytotoxic activities and Th1, Th2, and Th0 cytokine secretion patterns. J Immunol. 1999;163(4):2314-21.

[156] Barnaba V, Franco A, Paroli M, Benvenuto R, De Petrillo G, Burgio VL, Santilio I, Balsano C, Bonavita MS, Cappelli G. Selective expansion of cytotoxic T lymphocytes with a CD4+CD56+ surface phenotype and a T helper type 1 profile of cytokine secretion in the liver of patients chronically infected with Hepatitis B virus. J Immunol. 1994;152(6):3074-87.

[157] Cuss AK, Avery DT, Cannons JL, Yu LJ, Nichols KE, Shaw PJ, Tangye SG. Expansion of functionally immature transitional B cells is associated with human-immunodeficient states characterized by impaired humoral immunity. J Immunol. 2006;176(3):1506-16.

[158] Piqueras B, Lavenu-Bombled C, Galicier L, Bergeron-van der Cruyssen F, Mouthon L, Chevret S, Debré P, Schmitt C, Oksenhendler E. Common variable immunodeficiency patient classification based on impaired B cell memory differentiation correlates with clinical aspects. J Clin Immunol. 2003;23(5):385-400.

[159] Warnatz K, Denz A, Dräger R, Braun M, Groth C, Wolff-Vorbeck G, Eibel H, Schlesier M, Peter HH. Severe deficiency of switched memory B cells (CD27(+)IgM(-)IgD(-)) in subgroups of patients with common variable immunodeficiency: a new approach to classify a heterogeneous disease. Blood. 2002;99(5):1544-51.

[160] Wehr C, Kivioja T, Schmitt C, Ferry B, Witte T, Eren E, Vlkova M, Hernandez M, Detkova D, Bos PR, Poerksen G, von Bernuth H, Baumann U, Goldacker S, Gutenberger S, Schlesier M, Bergeron-van der Cruyssen F, Le Garff M, Debré P, Jacobs R, Jones J, Bateman E, Litzman J, van Hagen PM, Plebani A, Schmidt RE, Thon V, Quinti I, Espanol T, Webster AD, Chapel H, Vihinen M, Oksenhendler E, Peter HH, Warnatz K. The EUROclass trial: defining subgroups in common variable immunodeficiency. Blood. 2008;111(1):77-85.

[161] Giovannetti A, Pierdominici M, Mazzetta F, Marziali M, Renzi C, Mileo AM, De Felice M, Mora B, Esposito A, Carello R, Pizzuti A, Paggi MG, Paganelli R, Malorni W, Aiuti F. Unravelling the complexity of T cell abnormalities in common variable immunodeficiency. J Immunol. 2007;178(6):3932-43.

[162] Wright JJ, Wagner DK, Blaese RM, Hagengruber C, Waldmann TA, Fleisher TA. Characterization of common variable immunodeficiency: identification of a subset of patients with distinctive immunophenotypic and clinical features. Blood. 1990;76(10):2046-51.

[163] Bateman EA, Ayers L, Sadler R, Lucas M, Roberts C, Woods A, Packwood K, Burden J, Harrison D, Kaenzig N, Lee M, Chapel HM, Ferry BL. T cell phenotypes in patients with common variable immunodeficiency disorders: associations with clinical phenotypes in comparison with other groups with recurrent infections. Clin Exp Immunol. 2012;170(2):202-11.

[164] Viallard JF, Blanco P, André M, Etienne G, Liferman F, Neau D, Vidal E, Moreau JF, Pellegrin JL. CD8+HLA-DR+ T lymphocytes are increased in common variable immunodeficiency patients with impaired memory B-cell differentiation. Clin Immunol. 2006;119(1):51-8.

[165] Perreau M, Vigano S, Bellanger F, Pellaton C, Buss G, Comte D, Roger T, Lacabaratz C, Bart PA, Levy Y, Pantaleo G. Exhaustion of bacteria-specific CD4 T cells and microbial translocation in common variable immunodeficiency disorders. J Exp Med. 2014;211(10):2033-45.

[166] Marashi SM, Raeiszadeh M, Enright V, Tahami F, Workman S, Chee R, Webster AD, Milne RS, Emery VC. Influence of cytomegalovirus infection on immune cell phenotypes in patients with common variable immunodeficiency. J Allergy Clin Immunol. 2012;129(5):1349-1356.e3.

[167] Carter CR, Aravind G, Smalle NL, Cole JY, Savic S, Wood PM. CVID patients with autoimmunity have elevated T cell expression of granzyme B and HLA-DR and reduced levels of Treg cells. J Clin Pathol. 2013;66(2):146-50.

[168] Horn J, Manguiat A, Berglund LJ, Knerr V, Tahami F, Grimbacher B, Fulcher DA. Decrease in phenotypic regulatory T cells in subsets of patients with common variable immunodeficiency. Clin Exp Immunol. 2009;156(3):446-54.

[169] Fulcher DA, Avery DT, Fewings NL, Berglund LJ, Wong S, Riminton DS, Adelstein S, Tangye SG. Invariant natural killer (iNK) T cell deficiency in patients with common variable immunodeficiency. Clin Exp Immunol. 2009;157(3):365-9.

[170] Aspalter RM, Sewell WA, Dolman K, Farrant J, Webster AD. Deficiency in circulating natural killer (NK) cell subsets in common variable immunodeficiency and X-linked agammaglobulinaemia. Clin Exp Immunol. 2000;121(3):506-14.

[171] Cunningham-Rundles C, Radigan L. Deficient IL-12 and dendritic cell function in common variable immune deficiency. Clin Immunol. 2005;115(2):147-53.

[172] Bayry J, Lacroix-Desmazes S, Kazatchkine MD, Galicier L, Lepelletier Y, Webster D, Lévy Y, Eibl MM, Oksenhendler E, Hermine O, Kaveri SV. Common variable immunodeficiency is associated with defective functions of dendritic cells. Blood. 2004;104(8):2441-3.

[173] Rezaei N, Siadat SD, Aghamohammadi A, Moin M, Pourpak Z, Norouzian D, Mobarakeh JI, Aghasadeghi MR, Nejati M, Read RC. Serum bactericidal antibody response 1 year after meningococcal polysaccharide vaccination of patients with common variable immunodeficiency. Clin Vaccine Immunol. 2010;17(4):524-8.

[174] Pedersen G, Halstensen A, Sjursen H, Naess A, Kristoffersen EK, Cox RJ. Pandemic influenza vaccination elicits influenza-specific CD4+ Th1-cell responses in hypogammaglobulinaemic patients: four case reports. Scand J Immunol. 2011;74(2):210-8.

[175] Clemente A, Pons J, Matamoros N, Iglesias J, Ferrer JM. B cells from common variable immunodeficiency patients fail to differentiate to antibody secreting cells in response to TLR9 ligand (CpG-ODN) or anti-CD40+IL21. Cell Immunol. 2011;268(1):9-15.

[176] Escobar D, Pons J, Clemente A, Iglesias J, Regueiro V, Bengoechea JA, Matamoros N, Ferrer JM. Defective B cell response to TLR9 ligand (CpG-ODN), Streptococcus pneumoniae and Haemophilus influenzae extracts in common variable immunodeficiency patients. Cell Immunol. 2010;262(2):105-11.

[177] He B, Qiao X, Cerutti A. CpG DNA induces IgG class switch DNA recombination by activating human B cells through an innate pathway that requires TLR9 and cooperates with IL-10. J Immunol. 2004;173(7):4479-91.

[178] Chapel H, Lucas M, Lee M, Bjorkander J, Webster D, Grimbacher B, Fieschi C, Thon V, Abedi MR, Hammarstrom L. Common variable immunodeficiency disorders: division into distinct clinical phenotypes. Blood. 2008;112(2):277-86.

[179] Montoya CJ, Pollard D, Martinson J, Kumari K, Wasserfall C, Mulder CB, Rugeles MT, Atkinson MA, Landay AL, Wilson SB. Characterization of human invariant natural killer T subsets in health and disease using a novel invariant natural killer T cell-clonotypic monoclonal antibody, 6B11. Immunology. 2007;122(1):1-14.

[180] Meddows-Taylor S, Shalekoff S, Kuhn L, Gray GE, Tiemessen CT. Development of a whole blood intracellular cytokine staining assay for mapping CD4(+) and CD8(+) T-cell responses across the HIV-1 genome. J Virol Methods. 2007;144(1-2):115-21.

[181] Simms PE, Ellis TM. Utility of flow cytometric detection of CD69 expression as a rapid method for determining poly- and oligoclonal lymphocyte activation. Clin Diagn Lab Immunol. 1996;3(3):301-4.

[182] Chattopadhyay PK, Yu J, Roederer M. A live-cell assay to detect antigen-specific CD4+ T cells with diverse cytokine profiles. Nat Med. 2005;11(10):1113-7)

[183] Rakhmanov M, Keller B, Gutenberger S, Foerster C, Hoenig M, Driessen G, van der Burg M, van Dongen JJ, Wiech E, Visentini M, Quinti I, Prasse A, Voelxen N, Salzer U, Goldacker S, Fisch P, Eibel H, Schwarz K, Peter HH, Warnatz K. Circulating CD21low B cells in common variable immunodeficiency resemble tissue homing, innate-like B cells. Proc Natl Acad Sci U S A. 2009;106(32):13451-6.

[184] Isnardi I, Ng YS, Menard L, Meyers G, Saadoun D, Srdanovic I, Samuels J, Berman J, Buckner JH, Cunningham-Rundles C, Meffre E. Complement receptor 2/CD21- human naive B cells contain mostly autoreactive unresponsive clones. Blood. 2010;115(24):5026-36.

[185] Suryani S, Fulcher DA, Santner-Nanan B, Nanan R, Wong M, Shaw PJ, Gibson J, Williams A, Tangye SG. Differential expression of CD21 identifies developmentally and functionally distinct subsets of human transitional B cells. Blood. 2010;115(3):519-29.

[186] Warnatz K, Bossaller L, Salzer U, Skrabl-Baumgartner A, Schwinger W, van der Burg M, van Dongen JJ, Orlowska-Volk M, Knoth R, Durandy A, Draeger R, Schlesier M, Peter HH, Grimbacher B. Human ICOS deficiency abrogates the germinal center reaction and provides a monogenic model for common variable immunodeficiency. Blood. 2006;107(8):3045-52.

[187] Bossaller L, Burger J, Draeger R, Grimbacher B, Knoth R, Plebani A, Durandy A, Baumann U, Schlesier M, Welcher AA, Peter HH, Warnatz K. ICOS deficiency is associated with a severe reduction of CXCR5+CD4 germinal center Th cells. J Immunol. 2006;177(7):4927-32.

[188] Unger S, Seidl M, Schmitt-Graeff A, Böhm J, Schrenk K, Wehr C, Goldacker S, Dräger R, Gärtner BC, Fisch P, Werner M, Warnatz K. Ill-defined germinal centers and severely reduced plasma cells are histological hallmarks of lymphadenopathy in patients with common variable immunodeficiency. J Clin Immunol. 2014;34(6):615-26.

[189] Agematsu K, Nagumo H, Shinozaki K, Hokibara S, Yasui K, Terada K, Kawamura N, Toba T, Nonoyama S, Ochs HD, Komiyama A. Absence of IgD-CD27(+) memory B cell population in X-linked hyper-IgM syndrome. J Clin Invest. 1998;102(4):853-60.

[190] Weller S, Faili A, Garcia C, Braun MC, Le Deist F F, de Saint Basile G G, Hermine O, Fischer A, Reynaud CA, Weill JC. CD40-CD40L independent Ig gene hypermutation suggests a second B cell diversification pathway in humans. Proc Natl Acad Sci U S A. 2001;98(3):1166-70.

[191] Weller S, Braun MC, Tan BK, Rosenwald A, Cordier C, Conley ME, Plebani A, Kumararatne DS, Bonnet D, Tournilhac O, Tchernia G, Steiniger B, Staudt LM, Casanova JL, Reynaud CA, Weill JC. Human blood IgM "memory" B cells are circulating splenic marginal zone B cells harboring a prediversified immunoglobulin repertoire. Blood. 2004;104(12):3647-54.

[192] Berkowska MA, Driessen GJ, Bikos V, Grosserichter-Wagener C, Stamatopoulos K, Cerutti A, He B, Biermann K, Lange JF, van der Burg M, van Dongen JJ, van Zelm MC. Human memory B cells originate from three distinct germinal center-dependent and -independent maturation pathways. Blood. 2011;118(8):2150-8.

[193] Gao Y, Workman S, Gadola S, Elliott T, Grimbacher B, Williams AP. Common variable immunodeficiency is associated with a functional deficiency of invariant natural killer T cells. J Allergy Clin Immunol. 2014;133(5):1420-8, 1428.e1.

[194] Bosma A, Abdel-Gadir A, Isenberg DA, Jury EC, Mauri C. Lipid-antigen presentation by CD1d(+) B cells is essential for the maintenance of invariant natural killer T cells. Immunity. 2012;36(3):477-90.

[195] Mattner J, Debord KL, Ismail N, Goff RD, Cantu C 3rd, Zhou D, Saint-Mezard P, Wang V, Gao Y, Yin N, Hoebe K, Schneewind O, Walker D, Beutler B, Teyton L, Savage PB, Bendelac A. Exogenous and endogenous glycolipid antigens activate NKT cells during microbial infections. Nature. 2005;434(7032):525-9.

[196] Kinjo Y, Illarionov P, Vela JL, Pei B, Girardi E, Li X, Li Y, Imamura M, Kaneko Y, Okawara A, Miyazaki Y, Gómez-Velasco A, Rogers P, Dahesh S, Uchiyama S, Khurana A, Kawahara K, Yesilkaya H, Andrew PW, Wong CH, Kawakami K, Nizet V, Besra GS, Tsuji M, Zajonc DM, Kronenberg M. Invariant natural killer T cells recognize glycolipids from pathogenic Gram-positive bacteria. Nat Immunol. 2011;12(10):966-74.

[197] Miyamoto K, Miyake S, Yamamura T. A synthetic glycolipid prevents autoimmune encephalomyelitis by inducing TH2 bias of natural killer T cells. Nature. 2001;413(6855):531-4.

[198] Godó M, Sessler T, Hamar P. Role of invariant natural killer T (iNKT) cells in systemic lupus erythematosus. Curr Med Chem. 2008;15(18):1778-87.

[199] van der Vliet HJ, von Blomberg BM, Nishi N, Reijm M, Voskuyl AE, van Bodegraven AA, Polman CH, Rustemeyer T, Lips P, van den Eertwegh AJ, Giaccone G, Scheper RJ, Pinedo HM. Circulating V(alpha24+) Vbeta11+ NKT cell numbers are decreased in a wide variety of diseases that are characterized by autoreactive tissue damage. Clin Immunol. 2001;100(2):144-8.

[200] Parietti V, Chifflot H, Sibilia J, Muller S, Monneaux F. Rituximab treatment overcomes reduction of regulatory iNKT cells in patients with rheumatoid arthritis. Clin Immunol. 2010;134(3):331-9.

[201] Jin W and Dong C. IL-17 cytokines in immunity and inflammation. Emerging Microbes & Infections. 2013;2(9):e60.

[202] Snyder-Cappione JE, Nixon DF, Chi JC, Nguyen ML, Kirby CK, Milush JM, Koth LL. Invariant natural killer T (iNKT) cell exhaustion in sarcoidosis. Eur J Immunol. 2013;43(8):2194-205.

[203] Kyriakakis E, Cavallari M, Andert J, Philippova M, Koella C, Bochkov V, Erne P, Wilson SB, Mori L, Biedermann BC, Resink TJ, De Libero G. Invariant natural killer T cells: linking inflammation and neovascularization in human atherosclerosis. Eur J Immunol. 2010 Nov;40(11):3268-79.

[204] Molling JW, Kölgen W, van der Vliet HJ, Boomsma MF, Kruizenga H, Smorenburg CH, Molenkamp BG, Langendijk JA, Leemans CR, von Blomberg BM, Scheper RJ, van den Eertwegh AJ. Peripheral blood IFN-gamma-secreting Valpha24+Vbeta11+ NKT cell numbers are decreased in cancer patients independent of tumor type or tumor load. Int J Cancer. 2005;116(1):87-93.

[205] Suzuki Y, Onodera H, Tago H, Saito R, Ohuchi M, Shimizu M, Itoyama Y. Altered populations of natural killer cell and natural killer T cell subclasses in myasthenia gravis. J Neuroimmunol. 2005;167(1-2):186-9.

[206] Petrasca A, Doherty DG. Human Vδ2(+) γδ T Cells differentially induce maturation, cytokine production, and alloreactive T Cell stimulation by dendritic cells and B cells. Front Immunol. 2014;5:650

[207] Lynch L, Michelet X, Zhang S, Brennan PJ, Moseman A, Lester C, Besra G, Vomhof-Dekrey EE, Tighe M, Koay HF, Godfrey DI, Leadbetter EA, Sant'Angelo DB, von Andrian U, Brenner MB. Regulatory iNKT cells lack expression of the transcription factor PLZF and control the homeostasis of T(reg) cells and macrophages in adipose tissue. Nat Immunol. 2015;16(1):85-95.

[208] Zeng SG, Ghnewa YG, O'Reilly VP, Lyons VG, Atzberger A, Hogan AE, Exley MA, Doherty DG. Human invariant NKT cell subsets differentially promote differentiation, antibody production, and T cell stimulation by B cells in vitro. J Immunol. 2013;191(4):1666-76.

[209] Bender R, Lange S. Multiple test procedures other than Bonferroni's deserve wider use. BMJ. 1999;318(7183):600-1.

[210] Bender R, Lange S. Adjusting for multiple testing--when and how? J Clin Epidemiol. 2001;54(4):343-9.

[211] Kersten CM, McCluskey RT, Boyle LA, Kurnick JT. Escherichia coli and Pseudomonas aeruginosa induce expansion of V delta 2 cells in adult peripheral blood, but of V delta 1 cells in cord blood. J Immunol. 1996;157(4):1613-9.

[212] Sköld M, Behar SM. Role of CD1d-restricted NKT cells in microbial immunity. Infect Immun. 2003;71(10):5447-55.

[213] Pellicci DG, Uldrich AP, Le Nours J, Ross F, Chabrol E, Eckle SB, de Boer R, Lim RT, McPherson K, Besra G, Howell AR, Moretta L, McCluskey J, Heemskerk MH, Gras S, Rossjohn J, Godfrey DI. The molecular bases of δ/αβ T cell-mediated antigen recognition. J Exp Med. 2014;211(13):2599-615.

[214] Orsini DL, van Gils M, Kooy YM, Struyk L, Klein G, van den Elsen P, Koning F. Functional and molecular characterization of B cell-responsive V delta 1+ gamma delta T cells. Eur J Immunol. 1994;24(12):3199-204.

[215] Russano AM, Agea E, Corazzi L, Postle AD, De Libero G, Porcelli S, de Benedictis FM, Spinozzi F. Recognition of pollen-derived phosphatidyl-ethanolamine by human CD1d-restricted gamma delta T cells. J Allergy Clin Immunol. 2006;117(5):1178-84.

[216] Fenoglio D, Poggi A, Catellani S, Battaglia F, Ferrera A, Setti M, Murdaca G, Zocchi MR. Vdelta1 T lymphocytes producing IFN-gamma and IL-17 are expanded in HIV-1-infected patients and respond to Candida albicans. Blood. 2009;113(26):6611-8.

[217] Rush JS, Hodgkin PD. B cells activated via CD40 and IL-4 undergo a division burst but require continued stimulation to maintain division, survival and differentiation. Eur J Immunol. 2001;31(4):1150-9.

[218] Rousset F, Garcia E, Defrance T, Péronne C, Vezzio N, Hsu DH, Kastelein R, Moore KW, Banchereau J. Interleukin 10 is a potent growth and differentiation factor for activated human B lymphocytes. Proc Natl Acad Sci U S A. 1992;89(5):1890-3.

[219] Tangye SG, Ferguson A, Avery DT, Ma CS, Hodgkin PD. Isotype switching by human B cells is division-associated and regulated by cytokines. J Immunol. 2002;169(8):4298-306.

[220] Rutz S, Eidenschenk C, Ouyang W. IL-22, not simply a Th17 cytokine. Immunol Rev. 2013;252(1):116-32.

[221] van Kooten C, Banchereau J. CD40-CD40 ligand. J Leukoc Biol. 2000;67(1):2-17.

[222] Farrington M, Grosmaire LS, Nonoyama S, Fischer SH, Hollenbaugh D, Ledbetter JA, Noelle RJ, Aruffo A, Ochs HD. CD40 ligand expression is defective in a subset of patients with common variable immunodeficiency. Proc Natl Acad Sci U S A. 1994;91(3):1099-103.

[223] Hara T, Jung LK, Bjorndahl JM, Fu SM. Human T cell activation. III. Rapid induction of a phosphorylated 28 kD/32 kD disulfide-linked early activation antigen (EA 1) by 12-o-tetradecanoyl phorbol-13-acetate, mitogens, and antigens. J Exp Med. 1986;164(6):1988-2005.

[224] Biselli R, Matricardi PM, D'Amelio R, Fattorossi A. Multiparametric flow cytometric analysis of the kinetics of surface molecule expression after polyclonal activation of human peripheral blood T lymphocytes. Scand J Immunol. 1992;35(4):439-47.

[225] Marzio R, Mauël J, Betz-Corradin S. CD69 and regulation of the immune function. Immunopharmacol Immunotoxicol. 1999;21(3):565-82.

[226] Lougaris V, Baronio M, Vitali M, Tampella G, Soresina A, Badolato R, Plebani A. B cell responses to CpG correlate with CXCL16 expression levels in common variable immunodeficiency. ScientificWorldJournal. 2012:960219.

[227] Thon V, Wolf HM, Sasgary M, Litzman J, Samstag A, Hauber I, Lokaj J, Eibl MM. Defective integration of activating signals derived from the T cell receptor (TCR) and costimulatory molecules

in both CD4+ and CD8+ T lymphocytes of common variable immunodeficiency (CVID) patients. Clin Exp Immunol. 1997;110(2):174-81.

[228] Lin SJ, Chao HC, Chang KW, Yan DC. Effect of interleukin 15 and interleukin 2 on anti-CD3-induced T-cell activation and apoptosis in children with common variable immunodeficiency. Ann Allergy Asthma Immunol. 2003;91(1):65-70.

[229] Bradley JR. TNF-mediated inflammatory disease. J Pathol. 2008;214(2):149-60.

[230] Snapper CM, Finkelman FD, Paul WE. Differential regulation of IgG1 and IgE synthesis by interleukin 4. J Exp Med. 1988;167(1):183-96.

[231] Carolan E, Tobin LM, Mangan BA, Corrigan M, Gaoatswe G, Byrne G, Geoghegan J, Cody D, O'Connell J, Winter DC, Doherty DG, Lynch L, O'Shea D, Hogan AE. Altered distribution and increased IL-17 production by mucosal-associated invariant T cells in adult and childhood obesity. J Immunol. 2015;194(12):5775-80.

[232] Brière F, Servet-Delprat C, Bridon JM, Saint-Remy JM, Banchereau J. Human interleukin 10 induces naive surface immunoglobulin D+ (sIgD+) B cells to secrete IgG1 and IgG3. J Exp Med. 1994;179(2):757–762.

[233] Craft JE. Follicular helper T cells in immunity and systemic autoimmunity. Nat Rev Rheumatol. 2012;8(6):337-47.

[234] Crotty S. Follicular helper CD4 T cells (TFH). Annu Rev Immunol. 2011;29:621-63.

[235] Wykes M, Pombo A, Jenkins C, MacPherson GG. Dendritic cells interact directly with naive B lymphocytes to transfer antigen and initiate class switching in a primary T-dependent response. J Immunol. 1998;161(3):1313-9.

[236] Wykes M, MacPherson G. Dendritic cell-B-cell interaction: dendritic cells provide B cells with CD40-independent proliferation signals and CD40-dependent survival signals. Immunology. 2000;100(1):1-3.

[237] Thomas D, Dauwalder O, Brun V, Badiou C, Ferry T, Etienne J, Vandenesch F, Lina G. Staphylococcus aureus superantigens elicit redundant and extensive human Vbeta patterns. Infect Immun. 2009;77(5):2043-50.

[238] Li PL, Tiedemann RE, Moffat SL, Fraser JD. The superantigen streptococcal pyrogenic exotoxin C (SPE-C) exhibits a novel mode of action. J Exp Med. 1997;186(3):375-83.

[239] Douek DC, McFarland RD, Keiser PH, Gage EA, Massey JM, Haynes BF, Polis MA, Haase AT, Feinberg MB, Sullivan JL, Jamieson BD, Zack JA, Picker LJ, Koup RA. Changes in thymic function with age and during the treatment of HIV infection. Nature. 1998;396(6712):690-5.

[240] van Zelm MC, Szczepanski T, van der Burg M, van Dongen JJ. Replication history of B lymphocytes reveals homeostatic proliferation and extensive antigen-induced B cell expansion. J Exp Med. 2007;204(3):645-55.

[241] Routes JM, Grossman WJ, Verbsky J, Laessig RH, Hoffman GL, Brokopp CD, Baker MW. Statewide newborn screening for severe T-cell lymphopenia. JAMA. 2009;302(22):2465-70.

[242] Nakagawa N, Imai K, Kanegane H, Sato H, Yamada M, Kondoh K, Okada S, Kobayashi M, Agematsu K, Takada H, Mitsuiki N, Oshima K, Ohara O, Suri D, Rawat A, Singh S, Pan-Hammarström Q, Hammarström L, Reichenbach J, Seger R, Ariga T, Hara T, Miyawaki T, Nonoyama S. Quantification of κ-deleting recombination excision circles in Guthrie cards for the identification of early B-cell maturation defects. J Allergy Clin Immunol. 2011;128(1):223-225.e2.

[243] Borte S, von Döbeln U, Fasth A, Wang N, Janzi M, Winiarski J, Sack U, Pan-Hammarström Q, Borte M, Hammarström L. Neonatal screening for severe primary immunodeficiency diseases using high-throughput triplex real-time PCR. Blood. 2012;119(11):2552-5.

[244] Singh AK, Wilson MT, Hong S, Olivares-Villagómez D, Du C, Stanic AK, Joyce S, Sriram S, Koezuka Y, Van Kaer L. Natural killer T cell activation protects mice against experimental autoimmune encephalomyelitis. J Exp Med. 2001;194(12):1801-11.

[245] Oh K, Byoun OJ, Ham DI, Kim YS, Lee DS. Invariant NKT cells regulate experimental autoimmune uveitis through inhibition of Th17 differentiation. Eur J Immunol. 2011;41(2):392-402.

[246] Sharif S, Arreaza GA, Zucker P, Mi QS, Sondhi J, Naidenko OV, Kronenberg M, Koezuka Y, Delovitch TL, Gombert JM, Leite-De-Moraes M, Gouarin C, Zhu R, Hameg A, Nakayama T, Taniguchi M, Lepault F, Lehuen A, Bach JF, Herbelin A. Activation of natural killer T cells by alpha-galactosylceramide treatment prevents the onset and recurrence of autoimmune Type 1 diabetes. Nat Med. 2001;7(9):1057-62.

[247] Ortega C, Fernández-A S, Carrillo JM, Romero P, Molina IJ, Moreno JC, Santamaría M. IL-17-producing CD8+ T lymphocytes from psoriasis skin plaques are cytotoxic effector cells that secrete Th17-related cytokines. J Leukoc Biol. 2009;86(2):435-43.

[248] Res PC, Piskin G, de Boer OJ, van der Loos CM, Teeling P, Bos JD, Teunissen MB. Overrepresentation of IL-17A and IL-22 producing CD8 T cells in lesional skin suggests their involvement in the pathogenesis of psoriasis. PLoS One. 2010;5(11):e14108.

[249] Washington K, Stenzel TT, Buckley RH, Gottfried MR. Gastrointestinal pathology in patients with common variable immunodeficiency and X-linked agammaglobulinemia. Am J Surg Pathol. 1996;20(10):1240-52.

[250] Daniels JA, Lederman HM, Maitra A, Montgomery EA. Gastrointestinal tract pathology in patients with common variable immunodeficiency (CVID): a clinicopathologic study and review. Am J Surg Pathol. 2007;31(12):1800-12.

[251] Brown I, Mino-Kenudson M, Deshpande V, Lauwers GY. Intraepithelial lymphocytosis in architecturally preserved proximal small intestinal mucosa: an increasing diagnostic problem with a wide differential diagnosis. Arch Pathol Lab Med. 2006;130(7):1020-5.

[252] Gathmann B, Mahlaoui N; CEREDIH, Gérard L, Oksenhendler E, Warnatz K, Schulze I, Kindle G, Kuijpers TW; Dutch WID, van Beem RT, Guzman D, Workman S, Soler-Palacín P, De Gracia J, Witte T, Schmidt RE, Litzman J, Hlavackova E, Thon V, Borte M, Borte S, Kumararatne D, Feighery C, Longhurst H, Helbert M, Szaflarska A, Sediva A, Belohradsky BH, Jones A, Baumann U, Meyts I, Kutukculer N, Wågström P, Galal NM, Roesler J, Farmaki E, Zinovieva N, Ciznar P, Papadopoulou-Alataki E, Bienemann K, Velbri S, Panahloo Z, Grimbacher B; European Society for Immunodeficiencies Registry Working Party. Clinical picture and treatment of 2212 patients with common variable immunodeficiency. J Allergy Clin Immunol. 2014;134(1):116-26.

[253] Mannon PJ, Fuss IJ, Dill S, Friend J, Groden C, Hornung R, Yang Z, Yi C, Quezado M, Brown M, Strober W. Excess IL-12 but not IL-23 accompanies the inflammatory bowel disease associated with common variable immunodeficiency. Gastroenterology. 2006;131(3):748-56.

[254] Cho YN, Kee SJ, Kim TJ, Jin HM, Kim MJ, Jung HJ, Park KJ, Lee SJ, Lee SS, Kwon YS, Kee HJ, Kim N, Park YW. Mucosal-associated invariant T cell deficiency in systemic lupus erythematosus. J Immunol. 2014;193(8):3891-901.

[255] Dunne MR, Elliott L, Hussey S, Mahmud N, Kelly J, Doherty DG, Feighery CF. Persistent changes in circulating and intestinal γδ T cell subsets, invariant natural killer T cells and mucosal-

associated invariant T cells in children and adults with coeliac disease. PLoS One. 2013;8(10):e76008.

[256] Wilson RP, Ives ML, Rao G, Lau A, Payne K, Kobayashi M, Arkwright PD, Peake J, Wong M, Adelstein S, Smart JM, French MA, Fulcher DA, Picard C, Bustamante J, Boisson-Dupuis S, Gray P, Stepensky P, Warnatz K, Freeman AF, Rossjohn J, McCluskey J, Holland SM, Casanova JL, Uzel G, Ma CS, Tangye SG, Deenick EK. STAT3 is a critical cell-intrinsic regulator of human unconventional T cell numbers and function. J Exp Med. 2015;212(6):855-64.

[257] Smyth MJ, Thia KY, Street SE, Cretney E, Trapani JA, Taniguchi M, Kawano T, Pelikan SB, Crowe NY, Godfrey DI. Differential tumor surveillance by natural killer (NK) and NKT cells. J Exp Med. 2000;191(4):661-8.

[258] Crowe NY, Smyth MJ, Godfrey DI. A critical role for natural killer T cells in immunosurveillance of methylcholanthrene-induced sarcomas. J Exp Med. 2002;196(1):119-27.

[259] Galli G, Pittoni P, Tonti E, Malzone C, Uematsu Y, Tortoli M, Maione D, Volpini G, Finco O, Nuti S, Tavarini S, Dellabona P, Rappuoli R, Casorati G, Abrignani S. Invariant NKT cells sustain specific B cell responses and memory. Proc Natl Acad Sci U S A. 2007;104(10):3984-9.

[260] Cerundolo V, Silk JD, Masri SH, Salio M. Harnessing invariant NKT cells in vaccination strategies. Nat Rev Immunol. 2009;9(1):28-38.

[261] Toussirot E, Streit G, Wendling D. Infectious complications with anti-TNFalpha therapy in rheumatic diseases: a review. Recent Pat Inflamm Allergy Drug Discov. 2007;1(1):39-47.

[262] Genovese MC, Greenwald M, Cho CS, Berman A, Jin L, Cameron GS, Benichou O, Xie L, Braun D, Berclaz PY, Banerjee S. A phase II randomized study of subcutaneous ixekizumab, an anti-interleukin-17 monoclonal antibody, in rheumatoid arthritis patients who were naive to biologic agents or had an inadequate response to tumor necrosis factor inhibitors. Arthritis Rheumatol. 2014;66(7):1693-704.

[263] Hueber W, Sands BE, Lewitzky S, Vandemeulebroecke M, Reinisch W, Higgins PD, Wehkamp J, Feagan BG, Yao MD, Karczewski M, Karczewski J, Pezous N, Bek S, Bruin G, Mellgard B, Berger C, Londei M, Bertolino AP, Tougas G, Travis SP; Secukinumab in Crohn's Disease Study Group. Secukinumab, a human anti-IL-17A monoclonal antibody, for moderate to severe Crohn's disease: unexpected results of a randomised, double-blind placebo-controlled trial. Gut. 2012;61(12):1693-700.